HYDROTHERMAL ZEOLITE CRYSTALLIZATION FROM CLAY MINERALS

by

DAVID EDWARD MAINWARING, G.R.I.C.

A thesis submitted for the Degree of Doctor of Philosophy of the University of London

Physical Chemistry Laboratories,
Imperial College of Science and Technology,
South Kensington, London.

November, 1970.

Abstract

A study of the hydrothermal reactions of metakaolinite in alkaline solution has been made. Metakaolinite has proved to be a versatile starting material for aluminosilicate preparation, particularly zeolites. Approximately thirty zeolites crystallized from the compositions studied. This included the first preparation of the Rb analogue of phillipsite, and a siliceous form of the chabazite-like K-G which had a very high sorption capacity.

Highly alkaline solutions have permitted the temperatures required to produce both hydrated and non-hydrated products to be lowered considerably, for example zeolite K-F, analcime and kaliophilite. Syntheses from magmas containing two bases produced cancrinite at a temperature as low as 80°, and also new cationic variations of existing zeolite frameworks such as Na, Li-F.

The chemical, sorptive and crystallographic properties of many of the crystalline products have been investigated. Zeolite Ba-G has been re-indexed and identified as having the zeolite L framework. A new synthesis from the K,Ba system

has produced a zeolite which is the aluminous end member of the zeolite L family. This has the 7.5 Å channel system available for sorption and although aluminous it has a very high thermal stability.

A re-examination of zeolite Linde N has led to its confirmation as a single species and a new unit cell. The rubidium analogue of K-F has been indexed on a tetragonal unit cell and the relationship to the other members of the K-F family discussed.

The mechanism of zeolite crystallization has been followed by measurement of the rate of formation of the zeolites and of the change in composition of the solutions. This is discussed with respect to other systems, for example kaolinite and aluminosilicate gel syntheses. Where possible, syntheses and products have been compared to natural processes and natural zeolites.

Acknowledgements

I wish to express my appreciation to Professor R.M. Barrer, F.R.S. for his encouragement and interest during the course of this work. It has been a privilege and a pleasure to work in his laboratories on zeolite research.

I wish to thank the past and present members of this research school for the many helpful discussions on the diverse aspects of zeolite chemistry.

Finally I wish to thank English Clays Lovering Pochin Ltd. for the research scholarship which enabled me to carry out this work.

Contents

page

page

Section 1. Zeolites and Metakaolinite

1.1 Zeolite Characteristics

Silicates may be divided into groups on a structural basis (Wells) and one of the most important of these is the tectosilicate group. The various silica polymorphs may be represented by $(SiO_2)_n$ and are formed by the linking of each SiO_4-tetrahedron by shared oxygen atoms to four other identical tetrahedra. Many of the earth's minerals are formed by the substitution in the tectosilicates of Al^{3+} for Si^{4+} with the inclusion of cations to preserve electroneutrality. Thus there is a bonded framework containing alkali or alkaline earth ions in the aluminosilicates and a bonded silica framework needing no cations in their silica polymorphs.

These framework silicates include the felspars, which are the most important component of the lithosphere, the felspathoids, and the zeolites (Deer, Howie and Zussman). Between these groups there is a gradation of porosity. The anhydrous felspathoids such as nepheline, kaliophilite and kalsilite are the most dense (Barrer 1968). Next are the crystalline silicas which include quartz, cristobalite and tridymite, although the last two have sufficient porosity

to permit the encapsulation of helium and neon (Barrer and Vaughan 1967). The most porous of the aluminosilicates are the zeolites and the felspathoids. The felspathoids contain salts such as NaCl, Na_2SO_4 and Na_2CO_3 in their framework cavities. These 'guest molecules' can be replaced by excess alkali and water in their synthetic counterparts (Barrer and White 1952) and if removed, leave a framework with a porosity comparable to zeolites. Since zeolites can take up salts from either a concentrated solution (Barrer and Walker 1964) or from a molten salt bath (Meier 1957) there is no clear distinction between zeolites and felspathoids. For this reason, and bearing in mind the structural relationships, the felspathoids sodalite and cancrinite are often included in comparisons of the properties and structures of zeolites (Meier 1968, Breck 1970).

The very high porosity of zeolites is a result of the spacious internal cavities and channels of molecular dimensions containing weakly bonded cations and water molecules (Smith 1963). In solution zeolites exhibit both ion-exchange and ion-sieve characteristics (Amphlett 1964). These have largely been investigated by Barrer (for example Barrer, Buser and Grutter 1956 , Barrer and Falconer 1956), Ames (for example Ames 1964a and 1964b) and Sherry (for example Sherry 1966, 1968a and 1968b).

Many zeolites can undergo easy reversible dehydration (Eitel 1966) by moderate heating and/or by application of a vacuum without collapse of the aluminosilicate framework. Many important laboratory and industrial applications are based upon this ability. The activated zeolite thus possesses: (a) a three-dimensional lattice having uniform pores of molecular dimensions, (b) a high surface area accessible only to molecules small enough to diffuse through the pores, (c) a highly polar surface, and (d) remarkable thermal stability (Mays and Pickert 1968). These aluminosilicates are ideal for such uses as (a) molecular sieves (Barrer 1968), for example the separation of n-paraffins from naphthas and kerosene (Avery and Lee 1962), (b) selective sorbents (Barrer 1966), for example the removal of CO_2 and sulphur compounds from natural gas (Conviser 1965, Ebdon 1965), (c) desiccants (Barrer 1959), for example the drying of gases resulting from thermal cracking of petroleum oil (Pierce and Stiegham 1966) and (d) catalysts (Venuto and Landis 1968). Catalysis is probably the largest contribution of zeolites to industry at the present and in the immediate future. Some perspectives on zeolite catalysis have recently been noted by Venuto (1970) where much of the latest literature has been reviewed.

Zeolites have a very wide compositional range in both their cationic and framework content. The empirical oxide formula may be given as: $(M'_2, M'')O$, Al_2O_3, $nSiO_2$, mH_2O, where M' and M'' are the mono and divalent cations respectively. The values of n and m show considerable variation. A lower limit for n of 2 is placed on this formula for a completed aluminosilicate framework by the empirical rule of Lowenstein (1954): AlO_4 tetrahedra can only be linked to SiO_4 tetrahedra and never to other AlO_4 tetrahedra. Examples of zeolites with an alumina to silica ratio of 1:2 are sodalite (Loens and Schulz 1967) and gismondite (Fischer 1963). The upper limit appears to be in the range of 9-10. Here a group of four zeolites is important for their high silica content. These are mordenite (Meier 1961), ferrierite (Vaughan 1966), dachiardite (Gottardi and Meier 1963) and clinoptilolite (Ames 1961). Recently a ferrierite with an unusually high silica to alumina ratio of 14 has been reported by Wise, Nokleberg and Kokinos (1969).

The crystal structure of zeolites is a more characteristic property than chemical composition, and most of the structures of the framework zeolites have now been elucidated. Structural classification on a crystallographic basis began with Smith (1963) and later was refined by Meier (1968). Since then Barrer and Villiger (1969) have examined the

zeolites related to chabazite and produced a structural scheme within this group. The early structural determinations commencing with Taylor's study of analcime (1930) have been reviewed by Fischer and Meier (1965) and the more recent developments by Breck (1970). Meier and Olson (1970) have produced an atlas which shows stereopairs of twenty seven of the well established zeolite frameworks.

Meier (1968) has proposed eight structural building units common to zeolites. These units are small anionic rings or other groups of tetrahedra. The SiO_4 and AlO_4 tetrahedra were considered to be the primary building units and the larger assemblages to be the 'secondary building units' (SBU) of the framework. Barrer (1968) has listed the polyhedra that can be found in porous aluminosilicates. Most of these are considerably larger than the secondary building units of Meier and known silicate anions in solution. In Table 1.1.1 some of these characteristic structural units in zeolites have been described. To these has been added the cage (10-hedron type (11)) that is present in gismondite.

The structural characteristics and crystallographic data for the zeolites most commonly encountered have been collected in Table 1.1.2.

Table 1.1.1

Some Characteristic Structural Units in Zeolites

S4R	single four membered ring
S6R	single six membered ring
S8R	single eight membered ring
D4R	double four membered ring, 6-hedron
D6R	double six membered ring, 8-hedron
4-1	five membered assemblage of the natrolite group
5-1	six membered assemblage of the mordenite group
4-4-1	nine membered assemblage of the heulandite group
10-H (1)	10-hedron type (1), of paulingite
10-H (11)	10-hedron type (11), of gismondite
11-H	11-hedron of cancrinite
14-H (1)	14-hedron type (1), cubo-octahedron of sodalite
14-H (11)	14-hedron type (11), of gmelinite
17-H	17-hedron of levynite
18-H	18-hedron of paulingite and ZK-5
20-H	20-hedron of chabazite
23-H	23-hedron of erionite
26-H (1)	26-hedron type (1), truncated cubo-octahedron of A and ZK-5
26-H (11)	26-hedron type (11), of faujasite

Classification of Zeolites

Meier 1968 Group	Breck 1970	Some characteristic structural units	Framework density g/cc	Void fraction	Dimensional type of main channel system	Direction of main channels	Free apertures of channels in Å (No. of tetrahedra per ring in ( )	Fault planes	Crystal data
	Analcime $(Na_{16}Al_{16}Si_{32}O_{96}\cdot 16H_2O)$	S4R,S6R	1.85	0.18	111	-	2.6	*	Cubic Ia3d a = 13.74
I	Laumontite $(Ca_4Al_8Si_{16}O_{48}\cdot 16H_2O)$	S4R,S6R	-	-	1	11a	4-5.6(10)	*	Monoclinic Am a=7.57, b=14.75 c=13.10, γ=112.0°
	Phillipsite $(K,Na)_{10}Al_{10}Si_{22}O_{64}\cdot 20H_2O$	S4R,S8R	1.58	0.31	111	11a 11b 11c	4.2-4.4(8) 2.8-4.8(8) 3.3 (γ)	 (010) 	orthorhombic a=9.96 b=14.25, c=14.25 B2mb
IV	Gismondite $(Ca_4Al_8Si_8O_{32}\cdot 16H_2O)$	S4R S4R,S8R			111	11a 11c	2.8-4.9(8) 3.1-4.4(8)	(101) (011)	monoclinic $P2_1/C$ a=9.84, b=10.02 c=10.62, γ=92.4°
	Yugawaralite $(Ca_2Al_4Si_{12}O_{32}\cdot 8H_2O)$	S4R	1.81	0.27	11	11<101> 11a	3.6-2.8(8) 4.3-3.2(8)	*	monoclinic a= 6.73 b=13.95, c=10.03 γ=111.5° Pc
	Barrer's Pl [1] $(Na_6Al_6Si_{10}O_{32}\cdot 15H_2O)$	D4R,S8R	1.57	0.41	111	11a	3.5 (8)	-	cubic Im3m a=10.0
	Linde A $(Na_{12}Al_{12}Si_{12}O_{48}\cdot 27H_2O)$	D4R 26-H(1) 14-H(1)	1.27	0.47	111		4.1 (8)	*	cubic Pm3m a=12.32
VII	Paulingite $(K_2CaNa_2)_{76}Al_{152}-Si_{520}O_{1344}\cdot 700H_2O$	S4R, 10-H(1) 18-H, 26-H(1)	1.54	0.49	111		3.9 (8)	*	cubic Im3m a=35.1
	Faujasite $(Na_2CaMg)_{29}Al_{58}-Si_{134}O_{384}\cdot 240H_2O$	D6R 26-H(11) 14-H(1)	1.27	0.47	111		7.4 (12)	(111)	cubic Fd3m a=24.7
	X	D6R 26-H(11), 14-H(1)	1.31	0.50	111		7.4 (12)	(111)	
	Z-K-5 $(Na_{30}Al_{30}Si_{66}O_{192}\cdot 98H_2O)$	D6R 18-H, 26-H(1)	1.46	0.44	111		3.9 (8)	*	cubic Im3m a=18.7
	Chabazite $(Ca_6Al_{12}Si_{24}O_{72}\cdot 40H_2O)$	D6R D6R, 20-H	1.45	0.47	111		3.7-4.2(8)	(001)	hexagonal $R\bar{3}m$ a=13.17, c=15.06
	Gmelinite $(Na_2Ca)_4Al_8Si_{16}O_{48}\cdot 24H_2O)$	D6R, 14-H(11)	1.46	0.44	1	(111) 11c	6.9 (12)	(001)	hexagonal $P6_3/mmc$ a=13.8, c=10.0
	Linde L $(K_6Na_3Al_9Si_{27}O_{72}\cdot 21H_2O)$	D6R 11-H S12R	1.61	0.32	1	11c	7.5 (12)	(001)	hexagonal P6/mmm a=18.4, c=7.5
III	Cancrinite hydrate $(Na_6Al_6Si_6O_{24}\cdot CaCO_3$	S6R, 11-H	1.67		1	11c	6.2 (12)	(001)	hexagonal $P6_3$ a=12.75, c=5.14
	Sodalite hydrate $(Na_6Al_6Si_6O_{24}\cdot 2NaCl)$	S6R, 14-H(1)	1.72		111	11<111>	2.6 (6)	(111)	cubic $P\bar{4}3n$ a=8.87
	Levynite $(Ca_3Al_6Si_{12}O_{36}\cdot 18H_2O)$	D6R 17-H	1.56		111		3.3-5.1(6)		hexagonal $R\bar{3}m$ a=13.32, c=22.51
	Erionite $(Ca_{4.5}Al_9Si_{27}O_{72}\cdot 27H_2O)$	S6R, 11-H, 23-H	1.51	0.35	111		3.6-4.8(8)	(001)	hexagonal $P6_3/mmc$ a=13.26, c=15.12
	Offretite $(Na_2Ca)Al_4Si_{14}O_{36}\cdot 14H_2O$	D6R, 11-H 14-H(11)	1.55	0.40	111	11a 11c	3.6-4.8(8) 6.3 (12)	(001)	hexagonal $P\bar{6}m2$ a=13.3, c= 7.6
	Omega [2] $(6.8Na1.6(TMA)Al_8Si_{28}O_{72}\cdot 2H_2O)$	S6R S6R, 14-H(11)	1.65	0.38	1	11c	7.5 (12)	(001)	hexagonal a=18.15, c=7.59
	T [3]	S6R	1.50	0.40	111		3.6-4.8(8)		

V	Brewsterite $(Sr,Ba,Ca)_2Al_4Si_{12}O_{32}\cdot 10H_2O$	$T_{10}O_{20}$	4-4-1	1.75		ll	lla llc	2.3-5.0(8) (010) 2.7-4.1(8)	monoclinic $P2_1/m$ a= 6.77, b=17.51 c= 7.74, β=94.3°
	Heulandite $(Ca_4Al_8Si_{28}O_{72}\cdot 24H_2O)$		4-4-1	1.69	0.39	ll	lla llc	2.4-6.1(8) (010) 3.2-7.8(10)	monoclinic Cm a=17.73, b=17.82 c= 7.43, γ=116.3°
	Stilbite $(Na_2Ca_4Al_{10}Si_{26}O_{72}\cdot 28H_2O)$		4-4-1	1.64	0.39	ll	lla llc	4.1-6.2(10)(010) 2.7-5.7 (8)	monoclinic C2/m a=13.64, b=18.24 c=11.27, β=128.0°
VI	Mordenite $(Na_8Al_8Si_{40}O_{96}\cdot 24H_2O)$	T_8O_{16}	5-1	1.70	0.28	ll	llc llb	6.7-7.0(12)(010) 2.9-5.7 (8)	orthorhombic Cmcm a=18.13, b=20.49 c= 7.52
	Dachiardite $(Na_5Al_5Si_{19}O_{48}\cdot 12H_2O)$		5-1	1.72	0.32	ll	llb llc	3.7-6.7(10)(010) 3.6-4.8 (8)	monoclinic C2/m a=18.73, b= 7.54 c=10.30, β=107.9°
	Epistilbite $(Ca_3Al_6Si_{18}O_{48}\cdot 16H_2O)$		5-1	1.76	0.25	ll	lla llc	3.2-5.3(10) * 3.7-4.4 (8)	monoclinic C2/m a= 8.91, b=17.73 c=10.21, β=124.3°
	Ferrierite $(Na_2Mg_2Al_6Si_{30}O_{72}\cdot 18H_2O)$		5-1	1.77		ll	llc llb	4.3-5.5(10) * 3.4-4.8 (8)	orthorhombic Immm h=19.16, b=14.13 c= 7.49
	Bikitaite $(Li_2Al_2Si_4O_{12}\cdot 2H_2O)$		5-1	2.02		l	llb	3.2-4.9 (8) *	monoclinic $P2_1$ a= 8.61, b= 4.96 c= 7.61, β=114.4°
II	Natrolite $(Na_{16}Al_{16}Si_{24}O_{80}\cdot 16H_2O)$	T_5O_{10}	4-1	1.76	0.23	ll	1c	2.6-3.9 (8)(110)	orthorhombic Fdd2 a=18.30, b=18.63 c= 6.60
	Thomsonite $(Na_4Ca_8Al_{20}Si_{20}O_{80}\cdot 24H_2O)$		4-1	1.76	0.32	ll	1c	2.6-3.9 (8)(100) (010)	orthorhombic Pmm2 a=13.07, b=13.08 c=13.18
	Edingtonite $(Ba_2Al_4Si_6O_{20}\cdot 8H_2O)$		4-1	1.68	0.36	ll	1c	3.5-3.9 (8)(110)	orthorhombic $P2_12_12\bar{\omega}$ a= 9.54, b= 9.65 c= 6.50

Notes on Table 1.1.2

1. Barrer's P1 zeolite has been shown to have the gismondite framework (Baelocher and Meier 1970). These are characteristics of the cubic structure.

2. Proposed structure by Barrer and Villiger (1969).

3. Zeolite T has been shown to be a faulted offretite (Kerr, Gard, Barrer and Galabova 1970).

4. Gmelinite can be considered to have 3-dimensional channels of different sizes.

Many zeolite structures can be described by the stacking of some of the characteristic framework units shown in Table 1.1.1. The chabazite group is a good example of a series of zeolites produced by various stacking sequences of a framework unit (the six-membered ring S6R). The resulting cavities or polyhedral units have been illustrated by Barrer and Kerr (1959). If these single six rings are represented by A, B and C in the stacking sequence, then the members of the group are

AB	- cancrinite
ABC	- sodalite
AAB	- offretite
AABB	- gmelinite
AABBCC	- chabazite
AABAAC	- erionite
AABCCABBC	- levynite

Double rings (such as AA) are identical to the unit D6R (or 8-hedron) of Table 1.1.1. Other possible stacking sequences producing as yet hypothetical structures have been described by Kokotailo and Lawton (1964).

When columns of gmelinite cages (14-hedra (11)) parallel with the c-direction and produced by the AABB sequence are suitably linked to one another the resulting structure has wide twelve membered rings

(diameter 6.9 Å) parallel to the c direction. The extension of the chabazite cage (20-hedron) produced from the sequence AABBCC results in a framework possessing eight membered rings of diameter 3.7 - 4.2 Å. Stacking faults resulting from a change in stacking sequence (producing, for example, a chabazite layer in the gmelinite structure) are to be expected.

To the chabazite group the zeolites offretite, L and Ω can be added (Table 1.1.2). In this Table many of the common structural units have been shown. Recently the closely related members of this group, erionite, offretite and Linde L have been examined by various workers (for example, Kerr, Gard, Barrer and Galabova 1970).

Each of these three zeolites is composed of polyhedra in the stacking sequence

---- | 11-H, D6R | 11-H, D6R | ---

Zeolite L (Barrer and Villiger 1969 a) and offretite have the polyhedra in the same orientation (Figure 1.1.1 (a)) while erionite has alternate cancrinite cages (11-H) rotated by 60° in the c-direction (Staples and Gard 1959) (Figure 1.1.1 (b)). The joining of these columns of polyhedra in

Figure I.1.1.

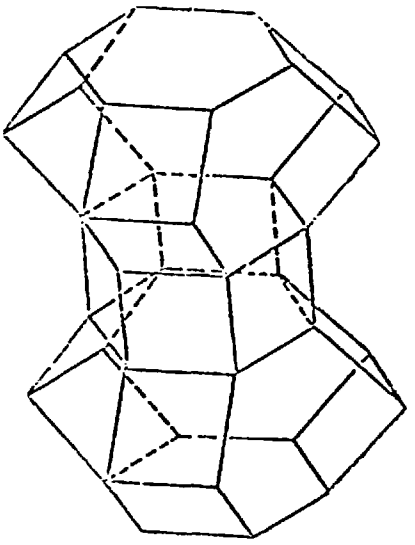

a
Column in Zeolite L
and Offretite

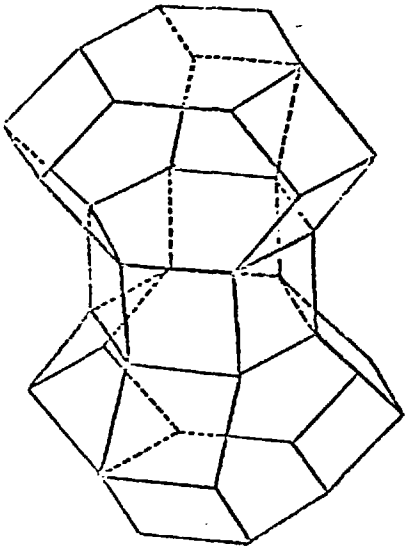

b
Column in Erionite

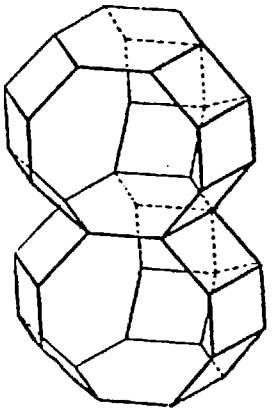

c
Column in Zeolite Ω

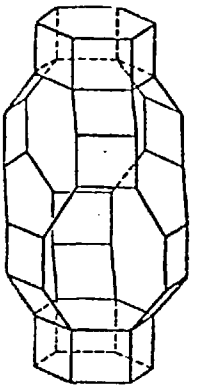

d
Cavity in Chabazite

offretite produces a distorted 12 member ring with a maximum free diameter of 6.3 Å. Thus cylindrical channels are formed in the c direction. Erionite has these channels interrupted every unit cell length (15.12 Å) by six membered rings. The largest opening into these cavities is the eight member ring which is part of the cavity wall. The columns of polyhedra in zeolite L are joined to form planar 12 membered rings. These give a channel in the c direction with a diameter at the ends of approximately 7.5 Å and at the centre a diameter of 13 Å. Barrer and Villiger (1969b) have proposed the probable structure of zeolite Ω . The Ω framework is based upon columns of gmelinite cages (14-H (11)) joined by the six membered ring windows (Figure 1.1.1 (c)). These columns are joined laterally to give wide channels parallel to c having free dimensions similar to those of zeolite L and circumscribed by 12 membered ring windows. The projection of the zeolite Ω structure onto a plane normal to the c direction is identical with that of the L structure.

An example of the stacking of larger structural units from Table 1.1.1 is shown below:

--- |	26-H (1), 18-H	26-H (1), 18-H | ---	ZK-5
--- |	26-H (1), 10-H (1), 18-H	26-H (1), 10-H (1), 18-H | ---	paulingite

Other sequences again produce structures which are as yet hypothetical.

In Table 1.1.2 many of the zeolites have isostructural species. These differ in cation composition, hydration or framework composition and thus in unit cell and space group. The analcime group provides examples of isostructural species, many of which are shown below.

Table 1.1.3

Species	Composition	Unit cell	Reference
analcime	$NaAlSi_2O_6.H_2O$	cubic a=13.7	Taylor (1930)
pollucite	$CsAlSi_2O_6$	cubic a=13.6	Strunz (1936)
leucite	$KAlSi_2O_6$	cubic a=13.4	
	$KAlSi_2O_6$	tetragonal a=13.0 c=13.8	Faust (1963)
wairakite	$CaAl_2Si_4O_{12}.2H_2O$	monoclinic a=13.69 b=13.68 (β=90.5) c=13.56	Coombs (1955)
viseite*		cubic a=13.65	McConnell (1952)
K-analcime*	$KAlSi_2O_6.H_2O$	cubic a=13.8	Barrer and McCallum (1953 b)
iron-pollucite*	$CsFeSi_2O_6.4H_2O$	cubic a=13.66	Kopp, Harris, Clark and Yakel (1963)
beryllium-analcime*	$Na_3Be_{1.5}Si_{5.0}O_{13}.NaCl$	cubic a=13.35	Ueda and Koizumi (1970)

* Unconfirmed by a complete structural analysis.

The ready isomorphous substitutions in the zeolite framework of Ga for Al and Ge for Si were demonstrated by Barrer, Baynham, Bultitude and Meier (1959). The series of gallosilicates, aluminogerminates and gallogermanates resembled, for example, thomsonite, faujasite and Linde Sieve A.

Attempts by Barrer and Marshall (1965) to substitute phosphorus in the framework appeared to be unsuccessful. Kühl (1967) has reported a synthesis of zeolite A containing imbibed phosphate (ZK-21) and recently Flanigen and Grose (1970) have described the crystallization of six alumino-silicophosphate zeolites which include analcime. The analcime (Table 1.1.3) framework has also been produced as a beryllosilicate by Ueda and Koizumi (1970), and as a ferro-silicate by Kopp, Harris, Clark and Yakel (1963). The common substitution of ferric iron, in natural erionite as found by Sheppard and Gude (1969) and in phillipsite as found by Hay (1964), suggests that further isomorphous substitutions can be carried out by hydrothermal syntheses.

1.2 Synthesis

Many of the techniques used in the hydrothermal synthesis of zeolites are imitative of natural geochemical processes. At present most zeolite crystallizations are from highly alkaline heterogeneous aluminosilicate gels. Typical sources of aluminium are sodium or potassium aluminate, amorphous aluminium hydroxide gel and aluminium salts such as aluminium phosphate. Silica sources are sodium and potassium silicate, silica gel, precipitated silica and stabilized silica sols. Alkali is added as hydroxides or hydrolysable salts such as phosphates and carbonates. The use of natural compounds such as kaolinite (Barrer and Marshall 1965, Taggart and Ruband 1964) allophane (Takahaski and Nishimura 1966), and pumice and natural glasses (Di Piazza, Regis and Sand 1959) has increased in zeolite technology.

Barrer (1960) has applied solution thermodynamics to these hydrothermal preparations to demonstrate the stabilization of the open zeolite frameworks by various space filling mineralisers such as water.

The stable product from the hydrothermal synthesis is that species with the minimum free energy under the given chemical and physical conditions. Fyfe (1960) has shown

that the crystallization from highly reactive gel mixtures increases the probability of metastable crystallization. According to Ostwald's Law of successive steps there are possible intermediate states through which a system passes towards the stable state of minimum free energy. Two non contradictory explanations have been proposed for this. One suggestion by Stranski and Totomanov (1933) is that the nucleation of species with the least surface energy will be favoured, resulting in the growth and perhaps persistence of a metastable phase. The other suggestion by Fyfe and Verhoogen (1958) is that the greatest rate of nucleation is obtained for a polymorphic transition when it involves the least decrease in entropy. Thus there is the tendency for a phase with a crystalline structure close to that of the reactant, or a previously formed species, to nucleate.

Goldsmith (1953) has attempted a qualitative explanation of nucleation in complex systems such as those in zeolite syntheses by means of the principle of simplexity. He postulates on a kinetic basis that the species of greatest simplexity (i.e. highest degree of randomness) should be those most readily nucleated in a complex random system, since the greater the disorder which can be tolerated and yet still produce a nucleus which can grow, the greater is

the probability of this occurring by random fluctuations in the solution. Kerr (1968) in a study of the two zeolites X and B (Na-P), which have essentially the same composition but widely different structures, found that zeolite X nucleates more readily than B but grows at a much slower rate than B.

The conversion of a zeolite after its growth to another zeolitic or non-zeolitic species is common. Some examples of this are zeolite A recrystallizing to Na-P (Barrer, Baynham, Bultitude and Meier 1959) and mordenite disproportionating into analcime and silica (Barrer 1949, and Coombs, Ellis, Fyfe and Taylor 1959). Senderov and Khitarov (1970) have concluded that the only thermodynamically stable zeolites in the Na_2O-Al_2O_3-SiO_2-H_2O system are analcime and natrolite.

The kinetics of zeolite formation have been investigated by a large number of workers in various systems. Some of these investigations are tabulated below.

Hydrothermal system	Method	Reference
mordenite from aqueous gels	nitrogen sorption	Dominé and Quobex (1968)
K-I from kaolinite	X-ray powder intensity	Barrer, Cole and Sticher (1968)
A and X from aqueous gels	X-ray powder intensity	Breck and Flanigen (1968)
A from aqueous gels	water sorption	Ciric (1968)
A from amorphous glass	water sorption	Kerr (1966)
X and B from aqueous gels	cyclohexane and water sorption	Kerr (1968)
Species P (ZK-5) from analcite	X-ray powder intensity	Barrer and Marcilly (1970)
sodalite from kaolinite	uptake of $NaClO_4$	Barrer and Cole (1970)
offretite from aqueous gels	X-ray powder intensity	Barrer and Aiello (1970)
A from aqueous gels	crystal size	Zhdanov (1970)

A characteristic of the kinetics of zeolite growth is the induction period. This has been found to increase with decreasing temperature and decreasing alkali concentration by Breck and Flanigen (1968) and Kerr (1966). Dominé and Quobex (1968) found it to vary with initial starting materials. Sticher and Bach (1968) have followed the rate of dissolution of kaolinite and metakaolinite in alkaline solutions during

zeolite production. They have found the period for the silicon and aluminium concentration in solution to reach a maximum with metakaolinite was shorter than with kaolinite. Zhdanov (1970) has concluded that the rate of dissolution of the solid phase in the heterogeneous aluminosilicate mixtures producing zeolites greatly influences the induction period. The induction period is probably also indicative of the time required for the growth of nuclei of a critical size, which then produce the rapid autocatalytic growth.

In all the above investigations the autocatalytic growth of the particular zeolite species has been noted. The rate of zeolite formation was shown to increase proportionally with the amount of product present by Kerr (1966, 1968). The influence of temperature upon the rate of formation of zeolite has been noted by Kerr (1966) and Zhdanov (1970). Breck and Flanigen (1968) and Dominé and Quobex (1968) have estimated the activation energy of the crystallization process for A, X, Y and mordenite to be 11, 14, 15 and 11 kcal/mole respectively. An increase of alkali concentration was found by Sand (1968) and Zhdanov (1970) to decrease both the crystallization time and the final crystal size. This is a consequence of the increase of nucleation rate with increasing alkali concentration.

The mechanism of zeolite crystallization during hydrothermal syntheses has lately been the subject of an increasing number of investigations. As yet no common opinion exists on this mechanism or the role of the solid and liquid phases in it.

Growth from solution is indicated by the large number of reactants from which one can grow the same zeolite. Kerr (1966) has grown zeolite A from a solution produced by passing a hot NaOH solution over an aluminosilicate glass and continually removing the zeolite A formed. Kerr states that there is some doubt as to whether the solution is a true or colloidal solution. Ciric (1968) in a more detailed investigation into the crystallization of zeolite A from gels in alkaline solution found that crystal growth occurred by a diffusion mechanism and that this was consistent with the observations of Kerr. Barrer (1967) has considered that the growth of the complex aluminosilicate framework is unlikely to proceed by the capture of single SiO_4^{4-} and AlO_4^{5-} tetrahedral ions and cations. The lattice is developed by the addition of polyhedral ions resulting from condensation polymerisation. The simple 'polyanions' could be the smallest secondary building units such as the single 4, 6 and 8 rings, the double 4 ring, or the double 6 ring.

Zhdanov (1967) and Dubin and Polstyanov (1966) have demonstrated by analysis and sorption measurements that alkali aluminosilicate gels have a definite chemical and physical structure. Zhdanov has found that the separate composition of the gel skeleton, liquid phase and the zeolite crystals indicate that zeolite growth cannot be attributed to the Si-O-Al network in the gel alone.

The direct crystallization of alkali aluminosilicate gels to form zeolites has been proposed by Flanigen and Breck (1960). They have found (Breck and Flanigen (1967)) that gel formation is the major nucleation controlling process. The initial gel formed during zeolite crystallization was found by Fahlke, Wieker and Thilo (1966) by chemical analysis and X-ray methods to have a definite structure.

A study of the stages of zeolite growth from clear alkaline aluminosilicate solutions has been reported by Aiello, Barrer and Kerr (1970). A solid phase initially appeared as laminae which were mostly amorphous. These were replaced by thicker laminae, at which stage the X-ray pattern showed clear arcs caused by zeolites. Finally, the laminae were completely replaced by zeolites, the nucleation of which appeared to be heterogeneous.

Zhdanov (1970) has concluded from investigations on the chemical structure of aluminosilicate gels that zeolite nucleation begins in the liquid phase of the gels or at the interface of gel phases. The growth of the nuclei proceeds at the expense of the hydrated anions in solution, and crystal growth leads to a dissolving of the solid phase of the gel throughout the crystallization.

As yet zeolite synthesis is largely empirical. The kinetics as well as the final product appear to depend on: (a) the preparation of the starting materials, (b) the chemical behaviour during crystallization and (c) the agitation of the magma.

The systematic investigation of zeolite crystallization began in the 1940's with the high temperature syntheses of mordenite (Barrer 1948b), analcite and a barium zeolite (Barrer 1948a). Barrer and Marcilly (1970) have now shown that the barium zeolite preparation was the first synthesis of the zeolite ZK-5, later reported by Kerr (1966b). Barrer (1968b) has reviewed the synthesis of about fifty zeolitic species produced in his research school up to 1967. Early zeolite syntheses in the laboratories of the Union Carbide Corporation resulted in the preparation of the two important

Table 1.2.1

Various Syntheses of Zeolitic Products

Synthesis system	Zeolitic products	Reference
Na aluminosilicate gels at 150°-450°	analcite, mordenite, basic sodalite, basic cancrinite, nepheline hydrate I	Barrer and White (1952)
at 60°-250°	analcite, mordenite, harmotome, faujasite (X), A, basic sodalite, gmelinite	Barrer, Baynham, Bultitude and Meier (1959)
Na aluminosilicate gels 150°	A, X, P	Milton (1959), Breck, Eversole and Milton (1956)
Na aluminosilicate gels	A, X, Y, basic sodalite	Ovsepian and Zhdanov (1965)
NaOH-$Na_2Al_2O_3$ + volcanic glass	analcime, phillipsite, X, A, sodalite and cancrinite	Di Piazza, Regis, Sand (1959)
NaOH + volcanic glass	A, sodalite, P	Sudo and Matsuoka (1959)
Na aluminosilicate gels	sodalite, cancrinite, X, A, cubic NaP, tetragonal NaP, orthorhombic NaP, analcime, sodalite, nepheline hydrate, cancrinite	Regis, Sand, Calmon and Gilwood (1960), Sand, Roy and Osborn (1957)
NaOH, KOH + metakaolinite	A, X, Y, L, T	Taggart (1964)
Na aluminosilicate gels	chabazite-gmelinite (S)	Breck (1962)

zeolites Linde A and Linde X (Milton 1959). Breck and Flanigen (1968) have reviewed many of the syntheses in those laboratories.

Some of the numerous zeolite syntheses carried out under various conditions have been listed in Table 1.2.1. Many of these are the first reported syntheses of the particular product. They illustrate the wide diversity of starting materials and hydrothermal conditions that have been employed.

Table 1.2.1 (continued)

Synthesis system	Zeolitic products	Reference
K aluminosilicate gels	K-F, chabazites K-G, phillipsites K-M, K-L	Barrer and Baynham (1956 a)
K aluminosilicate gels	K-G, K-M, K-I	Ovespyan and Zhdanov (1964)
KOH + kaolinite	K-G, K-I, K-F	Barrer, Cole and Sticher (1968)
K aluminosilicate gels	K-M, K-F, K-L	Breck and Flanigen (1968)
Na, K, alumino-silicate gels	Na, K-G; Na, K-M; Na, K sodalite; Na, K-P	Barrer, Baynham, Bultitude and Meier (1959)
Na, K alumino-silicate gels	Na, K-G; Na, K-F; Na, K-A; Na, K-X; Na, K-L	Zhdanov (1965)
Li-aluminosilicate gels	Li-A, Li-H	Barrer and White (1951)
Li-aluminosilicate gels and glasses	Li-A, Li-H	Ruiz-Menucho and Roy (1959)
Li-aluminosilicate gels	Li-A	Gusseva and Lileev (1965)
Li-aluminosilicate gels 250°	Li-clinoptilolite	Ames (1963)
Li-gmelinite at 250° and 1000 atm.	bikitaite	Hoss and Roy (1960)
Li-aluminosilicate gels 150°	Li-mordenite, Li-analcime, Li-phillipsite	Sand, Coblenz and Sand (1970)

Table 1.2.1 (continued)

Synthesis system	Zeolitic products	Reference
Li-aluminosilicate glass	ZSM-2	Ciric (1968b)
Na-Li alumino-silicate gels	Na-P, cancrinite, Na, Li-F, Li-A, phase O	Borer and Meier (1970)
kaolinite + LiOH	Li-A, Li-K	Barrer, Cole and Sticher (1968)
Rb and Cs alumino-silicate gels	Rb analcite, Rb-D, Rb-E, Cs-F, Cs-G (pollucite)	Barrer and McCallum (1953)
kaolinite + RbOH kaolinite + CsOH	Rb-D Cs-D	Barrer, Cole and Sticher (1968)
Ba aluminosilicate gels	Ba-G, Ba-M, Ba-J, Ba-K	Barrer and Marshall (1964)
$(CH_3)_4N$-OH + alumino-silicate gels	harmotomes, soda-lites, faujasites(X) and zeolite A	Barrer and Denny (1961)
sodium aluminate + tetramethylammonium silicate	ZK-4 (A)	Kerr (1966 b)
Na, K, $(CH_3)_4N$, aluminosilicate gels	Ω, offretite, erionite, sodalite, zeolite L, gmelinite (S), zeolite M	Aiello and Barrer (1970)
Na, $(CH_3)_4N$, alumino-silicate gels	zeolite Ω	Union Carbide (1967)

Table 1.2.1 (continued)

Synthesis system	Zeolitic products	Reference
Na, $(CH_3)_4N$ hydroxides + metakaolinite	Linde zeolite N	Acara (1968)
tetrapropylammonium hydroxide + NaOH + aluminosilicate gels	ZSM-5	Mobil Oil (1968)

1.3 The X-ray Examination of Zeolites

X-ray diffraction data for zeolite powders can be collected with a Guinier-de Wolff camera, a Debye-Scherer camera or a powder diffractometer. The Guinier camera has proved to be the most convenient for the initial investigation of zeolites. This includes the precise determination of the lattice d-spacings from which an accurate unit cell may be found.

Structural determinations on zeolites which involve the collection of intensity data should be done on a powder diffractometer with, if possible, provision for step counting.

The diffraction patterns of the four samples held by the Guinier-de Wolf camera are recorded one above the other on a strip of photographic film. The preparation of the powder samples is important if accuracy is to be attained. These procedures have been described in standard works (such as Azaroff and Buerger). To these must be added the precaution that, although zeolite powders must be ground sufficiently to produce diffraction arcs of even intensity, excessive grinding of zeolites quickly destroys their crystallinity. The internal standard which is used to correct for film shrinkage and for position of the initial (zero) mark

can either be placed in an adjacent sample location* or mixed with the sample. The positions of the powder diffraction arcs are then measured with respect to the zero mark for both the sample and the standard using a vernier instrument. If the measurement is in mm. this corresponds to the position of the arc in degrees of 4θ . This is done several times and the results are averaged. With each value an estimate of the experimental error is recorded. These values are put in a computer program (DELCOR[1]) with the known values of the standard (for example lead nitrate). This program first approximates to a correction function by means of a least squares polynomial of order up to 10, by computing the differences between observed and calculated values of the standard. The observed measurement of the zeolite is then corrected against the standard data by means of the polynomial function. From the corrected 4θ values and the wavelength of the X-radiation a set of corrected d-spacings for the zeolite sample is produced.

These d-spacings are used either for comparison with standard values such as those in the American Society of Testing Material (A.S.T.M.) Powder Diffraction Index or for further calculations in an attempt to determine the unit cell constants.

* This location has been found by Dr.H. Villiger to give an error of 3% in the calculated values (Personal Communication).

Two computer programs APOL[2] and LCLSQ[3] are frequently used. APOL is used to calculate lists of the d-spacings of powder lines from the unit cell constants and mark systematic absences if the space group is included in the input data. LCLSQ is used to calculate by a least squares procedure, the best unit cell constants for a prescribed set of d-spacings if these are indexed and the approximate unit cell constants are given. Thus if the zeolite has been identified the unit cell constants can readily be calculated.

Several methods may be employed to find the unit cell of a compound when only the measured d-spacings are known. The success of these methods greatly depends upon the accuracy of the d-spacing determination.

Graphical procedures can be used if the crystal system is isometric, tetragonal or hexagonal but the complex diffraction patterns, characteristic of zeolites, make this method inadequate or liable to errors. Systematic analytical methods such as those described by Azaroff and Buerger are to be preferred and these are outlined as follows.

1. 'DELCOR' FORTRAN IV program to calculate corrected powder d-spacings, Q values, and list all successive differences in Q values.
2. 'APOL', Cole, J.F. and Villiger, H. (1969), Min.Mag. 37, 300.
3. 'LCLSQ' A revised and expanded FORTRAN IV version of C.W. Burnham's Lattice Parameter Refinement Programme by J.F.Cole and H. Villiger.

Let the reciprocal cell dimensions of a general cell in reciprocal space be a^*, b^*, c^*, α^*, β^*, and γ^*. If the Miller indices of the crystal planes are h, k and ℓ, and the spacing of the crystal plane $d_{hk\ell}$ is related to the quantity $Q_{hk\ell}$ by

$$Q_{hk\ell} = \frac{1}{d^2_{hk\ell}} \qquad (1)$$

then

$$Q_{hk\ell} = h^2a^{*2} + k^2b^{*2} + \ell^2c^{*2} + 2\,hka^*b^* \cos\gamma^* + 2\,k\ell\, b^*c^* \cos\alpha^* + 2\,h\ c^*a^* \cos\beta^* \qquad (2)$$

also Bragg's law may be written as

$$Q_{hk\ell} = \frac{4\sin^2\theta}{\lambda^2}\ h\ k \qquad (3)$$

where λ is the wavelength of the radiation.

The observed set of $d_{hk\ell}$ values is transformed by the computer program DELCOR into a list of observed $Q_{hk\ell}$. The indexing procedure now is to find quantities on the right hand side of equation (2) to satisfy the list of observed $Q_{hk\ell}$. The $Q_{hk\ell}$ list is tested to determine if the crystals are isometric, tetragonal or hexagonal. If this is negative then the procedure may be extended to the orthorhombic system.

In the isometric system equation (2) becomes

$$Q_{hk\ell} = (h^2 + k^2 + \ell^2)\, a^{*2}$$
$$= N\, a^{*2} \qquad (4)$$

The values of $N = (h^2 + k^2 + \ell^2)$ are 1, 2, 3, 4, ---
The first observed $Q_{hk\ell}$ value is assumed to be $Q_{100} = (1)\, a^{*2}$, the other possible Q values are calculated and compared with the list. If the computed Q values do not correspond to the list then the first observed $Q_{hk\ell}$ value is assumed to be $Q_{110} = (2)\, a^{*2}$ and the procedure is repeated.

If the cubic unit cell edge is made large enough a very close agreement between observed and computed values will automatically result but many lines must be regarded as absent. This assumption in the past has led to many incorrect unit cells for zeolites (an example is shown in Section 3.7.2).

The $Q_{hk\ell}$ list can now be tested for tetragonal and hexagonal systems together.
In the tetragonal system equation (2) becomes

$$Q_{hk\ell} = (h^2 + k^2)a^{*2} + \ell^2\, c^{*2}$$
$$= N_T\, a^{*2} + \ell^2\, c^{*2} \qquad (5)$$

and in the hexagonal

$$Q_{hk\ell} = (h^2 + h\,k + k^2)\, a^{*2} + \ell^2\, c^{*2}$$
$$= N_H\, a^{*2} + \ell^2\, c^{*2} \qquad (6)$$

where N_T and N_H can have the following values

$$N_T = 1,\ 2,\ 4,\ 5,\ 8,\ 9,\ 10,\ 13,\ 16,\ ----$$

$$N_H = 1,\ 3,\ 4,\ 7,\ 9,\ 12,\ 13,\ 16,\ 19,\ ---$$

Thus the list can be examined for the presence of such a factor. This then is used in equation (5) or (6). Also equations (5) and (6) suggest relations of the type:

$$Q_{h_1k_1\ell_1} - Q_{h_2k_2\ell_2} = (N_1 a^{*2} + \ell_1\, c^{*2}) - (N_2\, a^{*2} + \ell_1^2\, c^{*2})$$
$$= \Delta N\, a^{*2} \qquad (7)$$

ΔN can have any integral value. Thus whenever two reflections have the same ℓ index, the difference between their respective Q values is simply $\Delta N\, a^{*2}$. There are only two other types of relations that can occur if the differences between Q values are considered. These occur when the hk values of the two reflections are the same but the ℓ values are not, for example,

$$Q_{h_1k_1\ell_1} - Q_{h_1k_1\ell_2} = (N_1\, a^{*2} + \ell_1^2\, c^{*2}) - (N_1 a^{*2} + \ell_2\, c^{*2})$$
$$= \Delta \ell^2\, c^{*2} \qquad (8)$$

and when neither hk nor ℓ have the same values, for example,

$$Q_{h_1k_1\ell_1} - Q_{h_2k_2\ell_2} = (N_1a^{*2} + \ell_1^2c^{*2}) - (N_2a^{*2} + \ell_2^2c^{*2})$$
$$= \Delta N\ a^{*2} + \Delta\ell^2\ c^{*2} \qquad (9)$$

Thus a list of differences between all pairs of observed Q values contains differences which can be used to find a^{*2} and c^{*2}. Since more difference relations are possible in equation (7) than (8), it follows that, if differences between all possible values of Q are considered, $\Delta N\ a^{*2}$ values should recur more often than $\Delta\ell^2\ c^{*2}$ values, whereas recurrences of specific differences in equation (9) are purely fortuitous. Thus it is possible to use the most frequently recurring differences to determine the values of a^{*2} and c^{*2}.

If these procedures are negative the experimental measurements (the corrected Q value list) are in a form suitable for the more lengthy Hesse-Lipson and Ito procedures. If the ΔQ values examined indicate the probability of orthorhombic symmetry then the Hesse-Lipson method should be used. Finally the Ito method can be used for the indexing of any powder photographs regardless of symmetry. But again this greatly depends upon the precision of the available data. Both these procedures have been well discussed by Azaroff and Buerger.

1.4 Metakaolinite

Kaolinite is a very common mineral: usually present in all clay and shale assemblages, where it often constitutes a major part of the clay fraction. It does not vary greatly from the oxide composition Al_2O_3, 2 SiO_2, 2 H_2O. The investigation of the structure of kaolinite began with Hendricks (1929) and Pauling (1930). The structure determinations have been reviewed by Brown (1961). A detailed refinement of the triclinic cell by Newnham (1956) gave the following lattice parameters:

$a = 5.139 \pm 0.014$ Å

$b = 8.932 \pm 0.016$

$c = 7.371 \pm 0.019$

$\alpha = 91.6 \pm 0.2^\circ$

$\beta = 104.8 \pm 0.2^\circ$

$\gamma = 89.9 \pm 0.1^\circ$

The general structural features of kaolinite are shown in Figure 1.4.1. The atoms are arranged in parallel sheets with the large anions, oxygen and hydroxyl, co-ordinated around the small cations Si^{4+} and Al^{3+}. The Si ions are surrounded by tetrahedral groups of four oxygen ions and

Figure I.4.I Diagram of the Crystal Structure of Kaolinite

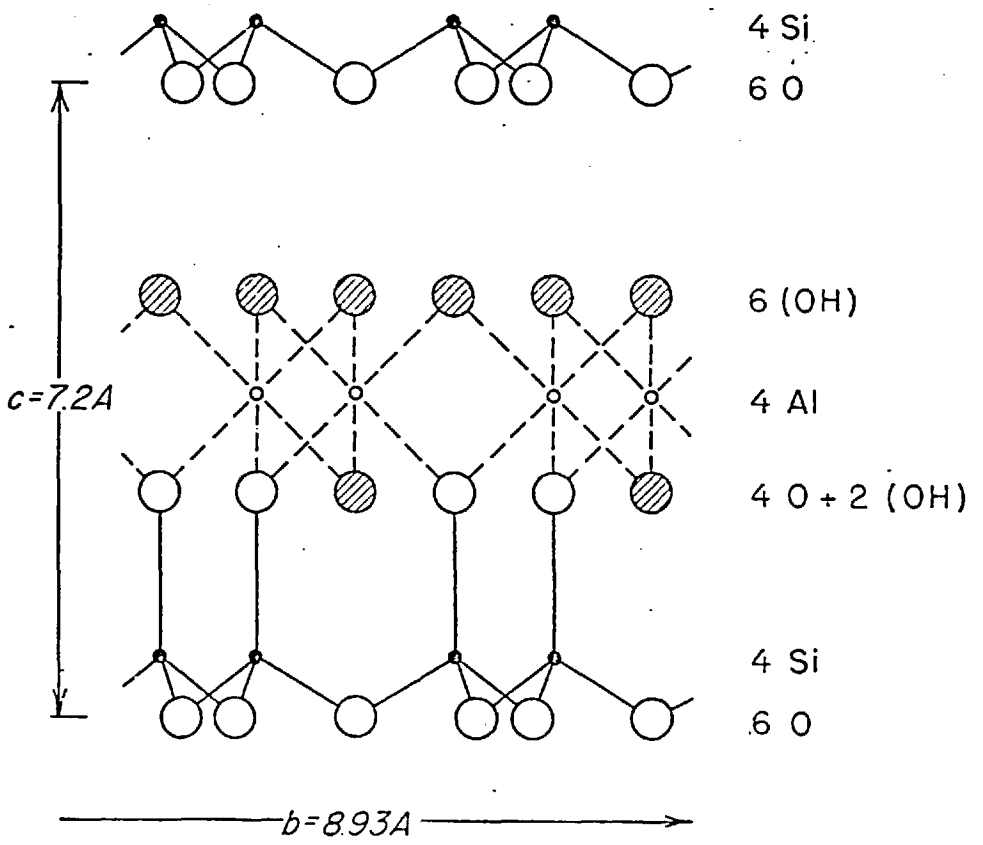

the Al ions by octahedral groups of six oxygen and hydroxyl ions. Thus the water molecules shown in the oxide formula do not exist in the structure but are hydroxyl groups. The water given off on heating is due to the decomposition of these hydroxyl groups.

Kaolinite undergoes thermal dehydroxylation at about 550° according to the reaction

$$2\ Al_2\ Si_2\ O_5\ (OH)_4 \longrightarrow 2\ Al_2\ Si_2\ O_7 + 4\ H_2O$$

Tscheischwiti, Buessem and Weyl (1939) have suggested that when kaolinite is dehydrated a considerable degree of order is maintained, and the product was called metakaolinite. Electron microscopy has shown that the external form of kaolinite particles persisted far above the dehydration temperature (Eitel, Müller and Radczewski, 1939). Roy, Roy and Francis (1955) concluded from X-ray, infra-red absorption and electron diffraction data that upon the dehydroxylation of kaolinite only a very minor change in the structural arrangement within the lattice takes place. The structure of metakaolinite is quite similar to that of kaolinite, at least in the two dimensions parallel to the original (001) cleavage plane. The decomposition of the hydroxyl sheets breaks up regularity in the c direction. Thus, on dehydroxylation the effective particle size is

radically reduced. The reduced particle size and the chemical instability of metakaolinite account for the increased solubility in alkaline solutions.

The dehydroxylation of kaolinite at temperatures between 400-540° and with a controlled water vapour pressure from 10^{-3} to 175 mm Hg was shown by Brindley, Sharp, Patterson and Narahari (1967) to be diffusion controlled having a rate constant dependent upon the temperature and the ambient water vapour pressure. Previously Brindley and Nakahira (1957) had found that heating of kaolinite to 497° produced a sample that showed 95% dehydroxylation at the surface and 40% dehydroxylation at the centre. These factors were considered in a choice of conditions for the preparation of bulk amounts of metakaolinite for synthesis (Section 2.1).

Section 2. The Experimental Apparatus and Methods Employed

2.1 The Starting Materials

The kaolinite used in this work was donated by English Clays Lovering Pochin Ltd. The chemical analysis supplied with the sample (Batch Number RLO 1016) is given in Table 2.1.1. The kaolinite was very well crystallized and the X-ray diffraction pattern is compared to a standard sample in Table 2.1.2.

Table 2.1.1

The chemical composition of the kaolinite

SiO_2	45.10%
Al_2O_3	38.57
Fe_2O_3	0.46
TiO_2	1.75
CaO	0.10
MgO	0.03
K_2O	0.08
Na_2O	0.18
Ignition loss	13.67
	99.94

Table 2.1.2

The X-ray diffraction pattern of the starting material and the impurity-anatase

Kaolinite		Kaolinite A.P.I. Project 49 Bath S.C.		Anatase
d (Å)	I	d (Å)	I	d (Å)
7.30	ms	7.512	10	4.755
7.02	ms	7.036	10	3.512
4.41	m	4.409	5	2.428
4.15	m	4.152	4	2.377
3.87	w	3.869	1	2.330
3.69	w	3.664	4	1.890
3.601	w			1.776
3.540	s	3.541	8	1.756
		3.366	0.5	1.699
3.120	mw			1.664
		3.093	0.5	1.585
3.072	vw	2.788	0.5	
2.550	w	2.550	4	
2.479	w	2.485	4	
2.368	w	2.366	3	
2.329	mw	2.324	7	
2.275	w	2.280	3	

The main impurity in the kaolinite was hydrous titanium dioxide. This was identified as anatase by measuring the very weak d-spacings in the metakaolinite produced from this sample and referring to the A.S.T.M. Fink Index. The diffraction pattern is shown in Table 2.1.2. The X-ray diffraction pattern of products synthesized from this batch of metakaolinite contained one or two of the strongest lines of anatase. These were removed from lists of the d-spacings of the products.

Bulk quantities of metakaolinite were prepared by loosely filling large porcelain dishes with kaolinite and heating in an electric furnace for twelve hours at 600°. Samples of metakaolinite from various levels were examined by X-ray diffraction to ensure a total conversion.

The hydroxides used in the following syntheses were analytical reagent grade, with the following exceptions: barium hydroxide of general purpose grade, and an aqueous solution of tetramethylammonium hydroxide containing 25% $(CH_3)_4NOH$. The hydroxides of rubidium and caesium were prepared by the reaction of the sulphates with barium hydroxide. The contact of all hydroxide solutions with air was kept to a minimum by making up the solutions immediately before use and keeping all containers tightly stoppered.

2.2 Syntheses

Syntheses at 100° and below were carried out in 250 ml. screw top polypropylene bottles (M.S.E. Ltd.). These were placed on rapidly rotating plates in an electrically heated air oven. The temperature was maintained to within ± 1° by a thermostatic device and a stabilized source of electricity. Syntheses above 100° were carried out in stainless steel autoclaves of about 16 ml. capacity, also rotated in the air ovens.

A known weight of solution of the desired composition was placed in the reaction container. To this were added known weights of the solid components (metakaolinite and silica). The container was quickly sealed. The autoclaves were placed in the oven which had been pre-heated to the synthesis temperature. It was found necessary to warm the polypropylene bottles while stationary to approximately 60° before sealing the screw caps. This ensured no leakage during the rotation.

The reaction products were removed from their solutions by filtration on No. 4 porosity sintered glass filters. They were then washed with a standard quantity of water (1 l. per 50 mls. of synthesis solution) then by alcohol.

All products were dried at 105° for 12 hours and then rehydrated over saturated calcium nitrate at 20° (relative humidity (R.H.) 56%) before they were examined.

2.3 Characterization of the Products

Samples of products were suspended in water and dried out on a microscope slide to be optically examined with a Leitz IIIc polarizing microscope. Many of the species crystallized were too small for optical examination. Some of these were examined on a Philips 100 desk model electron microscope with the help of Dr. I.S. Kerr of this Department or on a Cambridge Steroscan electron microscope with the help of Mrs. Culpitt of the Metallurgy Department.

All products from the synthesis runs were examined by X-ray diffraction. The Nonius Guinier-de Wolff cameras, which were used with quartz monochromators, were mounted on a Philips PW 1008/80 X-ray generator. The X-ray generator was operated at 40 KV and 13 mA with exposure times of between 1 and 1.5 hours. The diffraction pattern of each product was identified either by a visual comparison with those from a library of X-ray photographs of natural and synthetic minerals built up in this Department or by measurement of

the d-spacings directly with a perspex ruler (supplied by Solus-Scholl). The precise determinations of the d-spacings and the indexing procedures used after these initial investigations were those of Section 1.3

Having an indication of the nature of the product, that is the number of phases present, degree of crystallinity and approximate yield, the thermal dehydration was examined. The equilibrated samples (56% R.H.) were placed on a Stanton Thermobalance with a heating rate of 8°/min. This procedure was usually repeated twice. Initially the weight loss to 1000° C was measured and the resulting product kept for examination by X-ray diffraction. Then a new sample was heated only until the dehydration was complete, a specimen was taken for X-ray analysis and the remainder was rehydrated under the initial conditions. The water content of this second sample was again measured after about 1 week, if the X-ray analysis showed that it had remained crystalline.

Products were also examined by differential thermal analysis using a Du Pont 900 Thermoanalyser. The reference material used was Al_2O_3. Differential thermal analysis gave a more precise indication of the temperature range over which dehydration occurred than thermogravimetric analysis and also indicated the temperature at which the crystals were destroyed either by recrystallization or by glass formation.

Some of the products were examined by continuous X-ray diffraction while they were heated. For this a Nonius Lenné-Guinier camera was used. This was operated by Miss R.S. Osborne of the University of London X-ray Service.

Products that were stable on dehydration were examined for their ability to sorb other molecules. A standard volumetric apparatus (shown in Figure 2.3.1) was used for the determination of sorption isotherms for the gases oxygen, n-butane, and iso-butane. The operating procedure has been adequately described previously, for example Young and Crowell. The sorption of cyclohexane at a particular pressure was measured on a modified McBain-Bakr sorption balance.

Zeolites were ion-exchanged by allowing them to come to equilibrium with excess 2N metal chloride solutions. These were rotated at 80° in air ovens. The solution was changed after 1 day and the procedure repeated. The zeolite was washed with distilled water until free of chloride, washed with alcohol, dried at 105°, and finally equilibrated at 56% R.H.

Chemical analyses of zeolites were carried out on samples of known water content. The silica and alumina contents were measured by the standard methods (Vogel). Silica was determined as SiO_2 and alumina as aluminium 8-hydroxyquinolate.

Figure 2.3.1

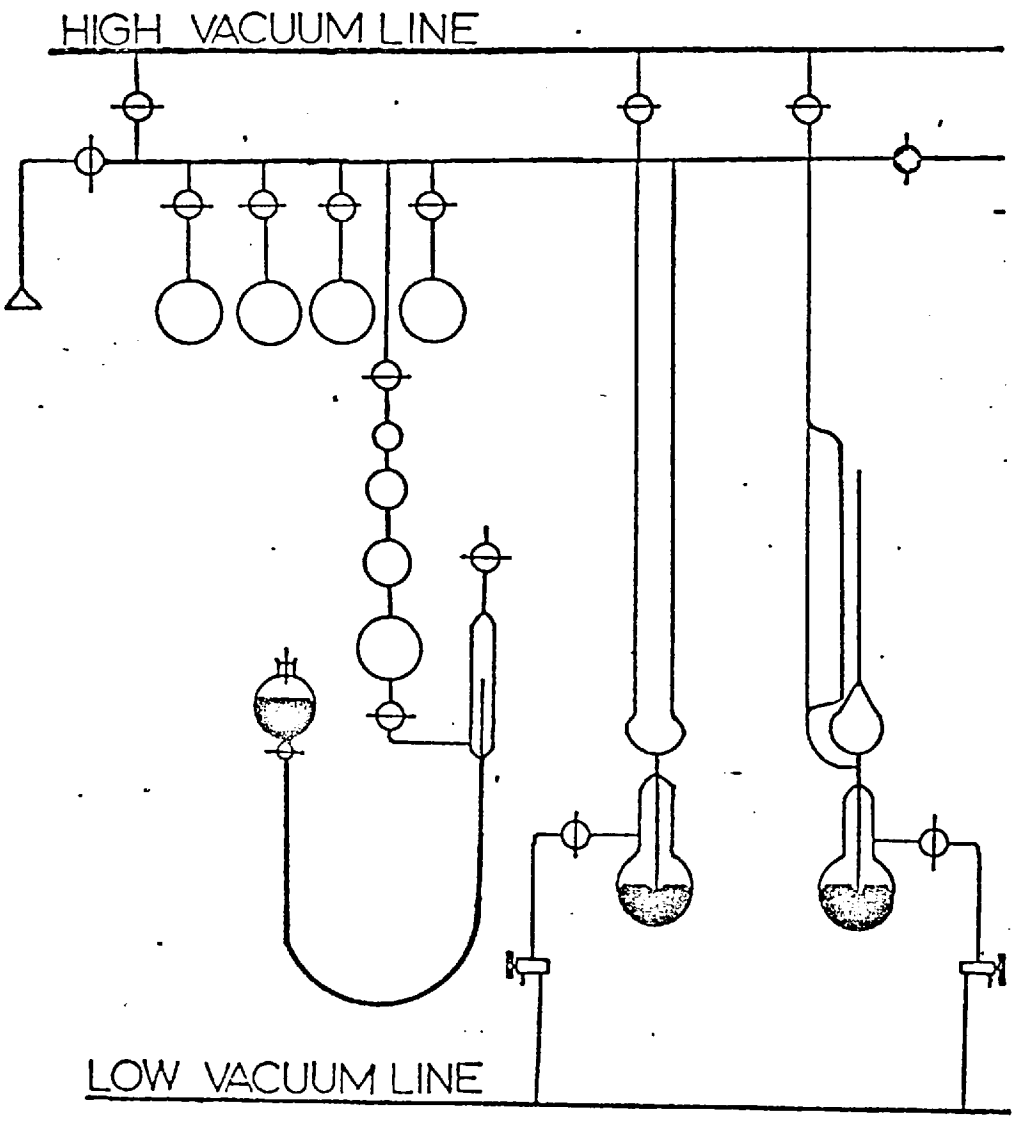

The alkali metal ions Na, K and Li were measured by flame photometry, using the Unicam SP 90 dual absorption-emission instrument. Barium was measured by atomic absorption photometry, using the same instrument. The preparation of the samples was as follows.

Approximately 0.2 g of sample was accurately weighed out into a platinum dish. This was treated with 5 ml. 10% H_2SO_4, and 40 ml. concentrated hydrofluoric acid (for barium 3 ml. of 70% perchloric acid was substituted for the sulphuric acid). The mixture was evaporated to dryness over a steam bath, and the procedure repeated. The resulting solid residue was dissolved in 5 ml. concentrated HCl and water by heating on a steam bath for half an hour. The clear solution was cooled and made up to 250 ml. in a volumetric flask with distilled water. This solution was then diluted to a suitable concentration for analysis on the flame photometer.

Powder X-ray diffraction intensities were used to quantitatively analyse a two component mixture. The method used, as described by Nuffield, consisted of the following procedure. A series of reference mixtures were prepared in which the weight fraction of a standard (zinc oxide) was kept constant, the weight fractions of the two components to be measured varied from 0 to 100% and a diluent

(metakaolinite) was added to bring the weights of the mixtures to the same total. To the samples of the mixtures to be analysed the same weight fraction of the standard was added. X-ray diffraction patterns were obtained for all the samples under identical conditions, and the intensities of the selected reflections of the two components in question and the standard were measured with a Hilger and Watts micro-densitometer. The intensity ratios for the reference samples were plotted against composition to give calibration curves. The weight fraction of each component was read from the respective calibration curve.

SECTION 3.1 THE SYSTEM METAKAOLINITE-K_2O-SiO_2-H_2O

3.1.1 Reactions in the System

The method of synthesis has been previously described in Section 2.2 where it was noted that contact between the metal hydroxide solutions and air was kept to a minimum. In Section 1.2 the criteria for the choice of the limits of the crystallization fields and the conditions employed were discussed. The overall objective was the preparation of zeolitic products which were free from contamination by gels and unreacted materials. In each of the syntheses carried out 0.005 moles of metakaolinite was reacted with a fixed weight of potassium hydroxide solution of known molality.

The silica to alumina ratio of the synthesis mix was increased beyond that of metakaolinite ($SiO_2:Al_2O_3=2$) by the addition of amorphous dry silica. Preliminary experiments showed that this method of silica addition led to the same product as obtained from different silica

sources (e.g. Syton 2X) but the crystallinity as shown by X-ray diffraction was increased. The influence of the nature of the starting material on zeolite formation has been discussed in the introductory chapter.

3.1.2 The Reaction of Metakaolinite with Potassium Hydroxide

Some of the reactions of metakaolinite with potassium hydroxide are given in Tables 3.1.1-3.1.3 as representative of the experiments carried out and the products formed. The approximate crystallization fields have been plotted in Figure 3.1.1.

Abbreviations used in the Description of Products

v. - very	cr. - crystallinity
gd. - good	yd. - yield
md. - moderate	tr. - trace
pr. - poor	Am. - amorphous
lo. - low	

Crystalline Products Formed

Short Reference	Zeolite Formula[+]	Oxide Composition	Description
K-G[*]	(K)-G_r(2.1-4.5) [Cha]	K_2O, Al_2O_3, $nSiO_2$, H_2O	chabazite-like phase
K-I	(K)-I_h(2) [ ]	K_2O, Al_2O_3, $2SiO_2$, H_2O	synthetic zeolite
K-F	(K)-F(2.0) [ ]	K_2O, Al_2O_3, $2SiO_2$, H_2O	synthetic zeolite
K-M	(K)-M_o(4.0) [Phi]	K_2O, Al_2O_3, $4SiO_2$, H_2O	phillipsite-like phase
K-L	(K)-L_h(5.0) [L]	K_2O, Al_2O_3, $5SiO_2$, H_2O	synthetic zeolite
K-Z	{KOH}(K)-Z (2.0) [ ]	K_2O, Al_2O_3, $2SiO_2$, H_2O, KOH	synthetic basic zeolite
K-D	-	K_2O, Al_2O_3, $2SiO_2$	synthetic kaliophilite
K-N	-	K_2O, Al_2O_3, $2SiO_2$	synthetic kalsitite

* K-G1 to K-G5 refer to the series of near chabazites increasing in silica content from K-G1 to K-G5

+ The zeolite formula is defined and discussed in Section 1.1 and appendix 1.

Table 3.1.1

Some typical syntheses, conditions and products in the system metakaolinite-SiO_2-KOH-H_2O. The general reaction compositions were: 1 metakaolinite ($Al_2O_3 2SiO_2$)+2.81-233K_2O + ~275H_2O rotated at 80° for 7 days.

Run No.	Concentration of Alkali	Product	Description
1-8	(0.5)	Am	unchanged metakaolin
1-30	(0.5) (14 days)	Am	" "
1-9	(1.0)	KG1	gd.cr./gd.yd.
1-11	(3.0)	KG1	gd.cr./md.yd.
1-14	(4.0)	KG1+KF	md.cr.
1-15	(5.0)	KF	md.cr./gd.yd.
1-18	(10.0)	KF	md.cr./md.yd.
1-21	(15.0)	KF	md.cr./md.yd.
1-22	(17.0)	KD	md.cr./lo.yd.
1-24	(28.0)	KD	md.cr./lo.yd.
1-28	(32.0)	KZ	gd.cr./v.lo.yd.

Table 3.1.2

1 metakaolinite ($Al_2O_3 2SiO_2$) + 2.6 - $7K_2O$ + ~$275H_2O$

rotated at 110° for 7 days

Run No.	Concentration of Alkali	Product	Description
1-32	0.5	KG1	pr.cr./lo.yd.
1-33	1.0	KG1	md.cr.
1-34	2.0	KG1	md.cr.
1-35	3.0	KF	gd.cr.
1-36	5.0	KF	gd.cr./gd.yd.
1-37	7.0	KF	gd.cr./md.yd.
1-39	8.0	KD	gd.cr./lo.yd.
1-42	12.0	KD	gd.cr./lo.yd.

Table 3.1.3

1 metakaolinite ($Al_2O_3,2SiO_2$) + 1.40 - $7K_2O$ + ~$275H_2O$

stationary at elevated temperatures, 3½ days

Run No.	Concentration of Alkali	Product	Description
1-45	0.25 (170°)	KI	pr.cr.
1-46	0.50 (170°)	KF	md.cr.
1-47	1.0 (170°)	KD	v.gd.cr.
1-48	1.4 (170°)	KD	v.gd.cr.
1-49	2.0 (170°)	KD + KN	md.cr.
1-50	4.0 (170°)	KD + KN	md.cr.
1-51	7.0 (170°)	KD	md.cr.
1-52	12.0 (170°)	KD	br.cr.
1-55	0.4 (250°)	KD	v.gd.cr.
1-56	0.8 (250°)	KN	v.gd.cr.
1-57	1.6 (250°)	KD	gd.cr.
1-59	3.0 (250°)	KD	md.cr.
1-60	0.6 (370°)	KN	v.gd.cr.

Figure 3.1.1

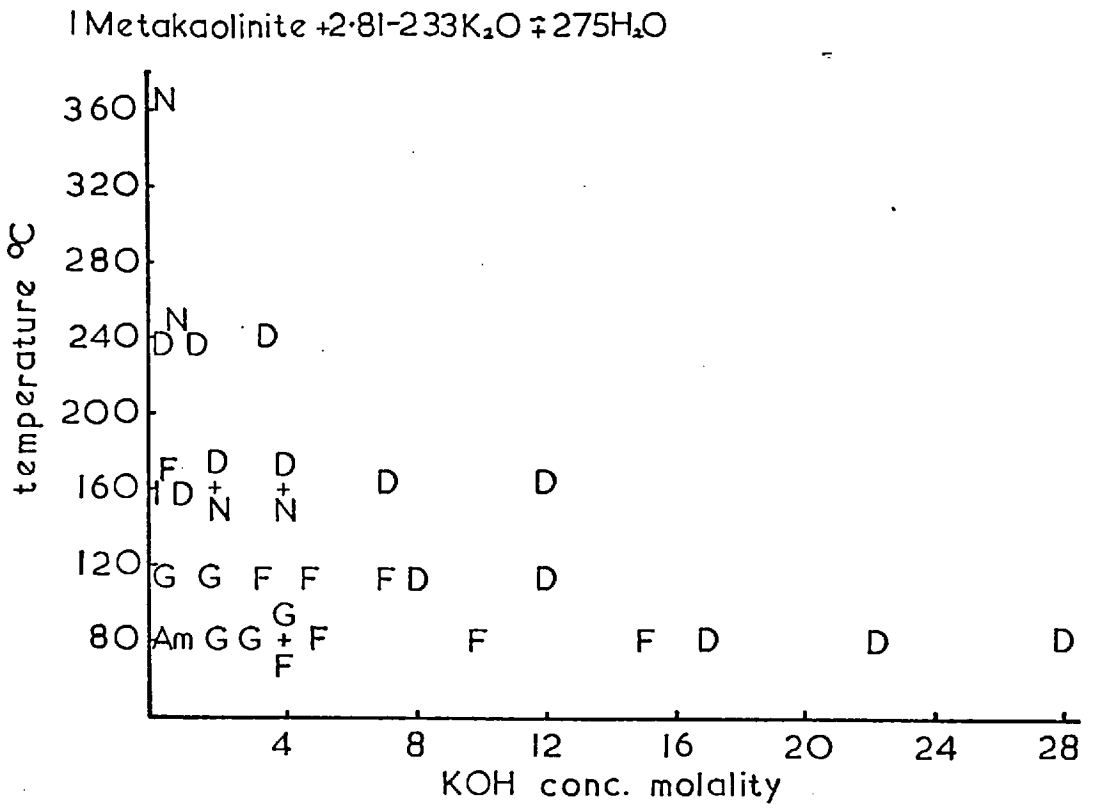

The effect of increasing the alkali concentration is to produce species which become less zeolitic. For example, in moving from 1 to 24 molal solutions of KOH at 80° there is a corresponding movement from the zeolites such as K-G and K-F to unhydrated phases such as K-D.

With the increase of temperature at constant alkalinity there is a similar movement to unhydrated phases. For example at 6 molal KOH a change from K-F to K-D is produced from a rise in temperature of 50°. Synthesis carried out at increased temperatures above 80° allows zeolite crystallizations to occur at lower concentrations of alkali. This may be a kinetic effect and is discussed further in subsequent sections.

Further characteristics of the crystallization in the system metakaolinite-SiO_2-KOH-H_2O are examined in a series of experiments described in Section 3.1.10.

3.1.3 The Reactions of Metakaolinite with Silica and Potassium Hydroxide

Some of the syntheses are recorded in the following Tables 3.1.4 - 3.1.7 along with a description of the resulting products. By the addition of silica it was possible not only to increase the number of phases that could be produced from metakaolinite but also to produce silica rich varieties of some products previously made.

Table 3.1.4

The general reaction compositions were:

1 metakaolinite (Al_2O_3, $2SiO_2$) + $2SiO_2$ + 2.8 - $233K_2O$ +~$275H_2O$

rotated at 80° for 7 days.

Run No.	Concentration of Alkali (molality)	Product	Description
1-63	0.5	Am	-
1-82	0.5 (14 days)	K-G3	pr.cr.
1-64	1.0	K-G3	md.cr.,gd.yd.
1-65	1.5	K-G3	gd.cr.
1-66	2.0	K-G2	md.cr.
1-69	3.0	K-G1	md.cr.
1-70	4.0	K-G1+K-F	Gmd.cr.,Klo.yd.
1-71	6.0	K-F	md.cr.
1-72	8.0	K-F	gd.cr.
1-74	10.0	K-F	gd.cr.
1-75	11.0	K-F	gd.cr.
1-76	12.0	K-F	gd.cr.
1-77	14.0	K-F+K-D	Fgd.cr.,Dmd.cr.
1-79	16.0	K-D	gd.cr.
1-80	18.0	K-D	gd.cr.

Table 3.1.5

1 metakaolinite + $2SiO_2$ + 2.8 - $7.0K_2O$ + $\sim 275H_2O$

rotated at higher temperatures for 7 days.

Run No.	Concentration of Alkali (molality)	Product	Description
1-84	0.3 (110°)	KG4	md.cr.
1-85	0.5 (110°)	KG3	md.cr.
1-86	1.0 (110°)	KG2	md.cr.
1-87	2.0 (110°)	KG1	gd.cr.
1-88	3.0 (110°)	KG+KF	Ggd.cr.,Fmd.cr.
1-89	5.0 (110°)	KD	gd.cr.
1-90	6.0 (110°)	KD	gd.cr.
1-91	7.0 (110°)	KD	gd.cr.
1-92	9.0 (110°)	KD	gd.cr.
1-96	0.5 (140°)	KM	md.cr.
1-97	1.0 (140°)	KM	md.cr.
1-98	2.0 (140°)	KD	gd.cr.
1-101	0.5 (170°)	KM	gd.cr.
1-102	1.0 (170°)	KM	v.gd.cr.
1-103	2.0 (170°)	KD+KN	Dgd.cr.,Ngd.cr.
1-104	3.0 (170°)	KN	v.gd.cr.

Figure 3.1.2 1 Metakaolinite $+2SiO_2+2{\cdot}8-233K_2O\mp275H_2O$

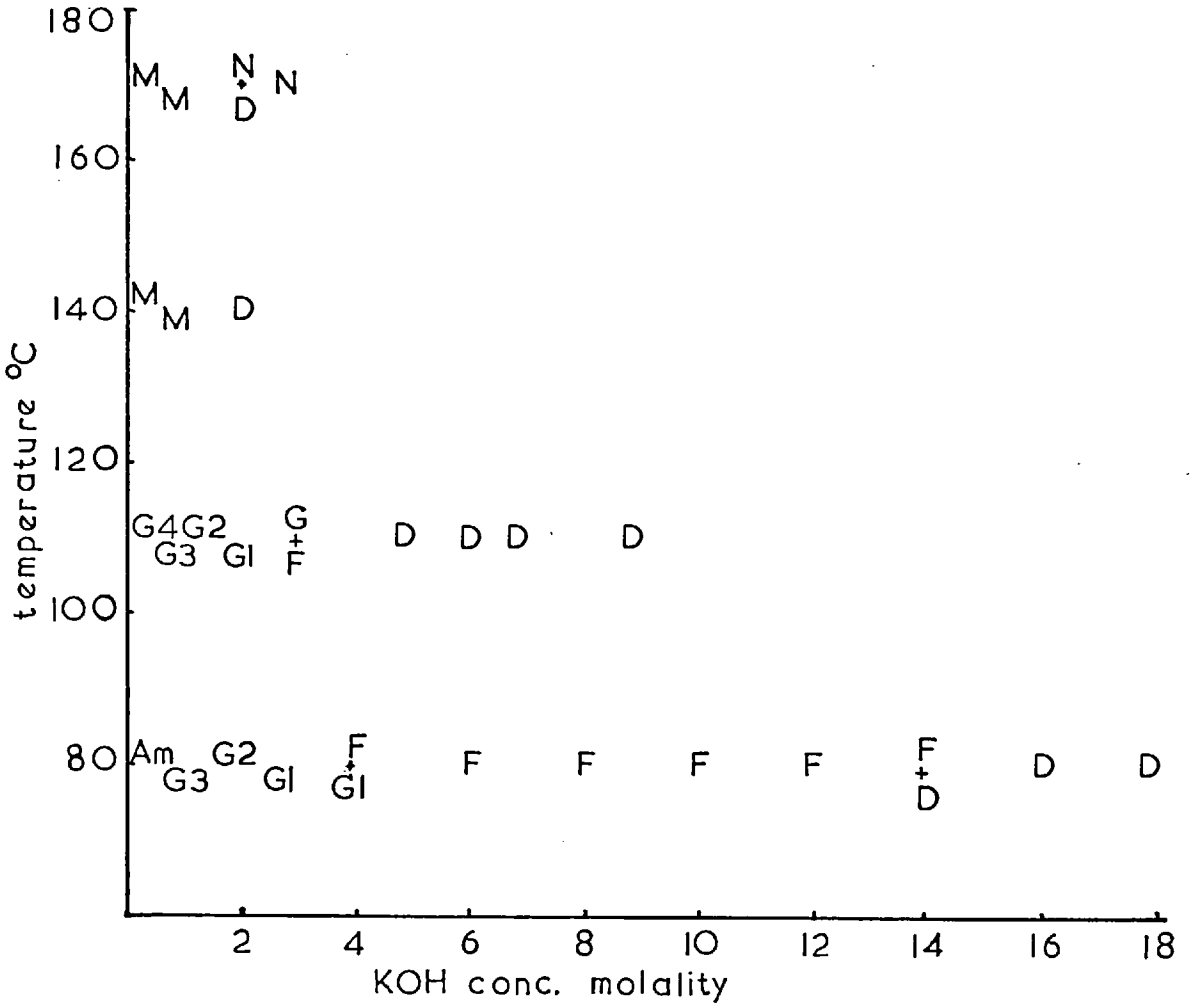

Table 3.1.6

1 metakaolinite + 4 SiO_2 + 2.8 - 233 K_2O + ~275 H_2O

rotated at 80° for 7 days.

Run No.	Concentration of Alkali (molality)	Product	Description
1-110	0.5	KM+KG	Mmd.cr.,Ggd.cr.
1-111	1.0	KG5	gd.cr.
1-112	2.0	KG4	md.cr.
1-113	3.0	KG2	md.cr.
1-115	4.5	KG1+KF	Gmd.cr.,Fmd.cr.
1-116	5.0	KF	Fmd.cr.
1-117	7.0	KF	Fmd.cr.
1-118	10.0	KF	Fpr.cr.
1-120	14.0	KD	gd.cr.
1-121	18.0	KD	gd.cr.
1-124	21.0	KD	gd.cr.
1-128	0.25	Am	-
1-129	0.25 (14 days)	Am	-
1-130	0.5 (14 days)	KM+KG	Mmd.cr.,Gmd.cr.
1-131	1.0 (14 days)	KG5	gd.cr.

1 metakaolinite + 4 SiO_2 + 1.4 - 7.0 K_2O + 275 H_2O

rotated at elevated temperatures for 7 days.

Run No.	Concentration of Alkali (molality)	Product	Description
1-165	0.5 (110°)	KG5	gd.cr.
1-166	1.0 (110°)	KM	v.gd.cr.
1-167	3.0 (110°)	KM	v.gd.cr.
1-169	5.0 (110°)	KF	v.gd.cr.
1-170	7.0 (110°)	KD	md.cr.
1-172	9.0 (110°)	KF+KD	gd.cr.
1-185	0.5 (170°)	KM	v.gd.cr./lo.yd.
1-186	1.0 (170°)	KM	md.cr.
1-187	2.0 (170°)	KN+KD	gd.cr./md.yd.
1-188	3.0 (170°)	KN+KD	gd.cr./md.yd.

Figure 3.13 1Metakaolinite + $4SiO_2$ + 2·8-233K_2O ∓ 275H_2O

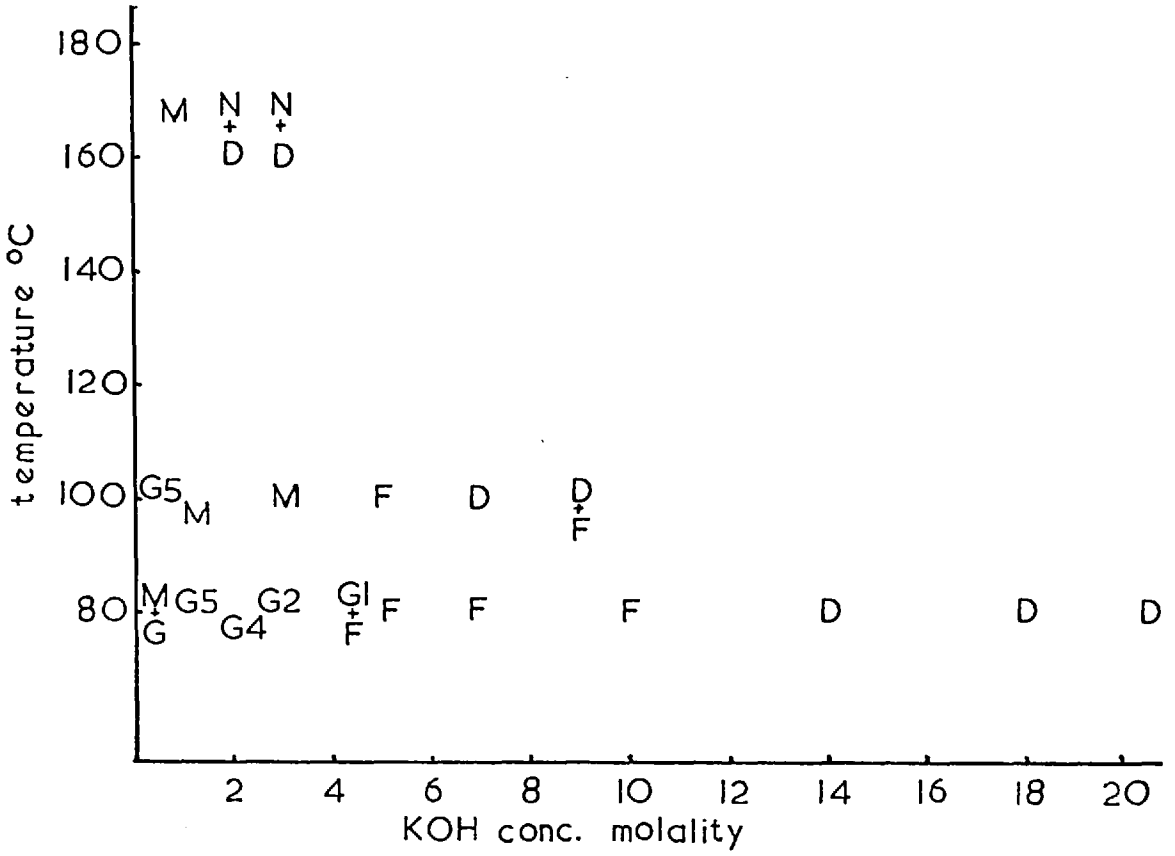

Table 3.1.7

1 metakaolinite + 8 SiO_2 + 2.8 - 233 K_2O + ~275 H_2O rotated at 80° for 7 days.

Run No.	Concentration of Alkali (molality)	Product	Description
1-140	0.5	Am	-
1-141	0.5 (14 days)	KL	pr.cr.
1-142	1.0	KM	md.cr.
1-143	2.0	KM+KG	Mmd.cr.,Gmd.cr.
1-144	3.0	KG	md.cr.
1-145	5.0	KG+KF	Gmd.cr.,Fmd.cr.
1-147	10.0	KD	md.cr.
1-148	15.0	KD	gd.cr.
1-151	20.0	Am	-
1-152	1.0 (14 days)	KM	md.cr.
1-155	20.0 (14 days)	Am	-

1 metakaolinite + 8 SiO_2 + 1.4 - 7.0 K_2O + 275 H_2O

rotated at elevated temperatures for 7 days.

Run No.	Concentration of Alkali (molality)		Product	Description
1-175	0.5	(110°)	KM+KG	Mmd.cr.,Gmd.cr.
1-176	1.0	(110°)	KG5	gd.cr.
1-177	3.0	(110°)	KM	gd.cr.
1-178	5.0	(110°)	KF	gd.cr.
1-179	7.0	(110°)	KD	gd.cr.
1-182	0.5	(140°)	KG2	gd.cr.
1-183	2.0	(140°)	KF	v.gd.cr.
1-184	4.0	(140°)	KD	gd.cr.
1-190	0.5	(170°)	KD	gd.cr.
1-191	1.0	(170°)	KD	v.gd.cr.
1-192	2.0	(170°)	KD+KN	Dgd.cr.,Nlo.yd.
1-193	3.0	(170°)	KD+KN	Dgd.cr.,Ngd.cr.

Figure 3.1.4 1 Metakaolinite +8SiO_2 +1·4-7K_2O ∓275H_2O

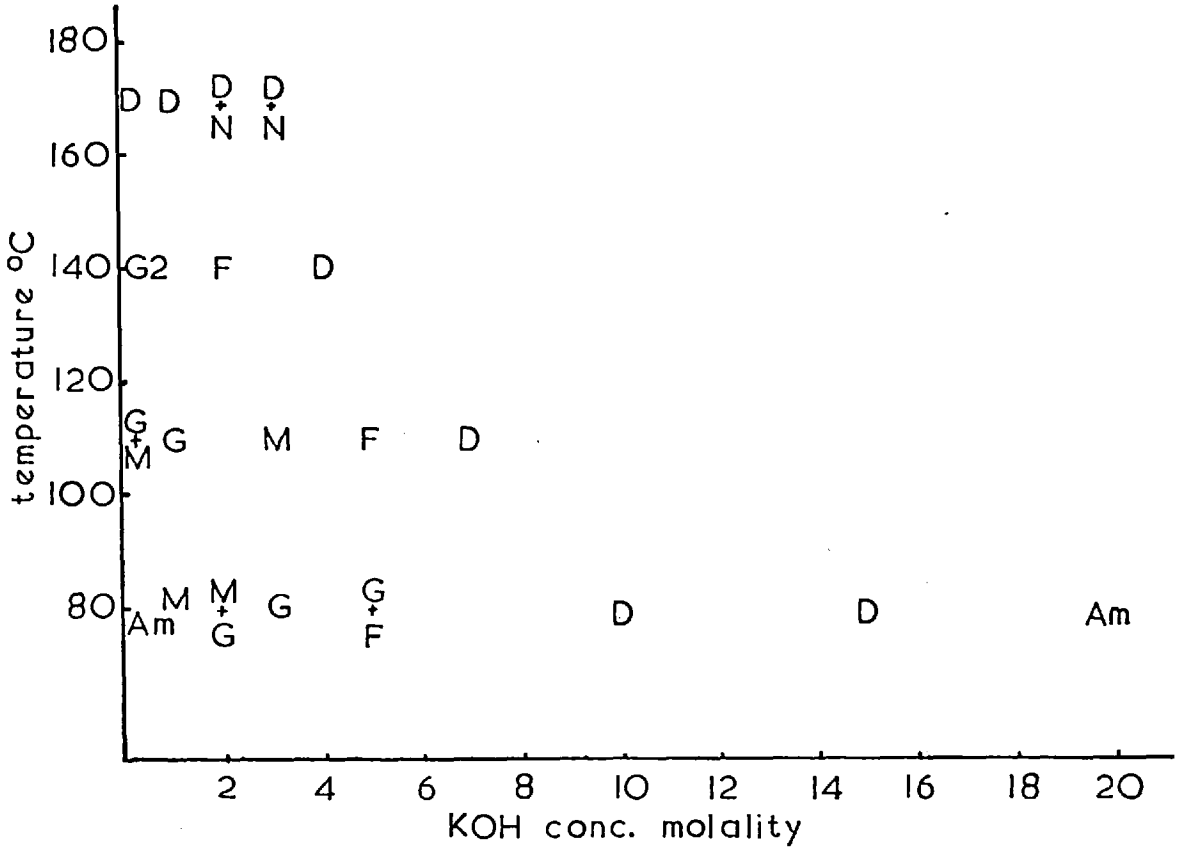

3.1.4 The Products of the Potassium Crystallization Fields

3.1.5 The Species K-G

These species formed a series of related hydrated products that crystallized consistently from reaction mixtures with silica to alumina ratios from 2:1 to 10:1. The temperature range over which they formed was 80° to 140°. These products were found by Barrer and Baynham (1956a) to be a series of near chabazites, the most siliceous member being the closest analogue to natural chabazite. It was found possible not only to produce the complete series of near chabazites but also to extend it both to higher and lower silica contents. Five samples of various silica to alumina ratios were prepared. Their chemical analysis gave the following composition in weight per cent and molar ratio respectively.

Table 3.1.8

Sample	$\%K_2O$	$\%Al_2O_3$	$\%SiO_2$	$\%H_2O^+$	Molar Composition
K-G1	25.5	27.7	34.7	12.2	K_2O, Al_2O_3, $2.13SiO_2$, $2.5H_2O$
K-G2	23.8*	25.8	37.9	12.8	K_2O, Al_2O_3, $2.50SiO_2$, $2.8H_2O$
K-G3	23.4*	25.2	39.0	13.2	K_2O, Al_2O_3, $2.67SiO_2$, $3.0H_2O$
K-G4	20.5*	22.3	39.4	15.7	K_2O, Al_2O_3, $3.00SiO_2$, $4.0H_2O$
K-G5	17.2	18.8	49.5	15.2	K_2O, Al_2O_3, $4.51SiO_2$, $4.5H_2O$

* determined by maintaining $K_2O:Al_2O_3 = 1$

\+ samples equilibrated at R.H. = 56%

A comparison of the compositional series of K-G with that obtained from gels illustrates the relative positions of the new products.

Products from Gels (Barrer and Baynham 1956a)		Products from Metakaolinite
		K-G1 $K_2O, Al_2O_3, 2.13SiO_2, 2.5H_2O$
$K_2O, Al_2O_3, 2.30SiO_2, 3.4H_2O$		
$K_2O, Al_2O_3, 2.56SiO_2, 2.62H_2O$		K-G2 $K_2O, Al_2O_3, 2.50SiO_2, 2.8H_2O$
$K_2O, Al_2O_3, 2.65SiO_2, 3.72H_2O$		K-G3 $K_2O, Al_2O_3, 2.67SiO_2, 3.0H_2O$
$K_2O, Al_2O_3, 2.71SiO_2, 3.94H_2O$		
		K-G4 $K_2O, Al_2O_3, 3.00SiO_2, 4.0H_2O$
$K_2O, Al_2O_3, 3.91SiO_2, 4.63H_2O$		
$K_2O, Al_2O_3, 4.15SiO_2, 4.38H_2O$		
		K-G5 $K_2O, Al_2O_3, 4.51SiO_2, 4.5H_2O$

The products were comparable with those of Barrer and Baynham in both analysis and X-ray diffraction patterns. In Section 3.1.10 the position of members of the series in the crystallization field and their composition relative to the growth conditions are examined. Finally, in Section 4. their formation is compared with the composition and conditions of natural chabazite occurrences. The new end members K-G1 and K-G5 are examined in more detail and their diffraction patterns recorded in Table 3.1.11. Both natural chabazite and two previous synthetic products are included for comparison.

The indexing of species K-G1 is considered in Section 3.6.10. During the reactions with mixed hydroxides the product G-1 crystallized in the sodium-potassium crystallization field with a very high degree of crystallinity. The diffraction pattern had all diffuse lines of K-G1 replaced by sharp lines. This product was examined and indexed and will be compared to the original K-G1 in that section.

Barrer, Cole and Sticher (1968) made K-G1 from kaolinite by reacting it with potassium hydroxide but no comparison can be made as their product was always mixed with the synthetic zeolite K-I.

Species K-G5 was crystallographically measured and the diffraction lines corrected using lead nitrate as an internal standard. The hexagonal unit cell had dimensions a=13.78±.01 and c=15.35±.03 Å. The diffraction pattern is compatible with the space group of natural chabazite, R$\bar{3}$m. The lattice dimensions could not be determined to a greater degree of accuracy due to the line width of the diffraction pattern. The broad diffraction lines were probably due to the small particle size. This was indicated by the

whole pattern having the same line width, unlike K-G1 where specific lines only were diffuse. This probably did not indicate poor crystallinity or low yield as very high sorption capacities were found for the K-G5 samples.

In Table 3.1.12 the unit cell parameters are compared with other parameters of synthetic chabazites and the natural counterparts chabazite and herschelite.

The least siliceous member of the series was thermally the least stable. In Figure 3.1.5 the T.G.A. and D.T.A. curves are shown for K-G1. The weight loss curve corresponds, for the most part, to the initial portion of the large endotherm shown in the D.T.A. trace. This endotherm is also produced by lattice collapse in the region 300-350°, as shown in a separate experiment where samples of K-G1 were removed from the thermobalance at 50° temperature intervals and examined by X-ray diffraction. These results are in agreement with those of Barrer and Langley (1958) who examined both the synthetic series of near-chabazites and natural chabazite.

The ignition product of K-G1 was kaliophilite. Recrystallization of the amorphous phase produced by the lattice collapse of K-G1 occurred at approximately 1000° C.

Figure 3.1.5

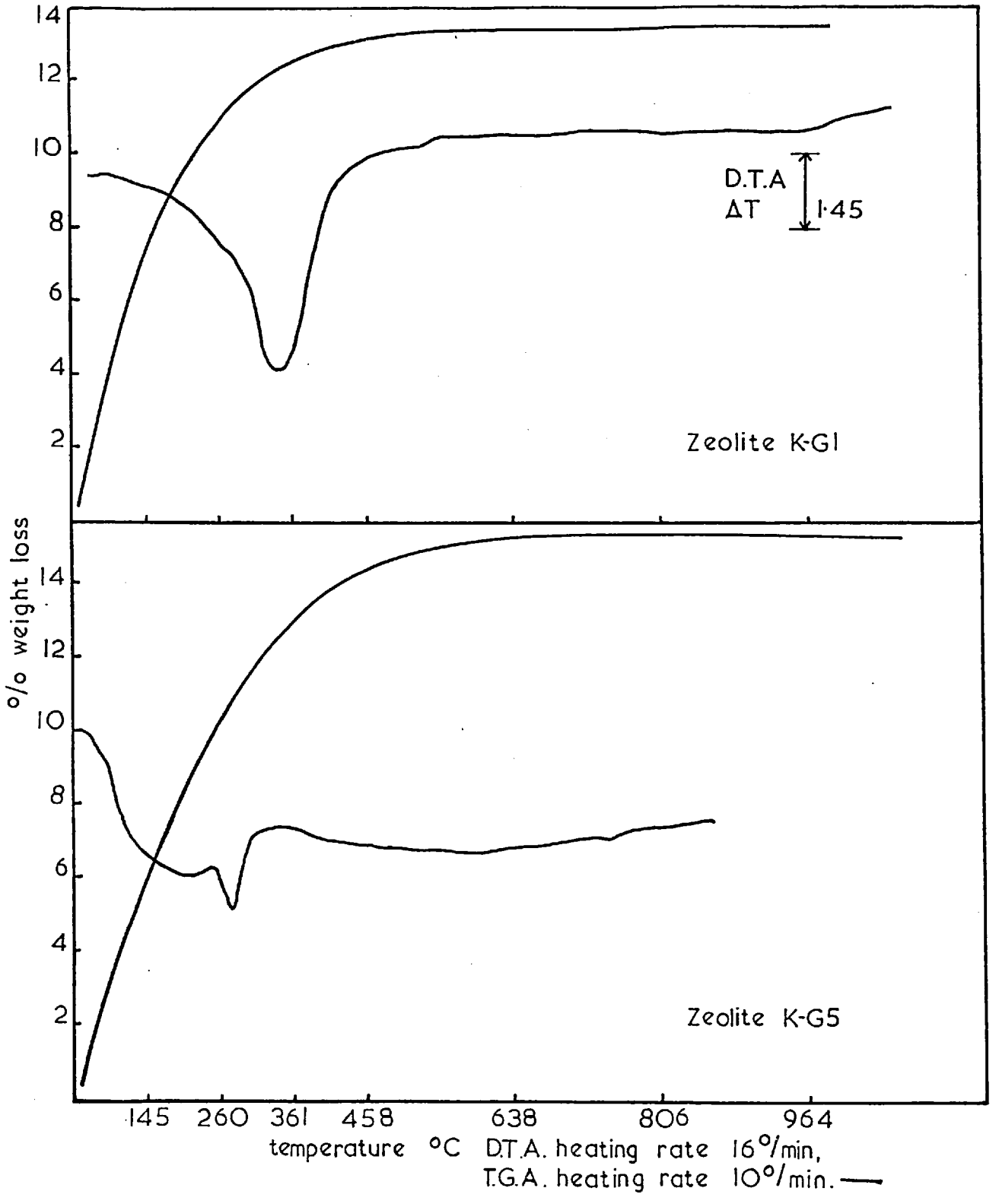
14
12
10
8
6
4
2
D.T.A
ΔT
1·45
Zeolite K-G1
% weight loss
14
12
10
8
6
4
2
Zeolite K-G5
145
260
361
458
638
806
964
temperature °C D.T.A. heating rate 16°/min,
T.G.A. heating rate 10°/min.

The potassium form of K-G1 was outgassed at 280° under vacuum and tested for oxygen sorption. No oxygen was sorbed at 78°K. A sample of K-G1 was extracted in a Soxhlet apparatus to determine whether its inability to sorb oxygen was due to impurities imbibed during crystallization. A loss in crystallinity resulted probably due to the instability of this aluminous form of K-G.

The lattice dimensions varied considerably with cation exchange. This effect was examined in the mixed Na/K synthesised product because of the sharper diffraction pattern. Such behaviour is in contrast to the most siliceous member K-G5 which showed little difference in the diffraction patterns of the ion-exchanged forms.

The water content of K-G1 and K-G5 varied with cation content. The ion-exchanged forms were dried at 200° and then equilibrated at R.H.=56%.

Thermogravimetric analysis gave the following results.

Table 3.1.9

Cationic form	Weight % equivalent to dry K-zeolite	
	K-G1	K-G5
H^+	-	17.9*
Li^+	25.4	26.1
Ca^{++}	24.0	25.5
Ag^+	20.5	20.0
Na^+	17.6	18.2
Ba^{++}	16.0	16.2
K^+	12.5	16.1

An exact comparison with the values for the species reported by Barrer and Baynham (1956) is not possible because their samples were equilibrated in air of unknown relative humidity. However, the same trend exists, demonstrating the increase of water content with polarising power of the cations.

* The hydrogen form, produced by thermal decomposition of the ammonium exchanged form, showed considerable lattice damage when examined by X-ray diffraction.

The kinetics of the growth of K-G1 were followed in a series of experiments extending in time from two hours to seven days. The method used is described below. Both the rate of formation of K-G1 at 80° and the concentration changes of the components, aluminium and silicon, in solution were determined. The results are given in Table 3.1.10.

The rate of conversion to zeolite was followed by plotting the water sorption of samples removed at intervals of time. This is shown in Figure 3.1.5%

As an initial experiment, metakaolinite was placed in a solution identical to that used in the kinetic runs and removed immediately. The metakaolinite was then treated in the same manner as the kinetic samples. The water content of the equilibrated metakaolinite was 0.5%, indicating surface hydration only. Thus the uptake of water in the samples is due almost entirely to species other than residual metakaolinite as yet unchanged at the time of sampling.

Figure 3.1.5a The Crystallization of K-G1

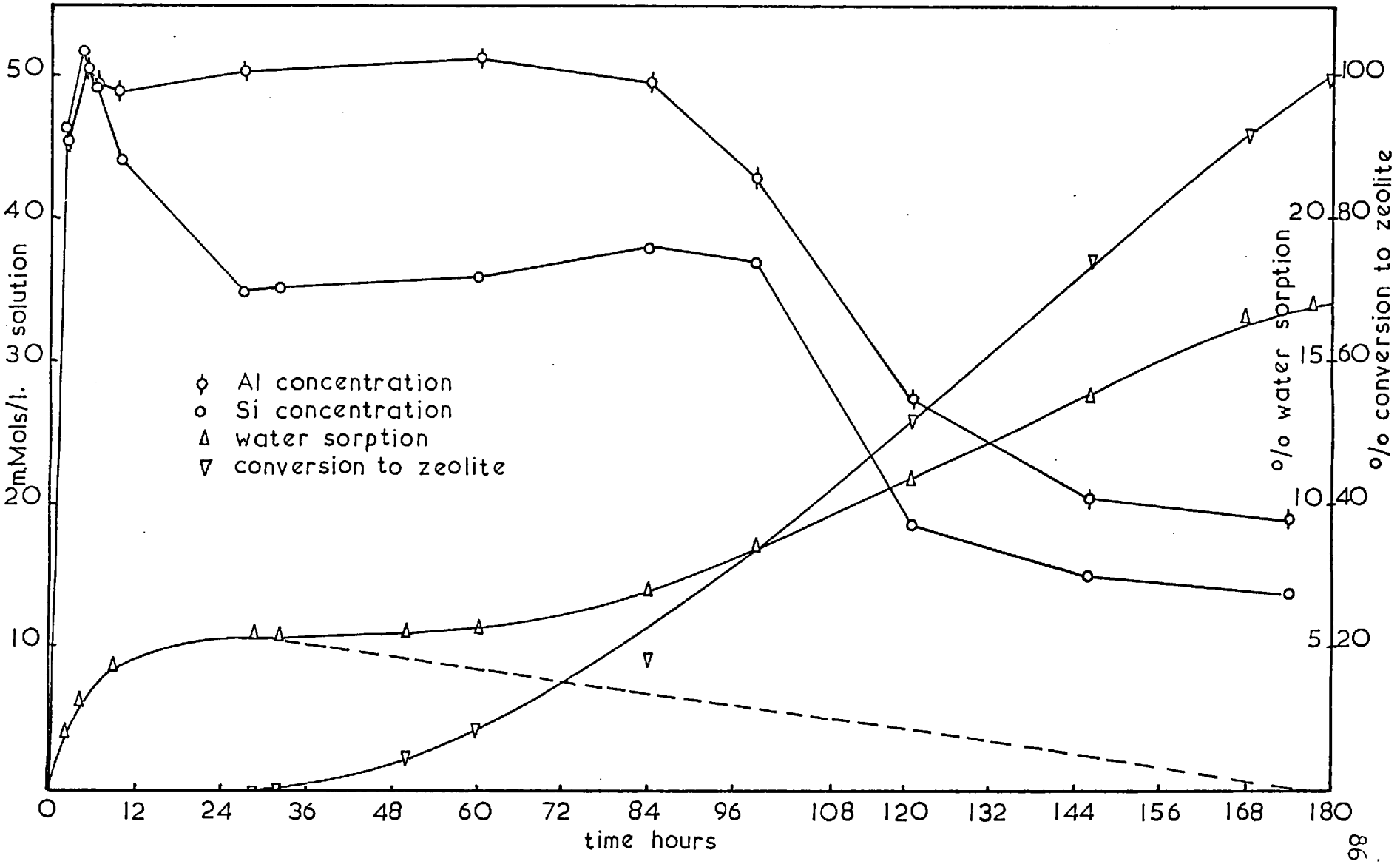

Table 3.1.10

A comparison of the composition of the solution with the rate of formation of zeolite K-G1.

Time hours	Concentration of Al mMols/l.	Concentration of Si mMols/l.	% weight H_2O sorption	% conversion to zeolite	
2	45.3	46.4	2.1	0	
5	50.7	51.8	3.2	0	
7	49.6	49.2	3.5	0	
10	49.1	44.0	4.4	0	1*
27	50.5	35.0	5.5	0	
32	50.5	35.2	5.4	1.2	
50	-	-	5.4	5.4	2*
60	51.5	36.0	5.7	8.9	
84	49.7	37.9	7.0	18.4	
99	42.8	37.1	8.6	34.5	3*
121	27.5	18.6	10.8	51.8	
146	20.6	15.0	13.7	74.4	
168	-	-	16.5	95.2	4*
170	19.1	13.9	16.8	100.0	5*

* Samples of these products were examined by X-ray diffraction; the results were:

1 showed no diffraction lines, only a very broad band

2-5 showed a diffraction pattern characteristic of K-G1 with increasing intensity.

The initial composition of the reacting magmas used in the kinetic runs are shown below per 50 mls of solution as used and per litre of solution for comparison with Figure 3.1.5a respectively.

Component	Composition	mMoles
Al	10	200
$Al_2Si_2O_7$ metakaolinite	5	100
Si	10	200
K	100	2,000
H_2O	2,780	55,600

The appropriate reaction may be represented by

$$Al_2Si_2O_7 + 2KOH \xrightarrow{H_2O} K_2[Al_2Si_2O_8]\,2.5\ H_2O$$

Thus both the alkali and the water were in excess.

The concentrations of aluminium and silicon rapidly reached a maximum of 50 mMoles per litre in four hours. Then followed a period where both the components maintained a constant concentration in solution with the aluminium always in a higher concentration. After 84 hours there was a decrease in both aluminium and silicon concentrations in solution until a constant lower value was reached. This behaviour was very similar to that reported by Sticher and Bach (1969), described in Section 1.2.

The water sorption increased initially to a low value of 5% which was maintained until about 80 hours, after which there began a rapid increase lasting up to 180 hours.

In Section 1.2 the evidence for the existence of gel formation prior to zeolite growth has been reviewed. A possible scheme of the processes involved in the growth of K-G1 from metakaolinite can be proposed in this context.

The rapid increase in aluminium and silicon in solution shows the rate of dissolution of metakaolinite forming a solution which becomes slightly super saturated. This is shown by the small peak values in the component concentrations. There then results a period when an alkali aluminosilicate gel is formed, which is hydrated to about 5%. Zhdanov (1968) has shown that alkali aluminosilicate

gels possess both pore structures and the ability to sorb greater amounts of water than either silica or alumina gels. After a time of approximately 48 hours, the more highly hydrated zeolitic phase appears. This produces the typical (Section 1.2.) sigmoidal curve resulting from autocatalytic growth of the zeolite. The rapid decrease in the component concentrations in solution during zeolite growth is probably due to the depletion of the starting materials.

The solution maintained a low concentration of aluminium and silicon which may be presumed to be in equilibrium at this alkalinity with the zeolite. Barrer, Cole and Sticher (1968) have shown the decrease in yield of a felspathoid-basic sodalite-with increasing alkalinity of solution. This is presumably due to its increased solubility in basic solutions.

Ciric, who studied the kinetics of growth of zeolite A from an amorphous starting material by the water sorption method, obtained the per cent conversion to zeolite in the following way (Ciric 1968). There is initial sorption due to the amorphous aluminosilicate phase and a final limiting value due to the product. The intermediate values were obtained by subtracting from the total sorption diminishing amounts of initial sorption. This procedure was used here

to account for the water uptake of the gel. The difference between successively smaller amounts of initial sorption due to the gel - taken along the dotted line in Figure 3.1.5a and the final limiting value were divided by the final sorption value to find the fraction conversion. This was then plotted as per cent conversion.

The resulting curve showing the conversion of metakaolinite to zeolite K-G1 is sigmoidal with a long initial induction period. The length of the induction period is probably due to:

a) a relatively low temperature of 80°,
b) a less reactive starting material than alkali aluminosilicate gels,
c) the process of gel formation prior to zeolite growth.

The increased concentration of aluminium in solution above that of silicon during the whole period of growth is consistent with the composition of the product K-G1 as shown in Table 3.1.8. Also this indicates that the chabazite grows with a uniform composition. Chemical analysis of the final product would not reveal this. The silicon to aluminium ratio in K-G1 was 1.06 indicating that there is ordering of the silicon and aluminium in the framework. This is possible in the chabazite framework as it possesses no closed rings containing odd numbers of

tetrahedra. These would not be allowed in an ordered structure which obeys Lowenstein's Rule (1954) (Goldsmith 1955). This rule requires that the maximum ratio of tetrahedrally coordinated aluminium and silicon is 1:1. The linkage of two AlO_4 tetrahedra is not permitted.

The most siliceous chabazite was the most thermally stable. The D.T.A. and T.G.A. curves are shown in Figure 3.1.5. The composition may be compared with both natural and synthetic analogues that have been analysed.

siliceous K-G (Barrer and Baynham 1956a)	K_2O, Al_2O_3, 4.15SiO_2, 4.38 H_2O
K-G5	K_2O, Al_2O_3, 4.51 SiO_2, 4.5 H_2O
natural chabazite (Barrer, Davies and Rees 1968)	0.15 Na_2O, 0.83 CaO, Al_2O_3, 4.89 SiO_2, 6.78 H_2O
K^{ex}nat.chabazite (Barrer, Davies and Rees 1968)	0.89 K_2O, 0.04 CaO, Al_2O_3, 5.15 SiO_2, 5.84 H_2O
natural chabazite (Mason 1962)	CaO, Al_2O_3, 4 SiO_2, 6 H_2O
herschelite (Mason 1962)	Na_2O, Al_2O_3, 4 SiO_2, 6 H_2O
*natural chabazite (Gude and Sheppard 1966)	0.19 CaO, 0.19 MgO, 0.84 Na_2O, 0.06 K_2O, 1.2 Al_2O_3, 9.51 SiO_2, 10 H_2O

Table 3.1.11

A comparison of the d-spacings of K-G1, K-G5, natural chabazite* and natural herschelite*.

K-G1		K-G5		chabazite		herschelite	
d	I	d	I	d	I	d	I
						11.89	8
9.56	md	9.39	m	9.35	50	9.36	51
6.89	m	6.96	mw	6.89	10	6.89	22
				6.37	5	6.38	3
5.57	wd	5.57	w	5.55	9	5.55	15
5.26	w	5.10	w			5.127	8
		5.00	m	5.021	30	5.032	40
4.75	wd	4.71	w	4.677	6	4.679	6
4.32	md	4.34	ms	4.324	76	4.500	3
4.17	w			4.044	1	4.322	67
3.96	w	3.96	w	3.976	2	4.109	9
3.90	mw			3.870	28	3.976	8
3.74	wd	3.63	w	3.590	23	3.877	23
3.51	w	3.47	w	3.448	13	3.600	21
3.27	wd	3.25	w	3.235	6	3.448	18
3.23	wd	3.17	w	3.190	5	3.235	11

* Gude and Sheppard (1966)

* This is a silica rich chabazite with a silica to alumina ratio of almost 8:1. The sample is of different origin (Gude 1966) from most chabazites being related to them in the same way as clinoptilolite to heulandite (Mumpton 1960, Mason 1960). The significance of its occurrence with respect both to other natural zeolites and to the sources and synthetic zeolite crystallization is discussed later.

The d-spacings and indexing of K-G5 are shown in Table 3.1.11, where it is compared with natural chabazites and K-G1. The unit cell parameters are listed below for comparison with related species.

Table 3.1.12

	a Å	c Å	Unit cell Vol. Å^3	SiO_2/Al_2O_3
K-G (Barrer and Baynham 1956a)	13.92	15.30		4.15
K-G5	13.78	15.35	2524	4.51
Natural chabazite (Mason 1962)	13.786	15.065	2479.5	
Silica rich chabazite (Gude 1966)	13.712	14.882	2423.1	7.74

Table 3.1.13

Cationic form of K-G5	Oxygen capacity c.c./gm. STP
Li^+	180
Ca^{++}	170
Na^+	109
K^+	9
H^+	100 *
NH_4^+	no sorption

* Lattice breakdown was shown by the diffuse nature of the diffraction pattern.

The hydrogen form was prepared by decomposition of the ammonium exchanged form at 400°. Both the water content and the oxygen sorption capacity decreased, confirming that lattice damage had taken place. Barrer and Baynham (1956b) produced the hydrogen forms of this series up to a silica to alumina ratio 4.15. This sample had a negligible oxygen sorption at -183° indicating that chabazite stability in the hydrogen form begins in the region of $\frac{SiO_2}{Al_2O_3} = 4.5$.

Figure 3.1.6 Sorption of Oxygen at 78°K in Zeolite G No. 5

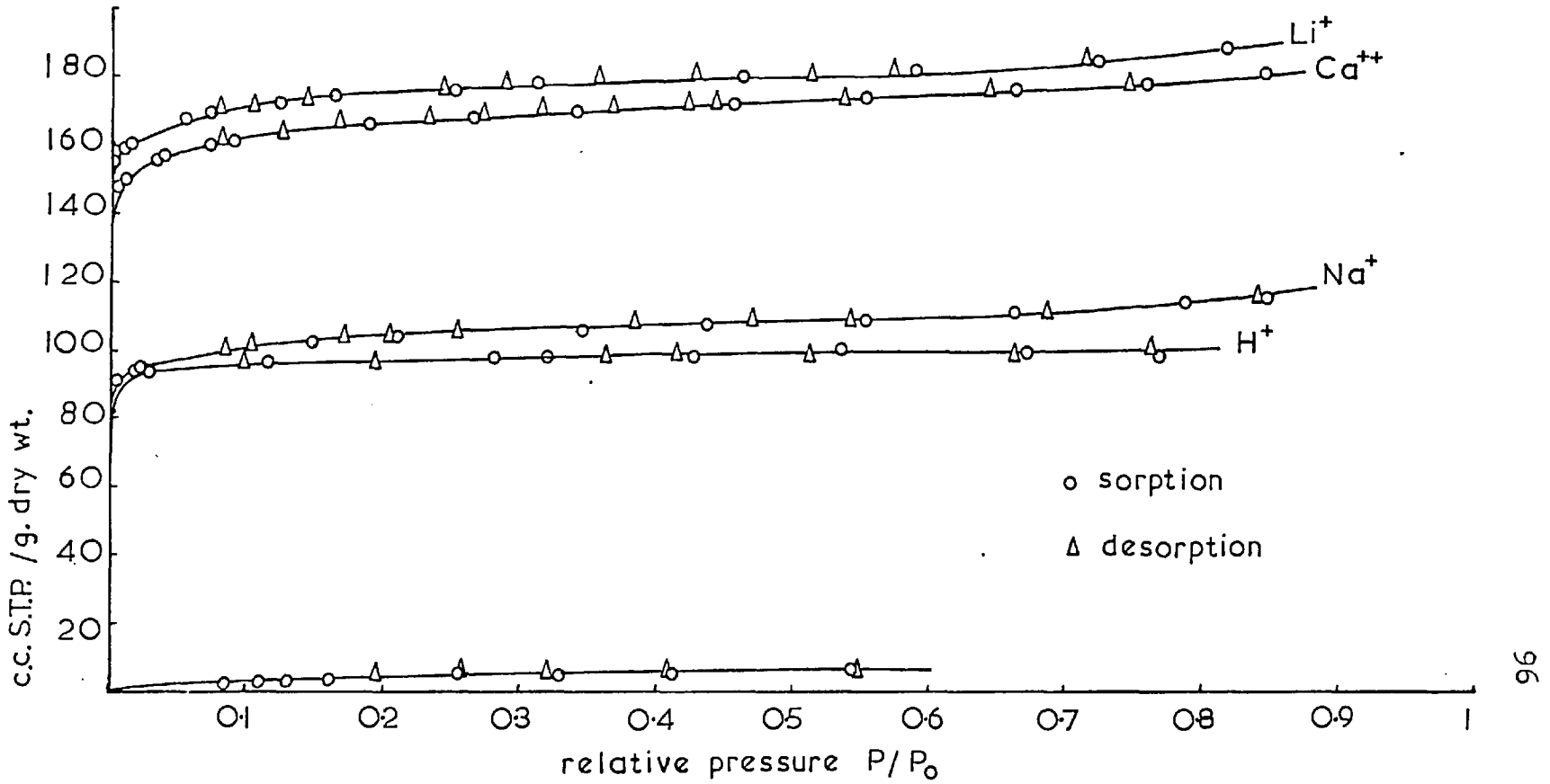

Cation exchange on K-G5 had only a very small effect upon the X-ray diffraction pattern unlike the larger effect shown in Table 3.1. on the more aluminous K-G1. This may be due to the smaller number of cations per unit cell in K-G5.

Cation exchange greatly influenced both the water content, as shown in Table 3.1.9 where this content is compared with that of K-G1, and the sorption capacity for oxygen. The oxygen sorption isotherms of various cationic forms are shown in Figure 3.1.6 and are tabulated in Appendix 2. The saturation capacities of various ion forms of K-G5 for oxygen at 78°K are given in Table 3.1.13 for K-G5 (silica to alumina ratio 4.51). Recently Barrer and Davies (1970) have carried out sorption measurements on the hydrogen form of natural chabazite.

If the decrease in the sorption capacities of the various cationic forms shown in Table 3.1.13 are compared with either the volumes of the unit cells not occupied by cations or the volumes indicated by the water contents, as shown in Table 3.1.9, then it may be seen that sorption capacity depends upon cation position.

The sample K-G5 was able to sorb unbranched paraffins such as n-butane in ion-exchanged forms. It acted as a molecular sieve by excluding larger and branched molecules such as iso-butane. The hydrocarbon isotherms are shown in Figure 3.1.7. and sorption values are tabulated in Appendix 2. The parent K^+ form would not sorb hydrocarbons which is consistent with the very low oxygen sorption. This behaviour is similar to that both of natural chabazite (Barrer 1944a,1953a,Addison 1955, Garden 1955) and of the synthetic chabazites of Barrer and Baynham (1958b).

The structural details of natural chabazite have been established by Smith et al (1958, 1962, 1963). In Figure 1.1.1d the cage-like unit of chabazite is shown. It can be seen that chabazite may either be considered as made up of hexagonal rings linked to form sheets which are then stacked in a layer sequence AABBCC, or as a system of shared chains of tetrahedra as shown in Figure 1.1.1d from which the structure is generated by applying a 3 operator (Villiger 1969).

The structure of chabazite contains cylindrical cavities of approximate dimensions 10 and 6.5 Å with access for molecules through six eight-membered rings. Barrer and Kerr (1959) have reported these to be slightly elliptical with free diameters 4.1 and 3.7 Å respectively.

Figure 3.1.7 The Sorption of n butane at 273°K by Various Cationic Forms of K-G5

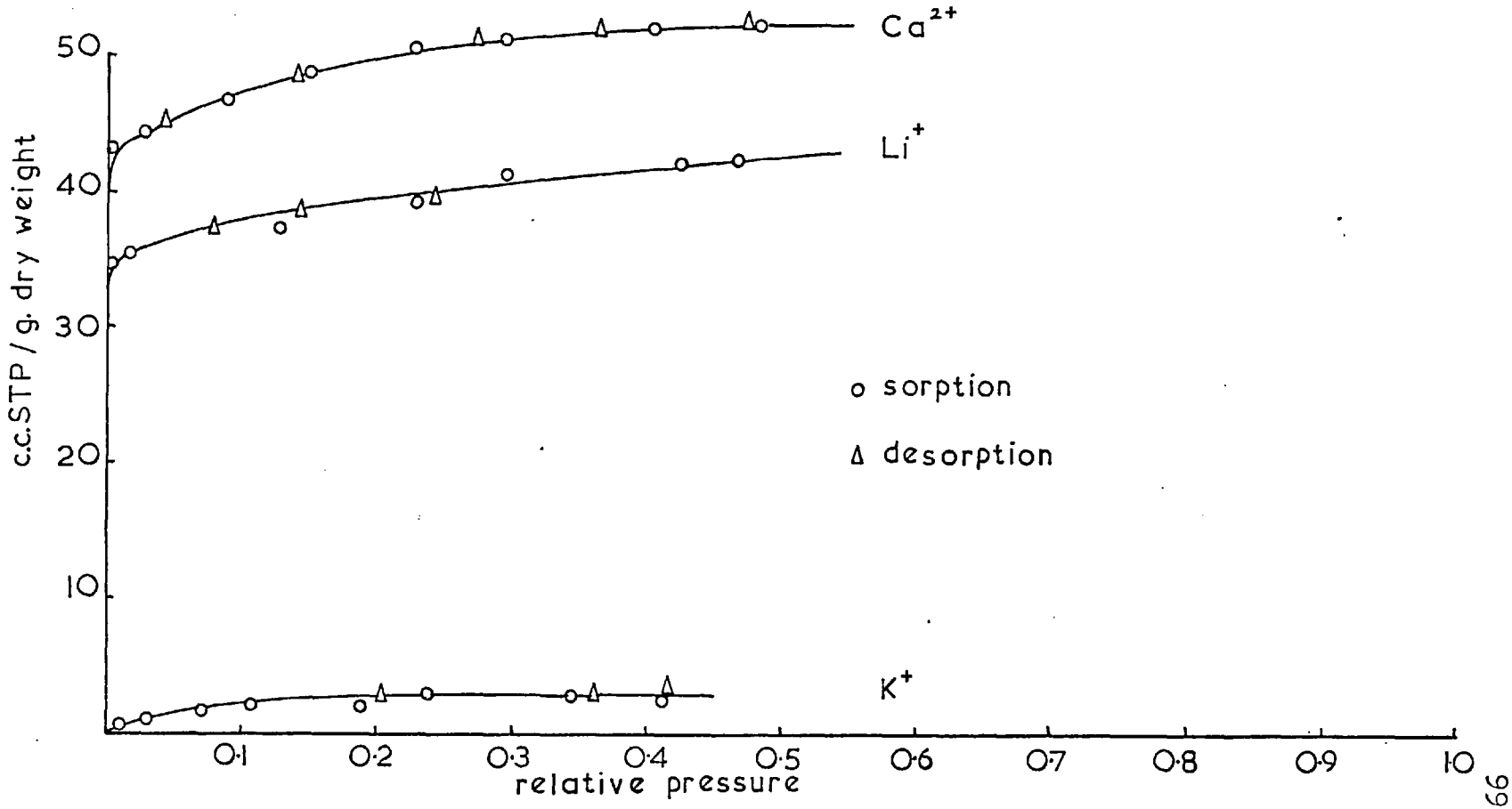

n-butane (diameter 4.9 Å) would be slowly sorbed through this window if it were left unblocked by cations. Both the sorbent molecule and the ring do not have completely rigid dimensions thus a molecule of slightly larger dimensions than the ring may pass through it (Barrer 1949b) (Barrer and Brook 1953b); but the energy of activation rises rapidly as the molecular dimensions increase (Barrer 1959). Smith (1964), from previous sorption measurements (Barrer and Baynham 1958b), has suggested that univalent cations may occupy sites in the eight-member rings. Barrer, Davies and Rees (1969) recently have found further evidence for this in the cation exchange isotherm contours and differential heat curves of natural chabazite.

Sorption in K-G5 can be seen to conform to the above picture, with the univalent cations, such as lithium, small enough and presumably sufficiently out of the plane of the eight-ring to allow the slow sorption of n-butane but the much larger potassium ion preventing access to the cavities. The divalent calcium ion is in the hexagonal prism (Smith 1962, 1963) in natural chabazite which would allow sorption through the eight-ring. Figure 3.1.7 illustrates that substitution of the larger cation calcium (ionic radius 1.02 Å) for lithium (0.68 Å) does not decrease the sorption

capacity. This is probably indicative of the divalent cation position being away from the eight-ring and, as Smith found, in the hexagonal prism. It should be noted that the calcium exchanged form has only half the number of cations as the lithium or potassium forms. This also would tend to increase access to the main cavities even if some of the Ca^{2+} ions were situated near the eight-rings.

This sample of K-G5 had a very high sorption capacity fully comparable with that of natural chabazite. For comparison typical sorption values of K-G5 and other zeolites are given below:

Sample	Oxygen	
Ca exch. K-G5	170 c.c./gm. STP - 195°	
Ca exch. natural chabazite	145 c.c./gm. STP - 183	(1)*
Ca exch. faujasite	190 c.c./gm. STP - 183	(1)
	n-butane	
Ca exch. K-G5	50 c.c./gm. STP - 0°	
Ca exch. natural chabazite	60 c.c./gm. STP - 140°	(2)

* early experimental results were expressed as sorption volume per g. of hydrated sample. This would tend to make the capacities of the natural and synthetic chabazites even more similar.

(1) Garden, Kington and Laing (1955)

(2) Barrer and Brook (1953a)

Plate 3.1.1 Scanning Electron Micrographs of K-G

The co-crystallization of K-G with K-M (radiating rods) magnification 3000X

The interpenetrating twins of K-G showing growth steps magnification 6000X

The crystal habit of the K-G series of near chabazites appeared by optical examination to be spherulitic, which may be due to aggregation of very tiny crystals. This is consistent with the previous synthesis of chabazite and gmelinite-like phases (Barrer and Baynham 1958a) (Barrer, Baynham, Bultitude and Meier 1959). Observations with the scanning electron microscope showed that each sphere was made up of a very complex series of inter-penetrating lenticular twins. This form of growth is very typical of the many occurrences of both gmelinite and chabazite studied by Walker (1951, 1959). Some of the scanning electron micrographs are shown in Plate 3.1.1. For comparison a sample of gmelinite* was examined optically and found to be identical to this. Walker (1951) has illustrated the possible crystal habits of chabazite from which the close relationship of K-G and the natural chabazite is apparent.

* This sample was kindly supplied by Dr. G.P.L. Walker of the Geology Department, Imperial College.

3.1.6 The Species K-M

This species first crystallized from compositions with silica to alumina ratios of 4:1 and continued to appear from those with ratios up to 10:1. In the compositions of low silica content its formation was favoured by increased temperature and low alkalinity. Preparations from crystallization fields of higher silica content were favoured both by higher temperature and higher alkali concentration. In Section 3.1.11. the conditions producing specific phases are correlated with their composition.

These syntheses of K-M are comparable with those of Barrer and Baynham (1958a)who, using gels, gave the optimum conditions of preparation to be a gel of composition K_2O, Al_2O_3, $3SiO_2$ maintained at 250°. Zhdanov (1968, Ovsepyan 1965) formed K-M from potassium aluminosilicate gels at 90° in their study of gel crystallization at lower temperatures. Some of the previous syntheses of this zeolite have been noted in the introductory section.

The diffraction pattern of K-M is given in Table 3.1.14 where it is compared with those of previous syntheses in the potassium crystallization field. Later, in Section 3.6.1 a preparation of Na, K-M was achieved having X-ray

and chemical properties very similar to those of natural phillipsite. This sample was indexed on an orthorhombic cell of comparable dimensions to phillipsite. A comparison of the diffraction patterns of K-M with those of both Na, K-M and phillipsite shows that considerable lattice changes occur as a result of cation exchange. This was found by Hoss and Roy (1960) who examined the influence of ion exchange upon a natural phillipsite. The variation in the unit cell will be discussed in respect to the perturbation of the phillipsite lattice (Section 3.6.8.). Included in Table 3.1.14 are the d-spacings of Linde zeolite W (Milton 1961) which is identical to K-M and which had been indexed on a cubic unit cell of edge 20 Å (Breck 1968). This unit cell should be replaced by the orthorhombic cell proposed later in Section 3.6.8.

The water content of various cation exchanged forms have been measured and these are given below in Table 3.1.15.

Table 3.1.15 showing the hydration of the cationic forms of K-M and Table 3.1.9 showing the same information for K-G1 and K-G5 illustrate that in general bivalent cations in a zeolite produce a greater degree of hydration than univalent cations. Barrer and Sammon (1955), Barrer and Langley (1958) and Barrer, Davies and Rees (1968)

Table 3.1.14

A comparison of d-spacings of species K-M with previously reported related zeolites.

K-M *	K-M (Barrer and Baynham, 1958a)		LINDE W Observed	(20 Å cubic) Calculated	
10.22			9.98	10.03	200
8.352	8.26	MS	8.18	8.19	211
7.149	7.15	S	7.08	7.09	220
5.384	5.37	M	5.35	5.36	321
5.067	5.05	MS	5.01	5.01	400
4.478	4.32	M	4.46	4.48	420
4.306	3.25	VS	4.29	4.28	332
4.115					
3.664	-		3.64	3.66	521
3.530	-				
3.245	-		3.25	3.25	611
3.185	3.18	VS	3.18	3.17	620
3.169					
2.973	2.97	MS	2.96	2.96	631
2.786					
2.736	2.73	S	2.73	2.73	721
2.678	-		2.66		
2.555	2.54	M	2.55		
2.426	2.42	M	-		
2.378					
2.185	-		2.18		
2.169	1.77	M	1.78		
2.150	1.72	MS	1.72		

* In Section 3.6.8 indexed as orthorhombic from the potassium exchanged Na, K-...

Table 3.1.15

The water contents of various cationic forms of K-M equilibrated at 25° and R.H. = 56%

Ionic form	equivalent volume occupied by cation Å	% by weight water	% water corrected to equivalent weight of K-form
K^+	9.84	14.9	14.9
Na^+	3.59	18.4	17.1
Li^+	1.31	19.0	17.3
Ba^{++}	5.15	14.8	18.6
Ca^{++}	2.22	20.2	22.2

in a series of investigations with the different cationic forms of chabazite found a similar relationship. Barrer and Bratt (1959) found that for faujasite there was not only a decrease of hydration with cationic volume but also a separate series for univalent, divalent and transition metal cations. Foster (1965) found that the sodium forms of the fibrous zeolites were less hydrated than the calcium forms in spite of their non-rigid framework. Natural phillipsite, which has a framework lacking overall rigidity (Steinfink 1962), was found by Gude and Sheppard (1966) to be less hydrated when it naturally contained univalent

cations. However, Taylor and Roy (1965) found that for tetragonal zeolite P2 there was a complex relationship resulting from the non-rigid framework, where both free volume and ionic potential were factors influencing hydration. The available volume for water sorption is influenced by the number and size of the cations and the inter-action between the cations and the anionic framework. The polarising power of the cation influences the degree of compactness of the hydration sphere about the cation.

Species K-M produced from the monoionic potassium crystallization field had the following chemical analysis.

	% by weight	Molar proportion
SiO_2	43.0	3.3
Al_2O_3	22.2	1.0
K_2O	20.2	1.0
H_2O	14.5	3.7

This may be compared with the composition $K_2O, Al_2O_3, 3\ SiO_2, 3\ H_2O$ found by Barrer and Baynham for their sample* and later with the di-cationic form in Section 3.6.8.

* This sample was examined by X-ray diffraction and shown to contain approximately 8% K-G. Thus a close comparison between samples cannot be made.

Figure 3.1.8 Oxygen Sorption on Ca^{2+} Exchanged K-M at 78°K

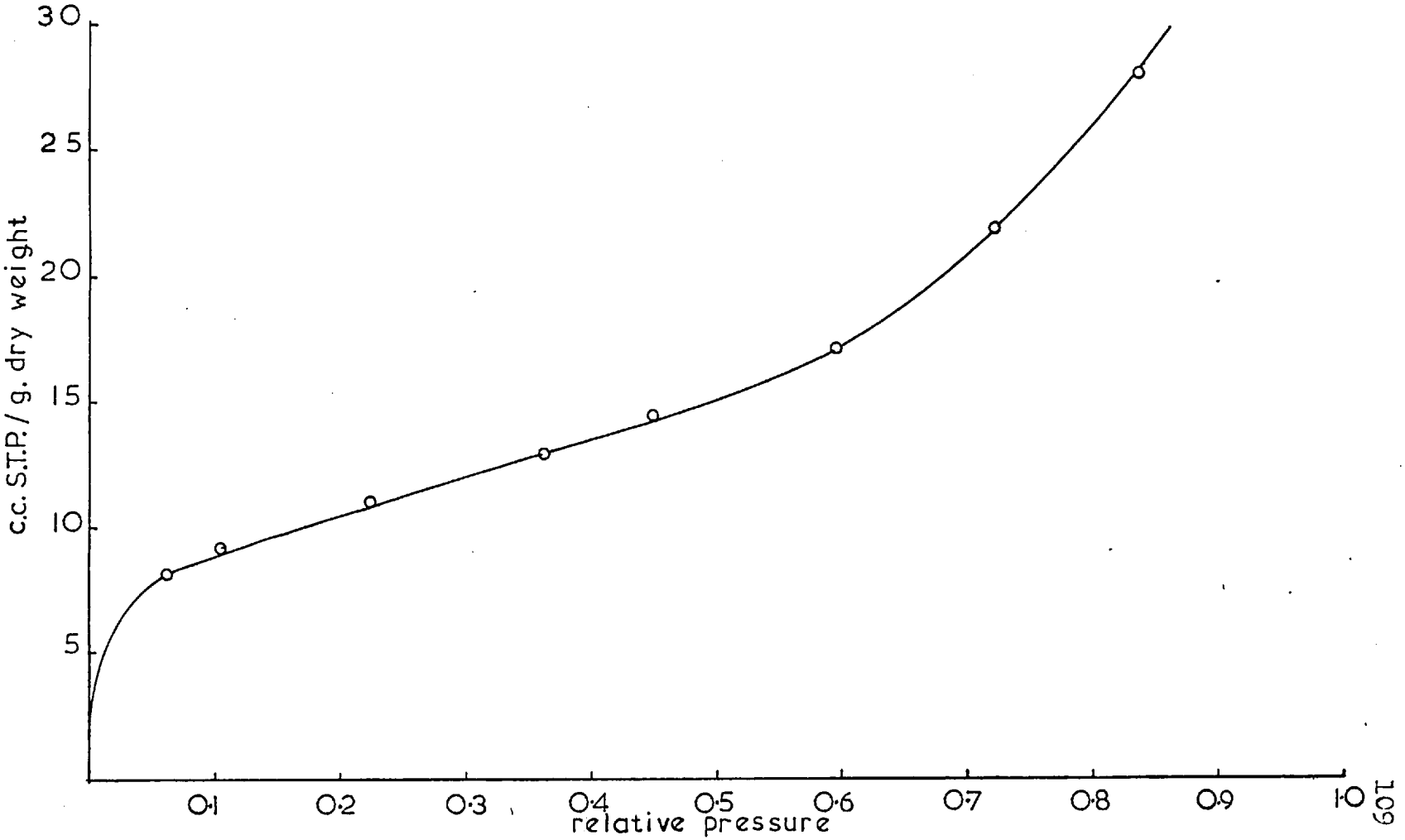

The oxygen sorption isotherm shown in Figure 3.1.8 indicates that no intra-crystalline sorption has taken place. This isotherm is characteristic of surface condensation on the small crystal particles. Thus the internal volume available for water sorption Table 3.1.15 and ammonia sorption (75 mls at N.T.P. per gram (Barrer and Baynham 1958a)) is not accessible to oxygen at low temperature (78°K). This sorption behaviour is similar to that of natural phillipsite which does not sorb oxygen or nitrogen but does admit ammonia (Barrer, Bultitude and Kerr 1959, Sameshima and Morita 1935).

The natural zeolite phillipsite occurs as inter-penetrating twins both separately and as radiating aggregates (Walker 1970, Sheppard and Gude 1968). Synthetic K-M previously prepared has been described as being composed of characteristic wheatsheaf bundles and spherulites (Barrer and Baynham 1958a and Ovsepyan and Zhdanov 1965) but close examination has been hindered by the small particle size. A number of preparations of K-M have been examined by the scanning electron microscope and are shown in Plate 3.1.2. The basic crystal habit is the tetragonal prism which may be produced by complex twinning. This appears to grow in three forms depending

Plate 3.1.2 Scanning Electron Micrographs of K-M

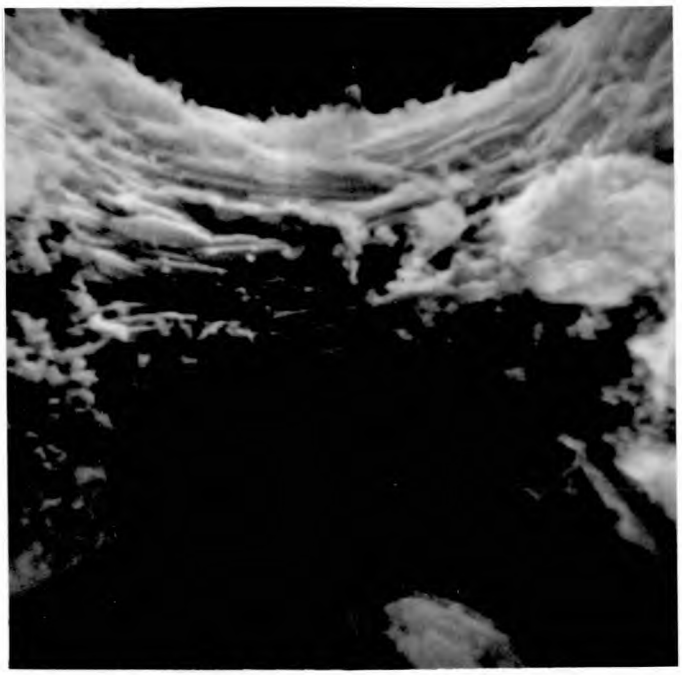

A X9000

B X7500

Plate 3.1.2

C X8000

D X5000

upon the crystallization conditions. These are summarised below:

Plate	Description	Synthesis conditions
3.1.2 A	wheatsheaf bundles composed of prismatic rods	1 Molar KOH, alumina :silica = 1:4 rotated at 110°
3.1.2 B C	prismatic crystals radiating from a common point	4 Molar KOH, alumina :silica = 1:4 rotated at 110°
3.1.2 D	single prismatic rods separated and very well formed	1 Molar KOH, alumina:silica = 1:4 rotated at 170°

Further properties of species K-M, such as thermal stability, were investigated on the mixed sodium/potassium crystallized form.

3.1.7 The Species K-F

This was the most abundently crystallized zeolitic species in the potassium crystallization field. It occurred from compositions with silica to alumina ratios of 2:1 up to those in which this ratio was 10:1. The temperature range producing K-F was 80 to 160°.

Some of the previous syntheses of K-F are noted in the introductory Section 1.2. There and in later sections other zeolites such as Rb-D, Cs-D and Li, Na-F are identified as different cationic preparations of the same framework.

Barrer and Baynham (1958a) in their original preparation of K-F found the optimum conditions of formation from potassium aluminosilicate gels were a composition K_2O, Al_2O_3, 4 SiO_2 + 130% molar excess of KOH maintained at 120°. Thus the temperature range for growth either from gels or metakaolinite is comparable, while the composition yielding K-F is dependent upon the alkali concentration as shown in Figures 3.1.1 - 3.1.4.

The d-spacings of the diffraction pattern of K-F were measured and corrected with lead nitrate as an internal

standard. These are given in Table 3.1.16 where they are compared with the original synthesis. The rubidium analogue Rb-D was indexed and from this a unit cell for K-F is proposed. The calculated unit cell* appears to be orthorhombic. Approximate cell dimensions are a=14.02, b = 13.92, c = 13.14 Å. The significance of this unit cell and those of various cationic analogues is discussed in Section 3.4.3.

The chemical analyses of species K-F are given below in Table 3.1.17. Two crystallizations are analysed, one of which was found to have an increased silica to alumina ratio beyond that previously reported.

Table 3.1.17

	% by weight		Molar ratio	
Sample	[1]	[2]	[1]	[2]
SiO_2	33.3	44.6	2.08	3.41
Al_2O_3	27.2	23.0	1.0	1.0
K_2O	25.1	21.0	1.0	1.0
H_2O	14.4	11.4	3.0	2.7

* The apparent extension of the symmetry to an orthorhombic unit cell from the tetragonal cells of other analogues of K-F (Section 3.4.3) was proposed by Ch. Baerlocher and will be reported later.

Table 3.1.16

The observed d-spacings of K-F compared with those of the original preparation

K-F	K-F (Barrer et al 1956a)	KF	K-F (Barrer et al)
7.86 W	7.45 VVS	2.384 W	
6.964 S		2.375 W	
6.553 W		2.356 MW	2.35 MW
5.930 V		2.331 VW	
5.609 VW		2.315 W	
4.769 W	4.78 VW	2.288 W	
4.622 W		2.254 W	
4.518 W		2.199 VW	2.20 W
4.178 MW		2.186 W	
3.994 W	3.98 M	2.173 W	
3.940 VW		2.159	
3.862 W		2.122	
3.509 W		2.099	2.11 M
3.474 M	3.47 M	2.087	
3.274 W	3.29 M	2.052	
3.186 VW		2.028	
3.123 W		1.999	
3.081 S	3.09 VS	1.973	
3.071 S	2.97 S	1.804	1.85 M
3.006 VS	2.82 VS	1.789	
2.966 M		1.749	
2.897 W		1.736	1.74 M
2.813 MS		1.724	
2.731 W		1.697	
2.685 W		1.685	1.68 MW
2.670 VW		1.666	
2.580 W		1.639	
2.465 VW		1.596	
2.433 VW		1.591	1.59 M

Sample 1 was the product obtained from metakaolinite and 3.2 KOH at 110° while sample 2 was from a metakaolinite and silica magma with a silica to alumina ratio of 6:1 and KOH concentration of 4.9 molal maintained at 110°. The lower water content of sample 2 may be accounted for by a lower yield of zeolite. If the less hydrated impurity was silica this would increase the silica ratio without isomorphous substitution of Si for Al + K. Also since isomorphous substitution of this type would decrease the cation density there would be a tendency to increase the degree of hydration.

These analyses may be compared with the sample prepared and analysed by B.M. Munday (1969) which had the composition

$0.99\ K_2O,\ Al_2O_3,\ 2.3\ SiO_2,\ 2.5\ H_2O$

The species K-F is reported to have a silica to alumina ratio of 2:1 by Barrer (1958a, 1968), Ovsepyan and Zhdanov (1965), and Borer (1969).

The low temperature sorption of oxygen was examined in both the samples of K-F with silica to alumina ratios of 2.08:1 and 3.41:1. Neither of them imbibed oxygen either in the original potassium or the calcium exchanged

Figure 3.1.9 Li Exchanged F $SiO_2 / Al_2O_3 = 3{\cdot}41$ Oxygen Sorption at 78°K

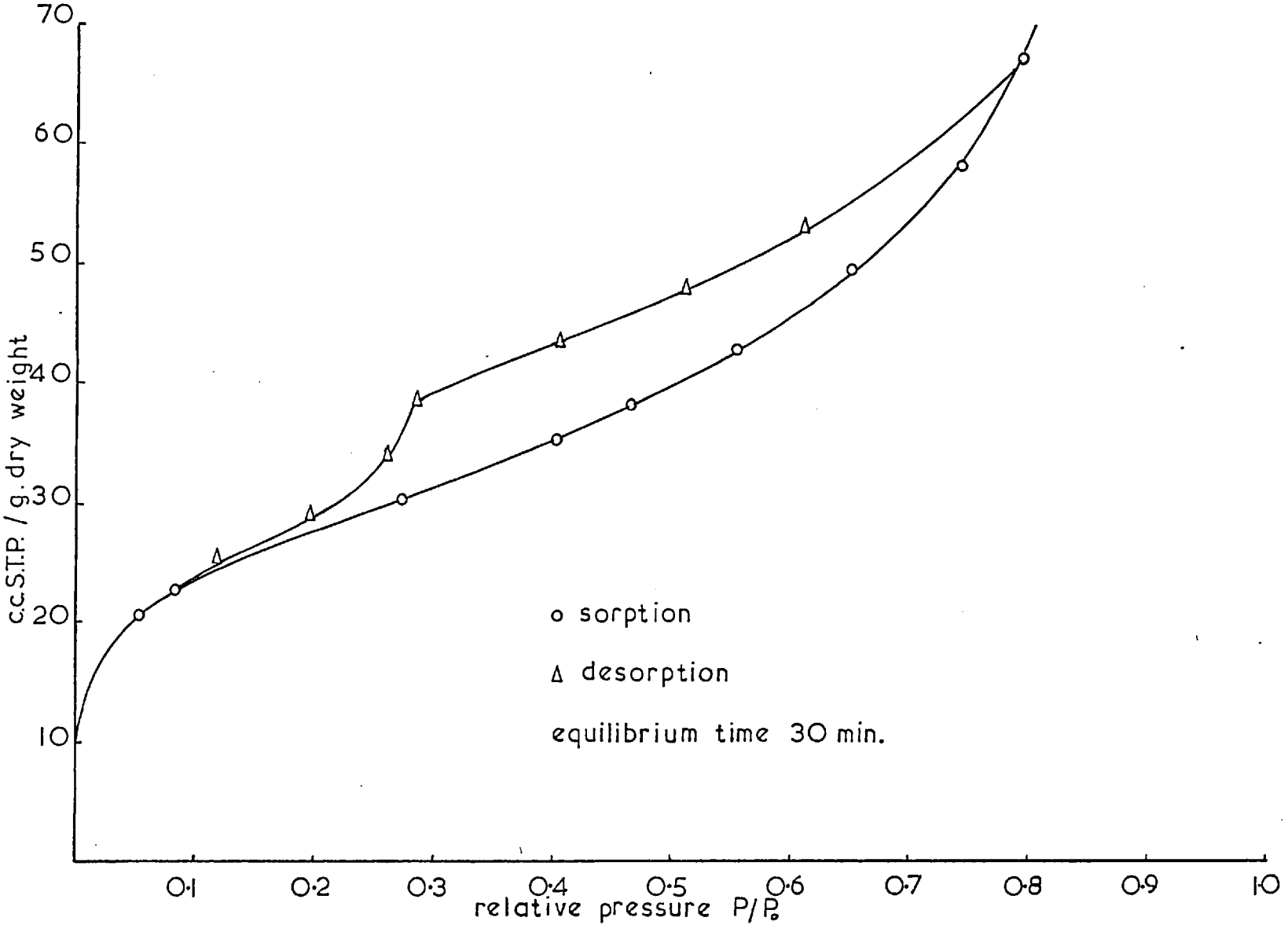

forms. An example of the isotherm produced by surface adsorption and condensation K-F is shown in Figure 3.1.9. This is consistent with the properties that would be expected of a small pore zeolite such as those of the natrolite group (Hey 1930, 1932).

The variation of water content with cation exchange has been determined by Barrer and Munday (1970) and with cationic type as synthesized by Barrer, Cole and Sticher (1968). The water content was found to decrease with increasing cation size in a manner similar to that described in Section 3.1.6.

The thermal stability of the cationic forms was examined first by differential thermal analysis, and then by removing samples heated to specific temperatures on the thermobalance for X-ray diffraction. In Figure 3.1.10 the D.T.A. curves obtained for various cationic forms are shown. Below, Table 3.1.18 shows the temperature at which the framework decomposed and the product obtained upon ignition of the sample.

Table 3.1.18

Form	Decomposition Temp.	Ignition Product
Cs	1060	Cs-F
Rb	1085	Rb-A
K	1095	synthetic kaliophilite
Na	~450	synthetic nepheline
Li	310	
Ca	~ 350	synthetic anorthite
Ba	~ 400	Ba-P

Figure 3.1.10 DTA of Various Cationic Forms of K-F

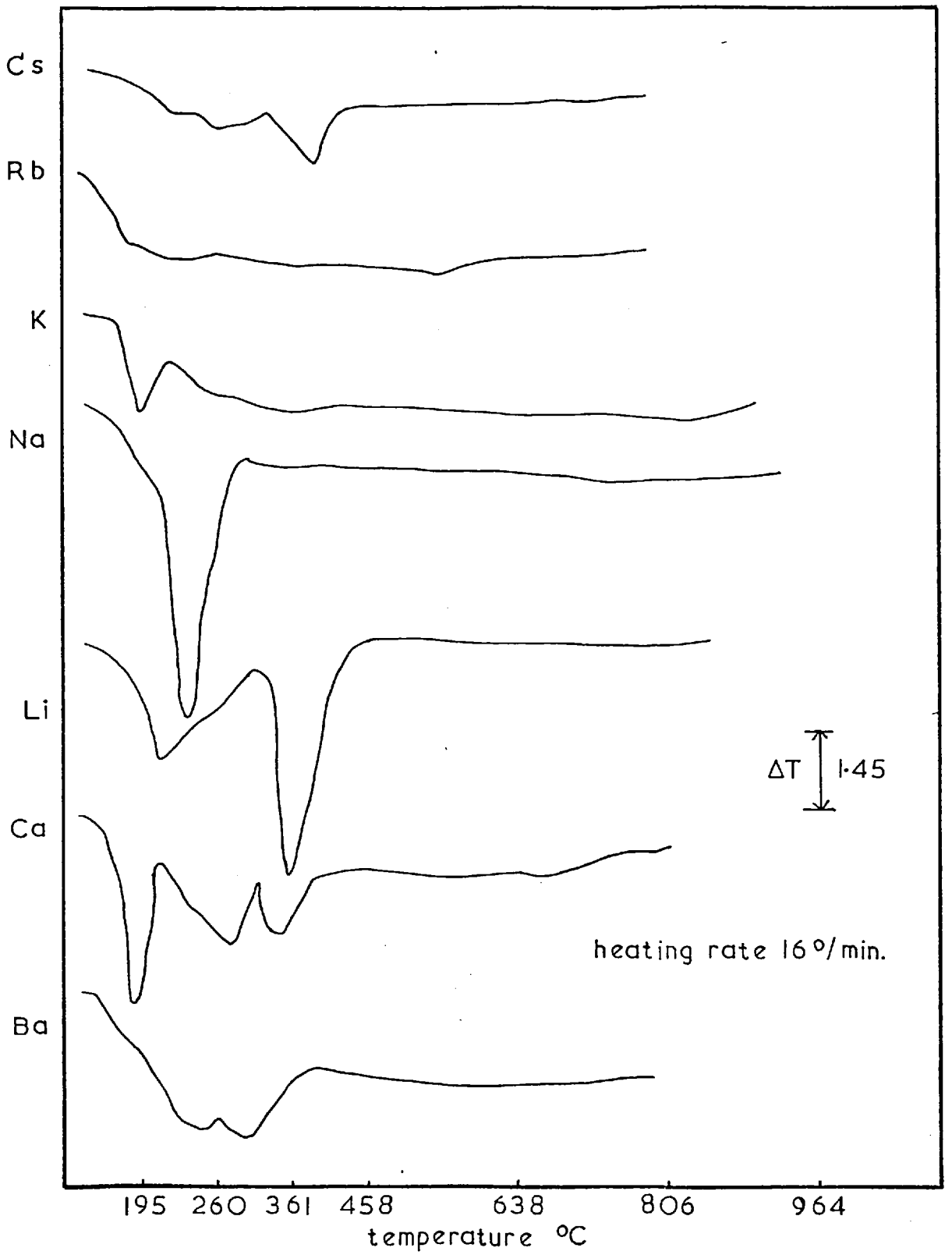

The cationic forms of K-F show a large variation in thermal behaviour. The caesium, rubidium and potassium forms are similar. They show endothermal water loss on D.T.A., while the lattice remains unchanged to a very high temperature, for example 1095° for K-F. At the decomposition temperature there is inversion to Cs-F, Rb-A and synthetic kaliophilite (K-D) for the caesium, rubidium and potassium forms respectively. Barrer, Cole and Sticher (1968) have identified Cs-F and Rb-A as synthetic species with similar frameworks but having no natural counterpart. The sodium form, like the lithium, calcium and barium forms, was amorphous between lattice decomposition and recrystallization at 1000°. The ignition product of Na-F was synthetic nepheline and a second phase, present in a small amount, which could not be identified. Decomposition of the lithium, calcium and barium forms took place almost exclusively in the region of the last endotherms on the D.T.A. curves. The ignition product of the lithium, calcium and barium forms were Li-O (Barrer, Cole and Sticher 1968), synthetic anorthite, and the hexagonal polymorph of barium celsian Ba-P (Section 3.5.7). The synthetic nepheline and anorthite were identified by their d-spacings compared with previously reported values. These are shown in Table 3.1.19. Here in the various cationic forms of K-F

Table 3.1.19

The d-spacings of the ignition products of cationic forms of K-F with their natural counterparts.

ignited Na^{ex} K-F		Smith (1957) natural nepheline		ignited Ca^{ex} K-F		Cole(1951) natural anorthite	
d	I	d	I	d	I	d	I
8.6*	W			6.5	VW	6.52	9
4.98	MW	5.030	3			6.42	1
4.32	M	4.354	10			5.79	1
4.29	M	4.319	10	4.65	W	4.69	11
4.19	S	4.211	35	4.00	MW	4.04	60
3.85	S	3.870	60	3.90	W	3.92	11
3.72	W	3.789	5	3.75	Md	3.78	20
3.59*	VW					3.76	13
3.25	S	3.294	40			3.69	1
3.01	M	3.065	10			3.68	1
2.99	VS	3.027	100	3.60	MW	3.62	25
2.88	M	2.905	35			3.61	7
2.69	W	2.670	1			3.51	3
2.64*	W					3.47	11
2.58	M	2.593	20			3.44	3
2.53	M	2.515	15			3.41	7
2.47*	MW			3.35	MW	3.37	25
2.41	MW	2.415	10	3.25	M	3.26	55
		2.390	3	3.21	M	3.21	35
2.37	M	2.359	30	3.19	Sd	3.20	100
2.32	S	2.322	20			3.18	75
2.17	VW	2.177	5	3.11	M	3.12	45
2.14	W	2.135	7			3.04	17
2.10	M	2.105	15	2.95	MW	2.953	25
2.08	W	2.092	5			2.935	17
				2.81	W	2.828	19
						2.655	11

* Lines of a second phase not identified.

there is multiple stage dehydration typical of the less rigid framework zeolites such as the fibrous zeolites (Peng 1955).

In Table 3.4.2 of Section 3.4.3 the compositions are compared of the different preparations of both K-F and other members of the group possessing the same framework. The product K-F as made from metakaolinite is very similar to the first preparation of K-F by Barrer (1948, 1953) which has recently been re-examined by Barrer and Marcilly (1970).

A possible structural relationship between the K-F zeolites and the naturally occurring fibrous zeolite, edingtonite, is demonstrated in Section 3.4.3. The mixed cationic forms of the K-F structures will be discussed in the sections on binary cationic systems where crystallization occurred within a large compositional range.

3.1.8 The Species K-L

This species was identified as zeolite L (Breck 1965). The diffraction pattern may be compared with Linde L in Table 3.1.20 and a related zeolite Ba-G in Table 3.5. The zeolite crystallized from a composition rich in silica (silica to alumina ratio = 10:1) and under conditions which would favour a silica rich zeolite, i.e. low alkalinity (0.5 molal KOH) and low temperature (80°).

The crystallinity and yield of zeolite K-L as it was produced here, from metakaolinite, was not good. This indicates that its growth is probably more favoured in a system using aluminosilicate gels (Breck 1965, Zhdanov 1967). The low yield is similar to that reported when K-L and other zeolites are produced in pelletized form, crystallized in situ. The resulting unreacted material is used both as a binder and a dilutant for the zeolite (Taggart 1964). This method of preparation is discussed later in Section 3.2. as it is applied more frequently to other zeolites. From the diffuse nature of the diffraction pattern it was estimated that up to a third of the product was gel and unreacted starting material.

Table 3.1.20

The d-spacings of species K-L compared with Union Carbide Linde K-L.

K-L		U.C. K-L (Breck 1965)	
16.0	sd	15.8	100
7.9	mw	7.89	14
7.5	mw	7.49	15
6.00	md	5.98	25
5.75	w	5.75	11
4.57	m	4.57	32
4.40	w	4.39	13
4.30	w	4.33	13
3.90	mwd	3.91	30
3.80	w	3.78	13
3.65	w	3.66	19
3.50	wd	3.48	23
3.25	w	3.26	14
3.17	md	3.17	34
-		3.07	22
-		3.02	15
2.90	md	2.91	23
2.65	w	2.65	19
2.62	vw	2.53	8
		2.45	9
		2.42	11
		2.19	11

Later in Section 3.5.1 it will be shown that this same framework can be grown with a very different composition in the barium-containing crystallization fields where, in contrast, a very high crystallinity was obtained. An approximate analysis was performed which gave the composition K_2O, Al_2O_3, 6.4 SiO_2, 3 H_2O. This may be compared with the sample obtained from gels which had a composition K_2O, Al_2O_3, 6.05 SiO_2, 4 H_2O (Barrer and Villiger 1970). The sample probably contained considerable excess silica as well as unreacted meta-kaolinite giving the high silica and low water contents.

3.1.9 The Species K-Z

This species was identified with the product Z first made by Barrer, Cole and Sticher (1968). It was crystallized by them from kaolinite in the presence of very concentrated solutions of potassium hydroxide. Metakaolinite crystallized to K-Z only from saturated solutions of potassium hydroxide, and then the silica to alumina ratio was 2. The composition was found previously to be

K_2O, Al_2O_3, 2 SiO_2, KOH, 3.5 H_2O

The d-spacings of the sharp diffraction pattern are listed in Table 3.1.21 where they are compared with those of the first synthesis.

Table 3.1.21

The d-spacings of species K-Z and the product Z from kaolinite.

K-Z (metakaolinite)		K-Z (kaolinite) (Barrer, Cole and Sticher 1968)	
5.351	ms	5.33	m
4.565	w	4.56	w
4.224	w	4.22	w
4.163	vw	4.16	w
3.932	w	3.93	w
3.661	ms	3.65	m
3.540	m	3.54	m
3.267	m	3.26	m
3.08	w	3.08	w
-		3.03	w
2.929	vs	2.92	s
2.895	w	2.89	w
2.871	w	2.87	w
2.750	mw	2.70	w
2.563	vw	2.56	vw
2.537	vw	2.53	vw
2.465	vw	2.46	w
2.341	mw	2.34	w

3.1.10 The Species K-D and K-N

Two anhydrous species, K-D similar to kaliophilite previously reported by Barrer, Cole and Sticher (1968) and K-N similar to kalsilite, crystallized from metakaolinite. The relatively low temperatures of formation of these species are compared below with those of previous syntheses from gels and with stability ranges found by Smith and Tuttle (1957) in the nepheline-kalsilite system.

Starting material	Temperature range °C	
	K-D	K-N
hydrothermal-gels (Barrer and Baynham 1956a)	no reproducability	300-400
pyrolytic-gels (Smith 1957)	~ 1000	> 850
hydrothermal-metakaolinite	80-250	140-370
pyrolytic-recrystallization of potassium zeolites	~ 1000	not formed

The two species K-D and K-N are polymorphs of potassium aluminosilicate with the composition K_2O, Al_2O_3, $2SiO_2$.

Table 3.1.22

The comparison of d-spacings of synthetic and natural kaliophilites.

K-D from metakaolinite		synthetic kaliophilite Smith and Tuttle (1957)		natural kaliophilite Smith and Tuttle (1957)	
d	I	d	I	d	I
				6.1149	2
				5.1523	4
				4.529	2
4.49	m	4.488	10	4.4883	7
4.27	ms	4.283	15	4.2624	15
		3.972	3	3.9706	5
				3.9145	10
				3.7596	12
				3.7323	7
				3.4964	10
				3.4257	1
				3.3659	2
				3.2826	8
3.099	vs	3.098	100	3.0909	100
				3.0248	12
				2.9393	4
				2.871	1
				2.8139	11d
				2.7280	1
				2.7043	7
2.590	ms	2.589	30	2.5931	30

Table 3.1.22 (continued)

K-D from metakaolinite		synthetic kaliophilite Smith and Tuttle (1957)		natural kaliophilite Smith and Tuttle (1957)	
d	I	d	I	d	I
				2.5516	4
				2.506	7d
				2.4430	1
				2.4203	2
				2.404	2d
				2.386	
				2.3521	2
				2.284	2d
2.245	w	2.243	3	2.2440	3
2.210	w	2.214	5	2.2134	9
				2.1849	7
				2.1621	5
				2.1564	5
2.129	m	2.139	12	2.1307	25

The X-ray diffraction patterns of K-D, produced either hydrothermally or by the ignition of potassium zeolites, were identical. This pattern is the same as that of the synthetic kaliophilite reported by Bowen (1917) and later studied by Smith and Tuttle (1957). The d-spacings of K-D, synthetic kaliophilite and natural kaliophilite are shown in Table 3.1.22. Here the same relationship between the synthetic phase and the natural mineral, as Smith found, is evident. Thus the synthetic product is related to but not identical with the natural mineral. Both hydrothermal crystallization and pyrolitic decomposition of potassium zeolites yielded a product with high crystallinity which gave a sharp diffraction pattern. Yet only the diffraction lines that corresponded with the more intense lines of natural kaliophilite were present in K-D. Natural kaliophilite has been indexed by Lukesh and Buerger (1942) whose work was confirmed by Smith and Tuttle (1957). The proposed unit cell was hexagonal with a = 26.93 ± 0.01, c = 8.522 ± 0.004 Å. But Lukesh and Buerger noted that kaliophilite may be orthorhombic with twinning producing the hexagonal appearance. Smith and Tuttle have suggested a hexagonal unit cell for synthetic kaliophilite with a = 5.180 ± .0.002, c = 8.559 ± 0.004 Å

which is related to a sub-cell of natural kaliophilite obtained by reducing the a dimension by a factor of $\sqrt{3}$.

Further examination of K-D was prevented by the very few diffraction lines produced.

The K-N was identical with its natural counterpart kalsilite. The d-spacings of K-N and a reference sample are given in Table 3.1.23.

The low temperature hydrothermal growth of synthetic analogues of kaliophilite and kalsilite considered together with the formation of potash felspar at 200° (Barrer and Hinds, 1950) provide examples of potassium species which were considered to be high temperature phases. The possible significance of these and other examples later found is of interest in the field of geological thermometry.

Table 3.1.23

The comparison of the d-spacings of K-N and kalsilite (Smith and Tuttle 1957).

K-N (from metakaolinite)		synthetic kalsilite a_{hex}= 5.159 ± .002 c_{hex}= 8.703 ± .002	
d	I	d	I
4.365	m	4.3512	12
3.970	s	3.9733	45
3.121	vs	3.1184	100
2.579	s	2.5789	50
2.471	mw	2.4724	15
2.428	w	2.4319	10
		2.236	3
2.220	w	2.2183	10
2.178	mw	2.1753	17
		2.164	5
		1.9868	5
		1.9546	3
1.925	w	1.9270	4
		1.7703	3
1.66	mw	1.6621	4
		1.6580	4
1.621	mw	1.6220	6
1.579	mw	1.5742	9
		1.5588	3
1.491	m	1.4895	10

3.1.11 Characteristics of the Potassium Crystallization Field

The effect of solid to solution ratio

The effect was investigated of the ratio of alkali hydroxide solution to solid metakaolinite upon the yield of crystalline zeolites. Separate crystallizations were made in which a fixed weight of metakaolinite (1.1 g) reacted with various weights of potassium hydroxide solution of fixed concentration (1 M and 4 M). One molal potassium hydroxide yielded the zeolite K-G and six molal yielded K-F. Figure 3.1.11 gives the weights of crystalline products as functions of the volume of potassium hydroxide solution.

The yield of zeolite decreases with increasing amount of solution gradually until a point above which both the 1 molal and 6 molal solutions produce a rapid decrease in yield.

The products were examined by X-ray diffraction. It was found that the best crystallinity occurred with reactions involving not less than 50 g of solution per 1.1 g of metakaolinite (0.005 moles). These were the reaction conditions in the syntheses described, unless otherwise indicated.

Figure 3.1.11 Effect of Metakaolinite Solid : KOH Solution Ratio on the Crystallization Products

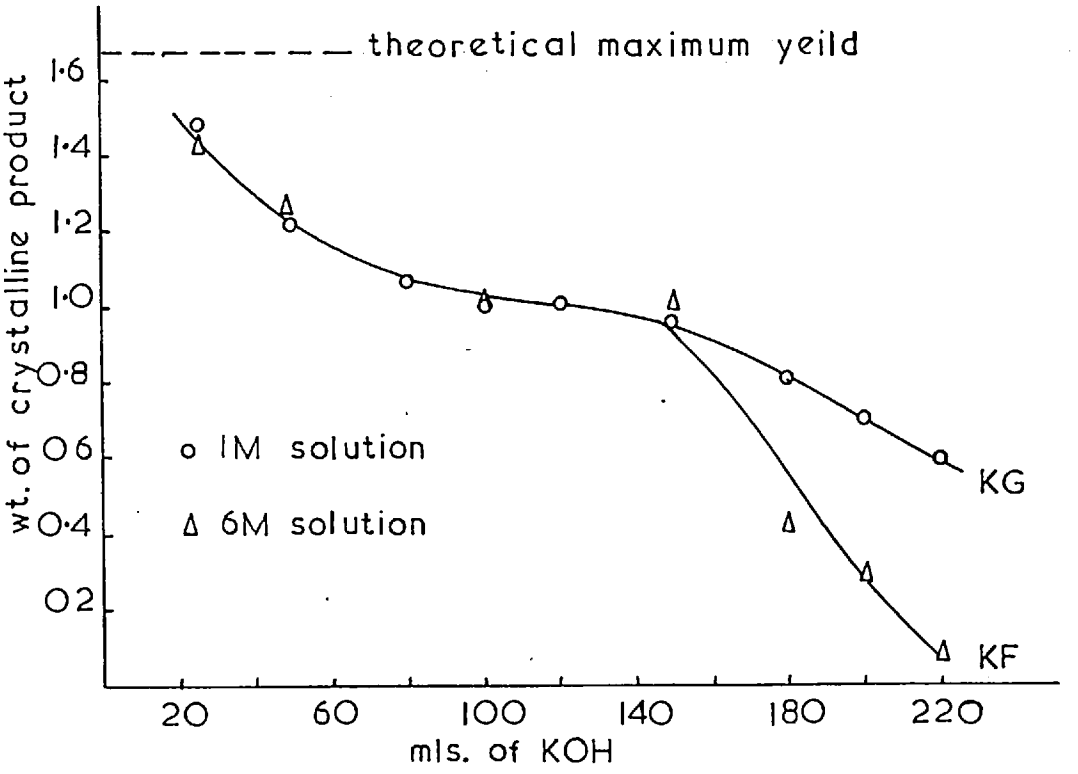

The effect of alkali concentration on the products.

Both the composition and nature of the final crystalline product can be related to the initial reacting composition. In Figure 3.1.12 the compositions are shown of crystalline products obtained from metakaolinite, silica and potassium hydroxide at 110°.

a) The crystallized product, whether zeolitic or not, tended to be less siliceous than the initial composition. The exceptions were found to be syntheses from metakaolinite alone, where analysis of K-G1 gave a silica to alumina ratio of 2.13 (Section 3.1.5). This probably indicates a tendency not to produce a perfectly ordered chabazite-like structure. Analysis of other products from metakaolinite showed almost the same silica to alumina ratio as metakaolinite, for example K-F (Section 3.1.7) had 2.08. This is probably a ratio of 2.00 within the limits of accuracy of the analysis; and indicates that K-F is growing with an ordered silicon-aluminium distribution.

b) The decrease in the silica to alumina ratio from the starting to the final composition was greater for larger initial ratios. For example at 1 molal KOH an initial composition of 10:1 gave a product with

Figure 3.1.12 Silica : Alumina Ratio (n) of the Synthesis Products

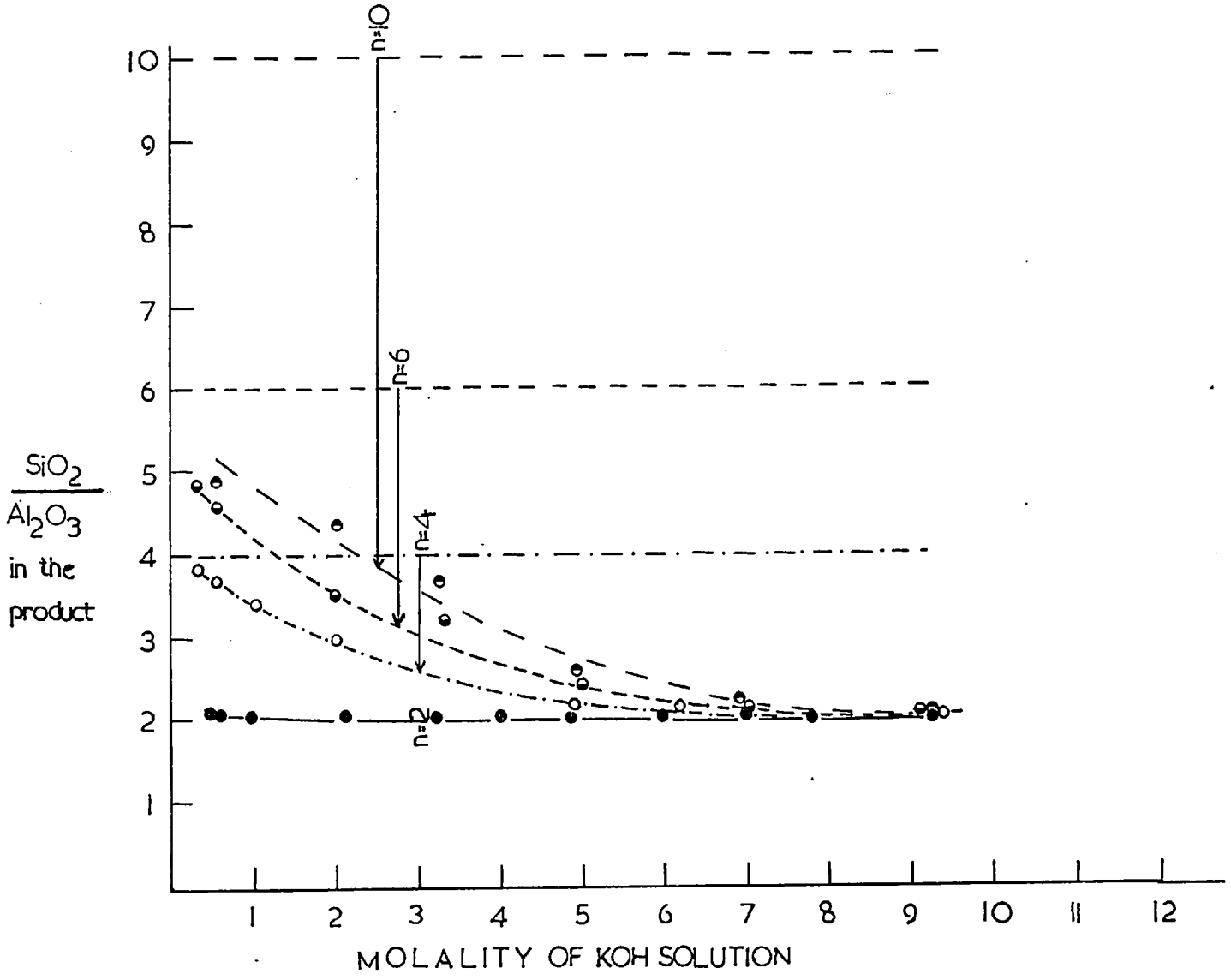

a ratio 4.4:1, whereas an initial composition of 4:1 gave a product with a ratio of 3.4:1. In the limiting case metakaolinite with a ratio of 2:1 crystallized to a product of the same composition.

c) The increase of the potassium hydroxide concentration produces a progressive decrease in the silica to alumina ratio in the products, until the lowest value of 2 is approached irrespective of starting composition. Zhdanov, Samulevich and Egorova (1963) found a similar dependence of final composition of sodium zeolites upon Na_2O content of aluminosilicate gels. Zhdanov (1968) plots the SiO_2/Al_2O_3 ratio of many zeolites against the excess alkali content of the parent gel to show that the same trend occurs in a large number of systems.

d) If the nature of the products from the crystallization of metakaolinite+silica with potassium hydroxide are considered (as in Section 3.1. and Figures 3.1.1-3.1.4) then it is seen that as the hydroxide concentration increases there is a corresponding trend from zeolitic species to non-hydrated products. Thus the open tectosilicate frameworks needing stabilization by occluded water (see Section 1.2) change to the denser frameworks not needing stabilization by a filler.

Section 3.2 The System Metakaolinite - Na_2O - SiO_2 - H_2O

3.2.1 Reactions in the System

The systematic study of the reactions between metakaolinite, silica and sodium hydroxide solutions yielded many products previously made from alkaline alumino-silicate gels. In Section 1.2 many of the syntheses previously reported have been noted. The Na_2O-Al_2O_3-SiO_2-H_2O system is the most widely studied of those producing zeolites. It has yielded three of the zeolites of greatest industrial importance, Zeolites A, X and Y. The significance of these and others in zeolite technology has been outlined in Section 1.1.

Crystalline Products

Short Reference	Zeolite formula	Oxide composition	Description
Na-Q	(Na)-Q_c(2.0) [A]	Na_2O, Al_2O_3, $2SiO_2$, 4 H_2O	synthetic zeolite similar to Linde A
Na-R	(Na)-R_c(2.8) [Fau]	Na_2O, Al_2O_3, $2.8SiO_2$, $6H_2O$	synthetic zeolite of faujasite X group
Na-I	{NaOH}(Na)-I_c (2.1) [Sod]	Na_2O, Al_2O_3, $2.1SiO_2$, 2NaOH, $1.5\ H_2O$	synthetic felspathoid sodalite
Na-J	-	Na_2O, Al_2O_3, $2SiO_2$, H_2O	nepheline hydrate I
Na-B	(Na)-B_c(4.0) [Ana]	Na_2O, Al_2O_3, $4SiO_2$, $2H_2O$	synthetic analcite
Na-C	{NaOH}(Na)-C_h (2.0) [Can]	Na_2O, Al_2O_3, $2SiO_2$, NaOH, H_2O	synthetic felspathoid cancrinite

Crystalline Products (continued)

Short Reference	Zeolite formula	Oxide composition	Description
Na-S	(Na)-S_h(4) [Gme]	Na_2O, Al_2O_3, $4SiO_2$, $6H_2O$	synthetic near gmelinite
Na-P1	(Na)-P1(3) [Gis]	Na_2O, Al_2O_3, $3SiO_2$, $6H_2O$	'cubic' sodium P *
Na-P2	(Na)-P_T2(3) [ ]	" "	tetragonal NaP
Na-P3	(Na)-P_o3(3) [ ]	" "	orthorhombic NaP

* Bärlocher and Meier (1970)

3.2.2 The Reactions of Metakaolinite with Sodium Hydroxide

Some of the typical syntheses carried out in this crystallization field and a description of the products are given in Tables 3.2.1-3.2.4. The corresponding crystallization field is shown in Figures 3.2.1-3.2.3.

Table 3.2.1

The general reaction compositions were:

1 metakaolinite (Al_2O_3, $2SiO_2$) + 2.5 - 50.0 Na_2O + ~$275H_2O$ rotated at 80° for 7 days.

Run No.	Concentration of alkali (molality)		Product	Description
2-2	0.5		Na-Q	gd.cr.
2-3	0.5	(4 days)	Na-Q	gd.cr.
2-4	1.0	(5 days)	Na-Q	gd.cr.
2-5	2.0	(5 days)	Na-Q	gd.cr.
2-6	3.0	(5 days)	Na-Q	gd.cr.
2-7	1.0	(10 days)	Na-Q	v.gd.cr.
2-8	2.0	(10 days)	Na-Q	v.gd.cr.
2-9	3.0	(10 days)	Na-Q	gd.cr.
2-11	4.0		Na-I	gd.cr.
2-12	6.0		Na-I	md.cr. *
2-14	10.0		Na-I	md.cr. *
2-16	4.0	(3 days)	Na-I	md.cr. *
2-17	6.0	(3 days)	Na-I	md.cr. *
2-18	10.0	(3 days)	Na-I	pr.cr.

* These sodalite products crystallized in a mixture of two different unit cells. This will be examined later in this section.

Table 3.2.2

The general reaction compositions were:

1 metakaolinite (Al_2O_3, $2SiO_2$) + 2.5 - $50Na_2O$ + ~$275H_2O$

rotated at elevated temperatures as indicated

Run No.	Concentration of alkali (molality)	Product	Description
2-20	0.5 (110°)	Na-Q	gd.cr.
2-21	1.0 (110°)	Na-C+Na-Q	md.cr.
2-22	3.0 (110°)	Na-I	gd.cr.
2-61	0.5 (140°)(3 days)	Na-C	md.cr.
2-62	1.0 (140°)(3 days)	Na-J	gd.cr. hi.yd.
2-64	3.0 (140°)(3 days)	Na-I	gd.cr.
2-65	5.0 (140°)(3 days)	Na-I	gd.cr. lo.yd.
2-75	0.5 (170°)(3 days)	Na-C	gd.cr.
2-76	1.0 (170°)(3 days)	Na-J	md.cr.
2-77	2.0 (170°)(3 days)	Na-J	md.cr.
2-78	3.0 (170°)(3 days)	Na-J	pr.cr.

Figure 3.2.1 I Metakaolinite +2·5–5ONa_2O ∓275H_2O

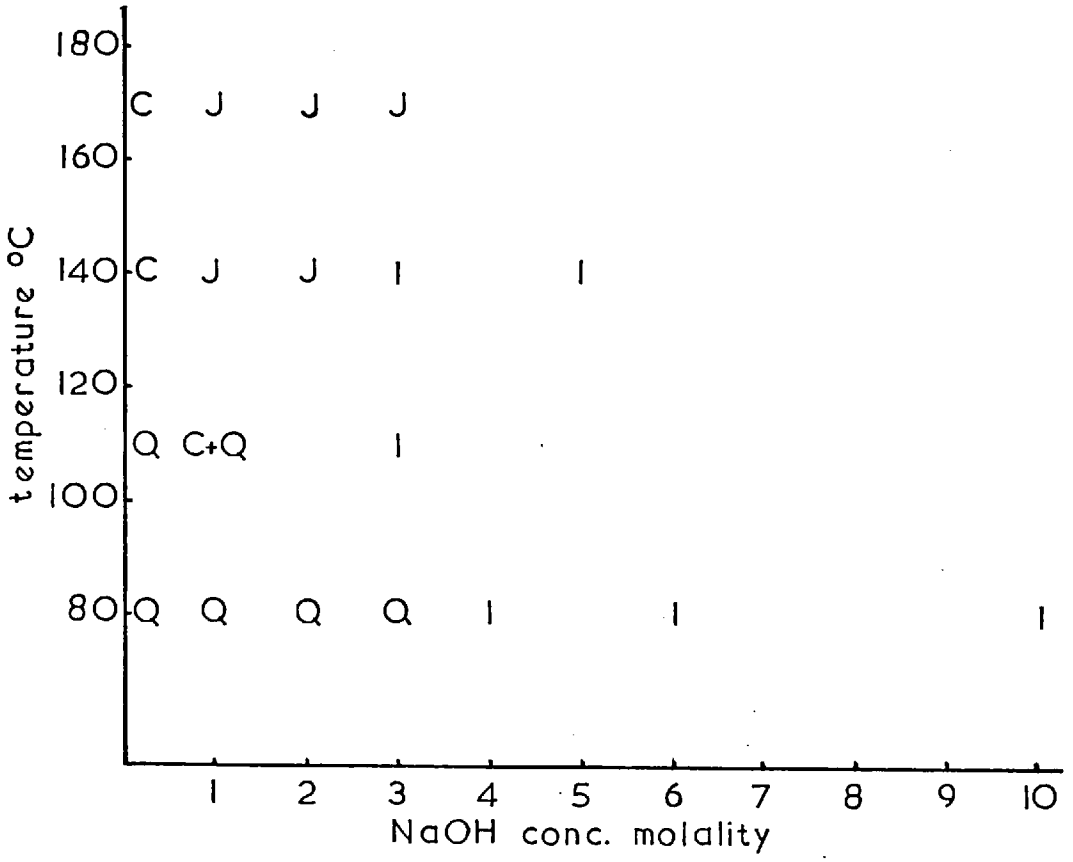

3.2.3 The Reactions of Metakaolinite with Silica and Sodium Hydroxide

Table 3.2.3

The general reaction compositions were:

1 metakaolinite ($Al_2O_3, 2SiO_2$) + $4SiO_2$ + 2.5 - 50Na_2O + ~ 275H_2O

rotated for 7 days at 80°.

Run No.	Concentration of alkali (molality)		Product	Description
2-30	0.5		Na-S	md.cr.
2-31	0.5	(14 days)	Na-S	gd.cr.
2-32	1.0	(3 days)	Na-R	md.cr.
2-34	1.0		Na-P2	md.cr.
2-35	1.5		Na-P2+Na-P1	gd.cr.P2,tr.P1
2-36	3.0		Na-P1+Na-I	md.cr.P1,lo.yd.I
2-38	5.0		Na-I	gd.cr.
2-39	8.0		Na-I	pr.cr.
2-23*	1.0	(3 days)(110°) $\left(\frac{SiO_2}{Al_2O_3} = 4\right)^*$	Na-B	v.gd.cr. 100%yd.
2-24	0.5	(3 days)(110°)	Na-B	v.gd.cr. 100%yd.
2-25	0.5	(7 days)(110°)	Na-B	v.gd.cr.
2-27	1.0	(3 days)(110°)	Na-P2+Na-B	gd.cr.P2,tr.B
2-28	3.0	(3 days)(110°)	Na-P2+Na-I	gd.cr.P2,tr.I
2-29	5.0	(3 days)(110°)	Na-I	gd.cr.
2-66	0.5	(3 days)(140°)	Na-B	v.gd.cr.
2-67	1.0	(3 days)(140°)	Na-B	v.gd.cr.
2-68	3.0	(3 days)(140°)	Na-B	v.gd.cr.
2-79	0.5	(3 days)(170°)	Na-B	v.gd.cr.
2-80	1.0	(3 days)(170°)	Na-B	v.gd.cr.
2-81	3.0	(3 days)(170°)	Na-B	v.gd.cr.
2-82	0.5	(8 days)(170°)	Na-B	v.gd.cr.

Figure 3.2.2.1 Metakaolinite+$4SiO_2$+2·5–50 Na_2O ∓ 275 H_2O

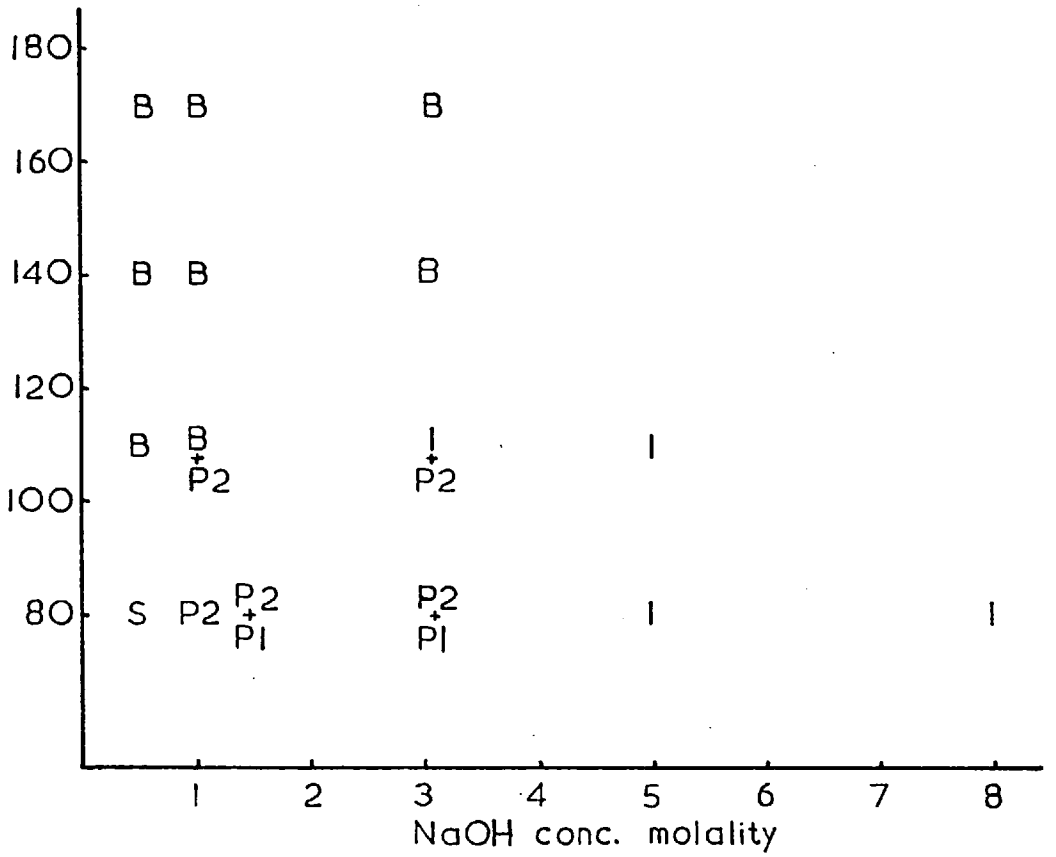

Table 3.2.4

The general reaction compositions were:

1 metakaolinite ($Al_2O_3,2SiO_2$) + $8SiO_2$ + 2.5 - 5.0Na_2O +~275H_2O

rotated for 7 days at 80°.

Run No.	Concentration of alkali (molality)	Product	Description
2-41	0.5	Am	-
2-50	0.5 (14 days)	Na-S	md.cr.
2-42	1.0	Na-S	md.cr.
2-43	1.5	Na-R	gd.cr.
2-44	1.5 (3 days)	Na-R+Na-Q	md.cr.R,tr.Q
2-45	2.0	NaP3	md.cr.
2-46	3.0	Na-P3+Na-I	md.cr.P3,tr.I
2-47	4.0	Na-P2+Na-I	md.cr.P2,tr.I
2-48	6.0	Na-I	md.cr. lo.yd.
2-49	8.0	Na-I	md.cr. lo.yd.
2-55	0.5 (3 days)(110°)	Na-P2	gd.cr.P2,
2-56	1.0 (3 days)(110°)	Na-B+NaP1	gd.cr.B,
2-57	3.0 (3 days)(110°)	Na-B+Na-P1	gd.cr.B,
2-58	5.0 (3 days)(110°)	Na-I	md.cr.
2-70	0.5 (3 days)(140°)	Na-B	v.gd.cr. hi.yd.
2-71	1.0 (3 days)(140°)	Na-B	v.gd.cr.
2-72	3.0 (3 days)(140°)	Na-B	v.gd.cr.
2-83	0.5 (3 days)(170°)	Na-B	v.gd.cr.
2-84	1.0 (3 days)(170°)	Na-B	v.gd.cr.
2-85	2.0 (3 days)(170°)	Na-C	v.gd.cr. lo.yd.
2-87	3.0 (3 days)(170°)	Na-C	v.gd.cr. lo.yd.
2-88	3.0 (7 days)(170°)	Na-C	v.gd.cr. lo.yd.

Figure 3.2.3 1 Metakaolinite+8 SiO_2 +2·5-5 Na_2O ∓ 275 H_2O

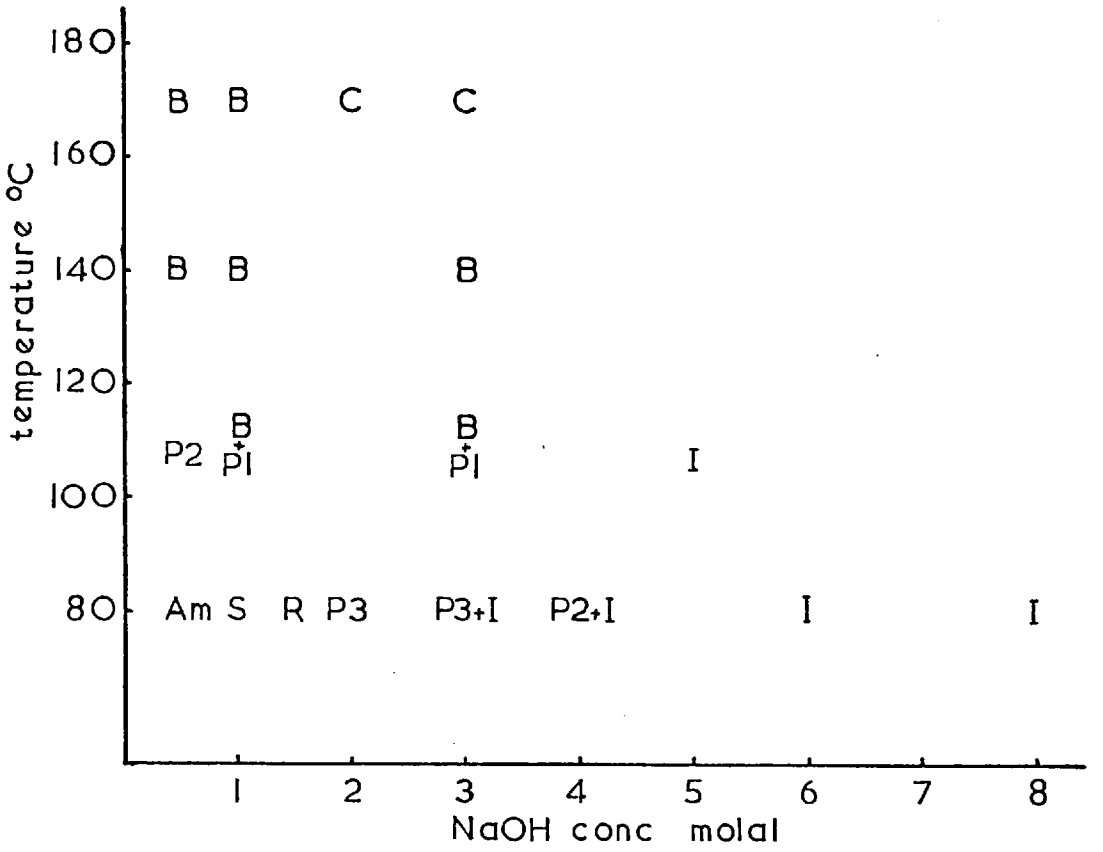

3.2.4 Properties of the Sodium Crystallization Fields

The crystallization fields in the metakaolinite-silica-sodium hydroxide system showed very similar trends to those of the potassium hydroxide system. As in Section 3.1.10, there is a tendency towards less siliceous products at higher alkali concentrations.

The yields of crystalline product decreased more in the sodium system with increasing temperature than in the potassium system. The same reduced yield was observed with increasing sodium hydroxide concentration. This corresponds with the decrease in yield of basic sodalite grown in sodium hydroxide solutions from kaolinite (Barrer and Cole (1970)).

3.2.5 Products of the Sodium Crystallization Fields

3.2.6 The Species Na-Q

The product is identical to the zeolite Linde A first reported by Breck, Eversale, Milton, Reed and Thomas in 1956. This zeolite crystallized only from the reaction mixtures with silica to alumina ratios of 2:1 (i.e. directly from metakaolinite without the addition of silica). In Table 3.2.5 the X-ray diffraction pattern is compared with that of the original synthesis by Breck (1956) and an early investigation by Barrer, Baynham, Bultitude and Meier (1959). Previous preparations have been noted in the introductory section, and now are compared with the present syntheses.

Na-Q formed at temperatures between 100° and room temperature. The best temperature range for a rapid crystallization producing yields approaching 100% was between 80° and 100°. The concentration of the sodium hydroxide varied between 0.5 molal and 3.0 molal. At concentrations of 4.0 molal co-crystallization of Na-Q and basic sodalite occurred.

Na-Q is known to be unstable in alkaline conditions. The ready re-crystallization of Na-Q to Na-P has been shown by Barrer, Baynham, Bultitude and Meier (1959) to take place at temperatures of 100° to 110°. In concentrated gels they found that the recrystallization was to basic sodalite. This is in agreement with the conditions of the crystallization field as shown in Figure 3.2.1. According to this figure high alkalinity produces basic sodalite, and low alkalinity at 80° results in Na-Q which is stable up to 14 days. Low alkalinity at 80° gives Na-Q in a very high yield and with good crystallinity as shown by the X-ray diffraction pattern. The method of synthesis may be compared with the industrial process described by Taggart (1964) where it is desired to produce zeolites in preshaped bodies such as pellets. Here metakaolinite is mixed with a hydroxide solution, formed into the desired shape, and then reacted with an aqueous hydroxide to crystallize the zeolite. The original shape is essentially retained.

The pseudo unit cell of species Na-Q was found to be cubic with a=12.30 Å. This corresponds with the value of 12.32 Å found by Reed and Breck (1956).

Table 3.2.5

Comparison of the d-spacings of species Na-Q with two early preparations.

	Na-Q		Na-Q (Breck 1956)		Na-Q (Barrer 1959)	
Indices	d	I	d	I	d	I
100	12.30	vs	12.294	100	12.36	vs
110	8.71	s	8.706	69	8.77	s
111	7.15	s	7.109	35	7.15	s
210	5.51	ms	5.508	25	6.35 5.52	w s
211	5.02	w	5.031	2	5.03	w
220	4.26	m	4.357	6	4.36	m
221,300	4.105	s	4.107	36	4.102	s
					3.899	w
311	3.714	ms	3.714	53	3.712	s
320	3.415	m	3.417	16	3.413	m
321	3.289	ms	3.293	47	3.287	ms
					3.072	vw
410,322	2.990	vs	2.987	55	2.982	vs
411,330	2,902	m	2.904	9	2.900	m
420	2.751	m	2.754	12	2.751	m
421	2.685	m	2.688	4	2.681	mw
332	2.625	ms	2.626	22	2.623	s
422	2.515	mw	2.515	5	2.512	mw
430,500	2.465	w	2.464	4		
511,333	2.370	w	2.371	3		

The rate of formation of zeolite Na-Q from gels has been investigated by Flanigen and Breck (1960), Kerr (1966) and Ciric (1968) (see Section 1.2). Their results are now compared with the kinetics of Na-Q formation from metakaolinite.

The method followed was that described in Section 2. The reaction is:

$$Al_2O_3.2SiO_2 + 2NaOH + xH_2O \xrightarrow{80^\circ} Na_2O,Al_2O_3,2SiO_2,4.5H_2O + (x - 4.5)H_2O$$

The results are given in Table 3.2.6 and are plotted in Figure 3.2.4. The crystallizing components in solution soon reach a maximum concentration very similar to the reactions of metakaolinite producing K-G (Section 3.1.5). Here, as with KOH solutions, there is a primary plateau region of the curve showing the per cent water sorption which probably indicates the presence of an intermediate gelatinous species. This product when dried and rehydrated contained about 5% by weight of water (see Figure 3.2.4). The kinetic curve for Na-Q shows the autocatalytic form typical for zeolite crystallization. The time to reach maximum yield is about 24 hours for metakaolinite magmas at 80° in 1N sodium hydroxide. This contrasts with the very short time required for

Figure 3.2.4 The Crystallization of Species Na-Q

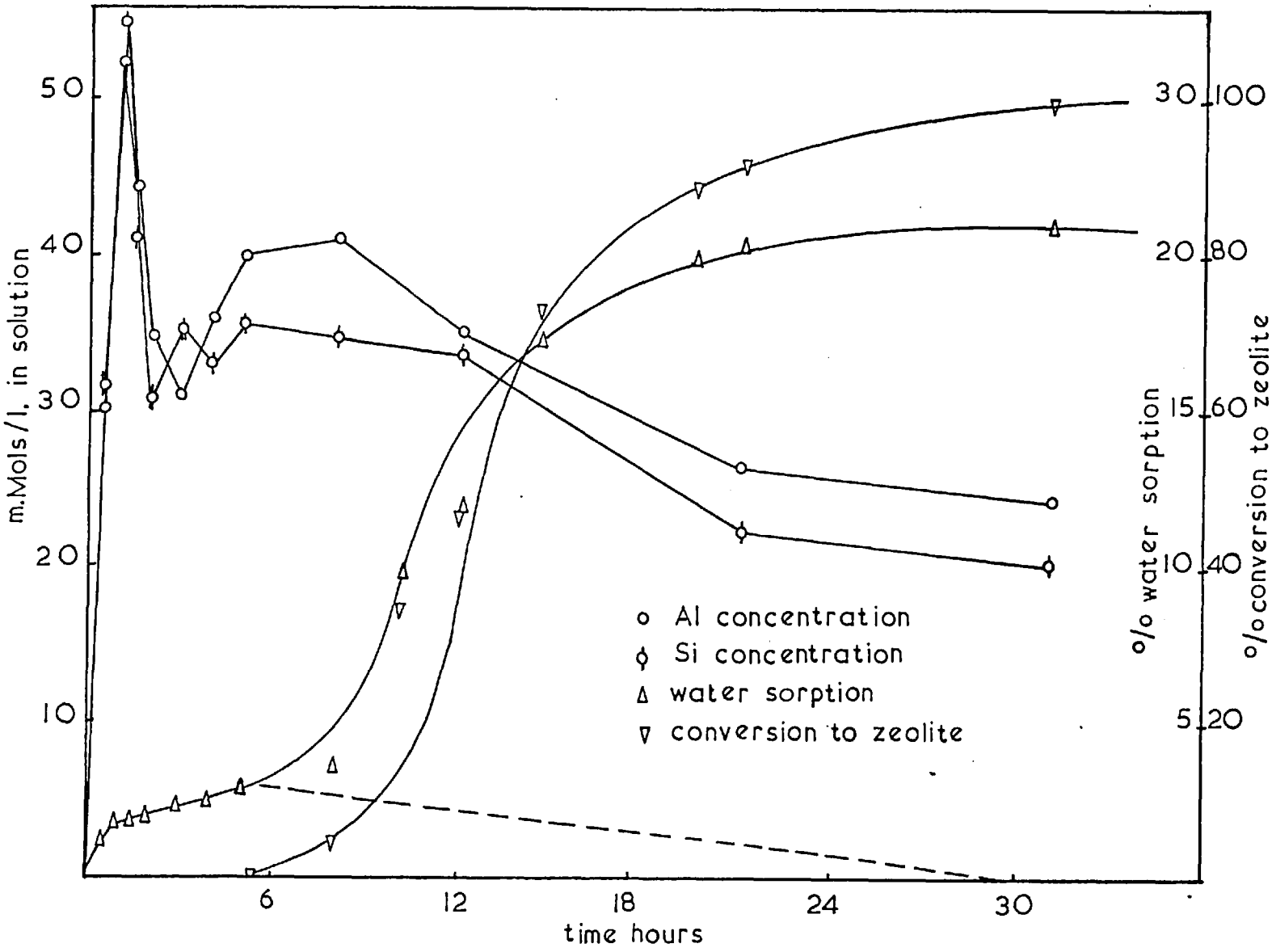

Table 3.2.6

Results of kinetic measurements and solution compositions for production of Na-Q at 80°C from metakaolinite in 1 N NaOH solution.

The initial concentration of metakaolinite = 100 mMols/l. of solution.

Time hours	Concentration of Al, Si in solution mMols/litre		% by weight water sorption	% conversion to zeolite
	Al	Si		
0.5	30.0	31.2	1.1	0
1.0	52.0	54.7	1.7	0
1.5	44.0	41.7	1.7	0
2.0	34.8	30.9	1.9	0
3.0	31.0	35.0	2.3	0
4.0	36.0	33.0	2.5	0
5.0	40.0	35.5	2.8	0
5.5	-	-	-	0
8.0	41.0	34.8	3.5	5
12.0	35.0	33.7	12.0	46
14.5	-	-	17.4	73
18.5	-	-	19.9	89
21.0	26.5	22.5	20.4	92
32.0	24.5	20.5	21.0	99

gels at 100° C. Ciric has found the time needed for complete crystallization at 100° to vary between two and six hours depending upon the Na_2O/Al_2O_3 ratio.

For the crystallization both of K-G and of Na-Q there is a decrease in the dissolved alumina and silica to values which appear to remain almost constant. Thus a solution of a definite composition comes to equilibrium with the zeolitic species. A further example of this general observation and an interpretation are given in subsequent sections.

The chemical analysis of one of the products obtained from metakaolinite and 2 molal sodium hydroxide is compared below with a typical product obtained from gels:

Mole Ratio	Metakaolinite	Gel (Breck 1956b)
Na_2O	1.0	0.96 ± 0.04
Al_2O_3	1.0	1.00
SiO_2	2.0	1.92 ± 0.09
H_2O	4.5	4.7

These compositions show no significant differences.

3.2.7 The Species Na-C

This product was identified as basic cancrinite. In the sodium system it formed only at higher temperatures (cf. Figure 3.2.3). 100% yields occurred at 170° to give perfectly shaped hexagonal rods (Plate 3.2.1). Barrer and White (1952), in their early study of the crystallization of sodium aluminosilicate gels, found the formation of basic cancrinite restricted to elevated temperatures of 330° - 450°. Recently Barrer and Cole (1970) have found that the presence of certain soluble salts such as nitrate preferentially results in cancrinite formation at temperatures as low as 80° in the kaolinite-NaOH system. In the present syntheses from metakaolinite, in the absence of salts, cancrinite was formed only at temperatures above this temperature. Nevertheless formation temperatures are significantly lower than those in the work of Barrer and White using gels. The crystallization of metakaolinite in the mixed sodium-lithium system yielded a basic cancrinite at 80° (Section 3.6.3).

The crystals formed at 170° gave sharp X-ray diffraction patterns. The d-spacings of one of these are given in Table 3.2.7 along with those of a standard sample.

Plate 3.2.1 Scanning Electron Micrographs of Na-C

Hexagonal rods of synthetic cancrinite X1530

X2700

Table 3.2.7

The d-spacings of species Na-C and basic cancrinite.

Na-C		Basic Cancrinite (Villiger 1970)
d	I	d
6.465	s	6.363
5.577	m	5.510
4.748	vs	4.697
4.205	ms	4.165
4.058	w	4.023
3.823	w	3.779
3.706	vs	3.673
3.274	vs	3.249
3.080	w	3.057
3.023	w	2.999
2.778	s	2.755
2.742	w	2.713
2.652	ms	2.634
2.611	s	2.596
2.544	m	2.528
2.449	s	2.434
2.422	m	2.405
2.287	m	2.273
2.213	w	2.203
2.195	m	2.182
2.132	s	2.121

The dimensions of the hexagonal unit cell were $a = 12.77$ and $c = 5.31$ Å, It was noticed that among different preparations there was a small difference in unit cell size. This is presumably due to small differences in either framework composition of the cancrinite or base content, and was also observed by Barrer and White (1952).

3.2.8 The Species Na-I

This product, basic sodalite, occurred over a large area of the sodium crystallization field and, as will be seen in Section 3.6, over a large part of the mixed cationic crystallization fields. Syntheses of Na-I were possible over the full range of silica to alumina ratios studied (i.e. 2:1 to 10:1), and over a temperature range from 80° to 140°. The position of basic sodalite in the sodium crystallization field corresponds with the general observations made on the potassium system. That is, this felspathoid with a low silica to alumina ratio of two grew from magmas of increasing silica content only in areas that had increased alkalinity. For example, at 110° with rotation, the alkali concentrations were:

Silica:alumina ratio of starting composition	Molality of NaOH in position of a major yield
2	3
6	5
10	>5

Siliceous sodalites are also possible. Thus, Baerlocher and Meier (1969) have made a sodalite of composition:

$$(CH_3)_4N,\ AlSi_5O_{12}$$

by employing tetramethyl ammonium ($(CH_3)_4N^+$) as the cation in syntheses. The size of this cation decreases the number which it is possible to fit into the framework and so necessitates formation of a sodalite having a high silica to alumina ratio of 10 and correspondingly low framework charge. Moreover the size of the $(CH_3)_4N^+$ ion is such that this product is anhydrous.

The chemical analysis of a Na-I product crystallized from metakaolinite at 4 molal NaOH and 80° was:

	weight per cent	Molar ratio
Na_2O	24.5	1.29
SiO_2	37.3	2.03
Al_2O_3	31.2	1.00
H_2O	6.8	1.25

This gives a compositional formula of

$$Na_2O,Al_2O_3,2.03SiO_2,0.58NaOH,1.25H_2O$$

A comparison may be made with the composition of the basic sodalite used by Barrer and Falconer (1956) in their ion-exchange investigations. This was:

$$Na_2O, Al_2O_3, 2.05SiO_2, 0.34NaOH, 1.51H_2O$$

Barrer, Cole and Sticher (1968) plotted the dependance of water and sodium hydroxide contents upon concentration of alkali in the synthesis. With increasing sodium hydroxide concentrations the water content decreased while the amount of intra-crystalline sodium hydroxide increased. From the composition of the gel used to prepare the sample of basic sodalite of Barrer and Falconer (Barrer and White 1952) the approximate concentration of alkali was calculated to be about 2.7 normal. Thus a comparison of the synthesis conditions of both Barrer and Falconer's sample and the one from metakaolinite in this work (4 M sodium hydroxide) with the final content of water and sodium hydroxide show the results to be compatible with the relationship found by Barrer, Cole and Sticher (1968). The starting materials varied in all three cases. Barrer and Falconer's basic sodalite was produced from gels, that of Barrer, Cole and Sticher from kaolinite, and in the present work from metakaolinite.

Thus for making basic sodalite a variety of starting materials is suitable and only the crystallization conditions need be changed.

In a number of syntheses the X-ray diffraction pattern of the product revealed a mixture of two basic sodalites having slightly different unit cell dimensions. Examples of these are given in Tables 3.2.8 and 3.2.9

Table 3.2.8

The d-spacings of basic sodalites prepared at various alkali concentrations from metakaolinite rotated at 80°.

Int.	4 molal	6 molal		10 molal		Indices
s	6.30	6.30	6.30	6.30	6.29	110
mw	4.45	4.46	4.45	4.47	4.44	200
vw	4.00	4.00	4.00	4.00	3.98	210
s	3.63	3.65	3.63	3.65	3.61	211
m	3.15	3.16	3.15	3.17	3.13	220
s	2.82	2.84	2.82	2.84	2.80	310
s	2.568	2.569	2.565	2.569	2.551	222
m	2.375	2.400	2.377	2.402	2.360	321
s	2.100	2.120	2.100	2.121	2.090	411
w	1.902	1.911	1.900	1.912	1.898	332
w	1.815	1.830	1.815	1.833	1.805	422
m	1.745	1.760	1.743	1.762	1.740	431
$\underline{a}$ =	8.905	8.949	8.910	8.957	8.863	

Table 3.2.9

The unit cell dimensions of basic sodalites from the reaction of metakaolinite with sodium hydroxide rotated at 80°.

Molality of NaOH	Unit cell determined Å		
4	$a = 8.905$		$\Delta a = 0$
6	$a_1 = 8.949$	$a_2 = 8.910$	$\Delta a = 0.039$
10	$a_1 = 8.957$	$a_2 = 8.863$	$\Delta a = 0.094$

Barrer and Cole (1970) have measured the kinetics of sodalite formation in the presence of $NaClO_4$ by determining the amount of salt in the product. A sigmoidal growth curve was observed similar to those in Sections 3.1.5 and 3.2.6.

3.2.9 The Species Na-B

This product was identified as synthetic analcite. The X-ray diffraction pattern is given in Table 3.2.10, which for comparison includes a natural analcite reported by Coombs (1955). Analcite has been synthesized in many crystallization fields with silica to alumina ratios from 4 to 10 (cf. Introductory Section). Barrer with White (1952) and with Baynham, Bultitude and Meier (1959) and Saha (1959) have found analcite to crystallize from gel and glass compositions with a silica to alumina ratio as low as 2. In the recrystallization of metakaolinite, analcite did not form when the silica to alumina ratio was 2 but appeared when, by addition of extra silica, the ratio was raised to 4.

Saha (1959), starting from glasses of albite, anhydrous analcite and anhydrous natrolite compositions, produced a range of analcite compositions. The unit cell was found to increase linearly with decreasing silica content. A variation of unit cell was also found by Guyer (1957). In this work two preparations of analcite were made under identical conditions apart from the concentration of sodium hydroxide in the synthesis mix. The name analcite is used for synthetic analcime (Na-B) consistent with all previous syntheses in these laboratories.

Table 3.2.10

The d-spacings of species Na-B and a natural analcite (Coombs 1955).

Species Na-B	Natural analcite	
-	6.87	5
5.603	5.61	80
4.852	4.86	40
3.664	3.67	20
3.433	3.43	100
2.926	2.925	80
2.795	2.801	20
-	2.693	50
2.503	2.505	50
2.423	2.426	30
	2.226	40
2.169	2.168	5
2.116	2.115	5
2.023	2.022	10
1.941	1.940	5
1.904	1.903	50
1.868	1.867	40
	1.833	5
a = 13.73	a = 13.72	

This resulted in two very good analcites with differing unit cell sizes. These were measured and corrected with the internal standard as described in Section 1.3 and the results are given below in Table 3.2.11.

Table 3.2.11

Molality of NaOH		Unit cell edge Å	Unit cell volume $Å^3$
(I)	0.5	13.694 ± 0.004	2568 ± 2.0
(II)	1.0	13.723 ± 0.002	2584 ± 0.5

Analcite crystallized from metakaolinite over a temperature range from 110° to 170°. Barrer, Baynham, Bultitude and Meier (1959) found the lowest temperature of synthesis of analcite from their sodium aluminosilicate gels to be 150° C, in agreement with the previous investigation of Barrer (1949). The analcite formed from metakaolinite and silica at 110° (Table 3.2.2) had a very good crystallinity. This was aided by the rapid rotation of the autoclave during synthesis which gave greater homogeneity to the reacting system. Such low temperature syntheses may be of geological interest in relation to the reports by Keller (1952, 1953) on the identification of large beds of analcite. The origin of which is suggested to be the circulation of sodium rich waters in lakes.

Plate 3.2.2 Scanning Electron Micrographs of Na-B

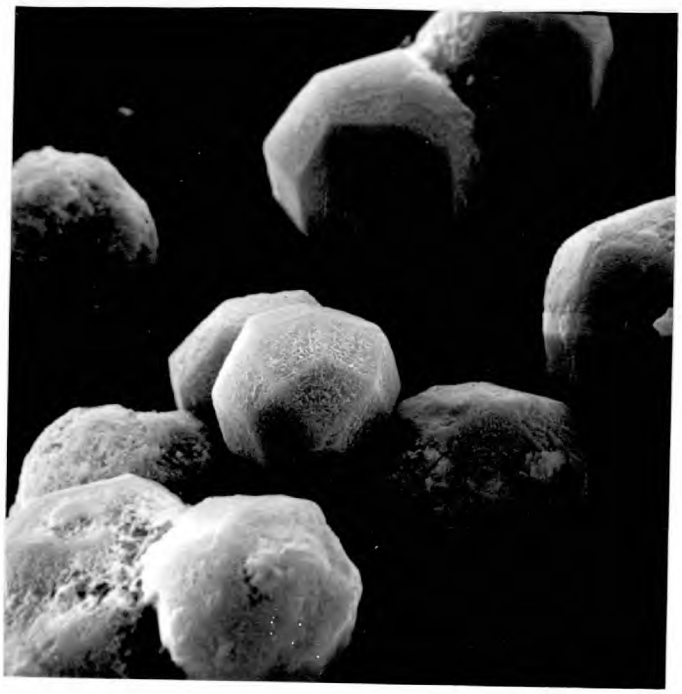

X1530

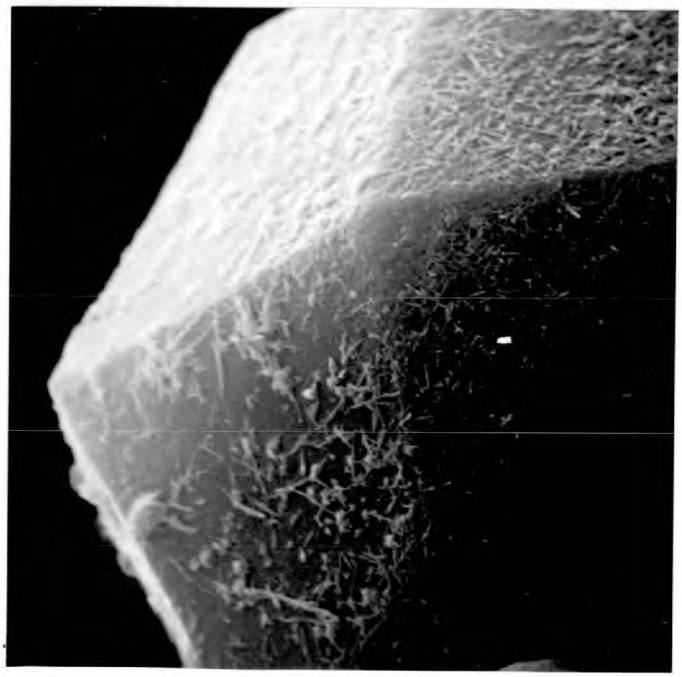

X8500

Barrer and White (1952) reported three crystal habits of synthetic analcite. These were icositetrahedra, spherulites and cubes. The preparations from metakaolinite produced only icositetrahedra. Scanning electron micrographs as shown in Plates 3.2.2 show the surface of these to have a fine web of needle-like particles which persistent washing would not remove. Very careful examination of the X-ray diffraction patterns failed to show the presence of a second crystalline phase. This was due to the very small amount present (less than 1%).

The differential thermal analysis and the thermogravimetric analysis of Na-B are shown in Figure 3.2.5 A comparison with the natural analcite reported by Koizumi (1953) shows that water loss in both natural analcite and in Na-B occurred in the relatively high temperature range for zeolitic dehydration of 300-500°. The slow water loss is a result of the very restricted channel system in analcite (Taylor 1930).

The sample was heated on a Guinier-Lenné camera to 800°. The resulting film is shown in Plate 3.2.3. The film was measured and the unit cell edge was calculated for various temperatures. The results obtained are shown in Table 3.2.12.

Plate 3.2.3

The continuous-heating X-ray diffraction pattern of synthetic analcite heated at 0.4°/min. in air (Plate 3.7.1*)

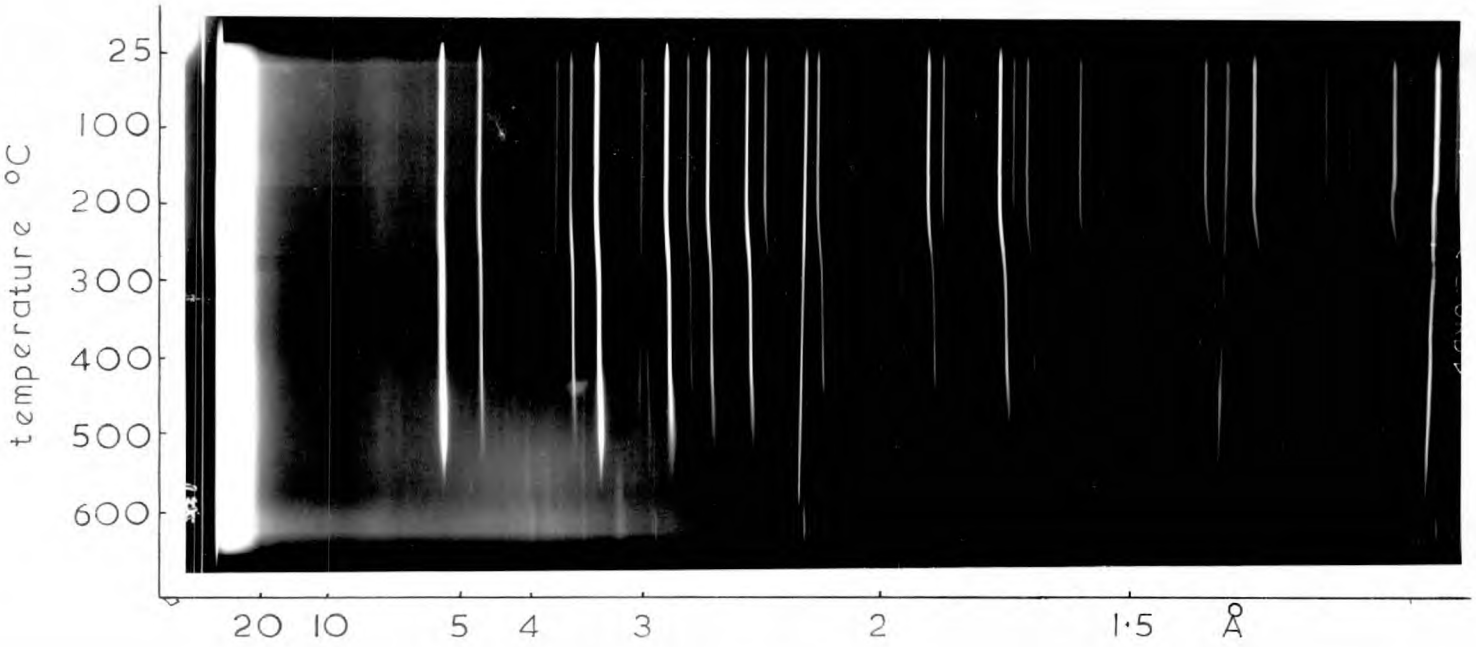

Table 3.2.12

Temperature °C	Unit cell edge a Å
25	13.78
275	13.77
360	13.73
420	13.67
590	13.63

In Figure 3.2.5 the unit cell edge for synthetic analcite is plotted below the T.G.A. and D.T.A. curves Although the heating rates for the thermogravimetric, differential thermal and Guinier-Lenné apparatus were different, Figure 3.2.5 shows the unit cell contracting with water loss up to 425° then becoming unstable as lattice breakdown occurs at higher temperatures.

The chemical analyses of both preparations described in Table 3.2.11 were found to be:

	Molar composition	
	I	II
Na_2O	1.0	1.0
Al_2O_3	1.0	1.0
SiO_2	4.32	4.09
H_2O	1	1

Figure 3.2.5 Effect of Heating on Zeolite Na-B Analcite

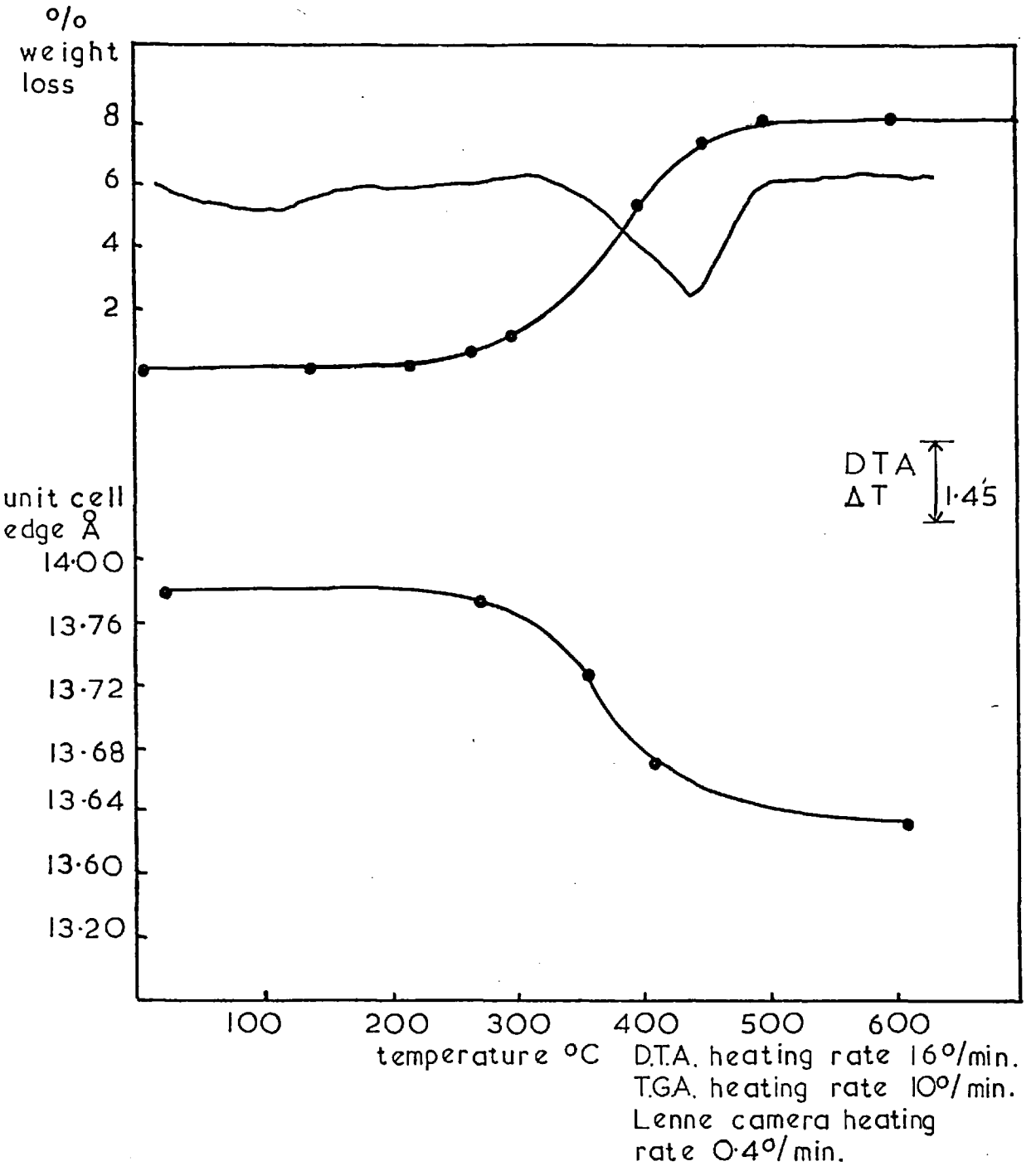

The analcites are compared with preparations of Saha (1959) and Barrer and White (1952a) below in Table 3.2.13.

In Table 3.2.13, the composition range for synthetic analcite was found by Saha to have silica to alumina ratios from 3 to 6. It should be noted that these values are the initial composition of the reacting mix and that no chemical analysis of the product was reported. The analcites synthesized from metakaolinite-silica reactions with silica:alumina ratios of 4 to 10 were found to have silica to alumina ratios of approximately 4 to 4.3. The composition of 68 natural analcites has been noted by Saha (1959) where it may be seen that the majority have silica to alumina ratios in the range of 4.0 to 4.6.

Table 3.2.13

Properties of synthetic analcites of Saha (1959), Barrer and White (1952a) and this work.

Analcite composition	SiO_2/Al_2O_3	Unit cell edge Å
$Na,Al,Si_{1.5}O_5,0.75H_2O$ (natrolite composition) (Saha)	3	13.77 +
Na,Al,Si_2O_6,H_2O (ideal analcite composition) (Saha)	4	13.73 +
$Na,Al,Si_3O_8,1.5H_2O$ (albite composition) (Saha)	6	13.67 +
$Na_2O,Al_2O_3,4.32SiO_2,H_2O$	4.32	13.69
$Na_2O,Al_2O_3,4.09SiO_2,H_2O$	4.09	13.72
$Na_2O,Al_2O_3,4SiO_2,H_2O$	4	13.67

+ Values read from the graph of Saha (1959).

3.2.10 The Species Na-J

This product was identified as nepheline hydrate I first synthesized by Barrer and White (1952a). Other previous syntheses are noted in Section 1.2. Na-J crystallized from metakaolinite as the sole product at temperatures above 140°. The crystal habit was rod shaped as seen under the electron microscope. It did not exhibit the twinning giving it the hexagonal appearance described by Barrer and White. The d-spacings of species Na-J were measured and indexed according to a unit cell proposed by Edgar (1964). The unit cell was found to be orthorhombic with a = 8.21, b = 7.47 and c = 5.23 Å. In Table 3.2.14 the observed and the calculated d-values are given together with the d-spacings of the original preparation for comparison.

The composition of Na-J was $Na_2O, Al_2O_3, 2SiO_2, H_2O$, which may be compared with the analysis of Guth (1965) who found $0.99Na_2O, Al_2O_3, 1.92SiO_2, 1.17H_2O$.

The differential thermal and thermogravimetric curves for Na-J are shown in Figure 3.2.6. There is a two-step dehydration where about 1% by weight is lost up to 200° and then a loss of approximately 4% to about

Table 3.2.14

The d-spacings, observed and calculated for Na-J compared with nepheline hydrate I of Barrer and White (1952a).

Na-J a=8.21 b=7.47 c=5.23 Å				Nepheline hydrate I	
I		d_{obs}	d_{calc}	I	d
m	(100)	8.3	8.21	60	8.3
m	(010)	7.47	7.47	60	7.4
				40	6.38
mw	(110)	5.52	5.52	50	5.52
w	(101)	4.72	4.41	10	4.72
s	(011)	4.39	4.28	90	4.39
w	(200)	4.10	4.10	10	4.11
w	(111)	3.79	3.80		
w	(210)	3.61	3.60	10	3.61
s	(120)	3.401	3.400	100	3.40
w	(201)	3.225	3.229	10	3.22
s	(211)	2.961	2.964	90	2.95
m	(121)	2.848	2.850	60	2.84
ms	(002)	2.602	2.615	70	2.60
s	(221)	2.443	2.443	70	2.43
w	(311)	2.304	2.306	10	2.30
w	(320)	2.200	2.207	40	2.19
w	(131)	2.172	2.168		
w	(212)	2.111	2.115	30	2.11

Figure 3.2.6 Species Na-J Nepheline Hydrate I

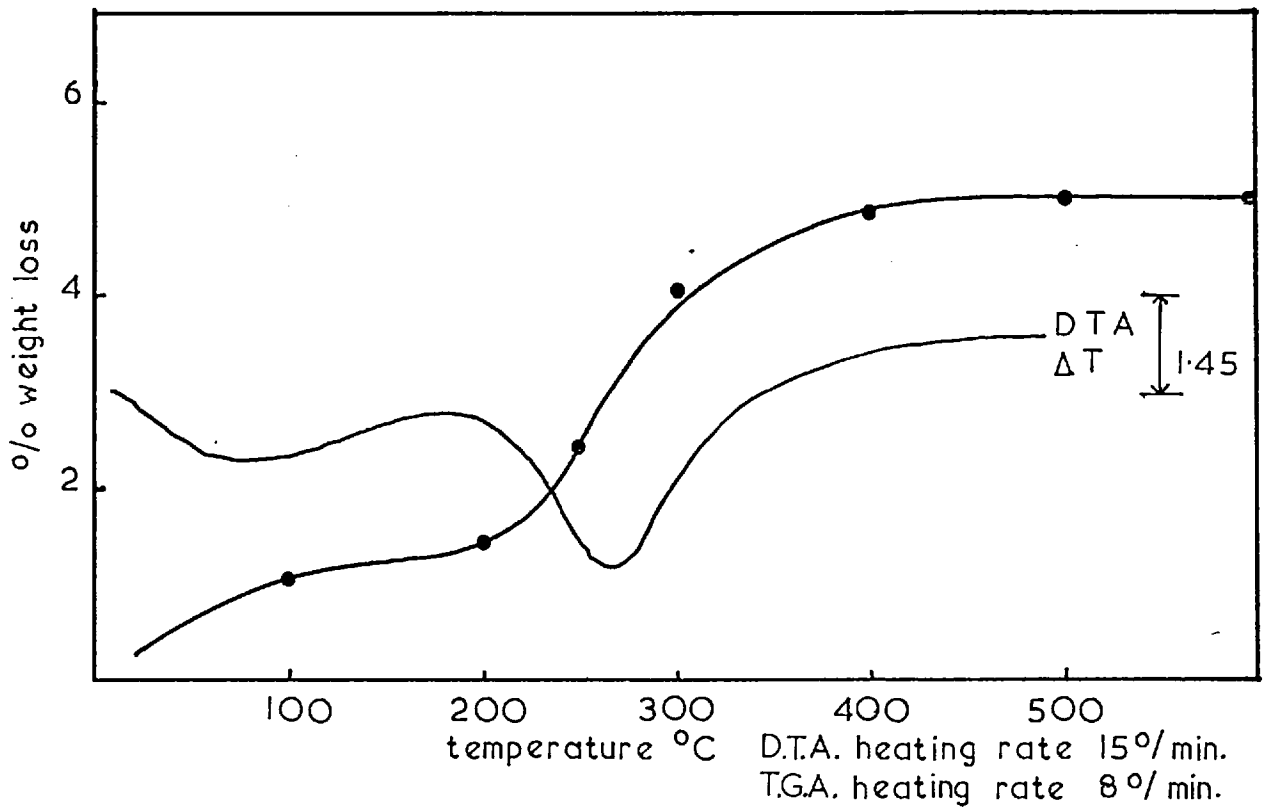

400°. Here the weight becomes constant. Heating Na-J to 500° resulted in lattice breakdown. A sample heated to 350° and then exposed to a relative humidity of 56% for seven days showed only surface water.

3.2.11 The Species Na-P

The previous syntheses and structural relationships of the members of this group P1, P2 and P3 have been discussed in Section 1 and here. Metakaolinite provided a source of the P1-pseudo cubic, P2-tetragonal and, in one synthesis, P3-orthorhombic member of this group. The orthorhombic form crystallized as approximately 60% of the product in a mixture with analcite. This synthesis was not reproducible.

The Na-P zeolites crystallized from mixtures with silica:alumina ratios of 4 to 10 and over a temperature range of 80° to 140°. None of the crystallizations from metakaolinite (with a ratio of 2) produced the P phases. Barrer et al (1959) found that P crystallized from gels with alumina:silica ratios of 1:12. Both Taylor and Roy (1964) and Saha (1961) have noted a linear decrease of refractive index with silica content, and Taylor has deduced from the refractive indices quoted by Barrer that his samples corresponded with a composition range having ratios 1:2 to 1:6.

From Tables 3.2.1 - 3.2.4 and Figures 3.2.2 and 3.2.3 there appears to be no correlation between the occurrence of P1 and P2 and magma or final crystal compositions other

Table 3.2.15

Mole ratio	Synthesis from metakaolinite + $2SiO_2$ 'cubic' Na P1	Synthesis from metakaolinite + $4SiO_2$ tetragonal P2	Na P Barrer et al (1959)	Na P Taylor and Roy (1964) tetragonal
Na_2O	0.99	1.00	1.0	0.89
Al_2O_3	1.00	1.00	1.0	1.00
SiO_2	3.40	4.10	3.3	3.18
H_2O	4.0	4.5	4.3	4.62

	Regis et al (1960)	Borer (1969) tetragonal	Borer (1969) cubic	Dyer (1968) cubic
Na_2O	0.7-0.9	1.00	1.00	1.00
Al_2O_3	1.0	1.00	1.00	1.00
SiO_2	7.6-7.8	4.40	3.03-3.65	3.80
H_2O	16.0-19.8	4.60	4.10-4.40	4.60

than the tendency for the 'cubic' P1 to form in lower temperature regions. Typical compositions of NaP for two preparations are given in Table 3.2.15 together with previous syntheses for comparison.

The orthorhombic P3 was not analysed due to its co-crystallization with analcite. But its position in the crystallization diagram at 110°, in a region dominated by analcite as the stable product, may be examined in the light of the hydrothermal stability studies of Taylor and Roy (1964). Some of their results are given in Table 3.2.16.

The P2 tetragonal framework undergoes recrystallization to the H (or M) structure in the case of the lithium and potassium ion-exchanged forms. The sodium and calcium forms convert respectively to analcite (Taylor 1930) and wairakite (Coombs 1955). The mixed potassium-sodium form produces a phase of the phillipsite type (see Section 3.6.8 for its synthesis and characterization) which is probably rich in potassium and analcite rich in sodium. The same division of cations occurs with mixed potassium-calcium forms to give K-M and the calcium analogue of analcite, called wairakite.

Table 3.2.16

	Initial product	Temperature	Final product
wet runs	$Na\text{-}P_T$	200°	analcime + P_T
	$Na\text{-}P_T$	260°	analcime
	$Li\text{-}P_T$	260°	H* + Li-A
	$K\text{-}P_T$	310°	(H)
	$Ca\text{-}P_T$	295°	wairakite + P_T
	$Ca\text{-}P_T$	310°	wairakite
	$Ba\text{-}P_T$	< 200°	H
dry runs	$Na_{56}K_{64}\text{-}P_T$	220°	H + analcime
	$Na_{28}K_{72}\text{-}P_T$	255°	H + analcime
	2 $K_{62}Ca_{38}\text{-}P_T$	220°	H
	2 $K_{62}Ca_{38}\text{-}P_T$	315°	H + wairakite
	2 $K_{34}Ba_{66}\text{-}P_T$	< 150°	H

* H refers to the phase previously called M (e.g. K-M in Section 3.1.6).

( ) indicates - not reproducible.

In the synthesis crystallization field (Figure 3.2.2) analcite is stable at a much lower temperature than that shown in Table 3.2.16 and P2 does not persist at temperatures of 200°. Here again is evidence of the lowering of the temperature of formation of species, considered high temperature phases, in highly alkaline media.

In Section 3.6 the systems containing NaOH + LiOH and NaOH + KOH as the bases were considered. The syntheses show the compositional limits in the formation of species P and M at relatively low temperatures. The stability of the P framework is increased with potassium content to such an extent that K-M is not reproducibly formed (Table 3.2.16) at 310°. Higher temperatures, where the recrystallization of K-P takes place readily, are beyond the stable region of K-M and the conversion to leucite.

The X-ray diffraction pattern of Na-P1 is shown in Table 3.2.17. This was indexed to give a pseudo-cubic cell with a unit cell edge of 9.99 Å.

Table 3.2.17

	$d_{(obs)}$	I	$d_{(calc)}$	Barrer (1959)	I	Borer (1969)	I
110	7.10	s	7.05	7.10	s	7.143	52.3
200	5.00	m	5.00	5.00	m	5.034	28.5
211	4.08	s	4.08	4.10	s	4.108	50.2
220	3.531	w	3.532	3.45	vw	-	
310	3.159	vs	3.159	3.18	vvs	3.177	100.0
222	2.887	w	2.885	2.90	vw	2.899	7.5
321	2.668	s	2.670	2.68	s	2.683	55.4
400	2.500	w	2.499	2.52	vw	2.513	5.0
410	-			2.41	vw	-	
411	2.357	m	2.355	2.36	w	2.364	10.9
420	2.246	w	2.235	2.23	vw	2.243	1.7
332	2.129	vw	2.130			2.140	1.6
422	2.044	mw	2.040			2.050	5.1
510	1.965	m	1.960			1.970	16.0
521	1.826	w	1.824			1.832	2.7
440	1.768	w	1.766			1.775	8.3
530	1.719	m	1.713			1.722	13.3
600	1.669	m	1.665			1.672	11.9

The X-ray diffraction pattern of P2 having a tetragonal unit cell a = 10.11, c = 9.80Å is given in Table 3.2.18. Here it is compared with its K and Ca exchanged forms and also the mineral *garronite*[*]. Barrer et al (1959) first indicated this similarity and later it was confirmed by Taylor and Roy (1964) who compared the K and Ca ion-exchanged forms of both the mineral and Na-P2. Included in Table 3.2.18 is the K-M phase produced by the hydrothermal recrystallization of the K exchanged Na-P2.

The effects of dehydration and heating have been investigated by Barrer, Bultitude and Kerr (1959), Taylor and Roy (1965) and lately by Borer (1969). Barrer showed that a distinct step occurred in the dehydration curve of Na-P1 between 73° - 83°. Upon rehydration hysteresis was observed. Taylor and Roy found that cubic Na-P and tetragonal Na-P were related by a reversible displacive transition at 60° ± 3. The transition point for the K-exchanged phase of composition $Na_{8.3}K_{17}$-P2 was 34° ± 3, while the K-exchanged K-P2 underwent a continuous reversible collapse on heating. Since the products were identical to those of Borer the T.G.A. and D.T.A. curves were not repeated but are reproduced in Figure 3.2.7. The weight loss curves are very similar

[*] This sample was kindly supplied by Dr. G.P.L. Walker of the Geology Department, Imperial College.

Table 3.2.18

A comparison of the d-spacings of Na-P2 with related species

	Na-P2		hydrothermal recrystallization ↓ 310° K-M	K$^{ex.}$-P2[1]		Ca$^{ex.}$-P2[1]		Garronite[2]	
a=	10.11		orthorhombic	9.93		9.88		9.85	
c=	9.80			9.67		10.30		10.32	
			9.8						
			8.27						
110	7.15	s	7.14						
101	7.05	s		6.943	101	7.13	82	7.15	ms
111	5.77	w	5.37						
200	5.05	s	5.04	4.966	200	4.95	62	4.95	ms
002	4.9o	s	4.74						
201	4.49	vw	4.48						
102	4.41	w	4.29						
211	4.10	vs	4.11	4.037					
112	4.04	mw		3.983	112	4.15	71	4.12	s
202	3.52	w	3.66	3.473	211	4.07	51	4.07	m
212	3.320	m	3.44		103	3.240	40	3.22	m
301	3.186	vs	3.25	3.132	301	3.140	100	3.14	s
103	3.110	s	3.18	3.066	222	2.893	3	2.88	w
311	3.033	mw	2.96		213	2.708	9	2.66	s
113	2.969	w	2.73		312	2.674	62	2.66	s
222				2.842	004	2.573	7	2.54	vw
302	2.769	vw			411	2.334	8	2.34	w
203	2.743	vw			420	2.211	3	2.22	w
321	2.690	ms	2.67	2.649	332	2.125	3	2.12	vw
312	2.673	vw		2.634	224	2.072	5	2.05	vw
213	2.646	ms		2.609	422	2.030	2	2.03	vvw
400	2.525	mw	2.55		314	1.985	6	1.970	w
410	2.447	vw			501	1.940	5	1.938	w
322	2.428	mw							
411				2.337					
331	2.314	vw							
204			2.17	2.175					

(1) Taylor and Roy (1964)

(2) Barrer, Bultitude and Kerr (1959)

Figure 3.2.7 The Effect of Heating on Zeolites Na P1 & Na P2 as found by Borer (1969)

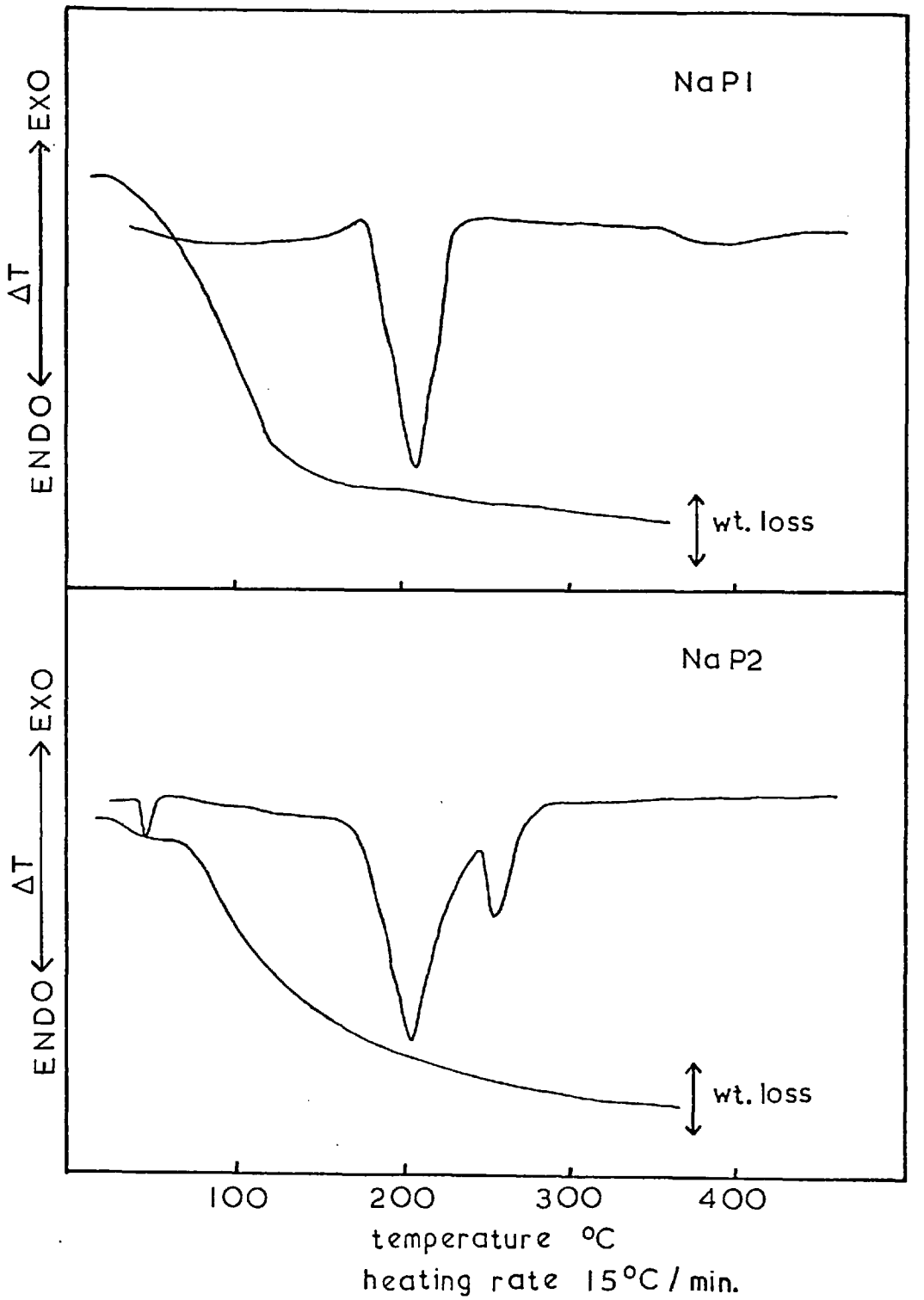

for P1 and P2 but the D.T.A. curves show marked differences. The Na-P1 shows one large exotherm corresponding to dehydration in the region of 150-200°. This peak in the Na-P2 sample is split into two which, if the Na-P1 and Na-P2 species have the same basic framework, has no apparent cause. Preceding the dehydration peaks the Na-P2 D.T.A. shows a small endothermic peak at 60° which corresponds very closely to the tetragonal-cubic transition mentioned earlier.

Properties of the species P1 and P2 which were influenced by cationic content during synthesis are examined in the section on crystallizations in the presence of two cations. These properties are discussed in relation to the quantitative ion exchange experiments of Barrer and Munday (1970).

The water content of various cationic forms of Na-P2 has been determined and are given below:

Cationic form	% weight loss on heating	% weight loss corrected to equivalent weight of Na- form
Cs^{+}	7.5	10.6
Rb^{+}	8.4	10.2
K^{+}	10.5	10.7
Na^{+}	15.2	15.2
Li^{+}	17.7	16.8
Ba^{2+}	14.9	23.8
Sr^{2+}	17.0	22.8
Ca^{2+}	19.3	21.6

In Figures 3.2.8 and 3.2.9 the thermogravimetric and differential thermal curves are shown.

Figure 3.2.8 Water Loss of Various Cationic Forms of Na-P2

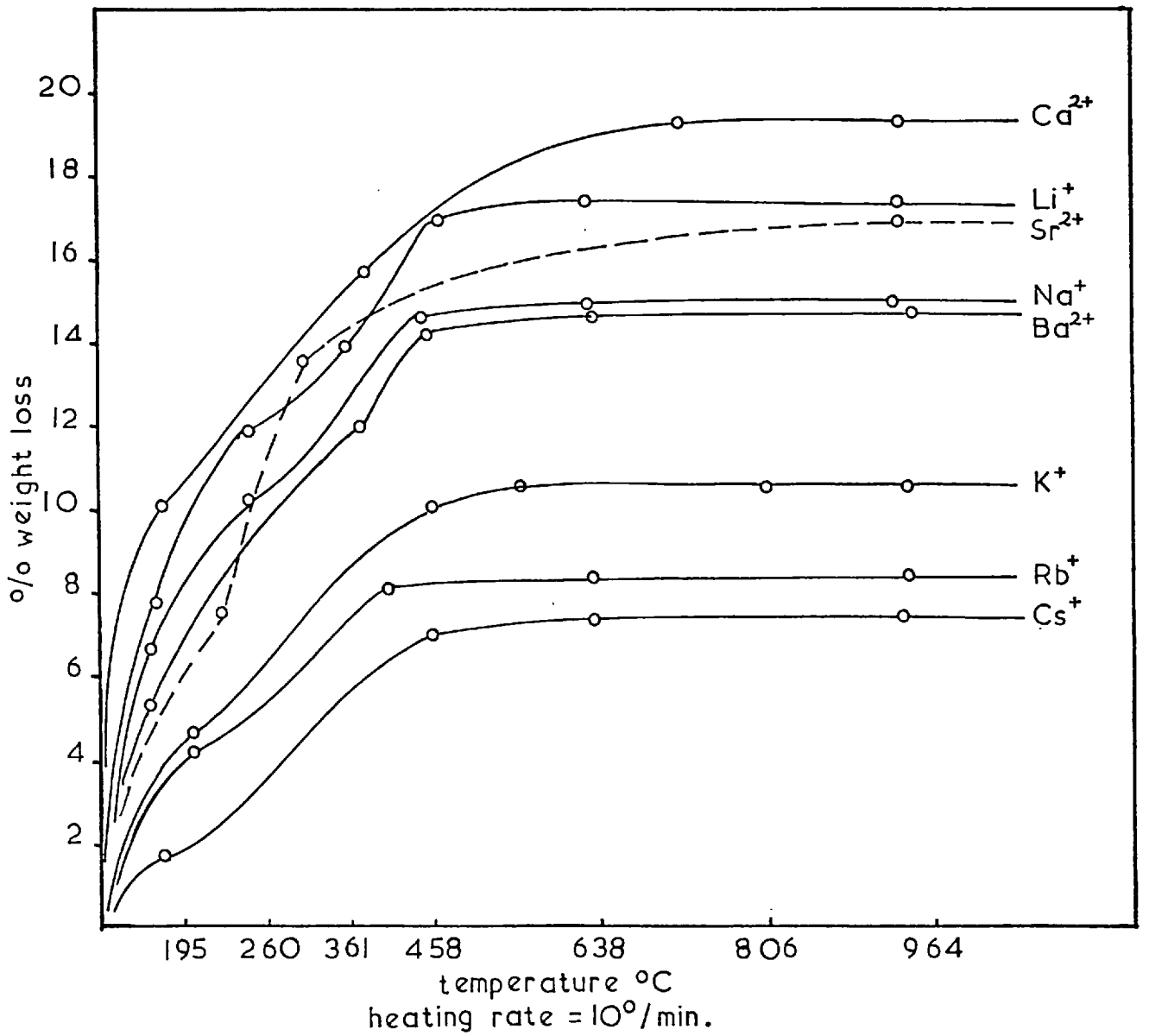

Figure 3.2.9 DTA of Various Cationic Forms of Na-P2

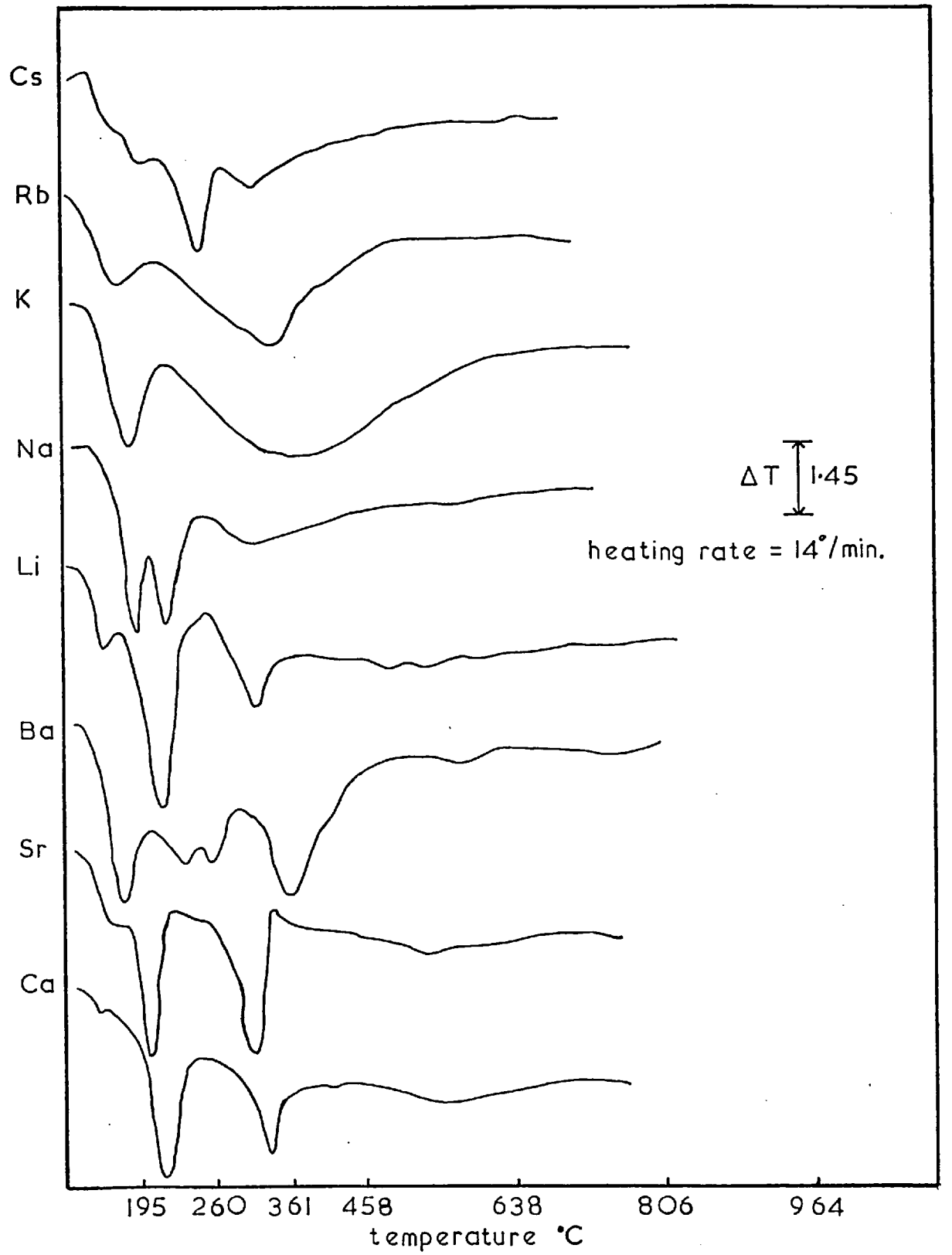

3.2.12 The Species Na-R

The product Na-R was identified as the synthetic analogue of faujasite (Bergerhoff, Baur and Nowacki, 1958) and corresponded to the synthetic zeolite Linde X (Milton 1959). Na-R crystallized from metakaolinite fortified with silica to give compositions more siliceous than that with $SiO_2:Al_2O_3 = 2$ which yields Na-Q. This may be because the final composition of Na-R is

$$Na_2O,\ Al_2O_3,\ 2.8\ SiO_2,\ 6\ H_2O$$

At 80°C the time required for maximum yield of Na-R was about 3 days (see Table 3.2.3). After this period there was a gradual conversion to Na-P2. This contrasts with species Na-Q (Section 3.2.7) which was stable under similar alkaline conditions up to 14 days. The observation that Na-Q at higher temperatures than those used for its synthesis from metakaolinite (100-110°) recrystallizes to Na-P and that the Na-R readily converts to Na-P2 at 80° is probably due to a greater compositional similarity between Na-R and Na-P than between Na-Q and Na-P. For example typical compositions are shown below.

Species	Typical molar compositions
Na-R	Na_2O, Al_2O_3, 2.8 SiO_2, 6 H_2O
Na-P	Na_2O, Al_2O_3, 3 SiO_2, 6 H_2O
Na-Q	Na_2O, Al_2O_3, 2 SiO_2, 4.5 H_2O

Kerr (1966) in a study of the relative rates of formation of zeolites Na-R and Na-P, found that Na-R nucleates more readily but has a slower growth rate than Na-P.

The yield of Na-R prepared from metakaolinite and silica, as estimated from X-ray diffraction and optical microscopy, was approximately 70% under the optimum conditions found. In Table 3.2.19 the X-ray diffraction pattern of a sample crystallized from metakaolinite and silica is compared both with natural faujasite and synthetic Linde X made from sodium aluminosilicate gels.

Table 3.2.19

A comparison of the d-spacings of Na-R with synthetic Linde X and natural faujasite.

Na-R (metakaolinite)		Natural faujasite		Linde X (Breck 1967)	
14.40	vs	14.25	vs	14.465	100
8.79	ms	8.70	s	8.845	18
7.51	m	7.38	s	7.538	12
5.70	m	5.66	vs	5.731	18
4.80	vw	4.76	s	4.811	5
4.40	w	4.36	s	4.419	9
-		4.16	w	4.226	1
-		3.90	w	3.946	4
3.79	m	3.76	vs	3.808	21
3.755	w	-		3.765	3
-		-		3.609	1
-		3.44	w	3.500	1
3.328	w	3.29	s (d)	3.338	8
-		3.19	w	3.253	1
3.050	w	3.01	w	3.051	4
2.940	w	2.93	s (d)	2.944	9
2.885	mw	2.81	s	2.885	14
2.800	w	2.75	m	2.794	8
2.710	vw	2.69	w		
2.625	mw	2.61	m		
2.589	w	2.58	mw		
		2.51	w		
		2.37	ms		
		2.29	w		
		2.17	m		
		2.15	w		

3.2.13 The Species Na-S

The product Na-S was identified as a member of the gmelinite family. The X-ray diffraction pattern exhibited both sharp and diffuse lines. There was only a minimal change in the diffraction pattern between various crystallizations of this species. This and sorption evidence indicated that Na-S was a gmelinite containing a certain amount of disorder such as stacking faults rather than a co-crystallization mixture of chabazite and gmelinite. The spacings derived from the X-ray powder diffraction pattern are shown in Table 3.2.20 where they are compared with spacings of chabazite and gmelinite.

The species crystallized from silica rich magmas with silica to alumina ratios of 6, 8 and 10. The crystallization took place in regions of low alkalinity (Figure 3.2.2) indicating that the product itself was stable only with high silica contents. Analysis of a sample gave the following composition.

	% by weight	Mole ratio
Na_2O	12.00	0.99
Al_2O_3	19.96	1.00
SiO_2	47.32	4.03
H_2O*	21.00	6.0

* equilibrated at a relative humidity of 56%.

This sample from the metakaolinite synthesis has a lower silica to alumina ratio than that of Barrer, Baynham, Bultitude and Meier (1959). This product had the following composition

$$Na_2O,\ Al_2O_3,\ 5.1\ SiO_2,\ 5.4\ H_2O$$

The product derived from metakaolinite was closer in composition to the natural gmelinite (Fischer 1966).

$$(Na_2Ca)_4\ Al_8Si_{16}O_{48} \cdot 24\ H_2O$$

giving mole ratios of

$$(Na_2O,\ CaO),\ Al_2O_3,\ 4\ SiO_2,\ 6H_2O$$

Evidence for the existence of stacking faults, other than diffuse lines in the sharp X-ray pattern is given by the sorption properties.

Table 3.2.20

A comparison of Na-S with chabazite and gmelinite.

Na-S		Gmelinite*	Chabazite*
a = 13.7 c = 10.0		a = 13.75 c = 10.05	a = 13.78 c = 15.06
11.84	m	11.911	9.355
9.00	md	7.681	6.892
6.86	s	6.877	6.369
5.99	w	5.955	5.548
-		5.123	5.020
5.01	s	5.025	4.677
-		4.630	4.322
4.46	m	4.502	4.058
-		4.108	3.979
4.00	w	4.057	3.870
3.964	mw	3.970	3.591
3.841	w	3.840	3.446
-		3.692	3.233
3.433	vs	3.438	3.184
3.510	m	3.535	3.118
3.300	vw	3.303	3.031

* Meier (1967)

The sorption capacities for oxygen of various cationic forms of Na-S are shown below. The isotherms are plotted in Figure 3.2.10 and the results of these experiments are given in Appendix 2.

Cationic form of Na-S	Oxygen sorption capacity
Li^+	160 c.c./gm. STP
Na^+	102
H^*	58
NH_4^+	18
Ca^{++}	142

* X-ray evidence showed that considerable lattice breakdown had occurred in this preparation, obtained by heating the ammonium form.

All the isotherms at 78°K in Figure 3.2.10 show surface condensation associated with hysteresis. The closure of the hysteresis loop at approximately the same relative pressure (about 0.25) for each of the cationic forms is ascribed to the sudden vapourization of the condensed oxygen as the partial pressure is lowered beyond a specific value. Hence this value appears to be characteristic of the gas and independent of both the particular zeolite and its cationic form.

Figure 3.2.10 Sorption of Oxygen at 78°K Zeolite Synthetic Gmelinite (D332)

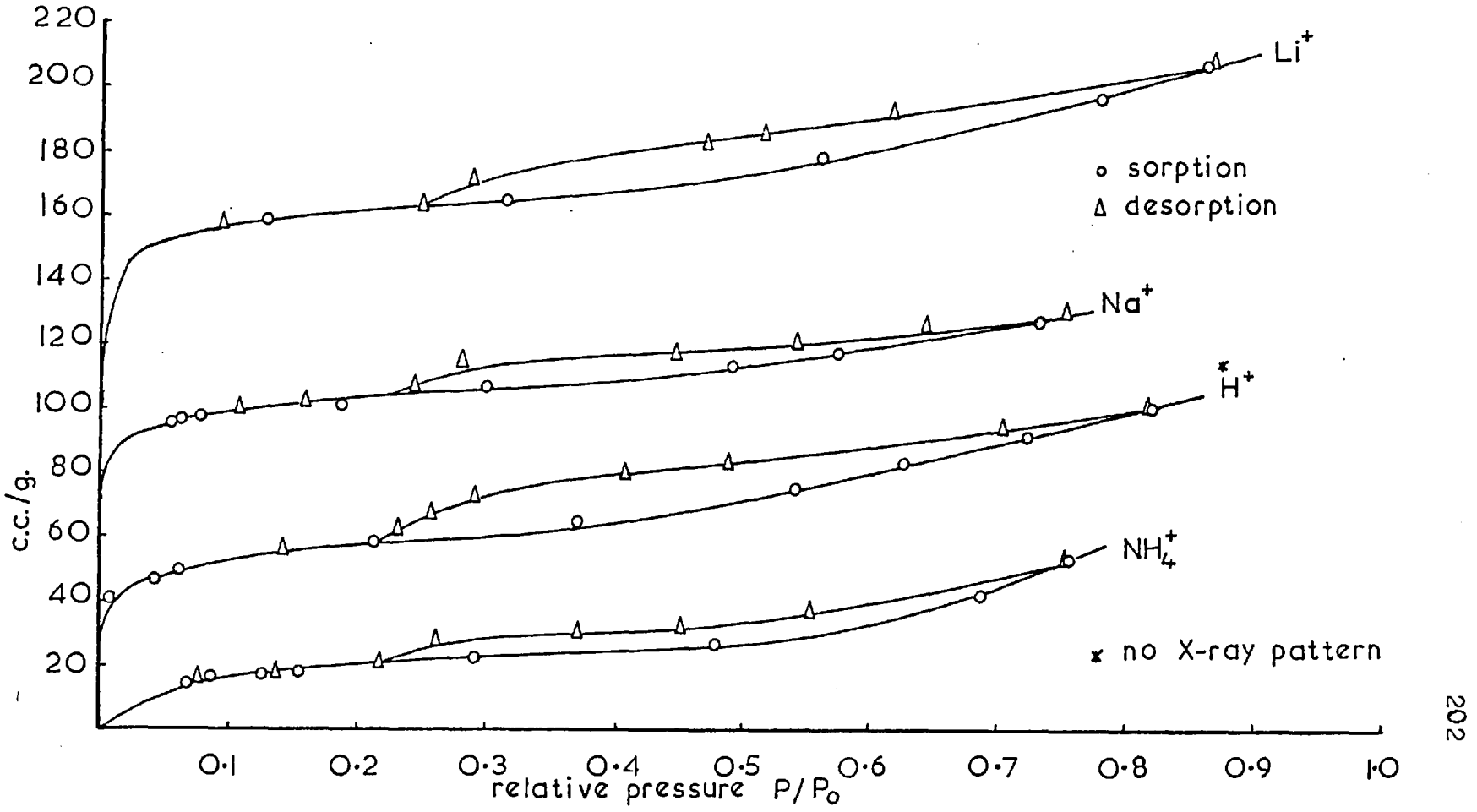

Figure 3.2.11 Li Exchanged Na Gmelinite Oxygen Sorption

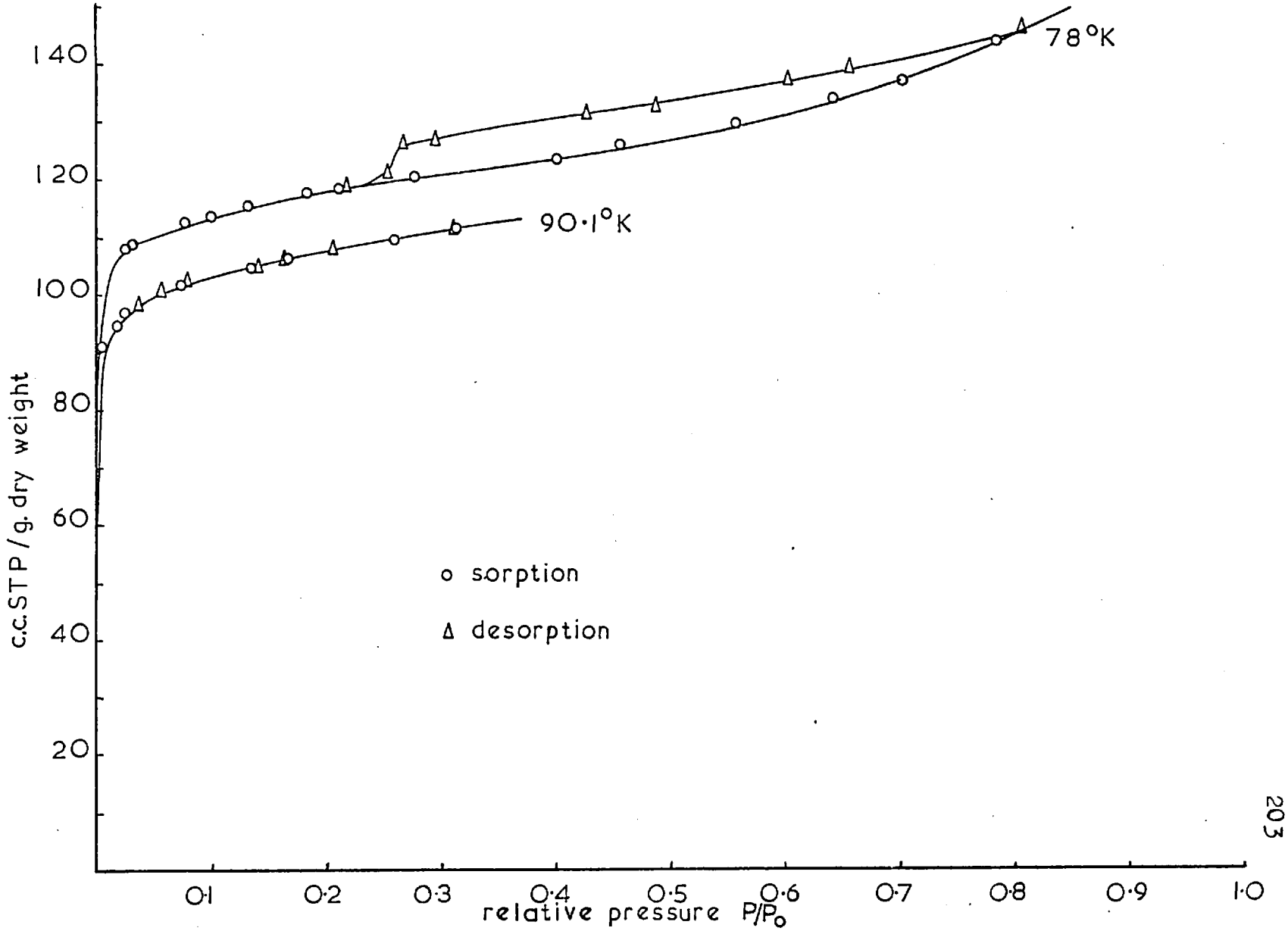

Figure 3.2.12 Sorption of n-Butane at 273 °K on $Li^{ex}(Na)-S_h(4\cdot03)[Gme]$

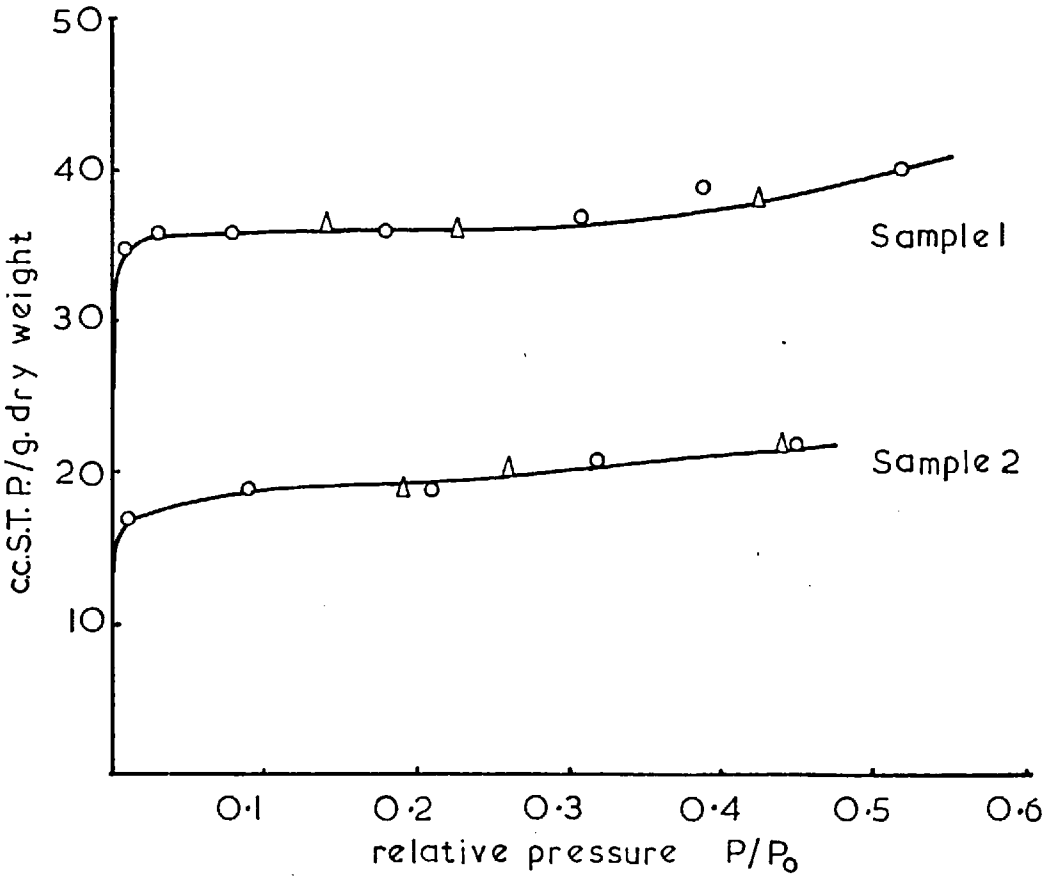

The effect of temperature upon sorption capacity and isotherm shape is shown in Figure 3.2.11 for another sample of Na-S ion-exchanged to the lithium form. The increase of temperature decreases the sorption capacity while removing the surface condensation. Thus at elevated temperatures reversible sorption takes place.

The lithium-exchanged Na-S sorbed n-butane but not iso-butane. Figure 3.2.12 shows the sorption of n-butane on two samples of Na-S. Sample 2 was made in these laboratories by Dr. J.F. Cole. By crystallizing gels in the presence of gelatine, he attempted to prevent the formation of stacking faults (Cole 1970). The results of hydrocarbon sorption on these samples were:

Sample	Sorption capacity c.c./gm. STP n-butane	iso-butane
1	36	0
2	18*	0

* This sample was heated in a stream of oxygen prior to sorption to remove any organic material occluded during synthesis. It was then checked for crystallinity by X-ray diffraction.

Both of the samples had effective channel dimensions reduced by stacking faults or in some other way from the free diameter of unobstructed channels, which is 7.0 Å (Table 1.1.2) to about 3.6 Å which is characteristic of chabazite (Dent 1958).

Since Na-S was silica rich (silica:alumina = 4) the stability of the hydrogen form was investigated. The zeolite was converted to the ammonium form and then heated until the ammonium cation decomposed. The product was examined as a sorbent and by X-ray diffraction. The sorption capacity fell to 58 c.c./gm. at S.T.P. for oxygen while the weakened diffraction pattern showed much reduced crystallinity.

Section 3.3 The System Metakaolinite - Li_2O-SiO_2-H_2O

3.3.1 The Reactions of Metakaolinite-Silica with Lithium Hydroxide

In the following Tables are given examples of syntheses carried out in the metakaolinite-silica-LiOH-H_2O system. Only two hydrated products and one silicate crystallized when the only cation present was lithium. Later, in Sections 3.6.3 and 3.6.5 it will be seen that in presence of a second cation the lithium cation promoted the growth of more diverse products. In nature there are only four purely lithium minerals commonly found. These are eucryptite, spodumene, petalite and the zeolite bikitaite. Two more minerals, the micas lepidolite and zinnwaldite, complete those minerals rich in lithium. A synthetic lithium zeolite ZSM-2 (Ciric 1968), the zeolites lithium mordenite, lithium phillipsite and lithium analcite produced by Sand, Coblenz and Sand (1970) and the lithium clinoptilolite of Ames (1963) were not found in these syntheses from metakaolinite. The products that were crystallized from metakaolinite-silica are listed below.

Short reference	Zeolite formula	Oxide composition	Description
Li-A	(Li)-A_0(2) [ ]	Li_2O, Al_2O_3, 2 SiO_2, 4 H_2O	synthetic zeolite
Li-H	(Li)-H(8) [ ]	Li_2O, Al_2O_3, 8 SiO_2, 5 H_2O	synthetic zeolite
Li-J	-	Li_2 SiO_3	lithium metasilicate

Table 3.3.1

The general reaction compositions were

1 metakaolinite (Al_2O_3 2 SiO_2) + 2.5 - 45 Li_2O + ~275 H_2O

rotated at 80° for 7 days

Run No.	Concentration of alkali (molality)	Product	Description
3-1	0.5	Li-A	md.cr.
3-2	1.0	Li-A	md.cr.
3-3	2.0	Li-A	md.cr.
3-4	5.0	Li-A	md.cr.
3-5	7.0	Li-J	pr.cr.
3-7	9.0	Li-J	pr.cr.
3-26	0.5 (110°)(3 days)	Li-A	md.cr.
3-27	1.0 (110°)(3 days)	Li-A	md.cr.
3-28	2.0 (110°)(3 days)	Li-J	md.cr.
3-40	0.5 (140°)(3 days)	Li-A	gd.cr.
3-41	1.0 (140°)(3 days)	Li-A	gd.cr.
3-48	0.5 (170°)(3 days)	Li-A	v.gd.cr.
3-49	1.0 (170°)(3 days)	Li-J	gd.cr.

Figure 3.3.1 1 Metakaolinite + 2·5–45 Li_2O ∓275 H_2O

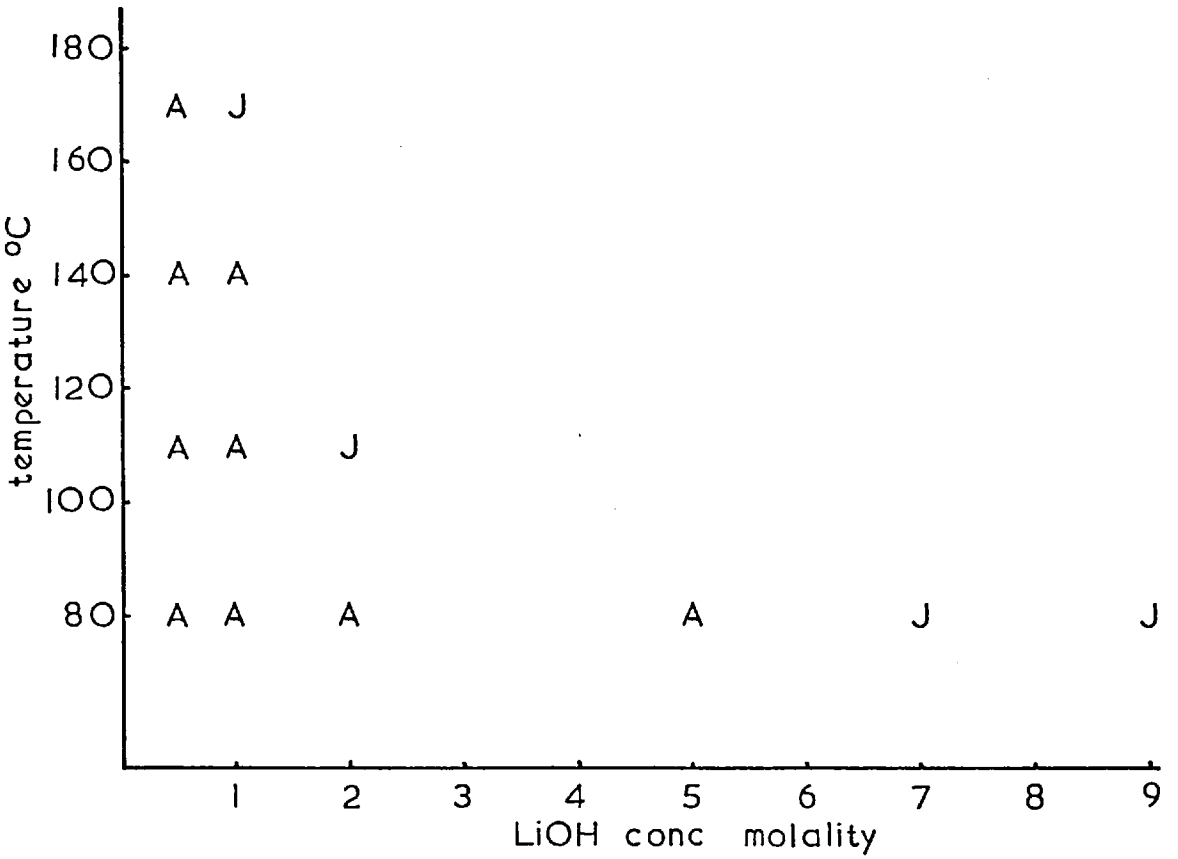

Table 3.3.2

The general reaction compositions were:

1 metakaolinite + 4 SiO_2 + 2.5 - 45 Li_2O + ~275 H_2O

rotated at 80° for 7 days.

Run No.	Concentration of alkali(molality)	Product	Description
3-10	0.5	Li-A	md.cr.
3-11	1.0	Li-A	md.cr.
3-12	2.0	Li-A	gd.cr.
3-13	3.0	Li-A + Li-J	Agd.cr.,Jpr.cr.
3-14	5.0	Li-J	pr.cr.
3-15	7.0	Li-J	pr.cr.
3-29	0.5 (110°)(3 days)	Li-A + Li-H	Agd.cr.,Htr.
3-30	1.0 (110°)(3 days)	Li-A + Li-J	Agd.cr.,Jmd.cr.
3-33	2.0 (110°)(3 days)	Li-J	md.cr.
3-42	0.5 (140°)(3 days)	Li-A + Li-H	Amd.cr.,Hpr.cr.
3-44	1.0 (140°)(3 days)	Li-A + Li-J	Agd.cr.,Jgd.cr.
3-51	0.5 (170°)(3 days)	Li-A + Li-H	Agd.cr.,Hpr.cr.
3-52	1.0 (170°)(3 days)	Li-A + Li-H + Li-J	Agd.cr.,Htr., Jgd.cr.

Figure 3.3.2 1 Metakaolinite + $4SiO_2$ + 2·5-45 Li_2O ∓275 H_2O

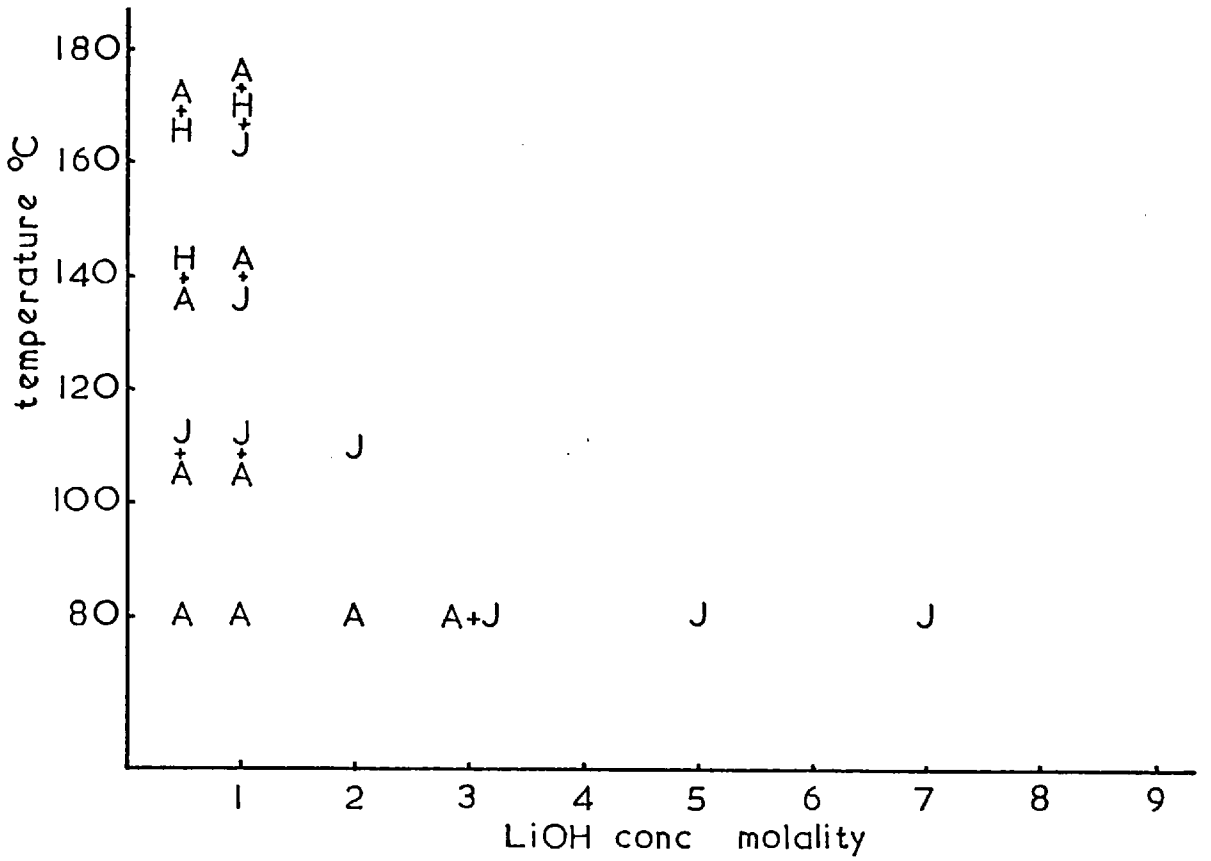

Table 3.3.3

The general reaction compositions were:

1 metakaolinite + 8 SiO_2 + 2.5 - 45 Li_2O + ~ 275 H_2O

rotated at 80° for 7 days

Run No.	Concentration of alkali(molality)	Product	Description
3-17	0.5	Li-A	md.cr.
3-18	1.0	Li-A	md.cr.
3-19	2.0	Li-A + Li-J	Amd.cr.,Jtr.
3-20	3.0	Li-A + Li-J	Apr.cr.,Jpr.cr.
3-22	5.0	Li-J	md.cr.
3-24	8.0	Li-J	md.cr.
3-36	0.5 (110°)(3 days)	Li-A + Li-H	Ap.cr.,Htr.
3-37	1.0 (110°)(3 days)	Li-A + Li-H	Ap.r.,Htr.
3-38	2.0 (110°)(3 days)	Li-J	md.cr.
3-45	0.5 (140°)(3 days)	Li-A + Li-H+ Li-J	Atr.,Htr., Jmd.cr.
3-46	1.0 (140°)(3 days)	Li-A + Li-J	Amd.cr.,Jmd.cr.
3-53	0.5 (170°)(3 days)	Li-A + Li-H	Agd.cr.,Hmd.cr.
3-54	1.0 (170°)(3 days)	Li-A + Li-J	Agd.cr.,Jgd.cr.

Figure 3.3.3. 1 Metakaolinite + $8SiO_2$ + 2·5–45 Li_2O ∓ 275 H_2O

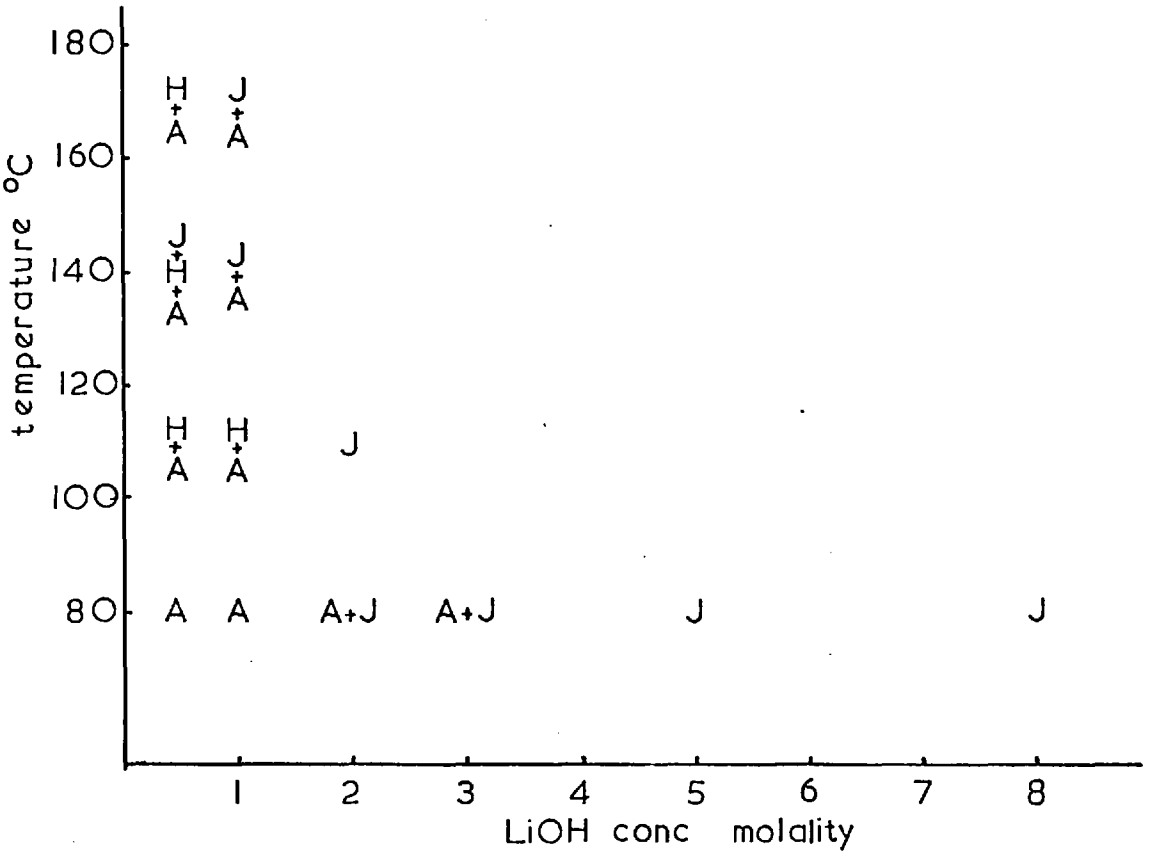

3.3.2 Properties of the Lithium Crystallization Field

The area of crystallization of lithium zeolitic phases was bounded by the lithium metasilicate crystallization area. From Figures 3.3.1 - 3.3.3 it can be seen that the crystallization area producing hydrated phases decreases as the total amount of silica in the system increases. For example, with a silica to alumina ratio of 2 Li-A can be grown in concentrations of alkali up to 5 molal, but with a ratio of 10 and with 2 molal lithium hydroxide, metasilicate has begun to form and by 5 molal the silicate is the only phase present.

In all the lithium aluminosilicate systheses with metakaolinite, or in other systems (Barrer and White 1951b), Ruiz-Menacho and Roy 1959 and Gusseva and Liliev 1965), no evidence was found for the crystallization of the only naturally occurring lithium zeolite-bikitaite (Hurlbut 1957 a,b). Hoss and Roy (1960) have described an interesting transformation of lithium exchanged gmelinite to bikitaite. Lithium gmelinite forms phillipsite at 200° when hydrothermally treated, and, depending on the extent of exchange, bikitaite at 250°. These workers also found all attempts to synthesise bikitaite directly unsuccessful.

3.3.3 Products of the Lithium Crystallization Fields

3.3.4 The Species Li-A

The product Li-A was identified as zeolite A first made by Barrer and White (1951 b). Li-A was a major product in areas of the crystallization field which were low in alkalinity and in temperature (Figures 3.3.1 - 3.3.3). The best crystalline product was obtained at 110° (for example run no. 3-27). As the silica to alumina ratio increased from 2 to 10 the region of formation of Li-A moved progressively to lower concentrations of lithium hydroxide.

Table 3.3.4 shows the measured d-spacings compared with those of the initial synthesis. Dr. I.S. Kerr (1970) has proposed a unit cell for Li-A from an electron microscopy study of single crystals. This is orthorhombic with $a = 10.31$, $b = 8.18$ and $c = 5.00$ Å.

A comparable synthesis of Li-A from kaolinite was reported by Barrer, Cole and Sticher (1968) but no crystallization field was described for comparison. They found that Li-A was an alteration product of a transient species Li-K when kaolinite was reacted with LiOH. In Table 3.3.5 the d-spacings of Li-K are recorded. It was

Table 3.3.4

The d-spacings of hydrated products of the Li_2O-metakaolinite-SiO_2-H_2O crystallization field.

Species Li-A		Li-A (Barrer and White 1951b)		Species Li-H		Li-H (Barrer and White 1951b)	
6.44	vs	6.42	vs	9.9	m	9.84	m
5.21	s	5.21	mw	8.4	w	8.39	mw
4.26	vs	4.29	vs	8.1	w	8.10	w
4.06	w	4.06	vw	6.7	ms	6.68	ms
3.27	w	3.27	vw	5.35	w	5.33	w
3.17	s	3.15	vs	4.85	sd	4.88	ms
3.02	vs	3.03	vs			4.55	vw
2.625	w			4.25	sd	4.27	s
2.495	s	2.490	s			3.97	vw
2.453	m			3.80	w	3.78	w
2.388	w	2.392	w	3.57	mw	3.58	mw
2.325	ms	2.326	m	3.50	w	3.49	w
2.241	w	2.243	vw	3.40	m	3.40	mw
2.169	m	2.173	mw	3.31	mw	3.32	mw
2.040	w	2.042	w			3.08	vw
1.958	m	1.952	mw	2.95	vw	2.97	w
1.867	vw	1.868	vw	2.81	vw	2.80	w
1.834	w	1.868	vw	2.65	w	2.66	w
1.751	m			2.52	m	2.52	m
		1.754	m			2.38	vvw
1.715	m	1.725	mw			2.02	vw
1.582						1.87	w
1.550	w	1.556	w				

observed that these were similar to an intermediate product formed during the growth of Na-P by Dr. R. Aiello (1970) from very dilute sodium aluminosilicate solutions. These preparations showed that dilute lithium alumino-silicate solutions first produced laminae before the appearance of Li-A. These laminæ were found by X-ray and electron microscopy to be largely amorphous. But sodium alumino-silicate solutions produced laminae which gave d-spacings by electron diffraction similar to Li-K.

Table 3.3.5

Comparison of the previously reported transient species.

Li-K (Barrer, Cole and Sticher 1968)		Na-lamina (Aiello, Barrer and Kerr 1970)	
4.40	35	4.50	vs
2.66	100	2.61	vs
2.42	30		
2.33	25	2.27	vw
1.79	20	1.71	m
1.536	30	1.52	vs
1.296	19d	1.31	s
		1.26	w
		1.04	vw
		0.99	vw
		0.87	vw

3.3.5 The Species Li-H

The product Li-H was identified with the Li-H originally made by Barrer and White (1952 b). The X-ray d-spacings are given in Table 3.3.4 where they are compared with those of the original preparation.

Li-H crystallized from compositions having silica to alumina ratios of 6 and 10. It was always co-crystallized with Li-A and no analysis could be carried out due to this admixture. The oxide composition found by Barrer and White was Li_2O, Al_2O_3, 8 SiO_2, 5 H_2O.

The formation of Li-H with a silica to alumina ratio of 8 from a reacting magma with a ratio of 6 is possibly due to the formation of Li-A (see Tables 3.3.2, 3.3.3) which has a silica to alumina ratio of 2 and when crystallized produces a solution of enriched silica content. This then can crystallize to form species Li-H.

3.3.6 The Species Li-J

Li-J was a lithium metasilicate. Previous syntheses were made by Barrer and White (1951 b), Gusseva and Liliev (1965), and Borer (1969) from gels. The crystallization of Li-J was from synthesis mixtures with silica to alumina ratios of 2 to 10 and temperatures from 80° to 170°. Elevated temperatures allowed lithium metasilicate to form at lower concentrations of lithium hydroxide (Figure 3.3.3). Synthesis of Li-J (composition $Li_2 SiO_3$) from metakaolinite produced solutions which contained increasing amounts of aluminate. Even in systems where the silica content had been increased initially, only a small part of the crystallization field produced phases other than Li-J. Again, in later sections on mixed cationic bases, the limiting of the area of zeolite crystallization in lithium containing fields by Li-J will be seen.

In Table 3.3.6 the diffraction pattern of Li-J is compared with a sample quoted in the A.S.T.M. index by Lam (No. 15-519). This had an orthorhombic unit cell with a = 5.43, b = 9.41 and c = 4.66 Å.

Table 3.3.6

Li-J		Li-metasilicate	
4.72	s	4.70	100
3.30	mw	3.31	20
2.70	s	2.71	90
2.35	mw	2.34	17
-		2.09	4
1.78	w	1.773	8
1.65	w	1.655	8
1.57	m	1.567	40
1.55	mw	1.560	40
-		1.412	4
-		1.355	4
1.30	w	1.299	8
1.257	w	1.255	6
		1.170	4
		1.138	4

Section 3.4 The System Metakaolinite-Rb_2O-SiO_2-H_2O and Metakaolinite-CS_2O-SiO_2-H_2O

3.4.1 Reactions in the Systems

The reactions of metakaolinite-silica with both rubidium and caesium hydroxide and the products obtained are given in Tables 3.4.1 and 3.4.2. The rubidium and caesium hydroxide were prepared as described in Section 2. They were then stored in sealed bottles until used. The period before use was kept to a minimum.

Rubidium hydroxide yielded two zeolites at 80°. One of these was the first preparation of the Rb-analogue of the phillipsite structure (K-M). Caesium hydroxide yielded three species, only one of which was hydrated. The products obtained from rubidium and caesium hydroxides are given below.

Crystalline Products Formed

Short reference	Zeolite formula	Oxide composition	Description
Rb-D	(Rb)-D_T(2) [ ]	Rb_2O, Al_2O_3, 2 SiO_2, H_2O	zeolite analogous with K-F
Rb-M	(Rb)-M_O(4) [Phi]	Rb_2O, Al_2O_3, 4 SiO_2, H_2O	zeolite analogous with K-M
Rb-A	-	Rb_2O, Al_2O_3, 2 SiO_2	unhydrated Rb alumino-silicate
Cs-D	(Cs)-D(2) [ ]	Cs_2O, Al_2O_3, 2 SiO_2, 2.4 H_2O	zeolite analogous with K-F
Cs-F	-	Cs_2O, Al_2O_3, 2 SiO_2	unhydrated Cs alumino-silicate
Cs-G	(Cs)-G_C(4) [Ana]	Cs_2O, Al_2O_3, 4 SiO_2	synthetic pollucite

Table 3.4.1

The general reaction compositions were:

1 metakaolinite (Al_2O_3, 2 SiO_2) + 0.25 - 20.0 Rb_2O + (n - 2)SiO_2 + ~ 275 H_2O rotated at 80°C for 7 days.

Run No.	Concentration of alkali(molarity)		Product	Description
4-3	0.5	n=2	Am	-
4-10	0.5 (14 days)	2	Am	-
4-4	1.0	2	Rb-D	pr.cr.
4-5	1.5	2	Rb-D	gd.cr.
4-7	3.0	2	Rb-D	gd.cr.
4-8	4.0	2	Rb-D + Rb-A	Dgd.cr., Amd.cr.
4-11	0.5	n=4	Am	-
4-12	1.0	4	Rb-M	pr.cr.
4-13	1.5	4	Rb-M	md.cr.
4-14	3.0	4	Rb-M	md.cr.
4-15	0.5	n=6	Am	-
4-16	0.5 (14 days)	6	Am	-
4-18	1.0	6	Rb-M	pr.cr.
4-19	1.5	6	Rb-M	md.cr.

Figure 3.4.1 1 Metakaolinite +·25-2O Rb_2O +(n-2)SiO_2 ∓275H_2O

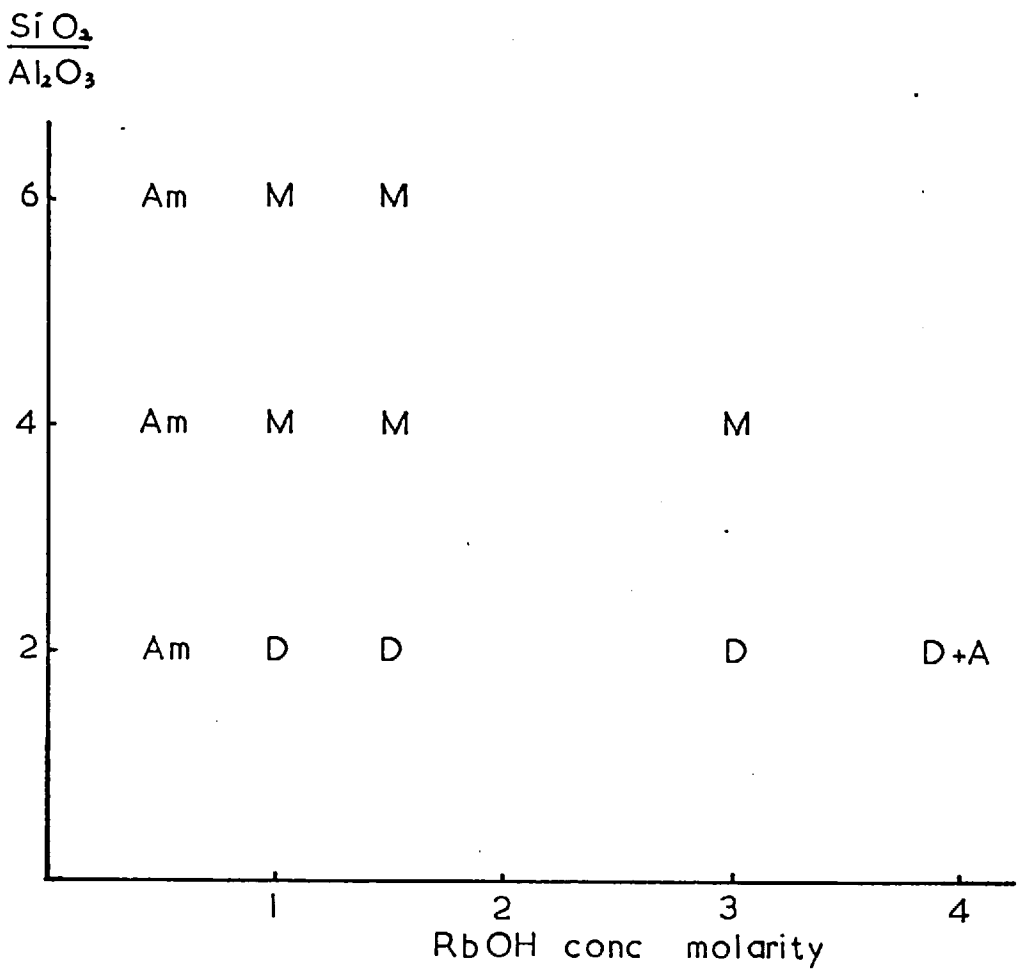

Table 3.4.2

The general reaction compositions were

1 metakaolinite (Al_2O_3, $2SiO_2$) + 0.25 - 20.0 Cs_2O + $(n-2)SiO_2$+

~ 275 H_2O rotated at 80°C for 7 days

Run No.	Concentration of alkali(molarity)		Product	Description
4-25	0.5	n=2	Am	-
4-31	0.5 (14 days)	2	Am	-
4-26	1.0	2	Am	-
4-27	2.3	2	Cs-D	
4-28	3.5	2	Cs-D + Cs-F	
4-29	4.5	2	Cs-D + Cs-F	
4-30	5.3	2	Cs-D + Cs-F	
4-32	1.0	n=4	Am	-
4-33	2.3	4	Cs-D	
4-34	3.5	4	Cs-D + Cs-F	
4-36	0.5	n=6	Cs-G +	
4-37	1.0	6	Cs-G +	
4-38	2.3	6	Cs-G	
4-39	3.5	6	Cs-G	

Figure 3.4.2

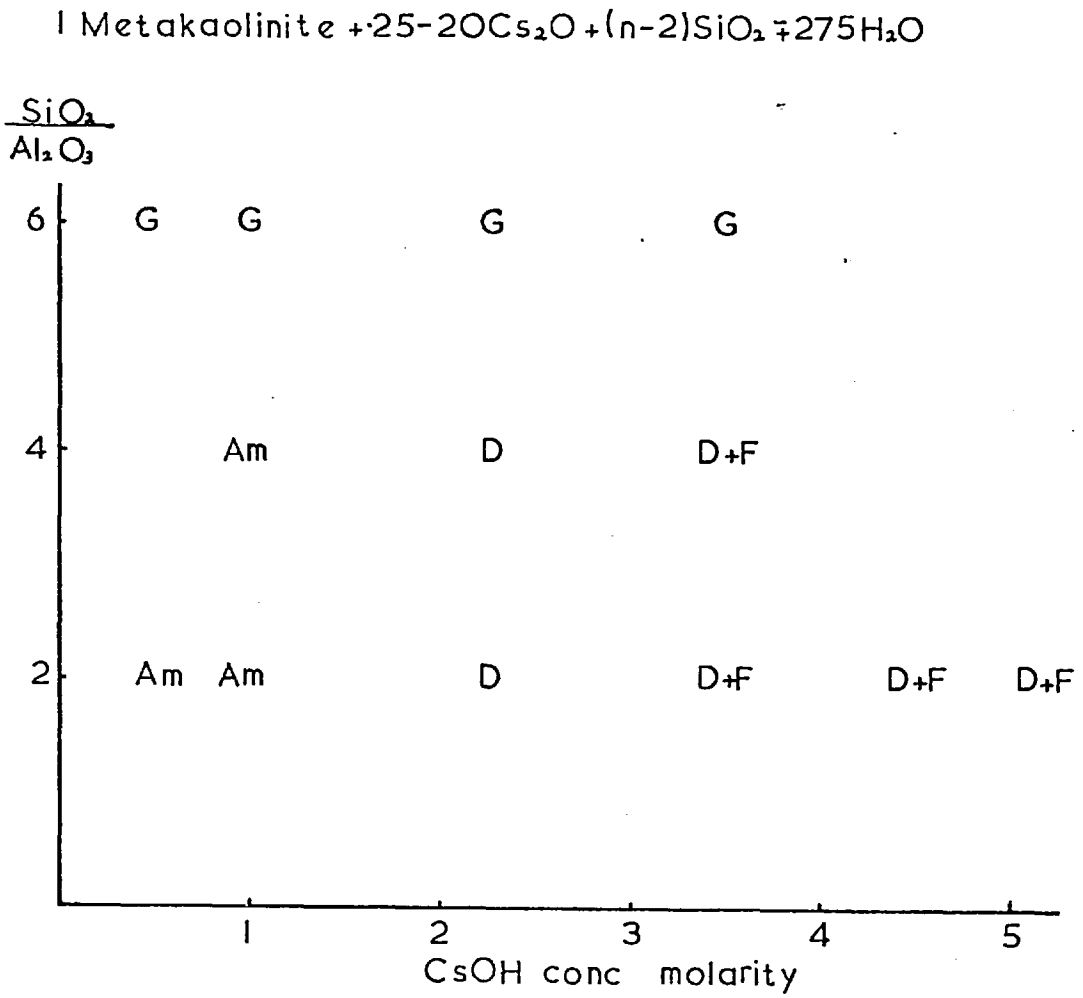

The crystallization of the two zeolites Rb-D and Rb-M took place readily at 80° when the alkali concentration was greater than 0.5 molar. Rubidium hydroxide, 0.5 molar, gave no crystalline products for periods of time up to 14 days. By comparison of Figures 3.1.1 and 3.4.1 it is seen that the crystallization fields

of potassium and rubidium show similarities. This is due to the chemical similarity of the ions K^+ (radius 1.33 Å) and Rb^+ (1.49 Å).

With caesium hydroxide-metakaolinite-silica-water as in the corresponding rubidium system, very low concentrations of caesium hydroxide yielded amorphous products, but now only in the low silica regions. With increased silica content pollucite (Cs-G) crystallized at alkali concentrations as low as 0.5 molar.

Natural occurrences incorporating both rubidium and caesium are found where they exhibit isomorphous substitutions for other cations such as sodium and potassium. An example is the rubidium microcline of Varutträsk (Adamson 1942) where rubidium is the major cation but also there is some substitution for caesium.

3.4.2 Products in the Rubidium and Caesium Crystallization Fields

3.4.3 The Species Rb-D and Cs-D

The species Rb-D and Cs-D were identified by X-ray diffraction with the species first made by Barrer and McCallum (1953) from gels and by Barrer, Cole and Sticher (1968) from kaolinite. The d-spacings have been compared in Table 3.4.3a with those of the original preparations.

Both Rb-D and Cs-D are isostructural with a large group of zeolites which occur in diverse crystallization fields. The original synthesis by Barrer (1948) was of K-F containing imbibed salts (Barrer and Marcilly, in press). Previous syntheses have been discussed in Section 1.2. The chemical analysis of a sample of Rb-D gave the molar formula:

$$Rb_2O,\ Al_2O_3,\ 2\ SiO_2,\ 2.5\ H_2O$$

In Table 3.4.2 the composition of the members of this family synthesized from metakaolinite are compared with products obtained from different starting materials.

Table 3.4.2

The composition of the 'F' group of zeolites synthesized here from metakaolinite and other starting materials.

Species	Oxide composition	Synthesis conditions
K-F	K_2O, Al_2O_3, $2SiO_2$, $3H_2O$	< 150°K aluminosilicate gels[1]
	K_2O, Al_2O_3, $2SiO_2$, $3H_2O$	80° KOH, kaolinite[2]
	K_2O, Al_2O_3, $2.1SiO_2$, $3H_2O$	80° KOH, metakaolinite
Rb-D	Rb_2O, Al_2O_3, $2SiO_2$, H_2O	165° Rb aluminosilicate gels[3]
	Rb_2O, Al_2O_3, $2SiO_2$, $2.6H_2O$	80° RbOH, kaolinite[2]
	Rb_2O, Al_2O_3, $2SiO_2$, $2.5H_2O$	80° RbOH, metakaolinite
Cs-D	Cs_2O, Al_2O_3, $2SiO_2$, $2.4H_2O$	80° CsOH, kaolinite[2]
	Cs_2O, Al_2O_3, $2SiO_2$, $2.2H_2O$	80° CsOH, metakaolinite
Na Li-F	$0.8Li_2O$, $0.2Na_2O$, Al_2O_3, $2SiO_2$, $3H_2O$	80° NaOH, LiOH, metakaolinite
Na Li-E	$0.75Li_2O$, $0.25Na_2O$, Al_2O_3, $2SiO_2$, $3.2H_2O$	100° Na, Li aluminosilicate gels[4]
N, K-F(KCl)	K_2O, Al_2O_3, $2.54SiO_2$, $0.8KCl$, $0.5H_2O$	200° KCl, K aluminosilicate gels[5,6]
K-F (Cl)	K_2O, Al_2O_3, $2SiO_2$, $0.3KCl$, $2.5H_2O$	80° KOH, KCl, kaolinite[2,7]
O, K-F (KBr)	K_2O, Al_2O_3, $2.53SiO_2$, $0.72KBr$, $0.4H_2O$	200° KBr, K aluminosilicate gels[5,6]
K-F(Br)	K_2O, Al_2O_3, $2SiO_2$, $0.2KBr$, $2.5H_2O$	80° KOH, KBr, kaolinite[2,7]
K-F (KI)	K_2O, Al_2O_3, $2.52SiO_2$, $0.45KI$, $0.5H_2O$	200° KI, K aluminosilicate gels[5,6]

NOTES 1. Barrer and Baynham (1958). 2. Barrer, Cole and Sticher (1968 a).
3. Barrer and McCallum (1953). 4. Borer and Meier (1970).
5. Barrer (1948). 6. Barrer and Marcilly (1970). 7. Barrer and Munday (1971).

Table 3.4.3

The indexed diffraction pattern of species Rb-D

$a = 9.983 \pm .001$ $\quad c = 13.229 \pm .002$ Å body centered*

Indices	d_{obs}	Intensity	d_{calc}
101	7.963	vvw	7.968
110	7.129	m	7.059
002	6.642	w	6.615
200	5.0155	w	4.9917
112	4.8359	mw	4.8268
211	4.2390	mw	4.2303
103	4.0416	w	4.0337
202	3.9902	mw	3.9844
220	3.5309	ms	3.5297
004	3.3080	w	3.3073
310	3.1565	vs	3.1570
222	3.1202	mw	3.1140
114	2.9955	vs	2.9949
312	2.8528	s	2.8491
204	2.7551	w	2.7570
321	2.7118	w	2.7102
400	2.4983	mw	2.4956
224	2.4131	vw	2.4134
411	2.3811	w	2.3818
330	2.3529	w	2.3531
314	2.2833	mw	2.2836
006	2.2070	w	2.2048
413	2.1212	mw	2.1224
206	2.0184	w	2.0169
500	1.9949	w	1.9967
431	1.9746	mw	1.9743
334	1.9163	w	1.9173
226	1.8678	w	1.8700

Table 3.4.3 (continued)

433	1.8195	w	1.8190
316	1.8065	w	1.8076
440	1.7635	ms	1.7648

* least squares refinement carried out on 34 of the first 39 powder lines.

One of the preparations produced a very sharp Guinier X-ray pattern. This was measured and corrected with an internal standard (Section 1.3). The powder lines were indexed using the Hesse-Lipson method. The unit cell was tetragonal with

$$a = 9.983 \pm 0.001$$

$$c = 13.229 \pm 0.002$$

and showed body centering. The calculated and observed d-spacings are given in Table 3.4.3. From this a related unit cell for K-F, having a c dimension twice that of Rb-D was found. On the basis of these unit cells Barrer and Marcilly (1970) have determined the unit cells of the halide containing species.

The unit cells of Rb-D, K-F and the halide-containing K-F species bear a close relationship to the natural fibrous zeolite edingtonite (Taylor and Jackson 1933). These unit cells are compared in Table 3.4.4. Further work is being carried out to determine the structural relationship between these species[3].

The product Rb-D crystallized only from compositions with a silica to alumina ratio of 2, which was that of the final product. This contrasts with Cs-D which crystallized from compositions with ratios of 2 and 4. A comparison of

Table 3.4.3a

A comparison of the d-spacings of species Rb-D and Cs-G with previous preparations

Rb-D * metakaolinite		Rb-D (Barrer, Cole and Sticher 1968)		Cs-D metakaolinite		Cs-D (Barrer, Cole and Sticher 1968)	
d (Å)	I	d (Å)	I/I_o%	d (Å)	I	d (Å)	I
7.963	vw						
7.129	m	7.05	36	7.20	mw	7.16	w
6.642	w	6.55	10				
-		5.65	10	5.60	vw		
5.015	w	5.15	9			5.07	w
-		4.95	13	4.90	w	4.87	w
4.836	mw	4.80	12				
4.239	mw			4.25	w		
4.042	w						
3.990	mw			4.00	w	4.00	w
3.531	ms	3.50	54	3.57	ms	3.56	m
3.308	w	3.28	7				
3.156	vs	3.09	100	3.15	vs	3.14	s
3.120	mw	3.03	11				
2.995	vs	2.965	100	3.00	vs	3.01	s
2.853	s	2.825	79	2.85	s	2.86	s
2.755	w	2.740	9.5				
2.712	w	2.680	6.5				
2.498	mw			2.51	w		
2.413	vw	2.400	4				
2.381	w			2.42	vw	2.36	vw
2.353	w					2.29	w
2.283	mw					2.22	w

* A complete list of indexed observed d-spacings is given in Table 3.4.3.

Table 3.4.4

Rb-D	tetragonal	a=9.98		c=13.23	body centered
K-F (KCl)	tetragonal	a=9.83		c=13.12[2]	body centered
Edingtonite	orthorhombic	a=9.54	b=9.65	c=6.50[1]	primitive
K-F	orthorhombic	a=14.02	b=13.92	c=13.14[3]	
K-F (KBr)	tetragonal	a=9.79		c=6.54[2]	primitive
K-F (KI)	tetragonal	a=9.81		c=6.59[2]	primitive

Notes 1. Taylor and Jackson (1933).

2. Barrer and Marcilly (1970).

3. Baerlocher, Barrer, Mainwaring and Marcilly (1970).

figures 3.4.1 and 3.4.2 shows that, at the silica ratio of 4, rubidium easily forms the near-phillipsite, Rb-M, itself having a ratio of 4. This eliminates the tendency, as with caesium, to form the corresponding D phase with a ratio of 2 and to leave a silica rich solution.

3.4.4 The Species Rb-M

This species was identified by the X-ray diffraction pattern as the rubidium analogue of synthetic near phillipsite. The potassium form of this was K-M described in Section 3.1.6. There is no naturally occurring counterpart nor any previously reported synthesis of Rb-M. The diffraction patterns of K-M and Rb-M are given in Table 3.4.5. A comparison of these values with those of the Na, K-M of Section 3.6.8 shows that there is a greater lattice change when sodium substitutes for potassium than when rubidium does so.

The water loss after equilibration at 56% R.H. was 12.6%. A sample ion-exchanged to the potassium form and equilibrated lost 14.4% weight upon heating. This value, if compared with those of Table 3.1.15 (Section 3.1.6) determined for the synthesized potassium form (14.9%), indicates that the yield of Rb-M was only very slightly lower than that of K-M. In Section 3.6.8 and Figures 3.6.13 - 3.6.16 the D.T.A. and T.G.A. curves are reproduced and are compared both with other members of the synthetic phillipsite family and with potassium exchanged natural phillipsite. An interesting property of Rb-M is its complete thermal stability. The sample remained unchanged when heated to 1000°.

Table 3.4.5

A comparison of the d-spacings of the rubidium and potassium near-phillipsite.

Rb-M		K-M (Section 3.1.6)
		10.22
8.37	ms	8.352
7.16	ms	7.149
5.40	m	5.384
5.07	sd	5.067
4.48	ms	4.478
4.32	sd	4.306
		4.115
3.67	mw	3.664
		3.530
		3.245
3.192	vsd	3.185
3.172	w	3.169
2.975	ms	2.973
		2.786
2.741	sd	2.736
		2.678
2.562	ms	2.555
2.429	mw	2.426
		2.378
2.194	mw	2.185
2.170	w	2.169
2.147	mw	2.150

This was also found by Barrer and Vaughan (1967a) in earlier experiments with rubidium exchanged K-M.

3.4.5 The Species Rb-A and Cs-F

The product Rb-A was obtained only in one synthesis where it formed a mixture with Rb-D. These species were first produced by Barrer and McCallum (1953) from rubidium and caesium aluminosilicate gels and are completely different from Linde Sieve A. The authors described the similarity between Rb-A and Cs-F and their mutual solid solubility. Neither of these two products could be identified with naturally occurring aluminosilicates. In Table 3.4.6 the X-ray diffraction patterns of the materials obtained from metakaolinite are given. Also included is a thallium aluminosilicate made by Taylor (1949) which has some similarities to the species Rb-A and Cs-D.

The products Rb-A and Cs-D had the compositions shown below where they are compared with those of other anhydrous phases.

Rb-A	Rb_2O, Al_2O_3, $2SiO_2$	
Cs-D	Cs_2O, Al_2O_3, $2SiO_2$	
K-D	K_2O, Al_2O_3, $2SiO_2$	Section 3.1.9
K-N	K_2O, Al_2O_3, $2SiO_2$	Section 3.1.9
thallium aluminosilicate	Tl_2O, Al_2O_3, $2SiO_2$	Taylor 1949

Table 3.4.6

The d-spacings of species Rb-A, Cs-D and a thallium aluminosilicate (Taylor 1949).

Rb-A		Cs-F		Tl_2O, Al_2O_3, $2SiO_2$	
-		-		6.5	vw
4.64	w	4.71	w	4.81	ms
-		-		4.24	vw
3.18	s	3.25	s	3.31	ms
-		-		3.11	s
2.91	w	2.95	w	2.96	mw
2.76	w	2.81	w	-	
2.66	s	2.71	s	2.71	m
2.27	m	2.31	m	2.36	vw
2.16	m	2.22	m	2.28	w
2.11	w	2.13	w	2.19	vw
1.978	mw	2.000	m	2.09	m
1.782	m	1.823	m	1.985	mw
1.708	m	1.751	msd	1.890	mw
1.684	w	1.685	w	1.840	w
				1.780	vvw
				1.705	mw

The species Cs-F occurred over a large part of the caesium crystallization field at higher concentrations of alkali (Figure 3.4.2). It, like Rb-A, crystallized in a mixture with the corresponding Rb-D or Cs-F species.

The products Rb-A and Cs-F do not appear to be related simply to synthetic kaliophilite (Table 3.1.22) or synthetic kalsilite (Table 3.1.23). A more detailed study may show a relationship between these, which may be expected due to the similarity in the potassium, rubidium and caesium crystallization fields. A comparison of the rubidium and caesium crystallization fields with those of potassium in Section 3.1 shows that Rb-A and Cs-F occur in positions close to those where kaliophilite crystallizes readily.

3.4.6 The Species Cs-G

This species is the synthetic analogue of the naturally occurring mineral pollucite. The relationship between the three minerals analcite, lencite and pollucite has been outlined in Section 1.1. A synthesis reported by Barrer and McCallum (1953) from caesium aluminosilicate gels at 165° produced a sample with a cubic cell edge of 13.7 Å. The d-spacings of this and of the sample from metakaolinite are given in Table 3.4.7. The reactions carried out with rubidium hydroxide did not produce a structurally related species although Barrer and McCallum reported that Rb-gels produced two modifications of rubidium analcite at temperatures only slightly higher than those producing pollucite. Taylor (1949) produced a thallium analogue of leucite at 220° from aluminosilicate gels. Thus where this framework does appear (i.e. for caesium) it does so at the remarkably low temperature of 80° C.

The species Cs-G was anhydrous like the synthetic pollucites made by Barrer and McCallum, and by Plyushchev (1959). This contrasts with natural pollucite which is partially hydrated and has the following composition

$$(Cs_x\ Na_{1-x})_2O,\ Al_2O_3,\ 4SiO_2,\ 2(1-x)\ H_2O$$

(Barrer and McCallum 1951).

Table 3.4.7

The d-spacings of Cs-G and synthetic pollucite

Cs-G (Å)		Pollucite		Cs-G		Pollucite	
5.64	mw	5.64	w	2.219	s	2.219	s
3.66	s	3.65	s	2.015	m	2.013	mw
3.43	s	3.434	vs	1.976	w	1.976	w
3.05	w	3.054	vw	1.861	s	1.862	s
2.90	s	2.912	s	1.735	s	1.737	s
2.67	w	2.680	vw	1.713	w	1.710	vw
2.495	w	2.496	m	1.635	w	1.681	vvw
2.415	mw	2.414	s			1.659	vvw

The isomorphous substitution of sodium for caesium thus allows the species to hydrate to an extent determined by the Na content.

3.4.7 Properties of the Rubidium and Caesium Crystallization Fields

The similarity between some of the hydrothermal crystallization reactions of rubidium hydroxide and caesium hydroxide with metakaolinite-silica and those of potassium hydroxide with the same compositions suggests that the absence in nature of any purely rubidium or caesium minerals except pollucite and the rubidium felspar (Section 3.4.1) is largely due to their low concentration in the lithosphere. Ion-exchange studies by Barrer and Munday (1970) and by Ames (1964) indicate that large cations are favoured by natural phillipsite. The main 8-ring channels in phillipsite (Section 1.1.) have an effective diameter of 4 Å (Steinfink 1962) which would allow even the caesium cation (3.3 Å diameter) to permeate the structure. However, synthetic near-phillipsite was produced in the potassium (K-M), sodium-potassium (Na, K-M) and rubidium (Rb-M) systems and not in the caesium system. This suggests a greater similarity between potassium and rubidium than between rubidium and caesium in such reactions. Perhaps the polycondensation processes in the case of potassium and rubidium, produce comparable secondary building units in solution.

Section 3.5 The System Metakaolinite-Silica-Barium Hydroxide-Water

3.5.1 Reactions in the System

The reactions between barium hydroxide solution and metakaolinite-silica were studied at 80°. Some of the syntheses, their conditions and products are given below in Table 3.5.2. The crystallization field has been plotted in Figure 3.5.1. Four crystalline products were obtained, three of which were hydrated. The fourth was the hexagonal polymorph of barium felspar, Ba-P. Two of the hydrated products were thermally unstable but the third was very stable.

Table 3.5.1

Crystalline products formed

Short reference	Zeolite formula	Oxide composition	Description
Ba-G	$(Ba)\text{-}G_h$ $(2.5)[L]$	$1.1BaO, Al_2O_3, 2.5SiO_2, 5.1H_2O$	barium zeolite
Ba-P	-	$BaO, Al_2O_3, 2SiO_2$	hex. barium celsian
Ba-T	$\{Ba(OH)_2\}$ $(Ba)\text{-}T(2)$ $[\ ]$	$BaO, Al_2O_3, 2SiO_2$ $1.2Ba(OH)_2, 2H_2O$	basic barium zeolite
Ba-N	$(Ba)\text{-}N\ (2)$ $[\ ]$	$BaO, Al_2O_3, 2SiO_2, 2.8H_2O$	barium zeolite

To prevent the production of barium carbonate a weighed amount of barium hydroxide was added to the synthesis mix immediately before sealing the reaction vessel.

Table 3.5.2

The general reaction composition was: 1 metakaolinite (Al_2O_3, $2SiO_2$) + 2.5 - 28.0 BaO + (n-2) SiO_2 + ~275 H_2O rotated at 80° for 7 days.

Run No.	Concentration of alkali (molality)		Product	Description
5-3	0.5	n=2	Ba-G	v.pr.cr.
5-4	0.5 (14 days)	2	Ba-G	pr.cr.
5-8	1.0	2	Ba-G	md.cr.
5-21	1.0 (10 days)(100°)	2	Ba-G	md.cr. gd.yd.
5-9	1.2	2	Ba-P	md.cr.
5-12	1.2 (10 days)(100°)	2	Ba-P	md.cr.
5-13	1.4	2	Ba-P + Ba-N	P,N,gd.cr.
5-15	1.6	2	Ba-N	gd.cr.
5-17	2.3	2	Ba-I	gd.cr.
5-19	2.8	2	Ba-I	v.gd.cr.
5-25	0.5	n=4	Ba-G	pr.cr.
5-26	1.0	4	Ba-G	pr.cr.
5-28	1.5	4	Ba-G + Ba-P	G,md.cr.,P,gd.cr.
5-30	2.0	4	Ba-P	md.cr.
5-34	0.3	n=6	Ba-G	pr.cr.
5-35	0.5	6	Ba-P	md.cr.
5-37	1.0	6	Ba-P + Ba-I	Pmd.cr.,Ipr.cr.
5-36	1.5	6	Ba-I	md.cr.
5-40	0.5	n=8	Am	-
5-49	0.5 (14 days)	8	Am	-
5-42	1.0	8	Ba-P	pr.cr.
5-43	1.5	8	Ba-P	pr.cr.
5-47	0.5	8	Am	-
5-48	0.5 (14 days)	8	Ba-P	md.cr.

Figure 3.5.1 | Metakaolinite +2·5-28 BaO +(n-2)SiO_2+275H_2O

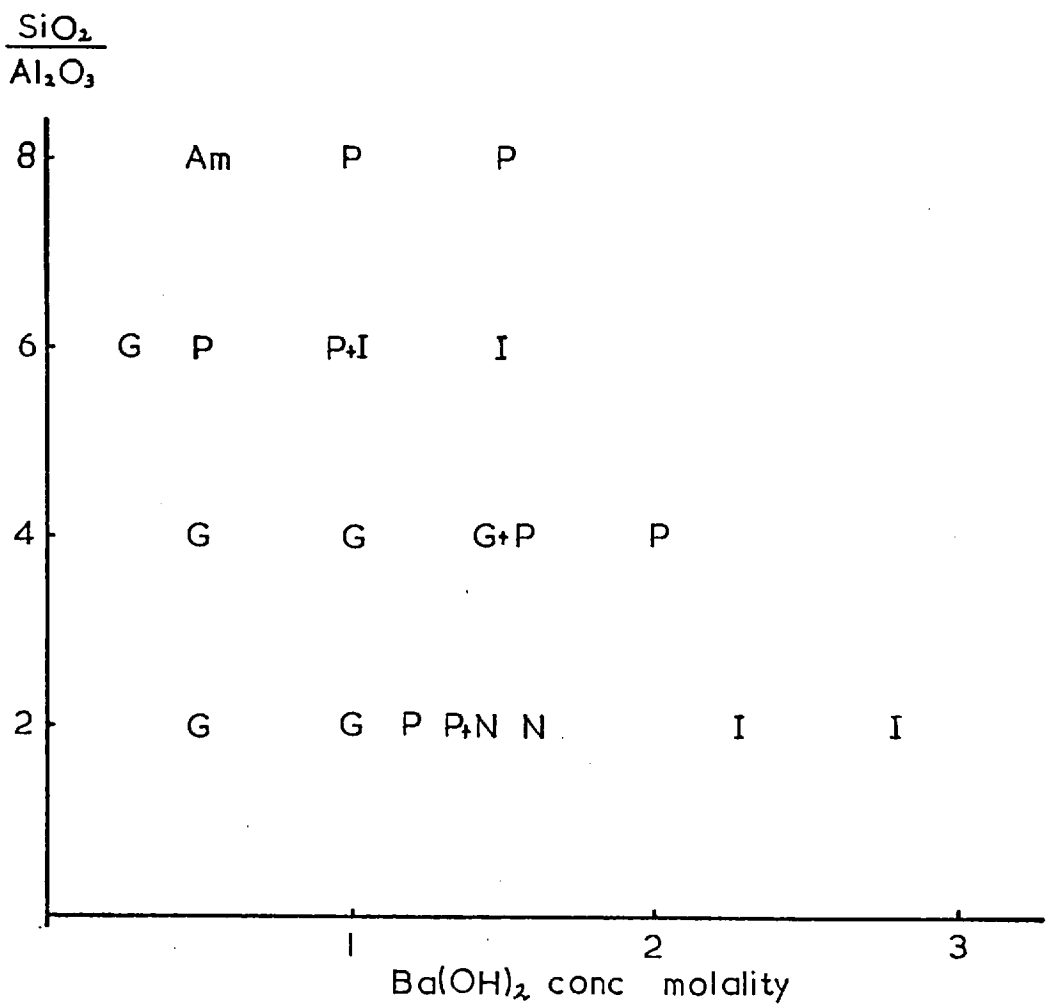

3.5.2 The Products of the Barium System

3.5.3 The Species Ba-G

This species was one of a series of zeolites produced in 1964 by Barrer and Marshall from aqueous alkaline gels of oxide composition BaO, Al_2O_3, $3SiO_2$ maintained at 150-200° for 3 to 4 weeks. The first 21 lines of the X-ray diffraction pattern were indexed by them to a tetragonal unit cell a=15.16 and c=18.89 Å. Figure 3.5.1 shows that Ba-G crystallizes from dilute barium hydroxide solutions (0.3 - 1.0 molal) at 80° when reacting with metakaolinite. The optimum growth was from a 1.0 molal solution at 100° for 10 days. Optical examination of the product showed that it was present as very small crystal aggregates in ~80% yield.

A method of synthesis which produced higher yields of product with better crystallinity was developed using mixed cationic bases, and will be described in Section 3.8.1.

The X-ray diffraction pattern gave the d-spacings shown in Table 3.5.3, and were indexed to a hexagonal unit cell whose dimensions are given below. This thus replaces the previously proposed tetragonal unit cell (Barrer and Marshall 1964). In Table 3.5.3 the d-spacings of Ba-G are compared

Table 3.5.3

d-spacings of Ba-G and related structures.

	Ba-G				K-L			Ω	
	d_{obs}	d_{calc}	I		d_{calc}	I		d_{calc}	I
100	16.64	16.197	vs	100	15.935	vs	100	15.722	m
110	9.47	9.351	w	110	9.200	vw	110	9.077	vs
200	8.10	8.099	w	200	7.967	vw	200	7.861	m
001	7.587	7.587	mw	001	7.520	mw	101	6.835	m
101	6.868	6.871	vw	101	6.801	vw	210	5.942	s
111	5.885	5.892	m	210	6.023	mw	201	5.460	w
300	5.412	5.399	m	111	5.822	mw	300	5.241	w
400	3.965	4.049	vw	300	5.312	vw	310	4.360	vw
311	3.850	3.865	mw	211	4.701	m	400	3.930	m
002	3.750	3.793	mw	220	4.600	m	002	3.795	vs
102	3.704	3.694	w	310	4.420	w	102	3.689	m
112	3.515	3.515	mw	301	4.339	w	320	3.607	m
202	3.477	3.435	w	400	3.984	vw	401	3.490	s
321	3.319	3.337	m	221	3.924	m	410	3.431	mw
212	3.224	3.225	mw	311	3.810	vw	321	3.258	w
411	3.192	3.204	vw	002	3.760	vw	411	3.126	s
302	3.076	3.104	m	320	3.656	m	302	3.074	m
402	3.052	3.061	mw	401	3.520	m	330	3.026	m
501	2.961	2.979	m	112	3.481	m	420	2.971	mw
510	2.920	2.909	w	202	3.400	vw	222	2.911	s
331	2.872	2.883	mw	321	3.288	mw	510	2.824	w
421	2.823	2.839	mw	212	3.189	m	421	2.767	w
402	2.744	2.768	w	302	3.069	mw	402	2.730	mw
600	2.687	2.699	vw	420	3.011	vw	511	2.646	mw
322	2.631	2.655	m	501	2.934	m	322	2.614	m
601	2.567	2.543	m	222	2.911	m			
003	2.529	2.529	vw	510	2.864	vw			
103	2.498	2.499	w	331	2.840	vw			
521	2.458	2.454	vw	421	2.796	vw			
113	2.441	2.441	vw	402	2.734	vw			

Table 3.5.3 (continued)

203	2.415	2.414	mw	511	2.675	m
422	2.389	2.382	m	600	2.656	m
611	2.365	2.349	vw	430	2.620	vw
213	2.331	2.337	vw	322	2.621	vw
512	2.304	2.308	w	502	2.552	vw

with those for two other zeolites without natural counterparts, zeolites L (Section 3.1.8) and omega (Union Carbide Corporation 1967). Zeolites L and Ω have related structures as shown in Section 1.1

	a Å	c Å
Ba-G	18.70	7.59
zeolite L	18.40	7.52[1]
zeolite Ω	18.15	7.59[2]

1. Barrer and Villiger (1969 a).
2. Barrer and Villiger (1969 b).

The data in Table 3.5.3 indicate that Ba-G is based upon the same aluminosilicate framework as zeolite L.

The chemical analysis of Ba-G synthesized under the optimum conditions gave the following oxide compositions and molar proportions respectively.

	% by weight	Molar proportion
SiO_2	30.55	2.5
Al_2O_3	20.77	1.0
BaO	34.28	1.1
H_2O (by difference)	14.60	5.1

The slight excess of BaO over Al_2O_3 may indicate that a little extra barium oxide is incorporated into the channel system, possibly as barium silicate or hydroxide. The silica to alumina ratio indicates that Ba-G is an aluminous form of the structure yielding zeolite L as a silica rich variety. This chemical difference accounts for the slightly larger unit cell of Ba-G, since the Al-O bond is a little longer than the Si-O bond (Smith and Bailey 1963). The composition of the mixed cation form crystallized in the barium-potassium system is discussed in Section 3.8.3.

The sorption properties of Ba-G were investigated with oxygen, n-butane and iso-butane. Ba-G and its sodium exchanged form sorbed respectively 88 c.c. and 68 c.c. at S.T.P. of oxygen at 78°K, but did not sorb significant amounts of normal or iso-butane at 273°K. The oxygen isotherms are shown in Figure 3.5.2. The sorption capacities are later shown in Table 3.8.6 for comparison with the Ba, K synthesis product. The sorption behaviour of Ba-G contrasts both with zeolite L (which has exceptionally large channels of about 7.5 Å parallel to c, Barrer and Lee 1969) and with the (Ba, K)-G produced from metakaolinite.

Figure 3.5.2 Sorption of Oxygen at 78°K on Ion-exchanged Forms of Ba-G

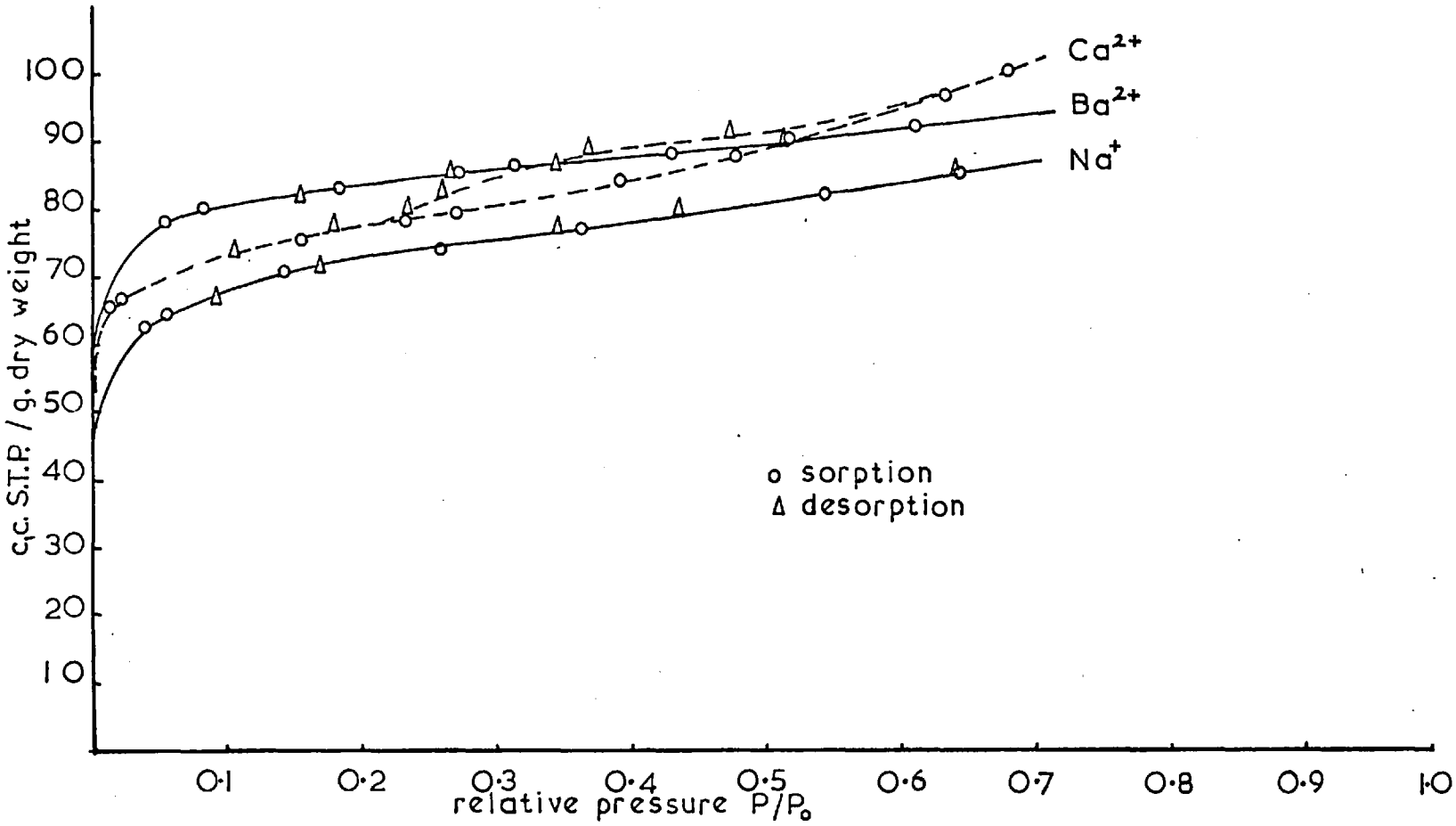

This behaviour may be due to included impurities in the channels which were absent in later syntheses in presence of mixed bases. Hydrothermal extraction in a Soxhlet apparatus, used in an attempt to remove these impurities, tended to decompose the zeolite, probably due to its high aluminium content.

A comparison of this product with that of Barrer and Marshall (1964) shows a greater sorption capacity for oxygen: 88 c.c./gm. at S.T.P. compared with 50 c.c./gm. for the earlier preparation. The water content, as shown in the T.G.A. and D.T.A. curves of Figure 3.8.6a was 14.1%. This was lower than the 15.0% reported by Barrer and Marshall. Thus in the earlier sample there probably was present a greater amount of barium alumino-silicate hydrated gel.

Further properties of this novel member of the L family of zeolites such as ion-exchange, thermal stability, decationation, and hydrocarbon sorption were investigated on the forms produced in the K + Ba and $(CH_3)_4N$ + Ba systems. These are described in Section 3.8.
Here the product had an unblocked main channel of about 7.5 Å diameter available for sorption.

3.5.4 The Species Ba-N

This species could not be identified with any synthetic aluminosilicate or naturally occurring mineral. It crystallized in very high yields from compositions with a silica to alumina ratio of 2. A very sharp X-ray diffraction pattern was produced by the sample, and the d-spacings are recorded in Table 3.5.4. The sample, when equilibrated to 56% R.H. lost 12.2% water on heating to 1000°. The dehydration curve, shown with the D.T.A., in Figure 3.5.3 indicated an inflexion occurring at ~ 200°, followed by a more rapid loss of weight. The D.T.A. curve shows this process to be endothermic. The sample was heated in a Lenné-Guinier camera and the diffraction pattern recorded. Lattice breakdown occurred in the region of 200°. This could account for the rapid loss in weight in this temperature region.

Chemical analysis of an equilibrated product gave the following composition.

	% by weight	Molar ratio
BaO	32.5	1 *
Al_2O_3	23.9	1
SiO_2	28.6	2
H_2O	12.2	2.8

* Determined by flame photometry.

Figure 3.5.3 Zeolite Ba-N Equilibrated at 56% R.H.

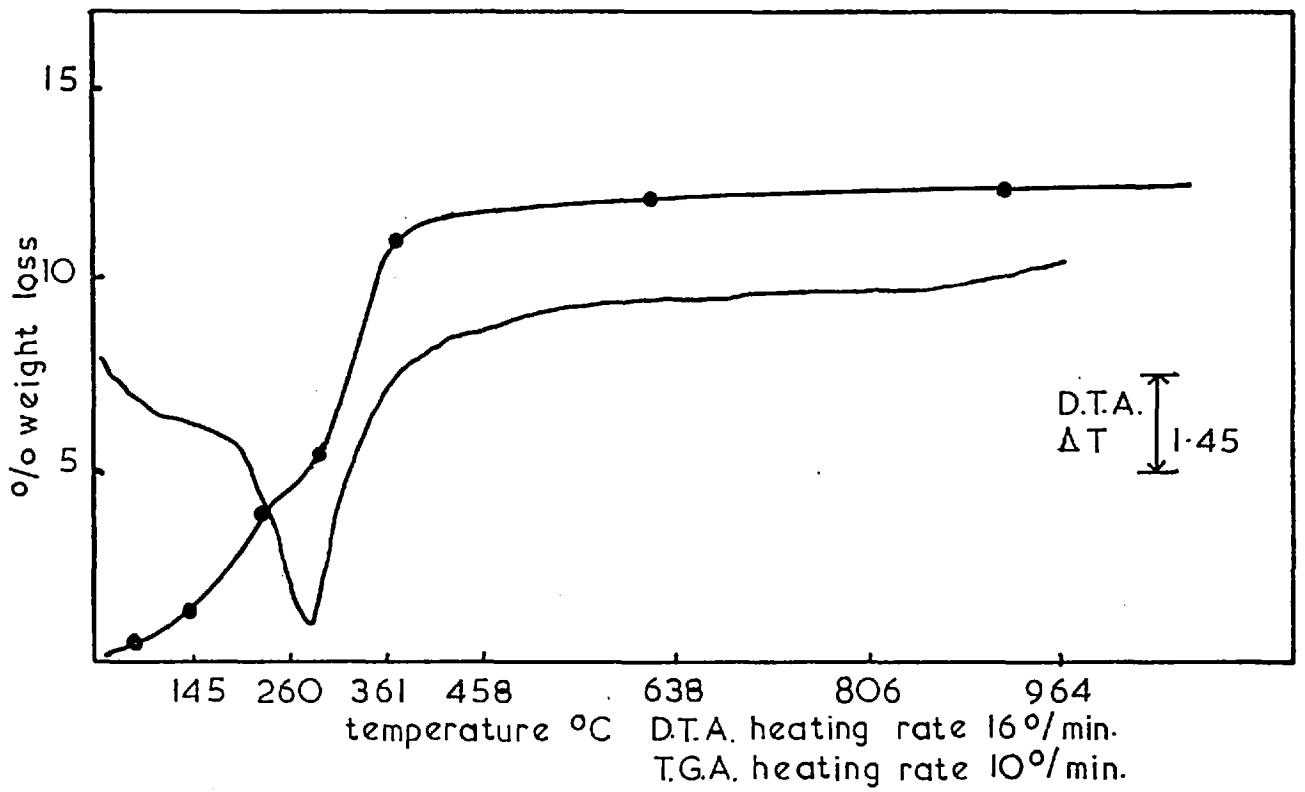

Table 3.5.4

The d-spacings of species Ba-N, Ba-P and the ignition product of Ba-N.

Ba-N		ignition product Ba-N		Ba-P (3.5.5)	
7.1	m	7.9	s	7.78	m
5.6	ms	4.6	vw	4.59	vw
5.2	ms	4.5	vw		
4.5	w	3.95	vs	3.97	vs
4.35	vw	2.96	vs	2.97	s
3.50	m	2.65	s	2.66	m
3.40	s	2.60	w		
3.15	mw	2.29	m	2.30	mw
2.92	ms	2.27	w		
2.84	w	2.25	m	2.25	m
2.79	w	2.196	ms	2.197	m
2.69	w	1.970	m	1.970	w
2.59	w	1.935	wd	1.935	mw
2.57	ms	1.855	mw	1.853	m
2.44	m				
2.40	w				
2.33	w				
2.24	m				
2.230	w				
2.165	w				
2.078	mw				
2.051	mw				
2.020	mw				
1.917	w				
1.893	m				
1.845	mw				
1.823	w				
1.762	mw				
1.741	w				

The sorption characteristics of Ba-N were not investigated due to the instability of the sample upon outgassing. The product formed by ignition was Ba-P, the d-spacings of which are given in Table 3.5.4.

3.5.5 The Species Ba-T

This species was synthesized in concentrated solutions of $Ba(OH)_2$ at 80°. Good crystallinity and a high yield were obtained by reacting metakaolinite with 2.5 - 3.0 molal $Ba(OH)_2$ at 80°. The composition of species Ba-T was BaO, Al_2O_3, $2SiO_2$, $1.2\ Ba(OH)_2$, $2H_2O$. The Lenné-Guinier heating camera showed that this product was stable to approximately 225° where it became amorphous. Gradual recrystallization took place between 500° and 800°. The T.G.A. and D.T.A. curves are given in Figure 3.5.4. The T.G.A. indicates a small loss of water initially followed by a more rapid weight loss to approximately 6%. This is confirmed by the two step endothermic peak of the D.T.A. The small exothermic peak at 710° is unaccounted for since the Lenné picture showed no lattice change at that temperature.

The X-ray diffraction pattern, given in Table 3.5.5, was very complex indicating a structure of low symmetry. The relative intensities of the powder lines showed no significant variation in different preparation within the crystallization area. This indicates that species Ba-T is probably a single phase. Optical or electron microscopy could not confirm this because the species was present as aggregates of very small crystals. The outgassed sample showed no tendency to sorb oxygen at 78° K.

Figure 3.5.4 Zeolite Ba-T

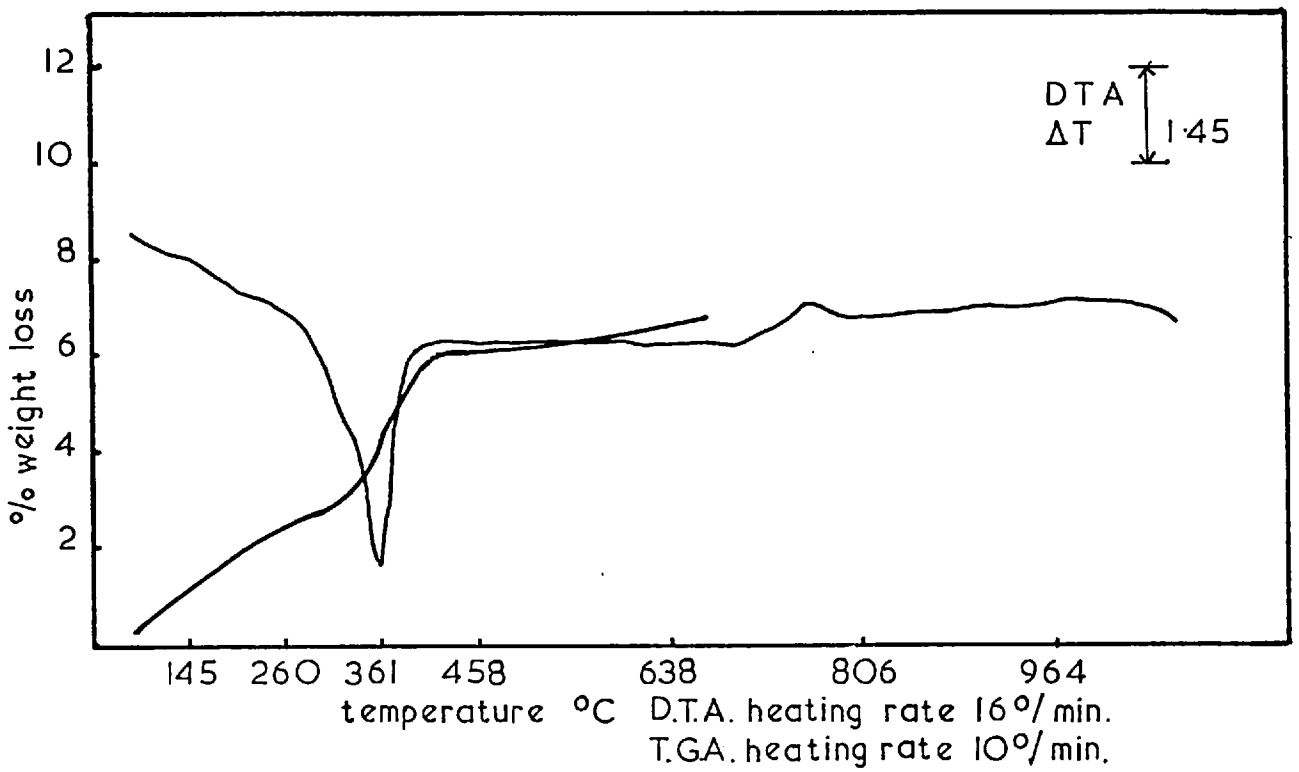

Table 3.5.5

The d-spacings of species Ba-T and the ignition product

Ba-T		Ba-T(cont.)		ignition product	
7.4	w	2.45	m	5.2	mw
7.2	w	2.43	ms	4.19	mw
5.2	ms	2.38	mw	3.96	mw
5.0	w	2.36	mw	3.70	s
4.3	m	2.35	mw	3.55	m
4.24	mw	2.33	m	3.42	vs
4.20	mw	2.32	vw	3.35	vs
4.16	m	2.31	vw	3.11	s
4.00	vw	2.27	w	3.09	m
3.79	s	2.25	mw	3.01	m
3.70	w	2.24	w	2.94	ms
3.68	s	2.22	m	2.91	ms
3.52	m	2.18	m	2.81	s
3.37	ms	2.15	w	2.75	w
3.30	mw	2.09	w	2.73	w
3.22	s	2.07	w	2.70	m
3.18	s	2.04	w	2.58	w
3.15	w	2.03	m	2.52	w
3.08	w	2.02	m	2.35	ms
3.03	w	2.00	m	2.30	ms
2.98	m	1.99	mw	2.08	ms
2.96	m	1.97	mw	2.04	ms
2.94	vw	1.96	mw		
2.92	w	1.95	w		
2.88	w	1.92	w		
2.84	w	1.89	w		
2.64	m	1.83	m		
2.63	w	1.78	m		
2.50	m	1.76	m		

3.5.6 The Species Ba-P

The product Ba-P was identified as the pseudo-hexagonal polymorph of barium celsian $BaO, Al_2O_3, 2SiO_2$ (Takeuchi 1958) previously prepared pyrolytically by Ginzberg (1923) and hydrothermally by Barrer and Marshall (1964). The X-ray diffraction pattern of Ba-P prepared hydrothermally is given in Table 3.5.4. Here it is compared with the ignition product from Ba-N. Thus, like synthetic kaliophilite (K-D, Section 3.1.10), Ba-P is the corresponding product from both the hydrothermal crystallization of metakaolinite and the decomposition of the zeolite.

Barrer and Marshall (1964) and Sorrel (1962) have found evidence in the hydrothermal and pyrolytic systems respectively that Ba-P was metastable and that it would produce celsian with more vigorous or prolonged treatments. In the present work neither prolonged hydrothermal treatments (Run No . 5-12) nor ignition at 1100° of Ba-N produced phases significantly different from Ba-P.

3.6 The Systems Metakaolinite - Na_2O - K_2O - SiO_2 - H_2O Metakaolinite - Na_2O - Li_2O - SiO_2 - H_2O Metakaolinite - K_2O - Li_2O - SiO_2 - H_2O

In the following section some reactions of metakaolinite + silica with mixed hydroxides are reported and discussed. Mixed bases allow one to investigate ion selectivity during crystallization. This selectivity may be then compared with the ion-exchange characteristics of the zeolite and if possible with the compositions of the naturally occurring forms. In Section 1.2 it was shown that some zeolites crystallize more readily in the presence of mixed bases than in the presence of either single base. It will be seen that some products previously thought of as homoionic are greatly improved when grown from dicationic systems. Also, in Section 1.2 it was noted that some zeolites do not crystallize in the presence of a single cation. The study of crystallization in presence of mixed bases thus offers the possibility of forming new phases absent from the previous homoionic crystallization fields. For example, in this work the ready growth of cancrinite at 80° from metakaolinite has been observed when both lithium and sodium hydroxides are present, but not at this temperature with caustic soda alone.

The nomenclature used to describe the mixed cationic species is consistent with their frequent prior identifcation as homoionic species. An example is the species Na Li-F which was identified as an analogue of the previously prepared K-F structures.

Due to the large number of synthesis experiments needed to explore the crystallization fields in presence of mixed bases only a representative number have been included. Generally these were chosen to delineate areas of crystallization or point out variations in conditions.

3.6.1 Reactions in the Sodium, Potassium System

The reactions carried out with metakaolinite, silica, and mixed sodium and potassium bases are described in Tables3.6.1 - 3.6.4. The crystallization fields have been plotted in Figures 3.6.1 - 3.6.4.

Table 3.6.1

The general reaction compositions were: 1 metakaolinite + 2.8 - 233 ($mK_2O + (1 - m)Na_2O$) + ~275 H_2O at 80° for 7 days

Run No.	Concentration of alkali (molality)	Cation fraction $\frac{Na_2O}{Na_2O+K_2O}$	Products	Description of products
6-22	0.5	0.1	G	md.cr.
6-23	0.5	0.2	G	md.cr.
6-24	0.5	0.3	G *	gd.cr.
6-25	0.5	0.5	G *	gd.cr.
6-29	0.5	0.6	G* + Q	Gmd.cr./Qlo.yd.
6-30	0.5	0.65	Q	md.cr.
6-31	0.5	0.9	Q	md.cr.
6-33	1.0	0.2	G	md.cr.
6-35	2.0	0.2	G	md.cr.
6-36	2.0	0.3	G *	gd.cr.
6-37	2.0	0.4	G *	gd.cr.
6-38	2.0	0.5	F	gd.cr.
6-40	2.0	0.6	F +	gd.cr.
6-42	2.0	0.8	F +	gd.cr.
6-46	3.0	0.1	G	md.cr.
6-48	3.0	0.5	F +	md.cr.
6-51	3.0	0.9	Q	gd.cr.
6-53	4.0	0.1	F	gd.cr.
6-55	4.0	0.5	F	gd.cr.
6-58	4.0	0.9	F + I	pr.cr.
6-60	7.0	0.2	F	gd.cr.
6-62	7.0	0.5	F +	gd.cr.

Figure 3.6.1 The Crystallization Field Resulting from:

1 Metakaolinite +2·8–233 $(mK_2O+(1-m)Na_2O)$ +275 H_2O

Rotated at 80° for 7 days

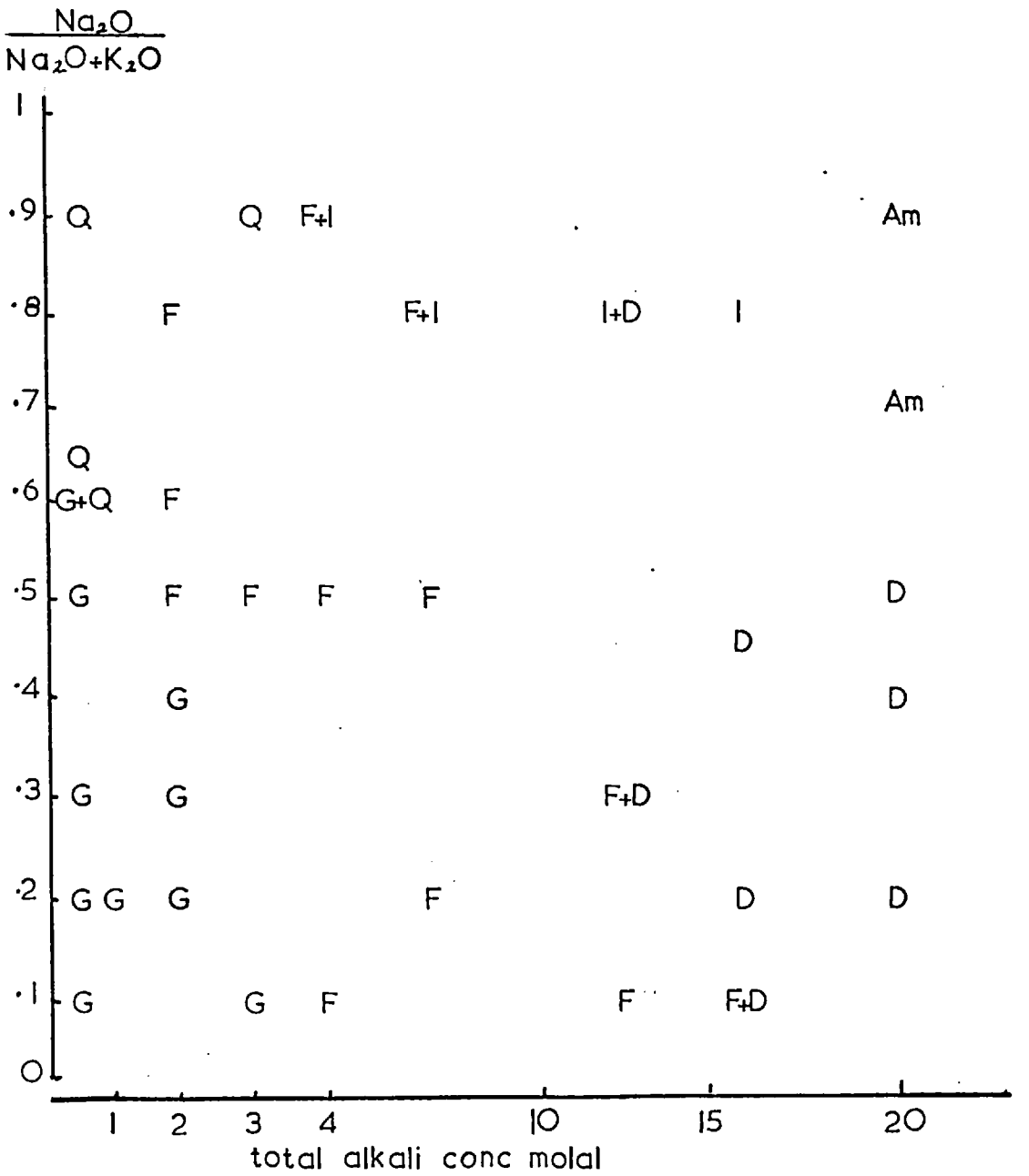

Table 3.6.1 (continued)

Run No.	Concentration of alkali (molality)	Cation fraction $\frac{Na_2O}{Na_2O + K_2O}$	Products	Description of products
6-65	7.0	0.8	F + I	md.cr.
6-68	13.0	0.1	F	md.cr.
6-69	13.0	0.3	F + D	md.cr.
6-70	13.0	0.8	I + D	Imd.cr./Dlo.yd.
6-71	16.0	0.1	F + D	F md.cr./D lo.yd.
6-72	16.0	0.2	D	md.cr.
6-74	16.0	0.45	D	md.cr.
6-76	16.0	0.8	I	gd.cr./lo.yd.
6-77	20.0	0.2	D	md.cr.
6-78	20.0	0.4	D	md.cr.
6-79	20.0	0.5	D	md.cr.
6-81	20.0	0.7	Am	-
6-83	20.0	0.9	Am	-

* The chabazite like phase G crystallized in the potassium rich part of the field. Where the sodium concentration was greater the pattern was much sharper. This is examined later in Section 3.6.10.

\+ The products here showed line splitting in the regions of higher sodium concentration. This is later interpreted as limited solid solubility between the potassium and sodium end members.

Table 3.6.2

1 metakaolinite + 2.8-233(mK_2O + $(1-n)Na_2O$) + $4SiO_2$ + ~ $275H_2O$

at 80° for 7 days.

Run No.	Concentration of alkali (molality)	Cation fraction $\frac{Na_2O}{Na_2O + K_2O}$	Product	Description of product
6-85	0.6	0.1	M	pr.cr.
6-86	0.6	0.3	M	pr.cr.
6-87	0.6	0.5	M + G	Mpr.cr.,Gmd.cr.
6-88	0.6	0.9	S	S pr.cr.
6-90	1.0	0.1	G	md.cr.
6-91	1.0	0.4	G	md.cr.
6-92	1.0	0.5	G + M	Gmd.cr.,Mlo.yd.
6-93	1.0	0.7	M	md.cr.
6-95	1.0	0.9	P2	gd.cr.
6-97	2.0	0.1	G	gd.cr.
6-98	2.0	0.4	G	gd.cr.
6-99	2.0	0.5	G + M	Ggd.cr.,Mmd.cr.
6-101	2.0	0.8	B + M	P2md.cr.,Mmd.cr.
6-102	2.0	0.9	P2	md.cr.
6-103	4.0	0.1	G + F	Gmd.cr.,Fgd.cr.
6-104	4.0	0.4	G	md.cr.
6-105	4.0	0.6	P2 + G	P2md.cr.,Gmd.cr.
6-107	4.0	0.8	P2	gd.cr.
6-108	7.0	0.1	F	gd.cr.
6-109	7.0	0.3	F	gd.cr.
6-111	7.0	0.6	F	gd.cr.
6-113	7.0	0.7	I + F	Ilo.yd.,Fmd.cr.
6-114	7.0	0.9	I	md.cr.
6-115	10.0	0.1	D	gd.cr.
6-116	10.0	0.3	D	md.cr.
6-117	10.0	0.5	D + I	Dmd.cr.,Ipr.cr.
6-118	10.0	0.7	I	pr.cr.
6-122	15.0	0.2	D	md.cr.
6-123	15.0	0.7	D	md.cr.

Figure 3.6.2 The Crystallization Field Resulting from :

$$1\,Metakaolinite + 2{\cdot}8-233(mK_2O+(1-m)Na_2O) + 4SiO_2 \mp 275H_2O$$

Rotated at 80° for 7 days

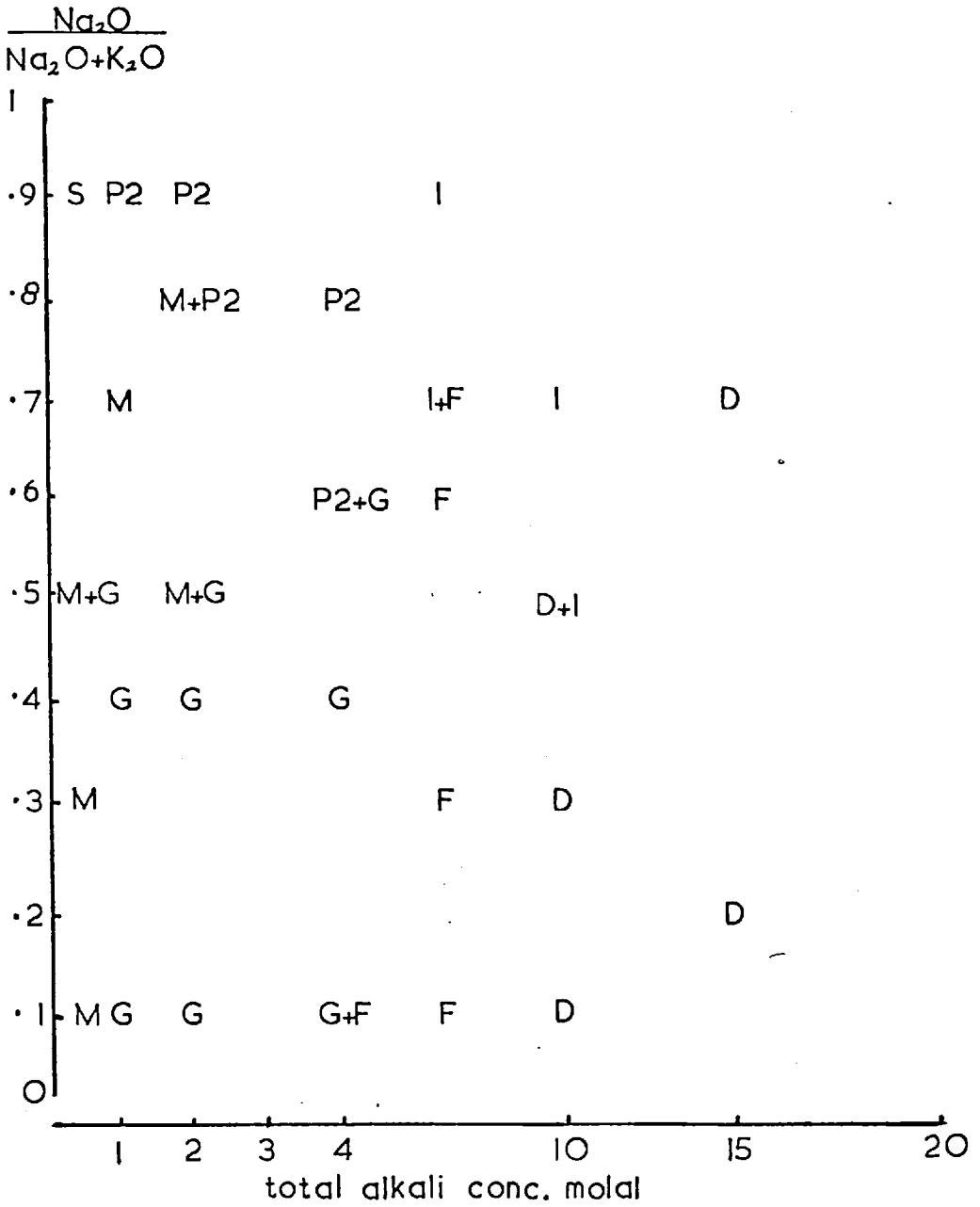

Table 3.6.3

1 metakaolinite + 2.8 - 233 (mK_2O + $(1-m)Na_2O$) + $.6SiO_2$ + $275H_2O$ at 80° for 7 days

Run No.	Concentration of alkali (molality)	Cation fraction $\frac{Na_2O}{Na_2O + K_2O}$	Product	Description of product
6-125	0.6	0.1	Am	-
6-126	0.6	0.5	Am	-
6-128	0.6	0.9	S	md.cr.
6-129	0.6	1.0	S	md.cr.
6-130	1.0	0.1	M + G	Mmd.cr.,Gpr.cr.
6-131	1.0	0.3	M	md.cr.
6-132	1.0	0.4	M + Pl	Mmd.cr.,Plo.yd.
6-133	1.0	0.9	Pl	gd.cr.
6-134	1.0	1.0	Pl + R	Plgd.cr.,Rmd.cr.
6-135	2.0	0.1	G	md.cr.
6-136	2.0	0.3	G	md.cr.
6-137	2.0	0.5	M + P2	Mmd.cr.,Plo.yd.
6-138	2.0	0.9	P2	Ppr.cr.
6-140	4.0	0.1	G	md.cr.
6-141	4.0	0.3	G + F	Gmd.cr.,Fmd.cr.
6-142	4.0	0.5	G + F	Glo.yd.,Fmd.cr.
6-144	4.0	0.8	P2	md.cr.
6-145	4.0	0.9	R	gd.cr.
6-146	7.0	0.1	F	md.cr.
6-147	7.0	0.4	F	md.cr.
6-149	7.0	0.9	I	pr.cr.
6-151	10.0	0.1	D	md.cr.
6-152	10.0	0.3	D	pr.cr.
6-153	10.0	0.5	D	pr.cr.
6-155	10.0	0.8	Am	-
6-156	15.0	0.1	D	md.cr.
6-157	15.0	0.5	Am	-
6-158	15.0	0.8	Am	-

Figure 3.6.3 The Crystallization Field Resulting from:

$$1\text{Metakaolinite} + 2{\cdot}8 - 233(mK_2O + (1-m)Na_2O) + 6SiO_2 \mp 275H_2O$$

Rotated at 80° for 7 days

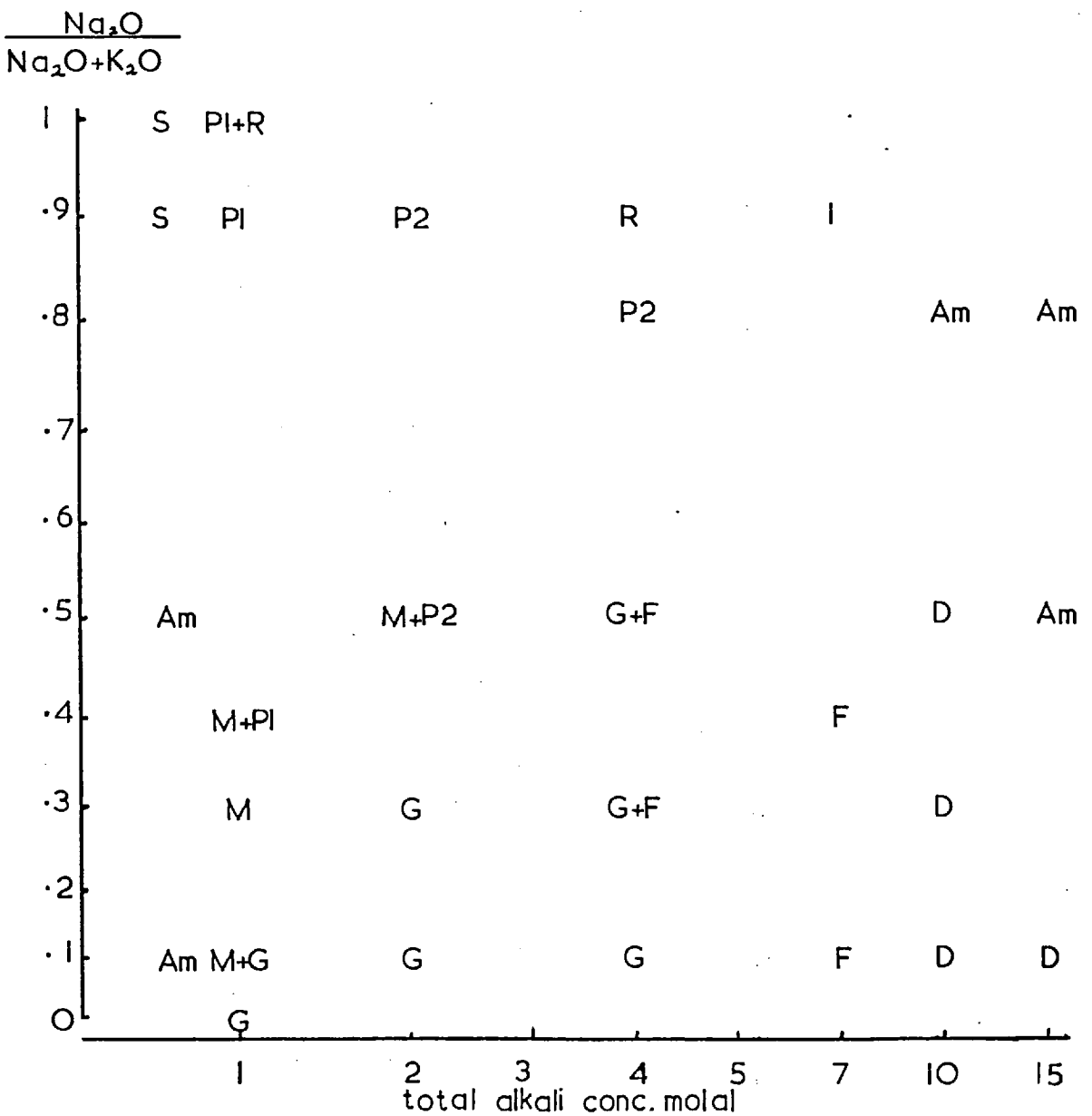

Table 3.6.4

1 metakaolinite + 2.8 - 233 (mK_2O + $(1-m)Na_2O$) + $8SiO_2$ + $275H_2O$ at 80° for 7 days.

Run No.	Concentration of alkali (molality)	Cation fraction $\frac{Na_2O}{Na_2O + K_2O}$	Product	Description of product
6-161	0.5	0.1	Am	-
6-162	0.5	0.5	Am	-
6-163	0.5	0.9	Am	-
6-165	1.0	0.1	M	md.cr.
6-166	1.0	0.5	M	md.cr.
6-168	1.0	0.9	M	pr.cr.
6-170	2.0	0.1	M + G	Mmd.cr.,Ggd.cr.
6-171	2.0	0.4	M + G	Mmd.cr.,Ggd.cr.
6-172	2.0	0.6	M	md.cr.
6-174	2.0	0.8	M	md.cr.
6-175	3.0	0.1	G	md.cr.
6-176	3.0	0.5	M + G	Mmd.cr.,Gpr.cr.
6-178	3.0	0.8	M	gd.cr.
6-179	3.0	0.9	Q + I	Qgd.cr.,Ilo.yd.
6-180	6.0	0.1	F	md.cr.
6-181	6.0	0.5	F	md.cr.
6-182	6.0	0.7	F	md.cr.
6-183	6.0	0.9	I	gd.cr.
6-184	6.0	1.0	I	gd.cr.
6-185	10.0	0.1	D	md.cr./lo.yd.
6-186	10.0	0.5	D	md.cr./lo.yd.
6-187	10.0	0.9	Am	-
6-190	0.5 (14 days)	0.1	M	pr.cr.
6-191	0.5 (14 days)	0.5	M	pr.cr.
6-192	0.5 (14 days)	0.9	S	md.cr.

Figure 3.6.4 The Crystallization Field Resulting from:

1 Metakaolinite +2·8–233(mK_2O+(1-m)Na_2O)+8SiO_2
∓275H_2O

Rotated at 80° for 7 days

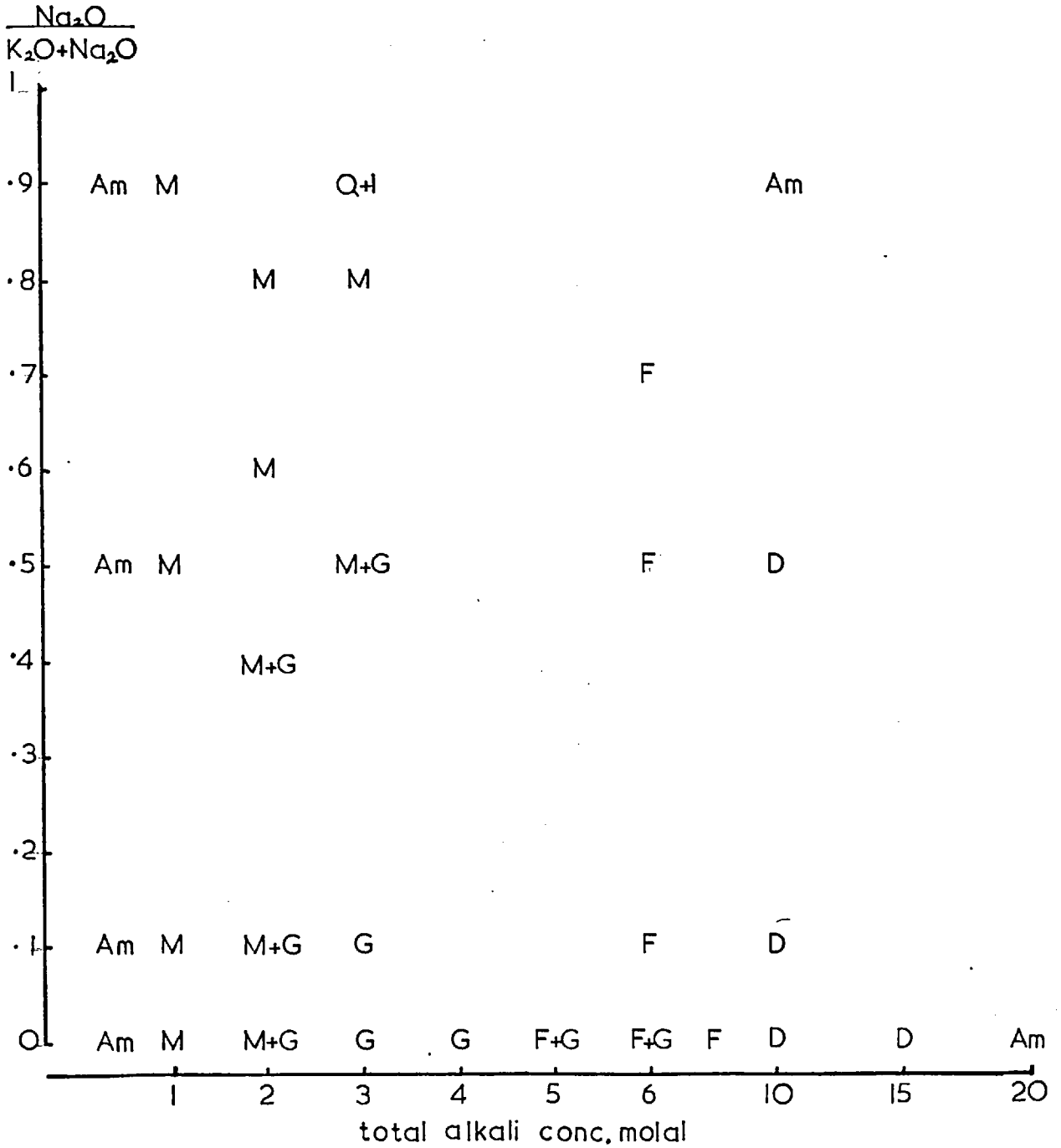

3.6.2 Properties of the Sodium-Potassium System

Throughout the crystallization fields in the presence of sodium and potassium hydroxides the products were predictable from a knowledge of the crystallization behaviour in presence of each base alone. Such prediction is not possible (Sections 3.7 and 3.8) with bases of widely different character such as tetra-methyl ammonium and sodium hydroxides.

In the NaOH - KOH - metakaolinite - silica - water systems as the cation fraction of, say, Na^+ declines, the initial product crystallizes with increasing amounts of the second cation, K^+. This continues until the more stable phase is that typical of the second cation, which then accommodates some of the initial cation.

An example from Figure 3.6.2 is the change in product at 1 molal concentration. When the sodium fraction varied from 0.0 to 0.5 the product was the chabazite-like phase G. At increased sodium fractions (0.6 - 0.8) the product was the more flexible lattice of phillipsite-like M. Predominantly sodium rich magmas (0.9 - 1.0) yielded the typical sodium zeolite P2. The effect upon the nature of the product when grown from mixed hydroxide systems is discussed later.

3.6.3 Reactions in the Sodium, Lithium System

The reactions carried out with metakaolinite, silica and mixed sodium and lithium bases are described in Tables 3.6.5 - 3.6.8. The crystallization fields have been plotted in Figures 3.6.5 - 3.6.8.

Table 3.6.5

1 metakaolinite + 2.5 - 75 ($mNa_2O + (1-m)Li_2O$) + ~ 275 H_2O rotated at 80° for 7 days.

Run No.	Concentration of alkali (molality)	Cation fraction $\frac{Li_2O}{Na_2O + Li_2O}$	Product	Description of product
6-200	0.5	0.1	Q + R	Qgd.cr.,Rtr.
6-201	0.5	0.3	C	md.cr.
6-202	0.5	0.5	C	md.cr.
6-204	0.5	0.75	C + A	Cmd.cr.,Agd.cr.
6-205	0.5	0.9	A	gd.cr.
6-206	1.0	0.1	Q	gd.cr.
6-207	1.0	0.3	Q	gd.cr.
6-208	1.0	0.5	Q	gd.cr.
6-209	1.0	0.6	F	md.cr.
6-210	1.0	0.7	F	md.cr.
6-213	1.0	0.75	F + C	Fmd.cr.,Cpr.cr.
6-211	1.0	0.9	C + F	Cmd.cr.,Ftr.
6-214	1.0	0.95	A + C	Agd.cr.,Cpr.cr.
6-215	2.0	0.1	P2	md.cr.
6-216	2.0	0.3	C + Q	Cmd.cr.,Qgd.cr.
6-217	2.0	0.5	C	md.cr.
6-218	2.0	0.8	C	md.cr.
6-219	2.0	0.9	A + C	Agd.cr.,Cmd.cr.
6-220	4.0	0.1	C + I	Cmd.cr.,Imd.cr.

Figure 3.6.5 The Crystallization Field Resulting from:

1 Metakaolinite +2·5–75(mNa_2O+(1-m)Li_2O)+275H_2O

Rotated at 80° for 7 days

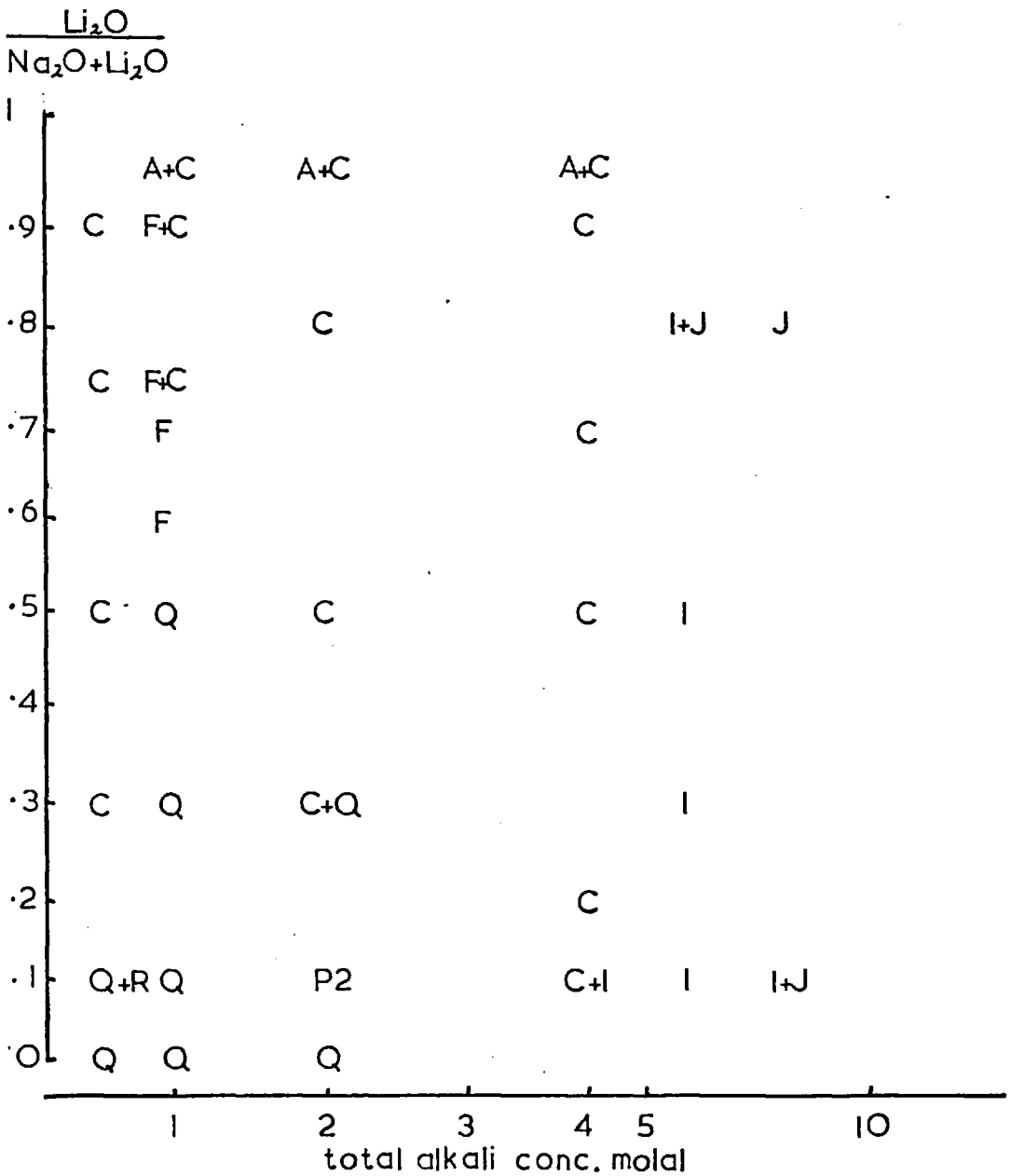

Table 3.6.5 (continued)

Run No.	Concentration of alkali (molality)	Cation fraction $\frac{Li_2O}{Na_2O + Li_2O}$	Product	Description of product
6-221	4.0	0.2	C	gd.cr.
6-226	4.0	0.9	C	md.cr.
6-228	4.0	0.95	A + C	Agd.cr., Cmd.cr.
6-227	6.0	0.1	I	md.cr.
6-230	6.0	0.5	I	pr.cr.
6-231	6.0	0.8	I + J	Ipr.cr., Jpr.cr.
6-232	8.0	0.1	I	md.cr.
6-233	8.0	0.5	I + J	Imd.cr., Jpr.cr.
6-235	8.0	0.8	J	pr.cr.

Table 3.6.6

1 metakaolinite + 2.5 - 75($mNa_2O + (1-m)Li_2O$)+ $4SiO_2$ + ~ $275H_2O$

rotated at 80° for 7 days.

Run No.	Concentration of alkali (molality)	Cation fraction $\frac{Li_2O}{Na_2O + Li_2O}$	Product	Description of product
6-237	0.5	0.1	S	md.cr.
6-238	0.5	0.3	S + P2	Smd.cr.,P2gd.cr.
6-239	0.5	0.5	Am	-
6-240	1.0	0.1	P1	md.cr.
6-241	1.0	0.2	P1	md.cr.
6-242	1.0	0.3	P2	md.cr.
6-243	1.0	0.5	P2	md.cr.
6-244	1.0	0.7	P2	md.cr.
6-245	1.0	0.9	P2 + A	P2pr.cr.,Agd.cr.
6-246	2.0	0.1	P1	gd.cr.
6-247	2.0	0.3	P2	md.cr.
6-248	2.0	0.8	P2	md.cr.
6-249	3.0	0.1	P1 + I	P1gd.cr.,Ipr.cr.
6-250	3.0	0.3	P1 + I	P1md.cr.,Imd.cr.
6-251	3.0	0.5	P1 + I	P1md.cr.,Imd.cr.
6-252	3.0	0.8	U	md.cr.
6-253	5.0	0.1	I	md.cr.
6-254	5.0	0.3	I	md.cr.
6-255	5.0	0.5	C + J	Cmd.cr.,Jpr.cr.
6-256	5.0	0.7	A	gd.cr.
6-257	8.0	0.1	I + J	Imd.cr.,Jpr.cr.
6-258	8.0	0.3	I + J	Imd.cr.,Jmd.cr.
6-259	8.0	0.6	J	md.cr.
6-260	9.0	0.1	I + J	Imd.cr.,Jmd.cr.
6-262	9.0	0.3	J	md.cr.
6-264	1.5	0.9	U	md.cr.
6-265	3.0	0.9	J + A	Agd.cr.,Upr.cr.

Figure 3.6.6. The Crystallization Field Resulting from:

1 Metakaolinite + 2·5–75($mNa_2O + (1-m)Li_2O$) + $4SiO_2$ ∓ $275H_2O$

Rotated at 80° for 7 days

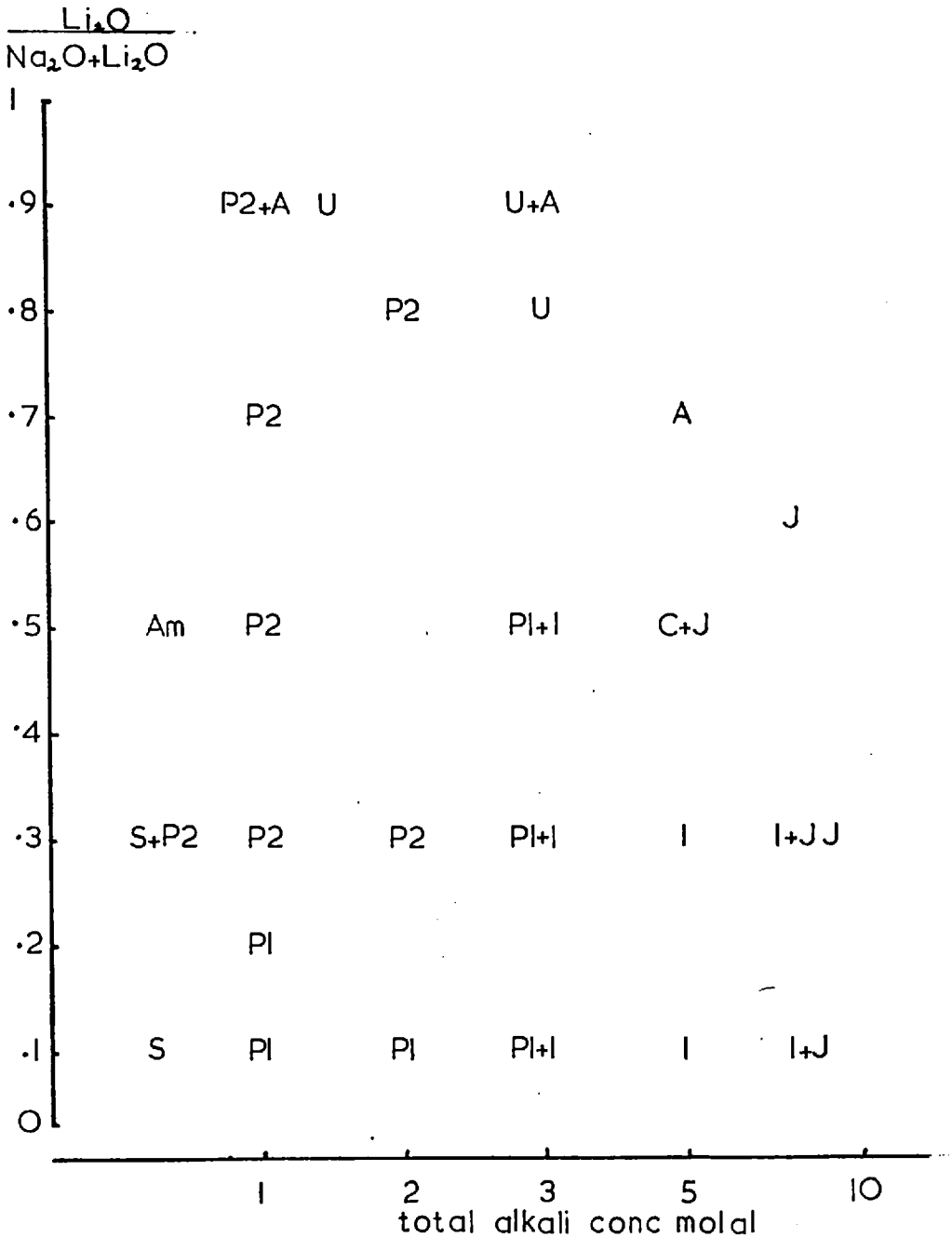

Table 3.6.7

1 metakaolinite + 2.5 - 75 ($mNa_2O + (1-m)Li_2O$) + $6SiO_2$ + ~ $275H_2O$

rotated at 80° for 7 days

Run No.	Concentration of alkali (molality)	Cation fraction $\frac{Li_2O}{Na_2O + Li_2O}$	Product	Description of product
6-270	0.5	0.1	S	md.cr.
6-271	0.5	0.2	S	md.cr.
6-272	0.5	0.4	Am	-
6-274	0.5	0.6	Am	-
6-277	1.0	0.1	R + P2	Rgd.cr.,P2md.cr.
6-278	1.0	0.3	P2	md.cr.
6-279	1.0	0.5	P2	md.cr.
6-281	1.0	0.8	P2 + J	P2md. Jpr.cr.
6-282	1.0	0.9	A	v.gd.cr.
6-283	2.0	0.1	P2 + R	P2md.cr.,Rgd.cr.
6-284	2.0	0.3	P2	md.cr.
6-285	2.0	0.5	P2 + J	P2md.cr.Jmd.cr.
6-286	2.0	0.8	P2 + J	P2md.cr.,Jmd.cr.
6-287	2.0	0.9	A + J	Amd.cr.,Upr.cr.
6-308	3.0	0.8	U + J	Upr.cr.,Jpr.cr.
6-309	3.0	0.9	U + J	Upr.cr.,Jpr.cr.
6-290	3.5	0.1	P2	md.cr.
6-291	3.5	0.3	P2	md.cr.
6-292	3.5	0.4	P2 + J	P2md.cr.,Jmd.cr.
6-295	3.5	0.8	I + J	Igd.cr.,Jmd.cr.
6-296	3.5	0.9	A + J	Agd.cr.,Jmd.cr.
6-298	6.0	0.1	I	md.cr.
6-299	6.0	0.3	I + J	Imd.cr.Jmd.cr.
6-301	6.0	0.8	I + J	Imd.cr.Jgd.cr.
6-302	6.0	0.9	J	gd.cr.
6-305	10.0	0.1	I	md.cr.
6-306	10.0	0.3	I + J	Imd.cr.Jmd.cr.
6-307	10.0	0.5	J	md.cr.

Figure 3.6.7 The Crystallization Field Resulting from:

1 Metakaolinite +2·5-75$(mNa_2O+(1-m)Li_2O)+6SiO_2$
$\mp 275H_2O$

Rotated at 80° for 7 days

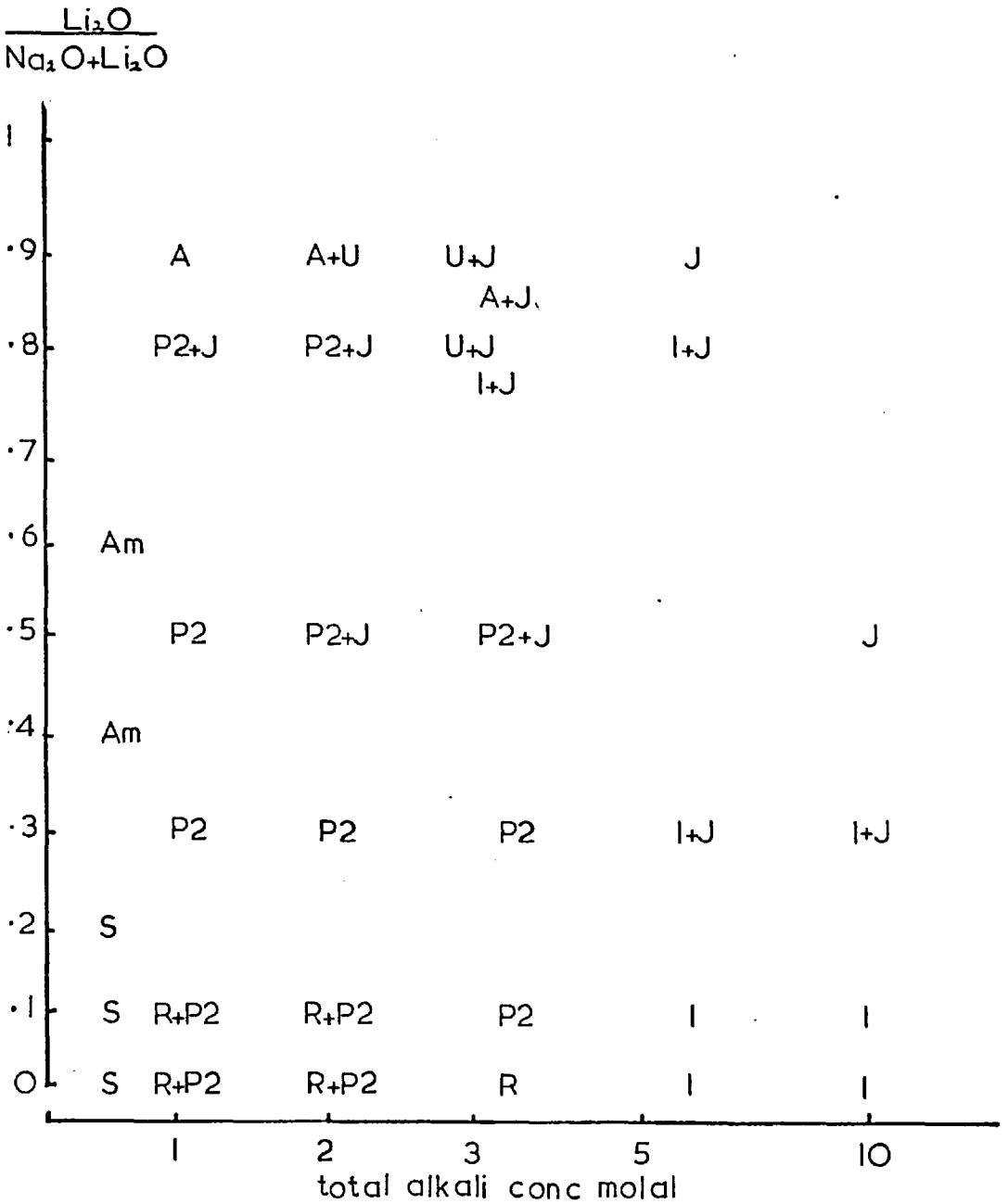

Table 3.6.8

1 metakaolinite + 2.5 - 75($mNa_2O + (1-m)Li_2O$) + $8SiO_2$ + ~$275H_2O$

rotated at 80° for 7 days.

Run No.	Concentration of alkali (molality)	Cation fraction $\frac{Na_2O}{Na_2O + Li_2O}$	Product	Description of product
6-310	0.5	0.1	Am	-
6-311	0.5	0.5	Am	-
6-312	0.5	0.9	Am	-
6-315	1.0	0.1	Pl	md.cr.
6-316	1.0	0.3	Pl + J	Plmd.cr.,Jpr.cr.
6-318	1.0	0.7	Pl + J	Plmd.cr.,Jpr.cr.
6-319	1.0	0.9	U	md.cr.
6-320	2.0	0.1	P2	md.cr.
6-321	2.0	0.2	P2 + J	P2md.cr.,Jlo.yd.
6-322	2.0	0.4	P2 + J	P2md.cr.,Jmd.cr.
6-325	2.0	0.9	P2 + J	P2md.cr.,Jmd.cr.
6-327	3.0	0.1	P2	md.cr.
6-328	3.0	0.3	P2 + J	P2md.cr.,Jpr.cr.
6-329	3.0	0.4	P2 + J	P2md.cr.,Jmd.cr.
6-331	3.0	0.9	P2 + J	P2gd.cr.,Jmd.cr.
6-332	6.0	0.1	P2 + J	P2md.cr.,Jpr.cr.
6-333	6.0	0.2	P2 + J	P2md.cr.,Jmd.cr.
6-334	6.0	0.3	P2 + I + J	P2md.cr.,Itr.
6-335	6.0	0.5	I + J	Ipr.cr.,Jmd.cr.
6-337	6.0	0.9	I + J	Igd.cr.,Jmd.cr.
6-338	8.0	0.1	I + J	Ipr.cr.,Jmd.cr.
6-340	10.0	0.1	I + J	Igd.cr.,Jgd.cr.
6-341	10.0	0.3	I + J	Igd.cr.,Jgd.cr.
6-344	10.0	0.8	J	gd.cr.
6-345	1.0	0.8	U	md.cr.
6-346	2.0	0.8	U + P2	Umd.cr.,P2pr.cr.

Figure 3.6.8 The Crystallization Field Resulting from:

1 Metakaolinite +2·5–75(mNa_2O+(1-m)Li_2O)+8SiO_2 ∓275H_2O

Rotated at 80° for 7 days

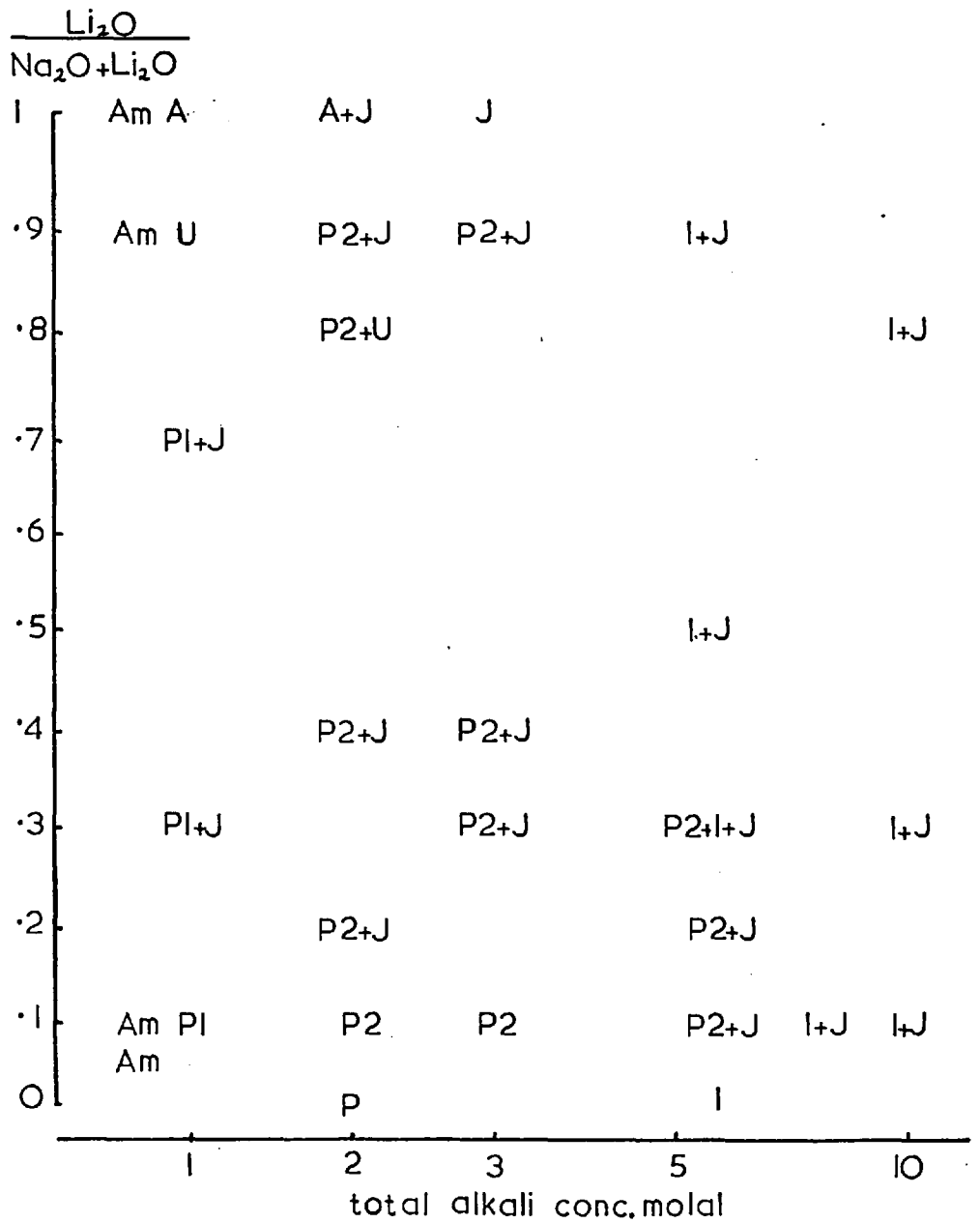

3.6.4 Observations on the Sodium-Lithium System

The reactions of metakaolinite + silica with the mixed aqueous sodium and lithium hydroxides gave products which were, with two exceptions, characteristic of either hydroxide reacting alone. Cancrinite was found in a large area of the crystallization field shown in Figure 3.6.5. This product was not typical of crystallizations at 80° with NaOH alone, but in the presence of lithium cations it formed readily.

With increased silica contents (silica:alumina ratio 6, 8 and 10) high lithium cation fractions produced species U which was related to the montmorillonite layer type minerals. The other crystalline product not synthesized using either hydroxide alone was Na, Li-F. This formed from less siliceous initial compositions (silica:alumina = 2) in regions of high lithium fractions.

3.6.5 Reactions in the Potassium, Lithium System

The reactions carried out with metakaolinite silica, and mixed potassium and lithium bases are described in Tables 3.6.9 - 3.6.12. The crystallization fields have been plotted in Figures 3.6.9 - 3.6.12.

Table 3.6.9

1 metakaolinite + 2.5 - 233 ($mK_2O + (m-1)Li_2O$) + ~275 H_2O

rotated at 80° for 7 days

Run No.	Concentration of alkali (molality)	Cation fraction $\frac{Li_2O}{Li_2O + K_2O}$	Product	Description of product
6-348	0.5	0.1	G	md.cr.
6-349	0.5	0.2	G	md.cr.
6-350	0.5	0.3	F	md.cr.
6-352	0.5	0.8	F + A	Fmd.cr.,Agd.cr.
6-355	1.0	0.1	F + G	Fmd.cr.,Gmd.cr.
6-356	1.0	0.2	F	md.cr.
6-357	1.0	0.3	F	md.cr.
6-359	1.0	0.65	F	md.cr.
6-362	1.0	0.9	A	gd.cr.
6-363	3.0	0.2	F	md.cr.
6-364	3.0	0.3	F	gd.cr.
6-365	3.0	0.4	F	gd.cr.
6-366	3.0	0.5	F + A	Fgd.cr.,Agd.cr.
6-369	3.0	0.65	F + A	Fgd.cr.,Agd.cr.
6-367	3.0	0.8	A	gd.cr.
6-370	5.0	0.9	F + J	Fgd.cr.,Jpr.cr.
6-372	7.5	0.2	F	gd.cr.
6-373	7.5	0.4	F	md.cr.

Figure 3.6.9 The Crystallization Field Resulting from:

1 Metakaolite + 2·5–233 $(mK_2O + (1-m)Li_2O) + 275H_2O$

Rotated at 80° for 7 days.

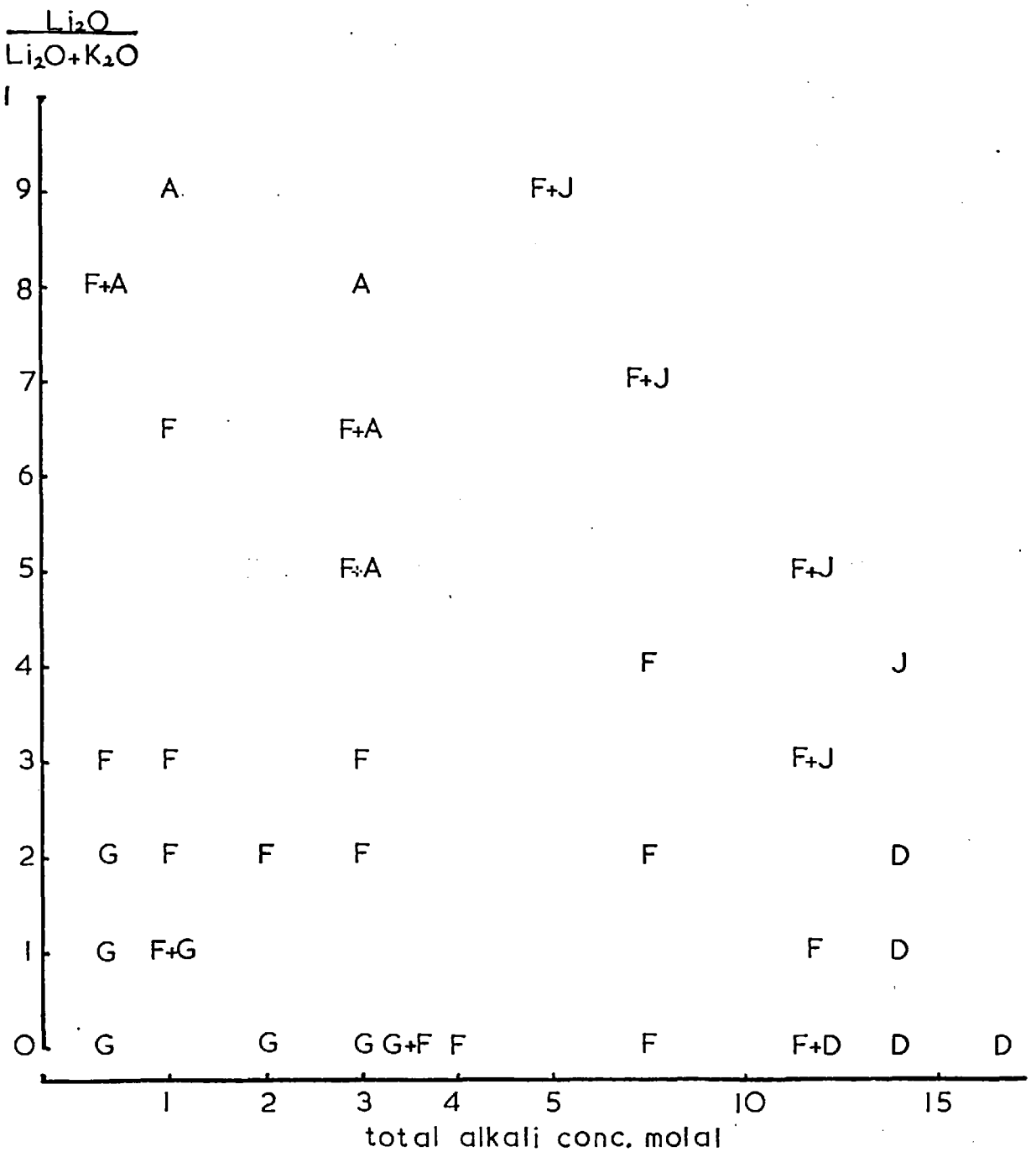

Table 3.6.9 (continued)

Run No.	Concentration of alkali (molality)	Cation fraction $\frac{Li_2O}{Li_2O + K_2O}$	Product	Description of product
6-374	7.5	0.7	F + J	Fmd.cr., Jtr.
6-378	12.0	0.1	F	md.cr.
6-379	12.0	0.3	F + J	Fmd.cr., Jpr.cr.
6-380	12.0	0.5	F + J	Fmd.cr., Jmd.cr.
6-381	14.0	0.1	D	md.cr.
6-382	14.0	0.2	D	md.cr.
6-383	14.0	0.4	J	md.cr.

Table 3.6.10

1 metakaolinite + 2.5 - 233(mK_2O + $(m-1)Li_2O$) + $4SiO_2$ + ~ $275H_2O$

rotated at 80° for 7 days.

Run No.	Concentration of alkali (molality)	Cation fraction $\frac{Li_2O}{Li_2O + K_2O}$	Product	Description of product
6-385	0.5	0.1	Am	-
6-386	0.5	0.5	Am	-
6-389	0.5	0.9	Am	-
6-390	1.0	0.1	S + F	Smd.cr.,Fmd.cr.
6-391	1.0	0.3	S + M	Smd.cr.,Mmd.cr.
6-392	1.0	0.5	M	md.cr.
6-393	1.0	0.7	M + G	Mmd.cr.,Gtr.
6-394	1.0	0.9	U	md.cr.
6-400	2.0	0.1	G + F	Gmd.cr.,Fpr.cr.
6-401	2.0	0.3	G	md.cr.
6-403	2.0	0.6	G	md.cr.
6-404	2.0	0.9	U	pr.cr.
6-406	3.0	0.1	G + F	Gmd.cr.,Fmd.cr.
6-407	3.0	0.3	G	md.cr.
6-408	3.0	0.6	G	md.cr.
6-409	3.0	0.9	G + J	Glo.yd.,Jpr.cr.
6-411	4.5	0.1	F	md.cr.
6-413	4.5	0.5	F	md.cr.
6-415	4.5	0.6	F	md.cr.
6-417	4.5	0.8	F + J	Fmd.cr.,Jmd.cr.
6-418	7.5	0.1	F	md.cr.
6-419	7.5	0.4	F + J	Fmd.cr.,Jmd.cr.
6-422	11.0	0.1	D	md.cr.
6-423	11.0	0.3	D + J	Dmd.cr.,Jmd.cr.
6-425	11.0	0.6	J	md.cr.
6-426	15.0	0.2	J	md.cr.
6-428	3.0	0.8	M + U	Mmd.cr.,Utr.

Figure 3.6.10 The Crystallization Field Resulting from:

1 Metakaolinite +2·5-233 ($mK_2O+(m-1)Li_2O$)+4SiO_2+~275H_2O

Rotated at 80° for 7 days

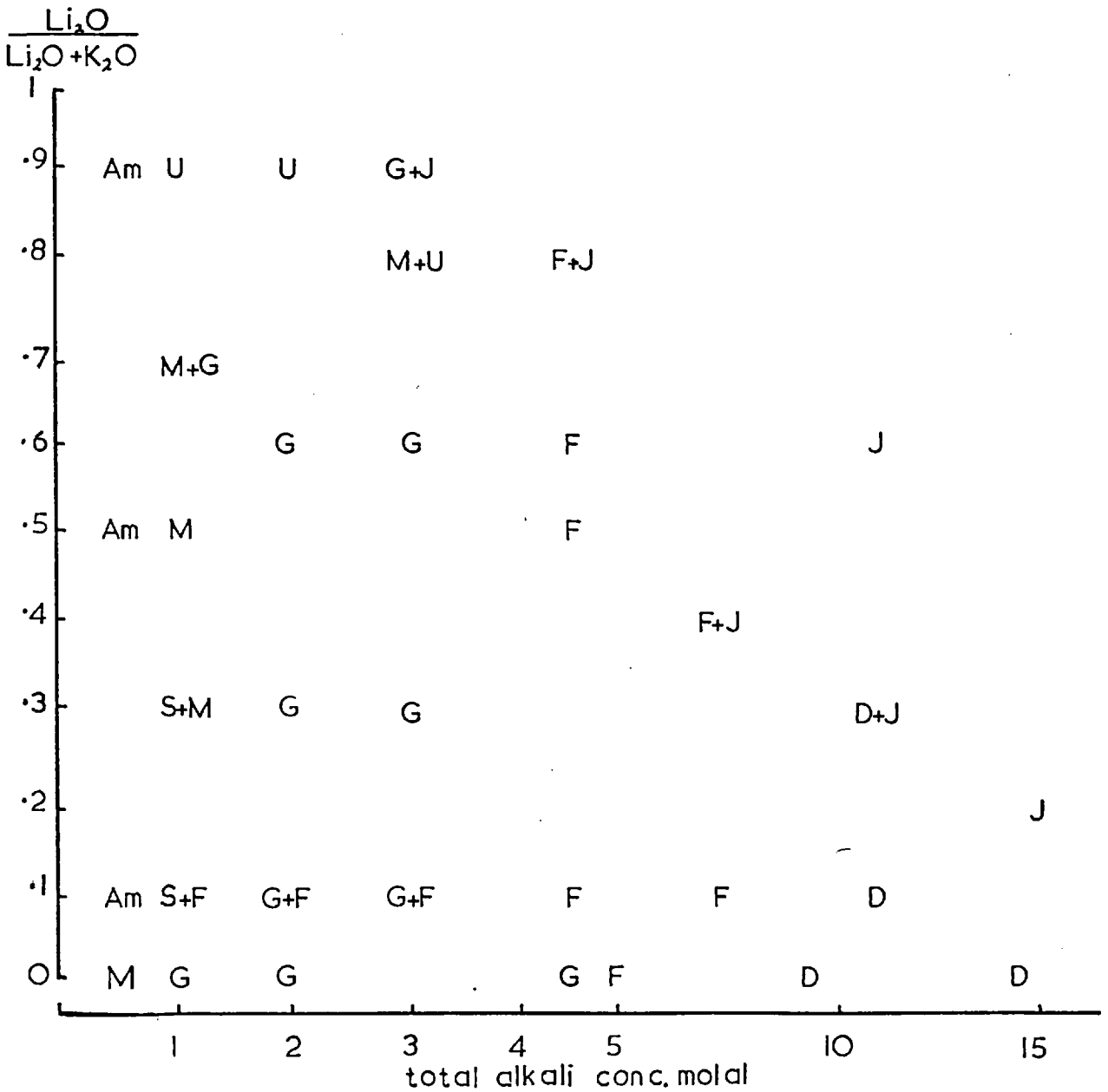

Table 3.6.11

1 metakaolinite + 2.5 - 233(mK_2O + $(m-1)Li_2O$ + $6SiO_2$ + ~ 275 H_2O

rotated at 80° for 7 days.

Run No.	Concentration of alkali (molality)	Cation fraction $\frac{Li_2O}{Li_2O + K_2O}$	Product	Description of product
6-430	0,5	0.1	Am	-
6-431	0.5	0.5	Am	-
6-432	0.5	0.8	Am	-
6-433	1.0	0.1	M	md.cr.
6-434	1.0	0.3	M	md.cr.
6-435	1.0	0.5	M + G	Mmd.cr.,Gmd.cr.
6-437	1.0	0.7	M + G	Mmd.cr.,Gmd.cr.
6-438	1.0	0.9	M + A	Mmd.cr.,Atr.
6-441	3.0	0.1	F	md.cr.
6-442	3.0	0.3	M + S	Mmd.cr.,Slo.yd.
6-445	3.0	0.5	M + S	Mmd.cr.,Spr.cr.
6-446	3.0	0.7	G+M+U	Gtr.,Mmd.cr.,Upr.cr.
6-447	3.0	0.8	G+M+U	Gtr.,Mmd.cr.,Upr.cr.
6-448	3.0	0.9	U + J	Upr.cr.,Jmd.cr.
6-450	5.0	0.1	F	md.cr.
6-452	5.0	0.3	F	md.cr.
6-454	5.0	0.5	F	md.cr.
6-458	5.0	0.7	F + J	Fpr.cr.,Jmd.cr.
6-459	8.0	0.2	F	md.cr.
6-460	8.0	0.7	F + J	Fpr.cr.,Jmd.cr.
6-461	10.0	0.1	D + J	Dmd.cr.,Jpr.cr.
6-463	10.0	0.5	J	md.cr.
6-465	5.0	0.9	U + J	Upr.cr.,Jmd.cr.
6-468	10.0	0.9	U + J	Upr.cr.,Jmd.cr.
6-471	15.0	0.3	J	md.cr.
6-472	15.0	0.5	J	md.cr.
6-473	15.0	0.7	J	pr.cr.

Figure 3.6.11 The Crystallization Field Resulting from: 1 Metakaolinite +2·5-233$(mK_2O+(m-1)Li_2O)+SiO_2+{\sim}275H_2O$ Rotated at 80° for 7 days

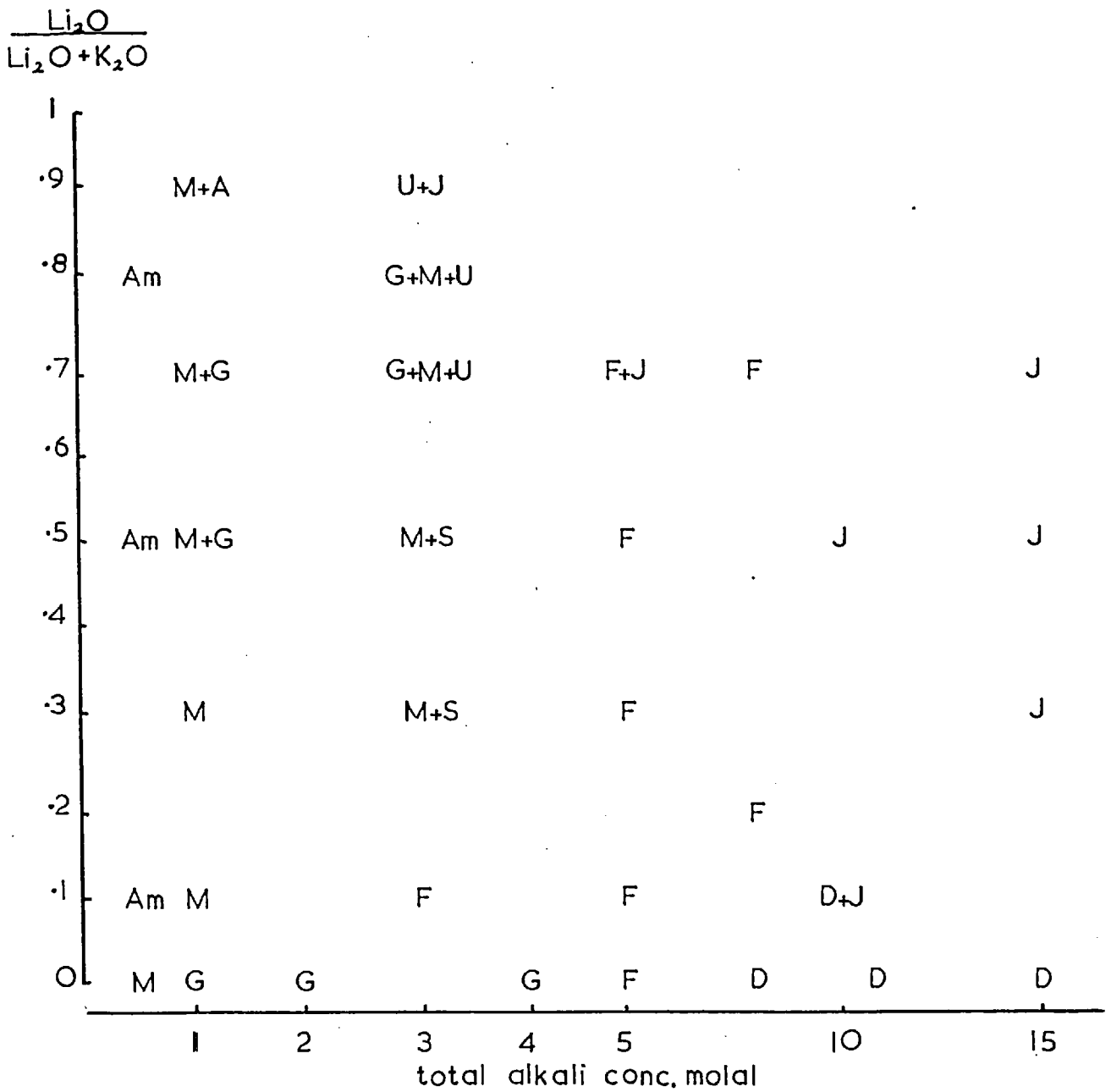

Table 3.6.12

1 metakaolinite + 2.5 - 233(mK_2O + $(m-1)Li_2O$) + $8SiO_2$ + ~ $275H_2O$

rotated at 80° for 7 days.

Run No.	Concentration of alkali (molality)	Cation fraction $\frac{Li_2O}{Li_2O + K_2O}$	Product	Description of product
6-475	0.5	0.1	Am	-
6-476	0.5	0.5	Am	-
6-478	0.5	0.9	Am	-
6-479	1.0	0.1	M	md.cr.
6-480	1.0	0.3	M	md.cr.
6-482	1.0	0.5	M	md.cr.
6-484	1.0	0.7	M	md.cr.
6-485	1.0	0.9	A	gd.cr.
6-486	2.0	0.1	G	md.cr.
6-488	2.0	0.3	M	gd.cr.
6-489	2.0	0.5	M	md.cr.
6-490	2.0	0.7	M + U	Mpr.cr.,Upr.cr.
6-491	2.0	0.9	M + J	Mpr.cr.,Jmd.cr.
6-493	5.0	0.1	F	md.cr.
6-494	5.0	0.3	F + J	Fmd.cr.,Jmd.cr.
6-495	5.0	0.5	F + J	Fmd.cr.,Jmd.cr.
6-497	5.0	0.7	F + J	Fmd.cr.,Jmd.cr.
6-498	5.0	0.9	J + U	Upr.cr.,Jmd.cr.
6-500	8.0	0.2	F + J	Fmd.cr.,Jmd.cr.
6-502	8.0	0.5	F + J	Fpr.cr.,Jgd.cr.
6-504	10.0	0.1	D	md.cr.
6-505	10.0	0.2	D + J	Dmd.cr.,Jmd.cr.
6-504	3.0	0.5	M	md.cr.
6-507	3.0	0.9	M + U	Mmd.cr.,Upr.cr.

Figure 3.6.12 The Crystallization Field Resulting from:

1 Metakaolinite + 2·5–233(mK_2O+(1-m)Li_2O)+8SiO_2 ∓275H_2O

Rotated at 80° for 7 days

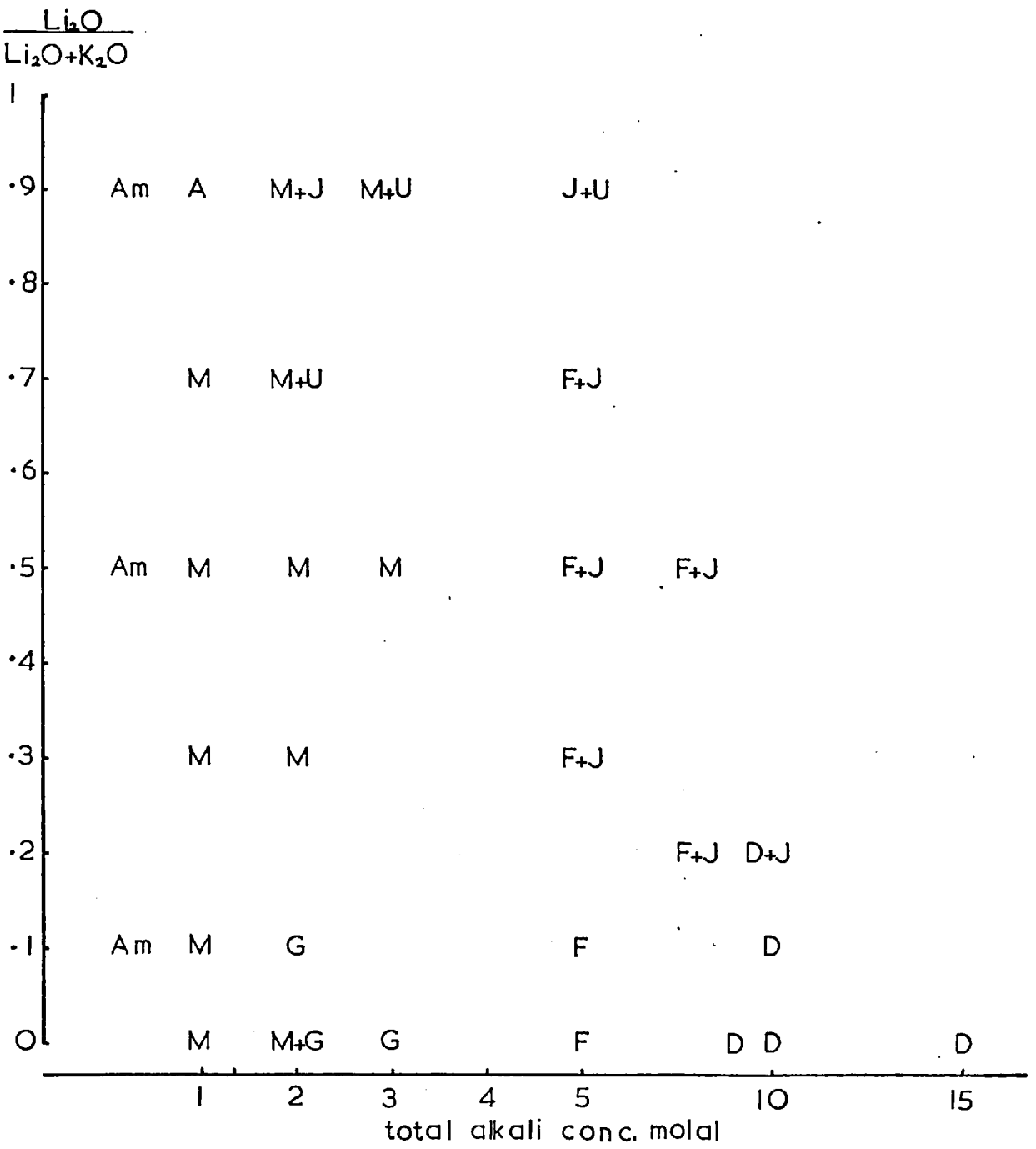

3.6.6 Observations on the Potassium-Lithium System

The reactions of aqueous potassium + lithium hydroxide with metakaolinite + silica again gave products, with the exception of species U, which were typical of syntheses using either potassium or lithium hydroxide alone. As with the sodium-lithium crystallization fields species U was formed from compositions rich in silica and lithium. The very large area in which the species F crystallized in the potassium-lithium field is noteworthy (Figure 3.6.9). The other structure, again typical of potassium crystallizations, which can accommodate lithium is species M. This replaces F in the crystallization fields from silica-rich compositions.

A comparison of the lithium-potassium crystallization field (Figure 3.6.9) with that of the lithium-sodium field(3.6.5) shows that the zeolite lithium A is able to form in regions of much higher potassium concentration than sodium.

3.6.7 A Comparison of the Mixed Cation Crystallization Fields

The three mixed hydroxide crystallization fields varied in producing species characteristic of the ion-pair involved. The sodium-potassium field gave only those products which were produced earlier by either one of the hydroxides when used alone. The potassium-lithium gave similar products and also the species U. While the sodium-lithium crystallization field yielded species U, a cancrinite at 80° and a product Na, Li-F related to K-F.

The syntheses of the zeolite F structure in the sodium-lithium crystallization field shows that this species crystallizes from all three dicationic magmas formed from the univalent alkali cations Li, Na and K. All syntheses of this zeolite are described in Table 3.4.2 of Section 3.4.3.

3.6.8 The Species Na, K-M and Li, K-M.

This product was the mixed cationic form of K-M (Section 3.1.6). It occurred as the product from both sodium-potassium and lithium-potassium systems. With sodium-potassium hydroxide and lithium-potassium hydroxide species M was formed from compositions with silica to alumina ratios of 6, 8 and 10. Previous syntheses of Na, K-M were reported by Barrer, Baynham, Bultitude and Meier (1959).

Chemical analysis of a sample from the sodium-potassium system gave the following composition.

	% by weight	Molar proportion
SiO_2	3	5.9
Al_2O_3	11	1
K_2O	17	0.7
Na_2O	58	0.3
H_2O (by difference)	11	4.0

This product is thus more silica rich than the K-M of Section 3.1.6 which had a silica to alumina ratio of 3.7. The composition may be compared with that of the natural phillipsite reported by Steinfink (1962) which

had a composition

$$(K_x, Na_{1-x})_5 Si_{11}Al_5O_{32}.10\ H_2O$$

giving an oxide ratio

$$(K_x, Na_{1-x})_2O,\ Al_2O_3,\ 4.4\ SiO_2,\ 4\ H_2O$$

and synthetic phillipsites reported by Kühl (1969) ZK-19:

$$(K_x\ Na_{1-x})_2O,\ Al_2O_3,\ 3.26 - 6.22\ SiO_2,\ 3.2\ H_2O.$$

The X-ray diffraction pattern of the mixed Na, K-M was sharp and very similar to that of the sedimentary phillipsite studied by Steinfink. The X-ray diffraction pattern of the potassium exchanged Na, K-M was corrected with an internal standard, and indexed by analogy to Steinfink's orthorhombic natural phillipsite. The observed and calculated d-spacings are given in Table 3.6.13. The orthorhombic unit cell constants were:

$$a = 9.959 \pm 0.003\ \text{Å}$$
$$b = 14.248 \pm 0.004$$
$$c = 14.246 \pm 0.010$$

Also included in Table 3.6.13 are the d-spacings of the sedimentary phillipsite used by Steinfink. A comparison

Table 3.6.13

X-ray d-spacings of Na, K-M and the natural phillipsite (Steinfink 1962).

K^{ex} (Na, K-M)			Natural phillipsite	
a = 9.959 ± 0.003			a = 9.965	
b = 14.248 ± 0.004			b = 14.25_2	
c = 14.246 ± 0.010			c = 14.25_2	
d_{obs}	d_{calc}	Ind	d_{obs}	hkl
10.29	10.07	011		
8.295	8.163	101	8.167	101
7.183	7.124	020	7.126	002
5.384	5.367	121	5.369	121
5.020	5.037	022	5.039	022
4.502	4.506	031	4.982	200
4.291	4.287	130	4.288	103
4.091	4.082	220	4.106	113
-	-		4.083	220
-	-		3.953	032
3.673	3.673	123	3.674	123
3.529	3.541	222	3.563	004
			3.457	014
3.258	3.265	141	3.266	141
3.243	3.233	310	3.235	301
			3.187	024
3.181	3.186	042	3.183	133
			3.155	311
			3.097	232
2.946	2.944	321	2.946	321
2.765	2.784	233	2.898	240
2.730	2.721	330	2.740	105,143
2.681	2.684	242	2.685	224
			2.558	125
2.549	2.542	332	2.543	323
2,513	2.519	044	2.519	044
2.398	2.394	341	2.395	341

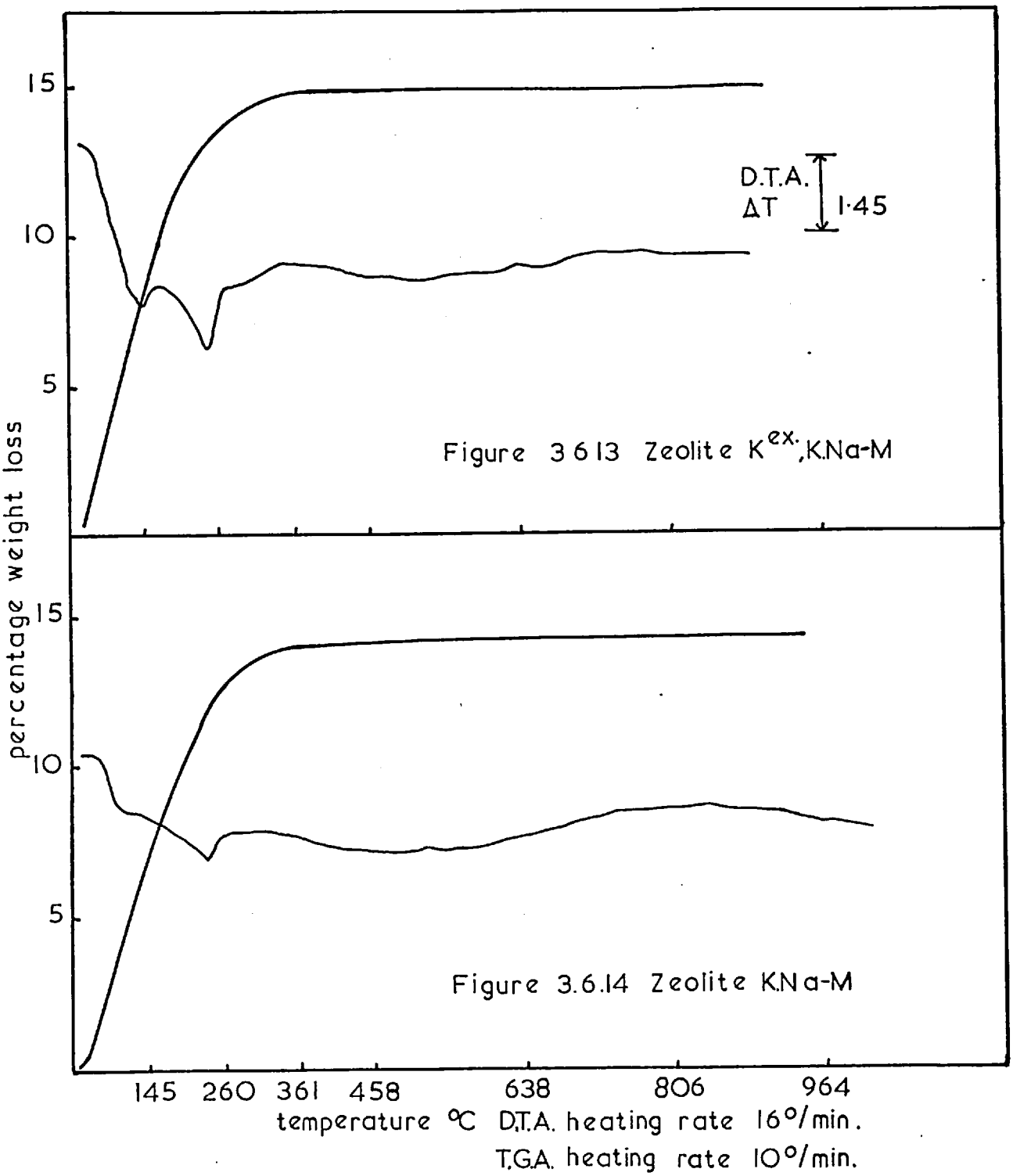

Figure 3 6 13 Zeolite $K^{ex.}$,K.Na-M

Figure 3.6.14 Zeolite K.Na-M

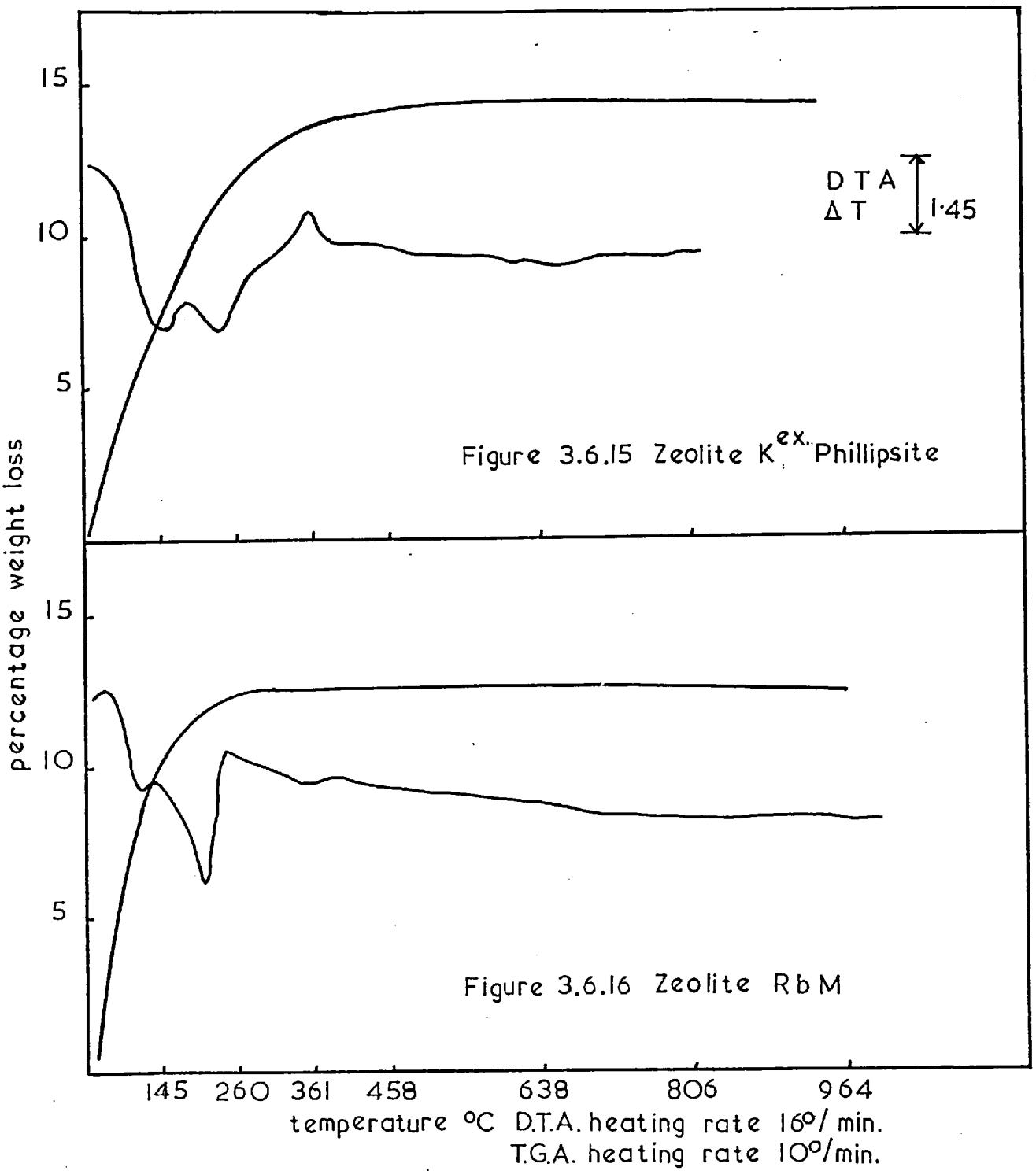

Figure 3.6.15 Zeolite $K^{ex.}$ Phillipsite

Figure 3.6.16 Zeolite Rb M

of the potassium exchanged form of Na, K-M and that of the potassium synthesized K-M (Section 3.1.6, Table 3.1.4) shows these to be identical.

Although the lattice dimensions varied with the cation present during crystallization or introduced by ion-exchange, no evidence was found, in the regions covered by Figures 3.6.2 to 3.6.4 and 3.6.10 to 3.6.12, that limited solid solubility occurred and that the product was a mixture of two forms.

The thermal properties of the sample of Na, K-M and the potassium exchanged product are given in Figures 3.6.14 and 3.6.13. Here they are compared with potassium exchanged natural phillipsite. Not only is the X-ray diffraction pattern of the mixed Na, K-M more like that of the phillipsite but also the D.T.A. of Na, K-M approximates to that of the natural mineral. Ion-exchange to the potassium form gives a product having a widely different D.T.A. curve (Figure 3.6.14).

The Na, K-M was outgassed at 350° and was found to be stable. As with K-M the sample would not sorb either oxygen at 78°K or n-butane at 273°K. This is consistent with observations of Kühl (1969) who found that synthetic phillipsites which were grown in the presence of phosphates

(Kühl 1967) sorbed 12% water but very little n-hexane. This low n-hexane sorption was probably surface condensation as shown in Figure 3.1.8 for oxygen on K-M.

3.6.9 The Species K, Na-F and K, Li-F

Both K, Na-F and K, Li-F crystallized from reacting compositions having silica to alumina ratios which varied from 2 to 10. A comparison of the K, Na crystallization field with that of the K,Li shows that the F structure tended to form in areas of greater lithium concentration. Thus at large values of $\frac{Na^+}{Na^+ + K^+}$ in the initial compositions the products were typical of crystallizations observed when only Na^+ was present. However, even for considerable values of $\frac{Li^+}{Li^+ + K^+}$ (≤ 0.9) and at high total concentrations of base the phase K,Li-F still appeared (Figure 3.6.9).

The X-ray diffraction patterns of the species F crystallized in the K-Na field showed that the unit cell size varied for various values of the ion fraction $\frac{Na^+}{Na^+ + K^+}$, and that for certain values of this fraction there were two complete diffraction patterns present with different d-spacings. The positions of the strong 2.93 Å line of K-F in these Na,F forms were compared by powder diffraction by the addition of an internal standard. The shifts in this line with the cation composition of the initial mixture are presented in Table 3.6.14 as the difference $\Delta 4\theta$ (where $\Delta 4\theta = 4\theta_{KF} - 4\theta_{K,Na-F}$). This difference is plotted against

cation fraction in solution in Figure 3.6.17. Also included for comparison is the potassium-sodium ion-exchange isotherm obtained by Barrer and Munday (1970).

Table 3.6.14

Cation fraction in solution $\left(\frac{K^+}{K^+ + Na^+}\right)$	$\Delta 4\theta$mm ($\Delta 4\theta = 4\theta_{K-F} - 4\theta_{K,Na-F}$)
0	0
0.9	0.150
0.8	0.275
0.7	0.350
0.6	0.388
0.5 (two complete diffraction patterns present)	0.588 0.988
0.4	1.088
0.3	1.113
1.0 (by ion-exchange)	1.117

From Table 3.6.14 it can be seen that a two-phase region exists where the cation fraction in the synthesis solution was 0.5. This is in contrast to the ion-exchange isotherm found by Barrer and Munday, who found limited solid solubility existed when the exchanging solution had a cation

Figure 3.6.17 Lattice Variation during Synthesis of K,Na F with the Ion exchange Isotherm (Barrer & Munday)

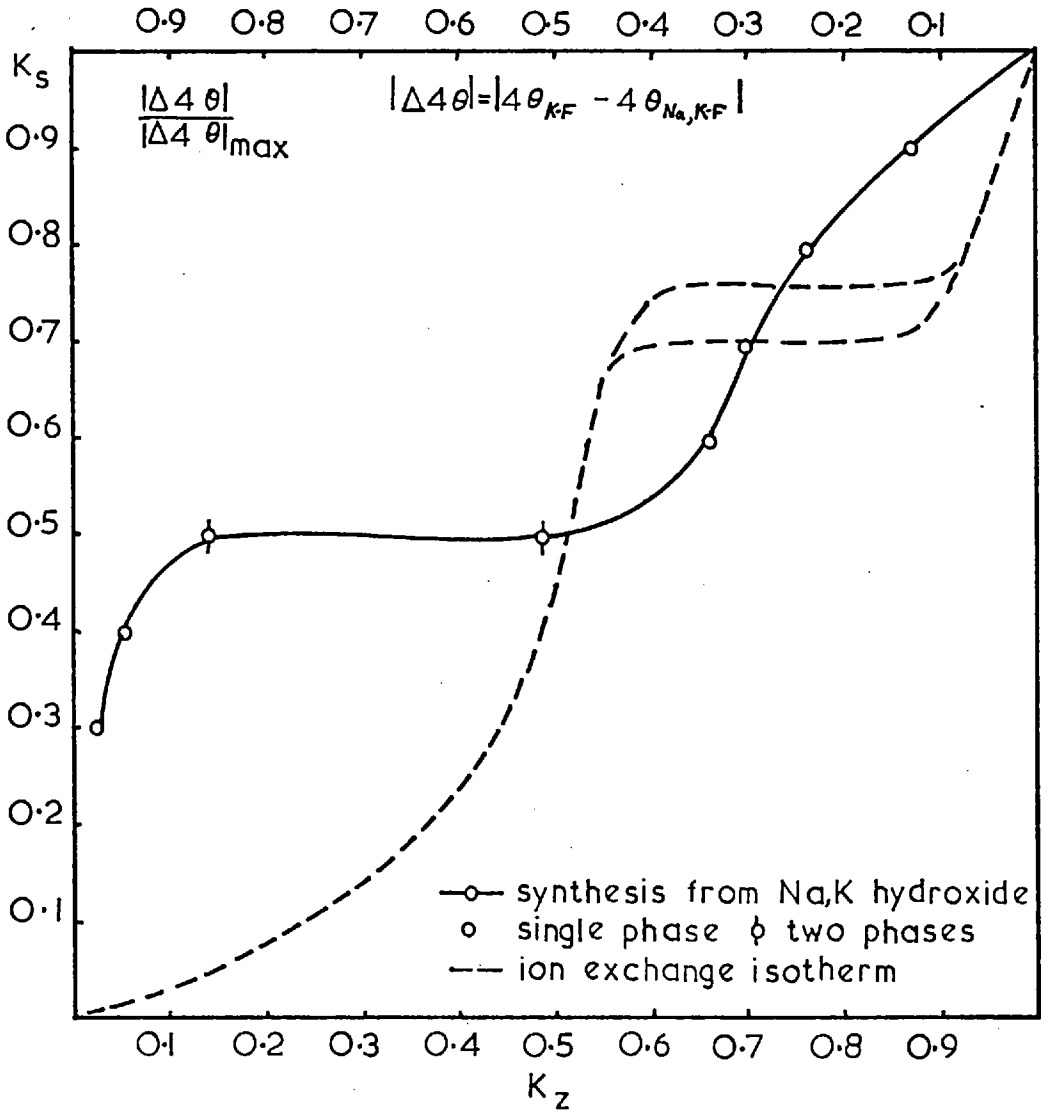

fraction of ~.725. If $\Delta 4\theta$ is assumed to vary linearly with composition then it can be seen that limited solid solubility between the potassium and sodium end-members for synthesis and ion-exchange occur in significantly different zeolite compositions. The ranges of composition as shown by the potassium fraction are 0.14 - 0.49 and 0.58 - 0.92 for synthesis and ion-exchange respectively.

No evidence for limited solid solubility in the potassium-lithium system was found. Various preparations of K, Li-F from the crystallization field shown in Figure 3.6.9 were analysed and the results are given below in Table 3.6.15.

Table 3.6.15

Cation fraction in solution $\left(\frac{Li^+}{Li^+ + K^+}\right)_s$	Cation fraction in zeolite $\left(\frac{Li^+}{Li^+ + K^+}\right)_z$
0.20	0.29
0.30	0.33
0.40	0.35
0.45	0.37
0.50	0.39
0.55	0.41
0.60	0.43
0.65	0.45

Figure 3.6.18 Cation Composition of Synthesis Products with the K,Li-F Ion exchange Isotherm

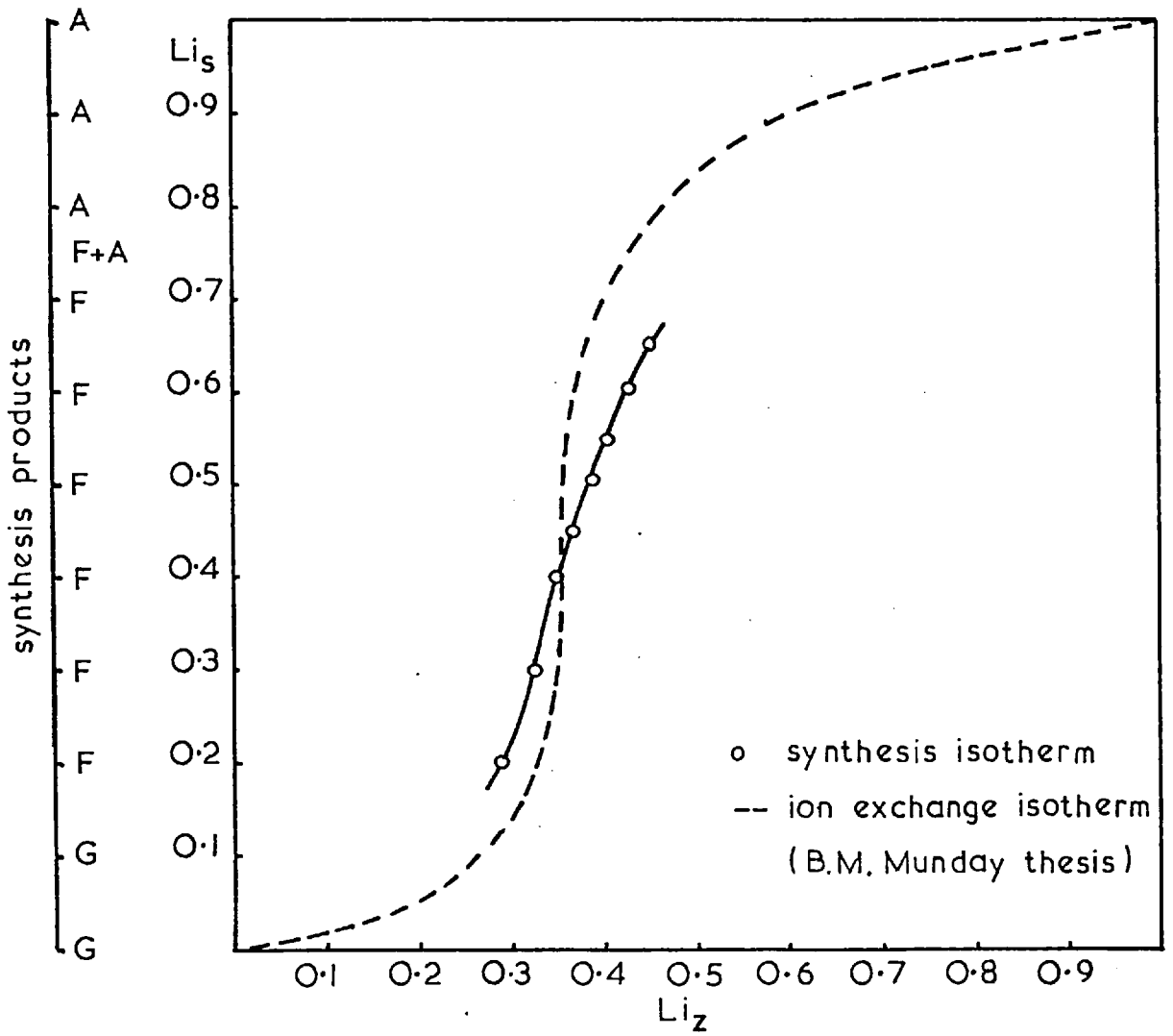

These values are plotted against the Li cation fraction in the initial mixture in Figure 3.6.18 together with the equilibrium ion-exchange isotherm found by Barrer and Munday. The composition of the synthesized products lie on a curve near but not coincident with the equilibrium ion-exchange isotherm. This small difference may be due to differences in temperature (synthesis 80°, ion-exchange 25°), solution concentration (synthesis 0.5 molal, ion-exchange 0.1 normal) and pH (synthesis was from mixed hydroxides whereas ion-exchange was measured using mixed chlorides).

The crystallization fields of zeolites do not show sharp boundaries. The products co-crystallize over large compositional ranges of the parent magmas. It was observed, however, that the boundary between K,Li-F and Li-A was relatively sharp (Figure 3.6.9). Syntheses were carried out in this region to examine as far as possible the change in yields of each on passing through this diffuse boundary. Product yields were determined by X-ray diffraction as described in Section 2.3. The results are shown in Table 3.6.16 and are plotted in Figure 3.6.19. The yield of K,Li-F began to decrease from a lithium cation fraction of 0.725 upwards where zeolite Li-A first appeared. When the cation fraction

was 0.8125 the only product was Li-A.

The intensities relative to an internal standard (ZnO) of the lines 2.95 Å for K-F and 3.01 Å for Li-A served to measure the yields of each. Although the hydroxide solution was in excess the shapes of the curves produced are not identical. The amount of Li-A increased gradually and smoothly up to 100% yield while that of K,Li-A showed a plateau region in the curve of yield against initial cation fraction of Li^+. The plateau occurred when this fraction lay between about.76 and .79 (see Table 3.6.16).

Table 3.6.16

Cation fraction in solution $\left(\frac{Li^+}{Li^+ + K^+}\right)$	Relative intensity $\left(I/I_o\right)$	
	K,Li-F	Li-A
0.7250	1.0	0.0
0.7375	6.8	0.5
0.7500	6.3	1.1
0.7625	5.9	1.9
0.7750	6.0	3.0
0.7875	5.7	4.1
0.8000	3.5	6.5
0.8125	0.0	1.0

Figure 3.6.19 The Yield of Products with Variation of Cation in Solution

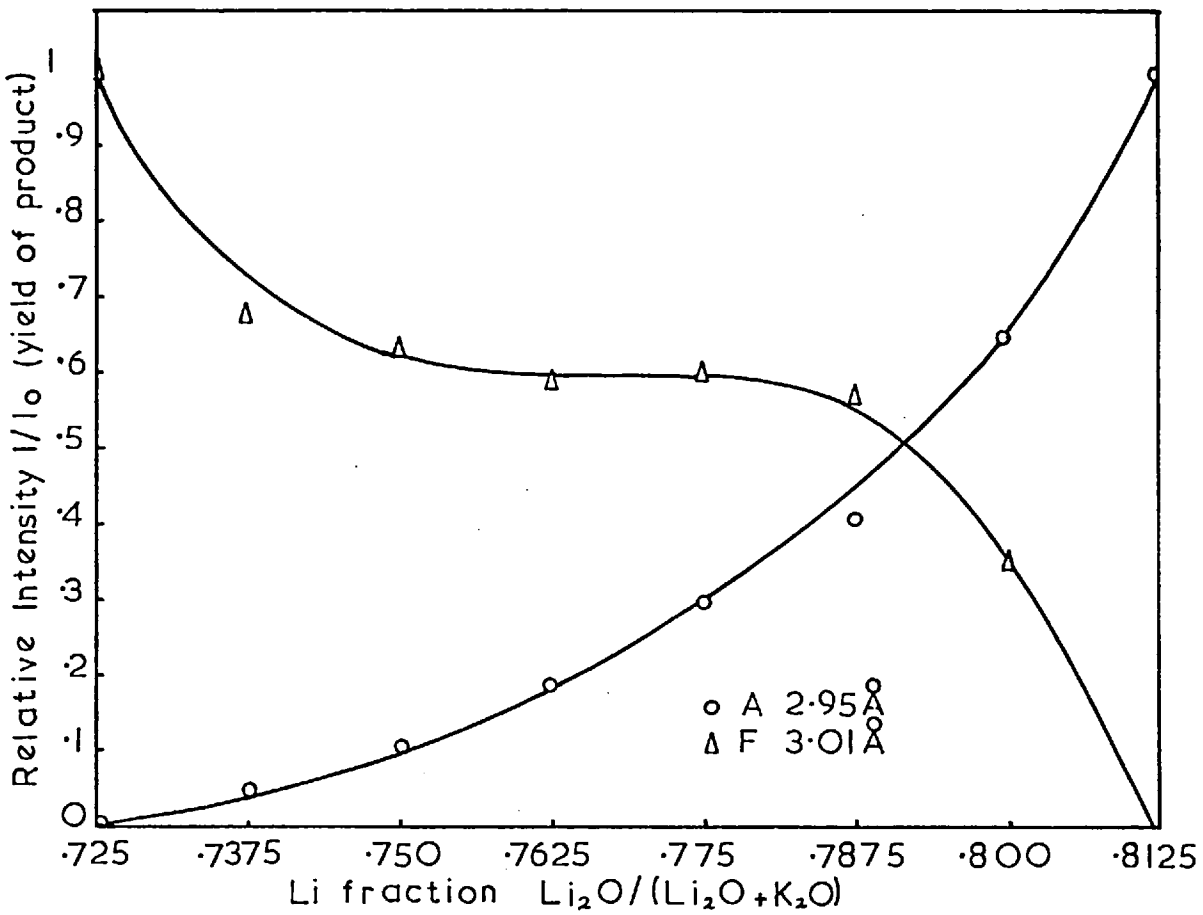

The Species Na,Li-F

The various members of the K-F type zeolites together with their compositions have been given in Table 3.4.2. Species Na,Li-F, which is of the same type, crystallized only from compositions with a silica to alumina ratio of 2, just as in the case of the rubidium member, Rb-D. In contrast, the potassium and caesium analogues, K-F and Cs-D, formed from compositions with ratios that varied from 2 to 10 and 2 to 4 respectively. An analysed sample of Na,Li-F had the composition

$$0.8\ Li_2O,\ 0.2Na_2O,\ Al_2O_3,\ 2\ SiO_2,\ 3\ H_2O$$

In Table 3.6.17 the X-ray diffraction pattern is compared with that of K-F (Table 3.1.16). It can be seen that Na,Li-F possesses basically the K-F framework. Li,Na-F was also found to be similar to a species produced in 1969 by Borer from mixed sodium-lithium alumino-silicate gels (Borer and Meier 1970).

Na,Li-F, unlike the Na,K-F previously described, showed no evidence of limited solid solubility. Figure 3.6.5 shows that Na,Li-F formed when the lithium cation fraction in the initial composition lay between 0.6 and 0.9.

According to Barrer and Munday (1969), who studied the ion-exchange isotherms in detail, a hysteresis loop resulted in the Na/Li isotherm of F due to a two-phase region when the equilibrium solution had a lithium fraction of 0.4 to 0.5. Thus during synthesis a single Na,Li-F phase nucleates and grows in a compositional region which is just outside that which gives two phases when cation equilibrium is reached with an exchanging solution.

Table 3.6.17

The d-spacings of species Na, Li-F

d	I	d	I
6.90	vs	2.60	m
6.50	m	2.58	w
4.75	m	2.47	m
4.20	w	2.16	w
3.95	mw	2.00	w
3.62	vw	1.85	mw
3.45	w	1.73	mw
3.30	mw	1.72	w
3.09	vs	1.69	w
2.95	s	1.66	w
2.80	s	1.57	vw

3.6.10 The Species K,Na-G

This product was identified as similar to the chabazite-like species K-G (Section 3.1.5). The X-ray diffraction pattern of the species G produced in the potassium rich part of the crystallization field was typical of K-G. This had both sharp and diffuse lines (Table 3.6.18). In the sodium rich part of the field the product had X-ray diffraction lines in the same position but here all lines were sharp. These were measured and indexed to give a hexagonal unit cell which showed extremely good agreement between observed and calculated d-spacings. The hexagonal unit cell had dimensions

$$a = 13.710 \pm 0.001$$

$$c = 15.713 \pm 0.003$$

The systematic absences showed rhombohedral lattice.

The diffraction pattern of the synthetic product having a composition

$0.4\ K_2O,\ 0.6\ Na_2O,\ Al_2O_3,\ 2\ SiO_2,\ 3\ H_2O$

the potassium and sodium exchanged were indexed and the unit cells calculated as shown below

	K	Na
a	13.737 ± 0.002	13.682 ± 0.006
c	15.772 ± 0.005	15.650 ± 0.011
Unit cell volume	2577.7	2537.1

In Table 3.6.18 the observed and the calculated d-spacings of the potassium exchanged K,Na-G are given. Sharp diffraction lines which appeared in these samples were diffuse in the preparations of K-G from compositions in which the base was potassium hydroxide only.

Previous workers (Barrer and Baynham 1956 a, Barrer, Baynham, Bultitude and Meier 1959, Zhdanov 1965, 1968) have not reported this difference between the diffraction lines of the synthetic K-G and Na,K-G. But the diffuse lines may be seen in the reproduction of the diffraction pattern of K-G by Barrer and Baynham (1956 a). An attempt to index the lines that changed in width between the preparations by the Hesse-Lipson method did not yield a unit cell of a possible second phase. This, together with the change in all line positions with ion-exchange and the very small error in the calculated unit cell dimensions indicated that the product was a single species.

Table 3.6.18

Indices	d_{obs}	d_{calc}	Indices	d_{obs}	d_{calc}
101	9.563 *	9.498	514 }	1.875	1.879
110	6.890	6.869	208 }		1.871
201	5.566 *	5.566	416	1.849 *	1.847
003	5.262	5.257	407	1.797 *	1.796
202	4.754*	4.749	515	1.770	1.769
211	4.324 *	4.323	434	1.751	1.752
113	4.174	4.175	336	1.727	1.727
300	3.962	3.965	440	1.717 *	1.717
212	3.906 *	3.906	318	1.691	1.692
104	3.745 *	3.743	435	1.667	1.662
302	3.514	3.543	614	1.646	1.648
204	3.273 *	3.286	606	1.582	1.583
311	3.227 *	3.230	418	1.571 *	1.570
303	3.167	3.166	534	1.560	1.561
105	3.051	3.049	704		1.561
214	2.967 *	2.965	526	1.541 *	1.542
401	2.922	2.923			
402	2.784 *	2.783			
410	2.594 *	2.596			
215	2.581 *	2.582			
314	2.533	2.530			
116	2.455	2.458			
413	2.329	2.328			
330	2.291 *	2.290			
324	2.244	2.244			
306	2.192 *	2.192			
405	2.164	2.164			
333	2.101 *	2.099			
325	2.065	2.064			
431	1.942	1.941			
520	1.905 *	1.905			

* indicated those diffraction lines whose width changed with synthesis conditions.

3.6.11 The Species Na,Li-C

The reactions of mixed sodium and lithium hydroxides with metakaolinite produced basic cancrinite at a relatively low temperature of 80°. The main crystallization area occurred with the silica to alumina ratio of 2 (Figure 3.6.5) but a small occurrence was observed when this ratio was 4 (Figure 3.6.6). This low temperature of formation contrasts with earlier syntheses from metakaolinite (Figure 3.2.1 . Section 3.2.2) where crystallization occurred only once at a temperature as low as 110° and where the main crystallization took place in the region 140 - 170°.

The composition of a series of cancrinites synthesized from solutions with varying lithium cation fractions were determined and gave the following results

Cation fraction in solution $\left(\frac{Li^+}{Li^+ + Na^+}\right)$	Cation fraction in product $\left(\frac{Li^+}{Li^+ + Na^+}\right)$
0.3	0.49
0.4	0.55
0.5	0.59
0.6	0.62
0.7	0.71
0.8	0.73

These are plotted together with the position of the sodium-lithium ion-exchange isotherm reported by Barrer and Falconer (1957) (Figure 3.6.20). The composition of the zeolite grown in the presence of sodium and lithium ions lies very close to the corresponding equilibrium compositions during ion-exchange. Barrer and Falconer have shown that for basic cancrinite the temperature of the isotherm does not significantly alter the shape or position of the isotherm.

Thus while the composition of synthetic Na,Li basic cancrinite is similar to its composition during ion-exchange that of K,Li-F (Section 3.6.9) is significantly different. A difference between the two alumino silicate frameworks is their rigidity when the cationic composition is changed. Basic cancrinite shows only a little contraction when smaller cations displace larger ones (Barrer and Falconer), whereas the F framework, as shown in this work (Sections 3.4 and 3.6) and by Barrer and Munday (1970), undergoes much larger changes in unit cell dimensions with changing cationic content.

Figure 3.6.20 The Composition of Cancrinites in the Sodium Lithium Systems

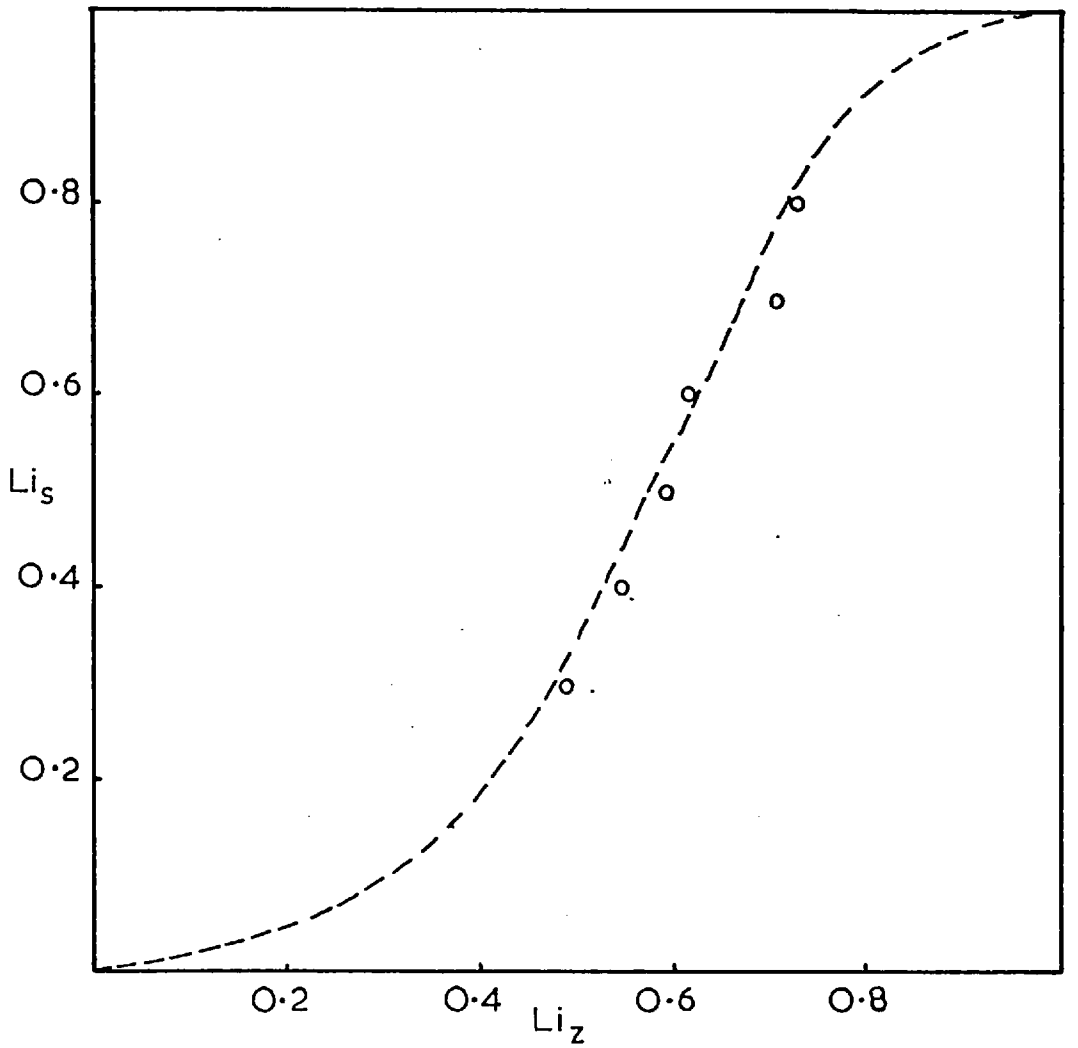

o composition of cancrinites from synthesis solution
---- ion exchange isotherm (Na,Li) Barrer & Falconer (1956)

3.6.12 The Species Na,Li-U and K,Li-U

This product occurred in mixed cation systems that were rich in lithium. Species U crystallized at 80° from compositions with an alkali concentration ranging from 1 to 5 molal. The species U did not show a high degree of crystallinity in its X-ray diffraction pattern. The pattern exhibited broad diffuse bands with the characteristic tailing of clay minerals such as montmorillonite (Brown 1961). A comparison of the diffraction pattern of species U with that of hectorite showed them to be almost identical. The d-spacings of these samples were:

K,Li-U Å	Hectorite Å
13	12
4.5	4.6
3.2	3.2
2.55	2.6
1.70	1.72
1.50	1.51

The product formed as very small aggregates of crystals unsuitable for optical examination. As a consequence of this and the diffuse nature of the X-ray diffraction pattern, no estimation of the yield was

possible. Lithium, the common cation in the syntheses, was probably not only an interlayer cation but also substituted in the octahedral layer of the structure.

3.7 The System Metakaolinite-Silica-Sodium-Tetramethylammonium Hydroxide-Water

Sodium hydroxide and tetramethylammonium hydroxide were selected for syntheses from metakaolinite in the presence of a cation pair having widely differing radii. The use of organic bases and mixtures of organic and inorganic bases has yielded both silica rich varieties of existing zeolites and also new zeolites (see introductory chapter).

This system yielded the following crystalline products:

Designation	Product	Reference-Section
Q	zeolite A type	3.2.7
R	faujasite type	3.2.13
I	sodalite	3.2.19
C	cancrinite	3.2.8
Pl	gismondite type	3.2.12
V	new synthetic zeolite $(Na,(CH_3)_4N)$-$V_T(2.0)[\ ]$	3.7.3

3.7.1 Reactions in the Sodium, Tetramethylammonium System

In Figures 3.7.1 - 3.7.3 have been plotted the crystallization fields of the crystals obtained in this field, while Tables 3.7.1, 3.7.2 and 3.7.3 give the crystallization conditions more explicitly.

Table 3.7.1

The general reaction composition was:

1 metakaolinite + 2.8 - 100.0($mNa_2O + (1-m)[(CH_3)_4N]_2O$) + ~ 275 H_2O

rotated at 85° for 4 days.

Run No.	Concentration of alkali (molality)	Cation fraction $\frac{[(CH_3)_4N]_2O}{[(CH_3)_4N]_2O + Na_2O}$	Product	Description of product
7-12	0.5	0	R + I	Rmd.cr., Ilo.yd.
7-13	0.5	0.1	R + I	Rmd.cr., Ipr.cr.
7-14	0.5	0.4	R + I	Rmd.cr., Imd.cr.
7-15	0.5	0.8	Q + Pl	Qgd.cr., Itr.
7-17	1.0	0.1	R + Q+I	Rmd.cr., QI tr.
7-20	1.0	0.3	R+Q+I	Rmd.cr., QI lo.yd.
7-21	1.0	0.5	R + Q	R.md.cr., Qmd.cr.
7-22	1.0	0.6	R+Q+Pl	Rlo.yd., Qmd.cr., Pl tr.
7-23	1.0	0.8	Pl + Q	Pllo.yd., Qmd.cr.
7-24	2.0	0.1	Q + V	Qmd.cr., Vmd.cr.
7-25	2.0	0.2	Q + V	Qmd.cr., Vmd.cr.
7-26	2.0	0.3	Q + V	Qgd.cr., Vpr.cr.
7-28	2.0	0.5	Pl+Q+V	Plmd.cr., Qmd.cr., V tr.
7-29	2.0	0.7	Pl + Q	Plmd.cr., Qpr.cr.

Table 3.7.1 (continued)

Run No.	Concentration of alkali (molality)	Cation fraction $\frac{[(CH_3)_4N]_2O}{[(CH_3)_4N]_2O+Na_2O}$	Product	Description of product
7-32	2.5	0.1	Q + V	Qmd.cr., Vmd.cr.
7-33	2.5	0.2	V	md.cr.
7-35	2.5	0.4	V	md.cr.
7-38	2.5	0.55	Pl + V	Plmd.cr., pr.cr.
7-39	3.0	0.1	V + I	Vmd.cr., Imd.cr.
7-40	3.0	0.2	V + I	Vmd.cr., Imd.cr.
7-41	3.0	0.4	V + I	Vlo.yd., Ipr.cr.
7-44	3.0	0.8	V + I	Vlo.yd., Ipr.cr.
7-45	4.0	0	Am	-
7-46	4.0	0.1	Am	-
7-47	4.0	0.3	I	md.cr.
7-48	4.0	0.5	I + Q	Imd.cr., Qtr.
7-49	4.0	0.8	I + Q	Imd.cr., Qtr.

Figure 3.7.1 The Crystallization Field Resulting from: 1 Metakaolite + 2·8 – 100 ($mNa_2O + (1-m)[(CH_3)_4N]_2O$) ∓ 275 H_2O Rotated at 85° for 4 days

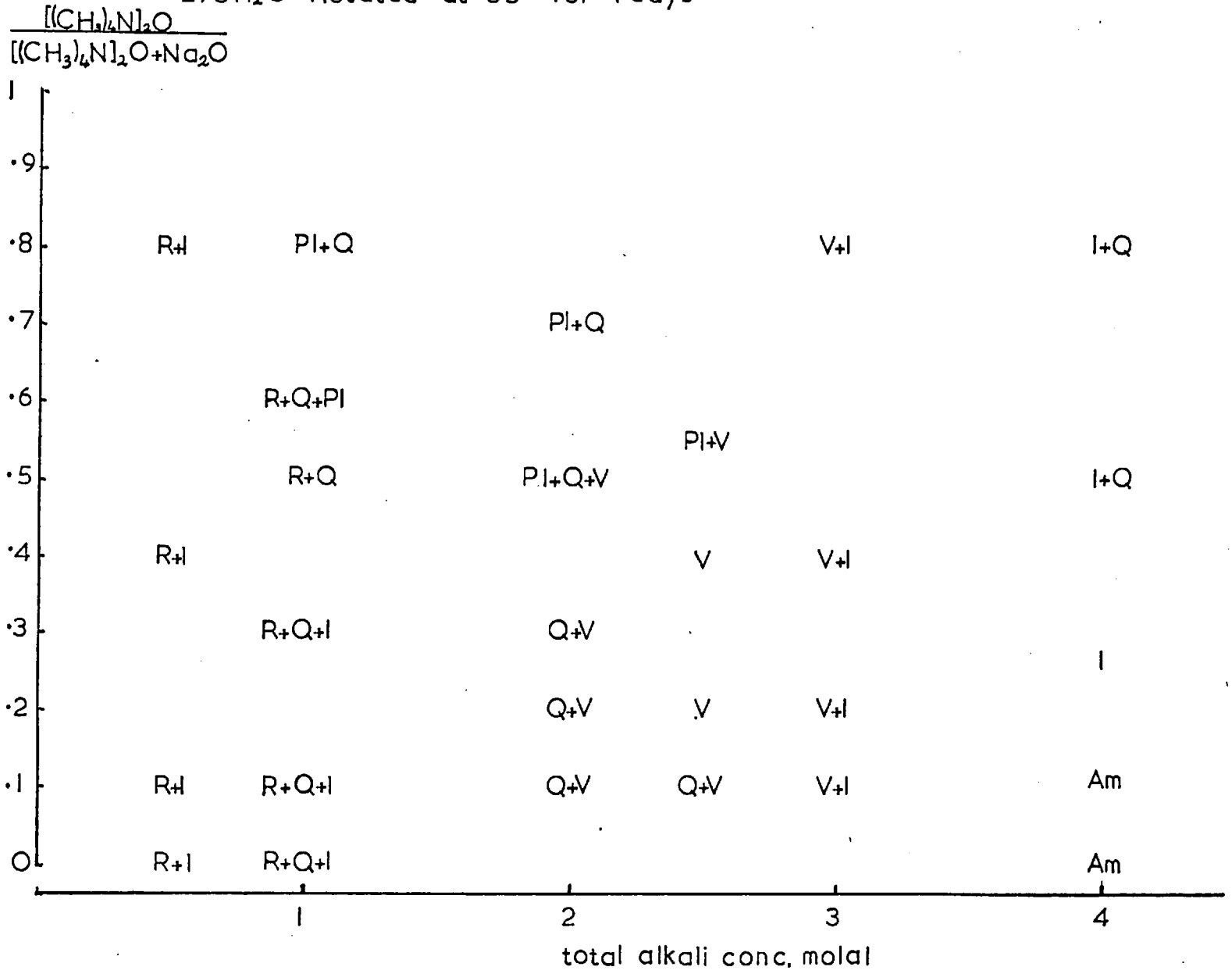

Table 3.7.2

1 metakaolinite + 2.8 - 100.0($mNa_2O+(1-m)[(CH_3)_4N]_2O$ + 4 SiO_2 + ~ 275 H_2O rotated at 85° for 7 days.

Run No.	Concentration of alkali (molality)	Cation fraction $\frac{[(CH_3)_4N]_2O}{[(CH_3)_4N]_2O+Na_2O}$	Product	Description of product
7-50	0.5	0	R + Q	pr.cr.
7-51	0.5	0.1	R + Q	Rmd.cr.,Q tr.
7-54	0.5	0.3	R + Q	Rmd.cr.,Qlo.yd.
7-55	0.5	0.4	R + Pl	Rmd.cr.,Plmd.cr.
7-56	0.5	0.7	R + Pl	Rlo.yd.,Plmd.cr.
7-57	0.5	0.8	Pl + Q	Plmd.cr.,Qmd.cr.
7-59	1.0	0.1	R+Q+I	-
7-60	1.0	0.2	R+Q+I	-
7-61	1.0	0.4	R + Q	Rmd.cr.,Qlo.yd.
7-63	1.0	0.6	Pl+R+Q	-
7-65	1.0	0.8	Pl + Q	Plmd.cr.,Qgd.cr.
7-66	2.0	0.1	R+Q+I	-
7-67	2.0	0.3	R + Q	Rgd.cr.,Qmd.cr.
7-68	2.0	0.5	Pl + Q	gd.cr.
7-69	2.0	0.7	Pl + Q	gd.cr.
7-70	2.5	0.05	I + V	md.cr.
7-71	2.5	0.2	I + V	md.cr.
7-72	2.5	0.4	V+Pl+Q	-
7-73	3.0	0	R + I	Rgd.cr.,Imd.cr.
7-75	3.0	0.1	V + I	Vmd.cr.,Ipr.cr.
7-76	3.0	0.3	V+Q+I	-
7-79	3.0	0.5	V+Q+I	-
7-80	3.0	0.7	Pl + I	Plmd.cr.,Ipr.cr.
7-81	4.0	0	Am	-
7-82	4.0	0.1	Am	-
7-83	4.0	0.2	I	md.cr.

Figure 3.7.2 The Crystallization Field Resulting from: 1 Metakaolinite + 2·8-10 O(mNa_2O + (1-m)$[(CH_3)_4N]_2O$ ∓ 275H_2O Rotated at 85° for 4 days

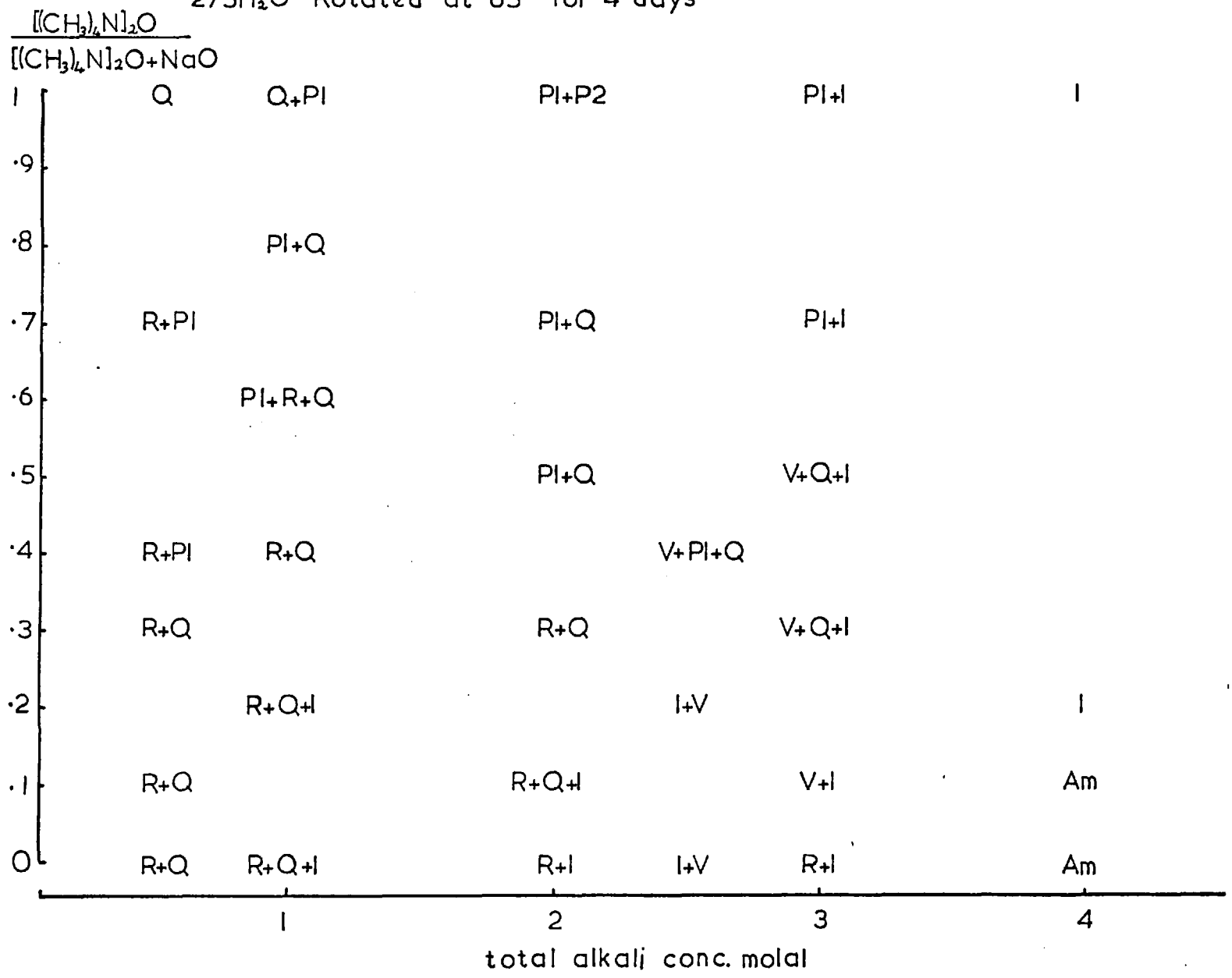

Table 3.7.3

1 metakaolinite + 2.8 - 100.0(mNa_2O+(1-m) $[(CH_3)_4N]_2O$ + 8 SiO_2 + ~ 275 H_2O rotated at 85° for 4 days.

Run No.	Concentration of alkali (molality)	Cation fraction $\frac{[(CH_3)_4N]_2O}{[(CH_3)_4N]_2O+Na_2O}$	Product	Description of product
7.85	0.5	0.1	R + Pl	Rpr.cr.,Plmd.cr.
7-86	0.5	0.3	R + Pl	Rpr.cr.,Plmd.cr.
7-87	0.5	0.5	R + Pl	Rmd.cr.,Plmd.cr.
7-88	0.5	0.7	R + Pl	Rgd.cr.,Plmd.cr.
7-89	1.0	0.1	R + Pl	Rpr.cr.,Plmd.cr.
7-90	1.0	0.2	R	R pr.cr.
7-91	1.0	0.4	R + C	Rgd.cr.,C tr.
7-92	1.0	0.6	Pl+R+C	Plmd.cr.,Rmd.cr., C tr.
7-93	1.0	0.8	Pl + Q	Plmd.cr.,Qgd.cr.
7-95	2.0	0.1	Pl + Q	Pllo.yd.,Qmd.cr.
7-96	2.0	0.3	R+Q+Pl	Rlo.yd.,Qmd.cr., Pl lo.yd.
7-98	2.0	0.55	R+Q+Pl	Rtr.,Qmd.cr., Pl pr.cr.
7-100	2.0	0.7	R + Q	Rtr.,Qgd.cr.
7-101	2.0	1.0	R + Q	Rtr.,Qgd.cr.
7-102	2.5	0	Pl + Q	Plmd.cr.,Qgd.cr.
7-104	2.5	0.1	C + I	Cmd.cr.,Imd.cr.
7-106	2.5	0.2	Pl+R+Q	Plmd.cr.,Rtr., Q md.cr.
7-107	3.0	0	I + C	C tr.,Imd.cr.
7-109	3.0	0.1	I + C	C tr.,Imd.cr.
7-110	3.0	0.2	I + V	Ilo.yd.,Vmd.cr.
7-111	3.0	0.5	P2 + I	P2md.cr.,Imd.cr.
7-115	3.0	0.7	P2 + I	P2md.cr.,Imd.cr.
7-117	3.5	0	I	md.cr.
7-118	3.5	0.1	I + V	Imd.cr.,Vmd.cr.
7-119	3.5	0.2	I + V	Imd.cr.,Vmd.cr.
7-120	3.5	0.35	P2 + I	P2md.cr.,Igd.cr.

Figure 3.7.3 The Crystallization Field Resulting from: 1 Metakaolinite + 2·8-100($mNa_2O + (1-m)[(CH_3)_4N]_2O$ $8SiO_2 \mp 275 H_2O$ Rotated at 85° for 4 days

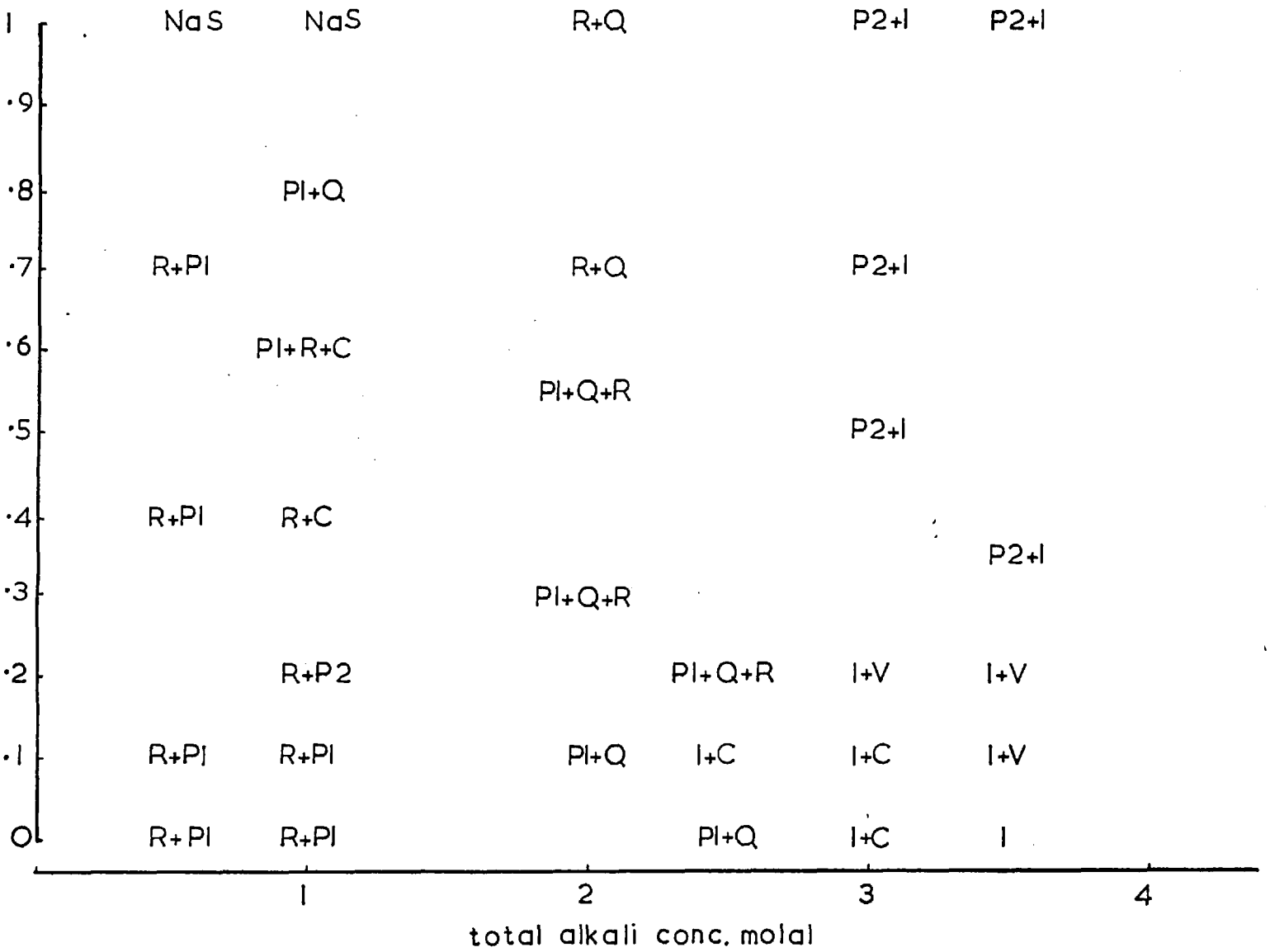

The crystallites were very small and irregular in shape. It was not possible to observe the yields of products optically or by electron diffraction. Both the yield and degree of crystallinity were estimated from the diffraction patterns, most of which had broad lines. This tendency increased in the tetramethyl ammonium rich part of the crystallization field.

The crystalline products from the sodium-tetramethyl-ammonium system usually paralleled those obtained using NaOH as the only base. The only new product, unique to this system, was $Na,(CH_3)_4N$-V which is discussed in the next section. Thus the principal effect of the tetramethyl-ammonium cations in the sodium system is to replace some of the sodium cations in the products. Accompanying this there is an isomorphous substitution Na,Al=Si so that silica rich modifications tend to be formed. This was first observed by Barrer and Denny (1961).

Some of the crystallizations from magmas having a silica to alumina ratio of ten produced cancrinite. This product was never as well crystallized as that grown at 80° with the cation pair Na/Li, but always formed together with either R or I. The previous syntheses of the other products grown in this section have been discussed earlier in Section 1.2.

The polyhedra found in the frameworks of the crystals grown from metakaolinite + sodium hydroxide + tetramethylammonium hydroxide mixtures (Table 3.7.1 and Figure 3.7.1(a)) have been plotted on a diagram similar to the crystallization field. The limits of occurrence of these polyhedra have been marked on the diagram, the polyhedra being identified as indicated below:

sodalite cage	14-H (1)
truncated cuboctahedron	26-H (1)
faujasite cage	26-H (11)
gismondite cage	10-H (11)
cube	6-H
hexagonal prism	8-H

The occurrence in zeolites of these polyhedra, and of other building units, has been discussed in Section 1

Figure 3.7.1a Polyhedra in the Products of the Crystallization Field in Figure 3.7.1

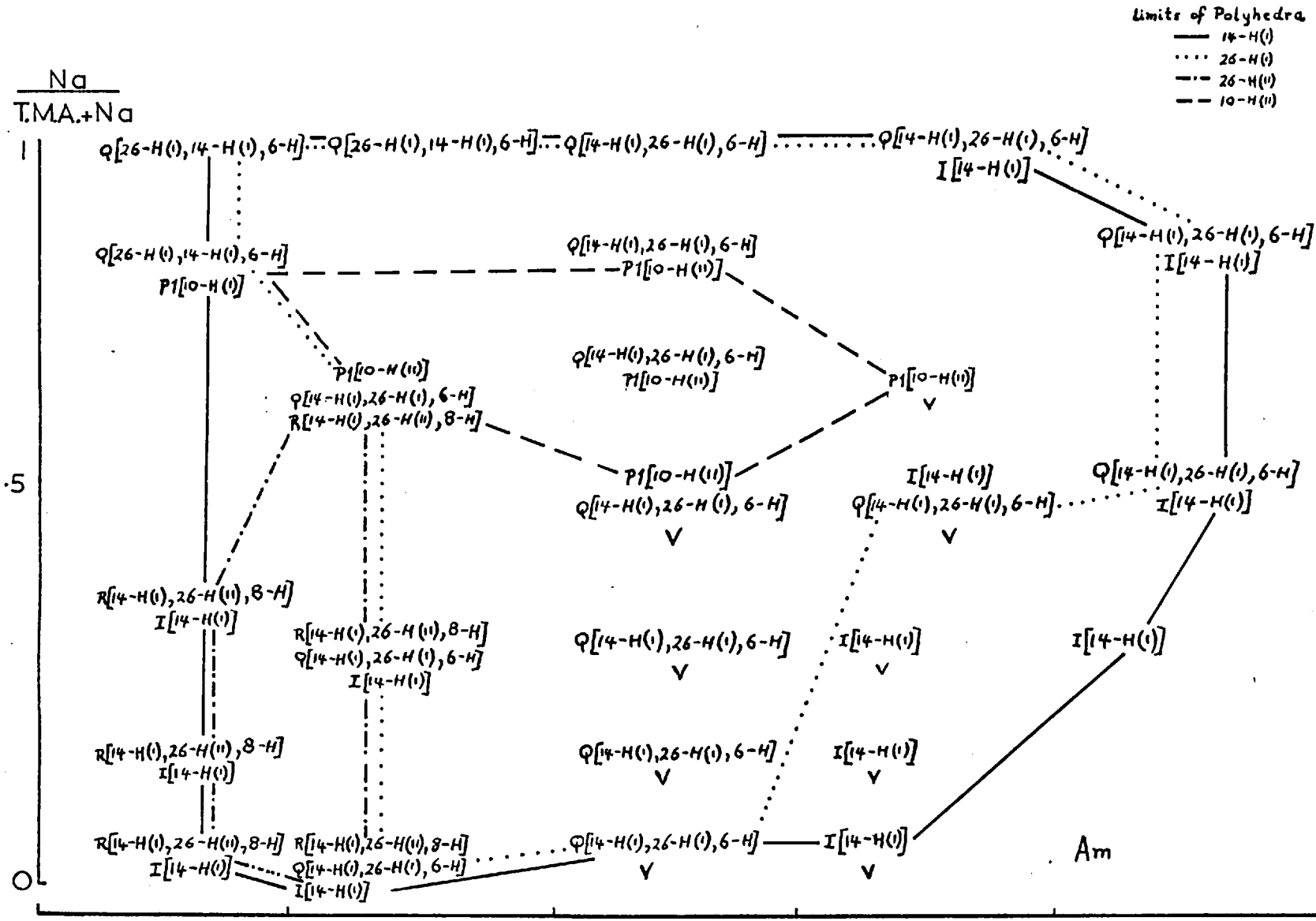

3.7.2 The Species $Na,(CH_3)_4N$-V

$Na,(CH_3)_4N$-V occurred in syntheses with silica to alumina ratios of 2, 6 and 10. Formation was always in the part of the crystallization field rich in tetramethylammonium cations. Figures 3.7.1 - 3.7.3 show that as the silica to alumina ratios of the magmas increased species V crystallized in areas of higher alkalinity. The analysis revealed that the silica to alumina ratio of the product was two. This is consistent with earlier observed trends in zeolite crystallization (for example Section 3.1.11).

Product V gave an intense, characteristic X-ray diffraction pattern. The diffraction lines were broader than those of the well crystallized zeolites previously made. The product occurred as spherical aggregates of very small crystals. This did not allow the purity to be judged optically. However, the water content and the analysis indicated a high yield. The line broadening appeared to be due to the very small particle size (Nuffield 1966). From the X-ray diffraction pattern shown in Table 3.7.4 this product was identified as being similar to the new zeolite Linde N, (Acara, 1968). The zeolite Linde N was originally indexed as body centered cubic with a unit cell edge of 37.219 Å (U.S.P. 3,414,602). The diffraction pattern of

V was measured and corrected with an internal standard. It was then indexed using the Hesse-Lipson analytical method, previously described in Section 1.3. The unit cell was found to be tetragonal with

$$a = 13.08 \pm 0.01 \text{ Å}$$
$$b = 21.56 \pm 0.04 \text{ Å}$$

The agreement between observed and calculated d-spacings, given in Table 3.7.4, was within the accuracy of the measurement of the diffraction pattern. Unlike cubic indexing, also shown in Table 3.7.4, there were not many absent lines which could not be accounted for.

Chemical analysis of one of the preparations of species V gave the following oxide compositions and molar proportions respectively:

	% by weight	Molar proportions
Na_2O	14.8	0.88
$[(CH_3)_4]_2O$	4.7	0.1 *
Al_2O_3	29.5	1
SiO_2	35.0	2.0
H_2O	16.0	3.0

* Analysis by the Microanalytical Laboratory of Imperial College.

The composition of this preparation is very similar to that found by Acara (1968), viz.

$$0.83 \pm 0.05\ Na_2O,\ 0.03 \pm 0.01[(CH_3)_4N]_2O,\ Al_2O_3,\ 2.0 \pm 0.2\ SiO_2,\ y\ H_2O$$

Here the zeolite N was also made by the reaction of metakaolinite with sodium and tetramethylammonium hydroxide. No synthesis has yet been reported from crystalline products. In the analysis of Na,$(CH_3)_4$N-V the total cations in the formula did equal the aluminium content but in Linde N it was significantly less.

The thermogravimetric analysis curvesof both the original hydrated product and the product after removal of the tetramethylammonium cations and rehydration are shown in Figures 3.7.4 (a) and 3.7.4 (b) respectively. The weight loss in both cases was approximately 16.5%. This is comparable with the 15.1% found by analysis when the inaccuracy of the microanalytical determination of the tetramethylammonium cation is considered. The weight loss curve in both cases was a smooth one. This curve for the initial sample showed an inflection corresponding to the decomposition of the organic cations.

Table 3.7.4

The calculated and observed d-spacings of species V are compared to those values found by Acura (1968).

	Na,$(CH_3)_4$N-V				Linde N		
	d_{obs}	d_{calc}	Int		d_{obs}	d_{calc}	Int
001	21.54	21.56	m	111	21.655	21.488	41
100	13.094	13.082	ms	220	13.173	13.159	68
101	11.192	11.185	ms	311	11.191	11.222	73
110	9.276	9.250	m	400	9.299	9.305	50
003	7.101	7.188	w	511,333	7.138	7.163	14
200	6.541	6.541	vs	440	6.569	6.579	100
				531	6.268	6.291	36
210	5.846	5.850	w	620	5.864	5.885	23
211	5.644	5.646	w	533	5.655	5.676	16
004	5.337	5.391	mw				
212	5.153	5.142	w				
203	4.799	4.838	mw	731,553	4.826	4.845	27
221	4.514	4.522	w	820,644	4.522	4.513	14
300	4.349	4.361	w	661,830	4.358	4.356	20
301	4.267	4.274	mw				
310	4.128	4.136	w				
302	4.046	4.042	s	842	4.056	4.061	89
214	3.945	3.965	w				
303	3.765	3.728	ms	940,665	3.776	3.779	57
320	3.709	3.628	s		3.718		80
321	3.567	3.578	w		3.574		23
224	3.519	3.510	w				
322	3.433	3.438	w		3.482		20
116	3.367	3.350	w		3.377		20
401	3.227	3.233	m		3.347		41
225	3.163	3.154	w				
402	3.131	3.129	m		3.139		41

Table 3.7.4 (continued)

	$Na,(CH_3)_4N$-V			Linde N		
	d_{obs}	d_{calc}	Int	d_{obs}	d_{calc}	Int
412	3.045	3.044	w	3.051		20
315	2.993	2.986	ms	2.991		61
420	2.917	2.925	w			
421	2.884	2.898	w			
422	2.828	2.823	mw	2.827		25
325	2.761	2.776	m	2.763		59
414	2.725	2.734	w			
423	2.700	2.709	mw			
334	2.664	2.677	m	2.668		30
500	2.610	2.616	w			
424	2.590	2.571	w			
511	2.548	2.548	m			
415	2.517	2.556	w			
503	2.450	2.458	m	2.452		32
416	2.382	2.379	w			

The D.T.A. curve of the original sample showed first the endothermic loss of zeolitic water. After this, a large exotherm occurred which corresponded with the oxidation of the tetramethylammonium cation. The weight then remained constant and the D.T.A. trace smooth until approximately 930° when a small endotherm probably indicating lattice collapse, and a larger exotherm indicating recrystallization, were observed. The product when heated to 1100° on a Meker burner was poorly crystallized nepheline. The thermal behaviour of the sample first heated to 600° and then rehydrated was very similar to that of the original product but with no large exotherm due to combustion of the tetramethylammonium cations.

The sample was heated on a heating Lenné-Guinier camera. The diffraction record is shown in Plate 3.7.1. The lattice remained stable until approximately 650° when it recrystallized to the first of the two high temperature products, Na-V1. This phase was stable only over an interval of 50° after which the second product Na-V2 began to appear. The d-spacings of the two species are given in Table 3.7.5.

Na-$(CH_3)_4$N-V was examined both before and after the removal of the tetramethylammonium cations for sorption of oxygen. Neither of these forms showed any uptake of oxygen at 78°K.

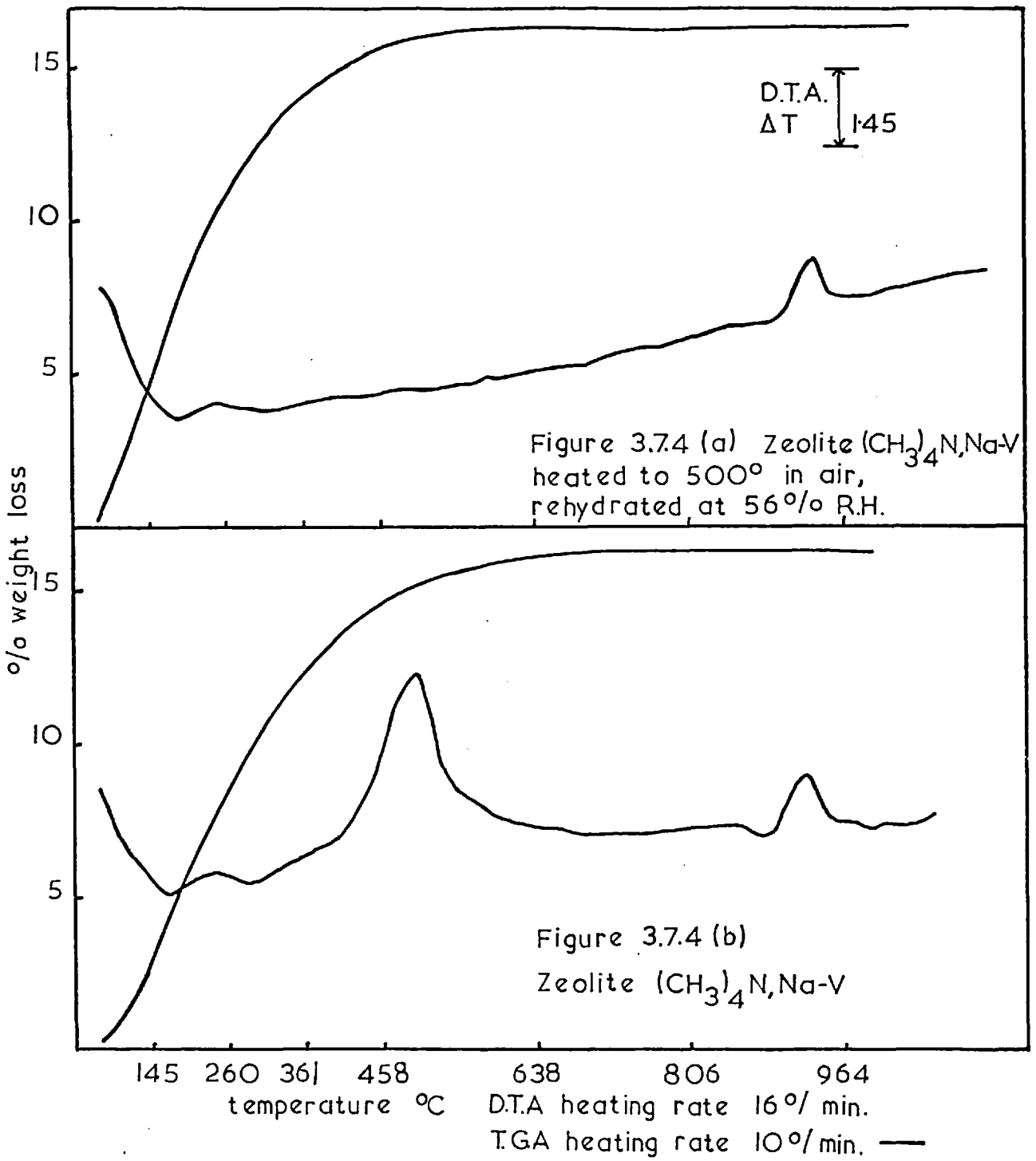

Figure 3.7.4 (a) Zeolite $(CH_3)_4N$,Na-V heated to 500° in air, rehydrated at 56% R.H.

Figure 3.7.4 (b) Zeolite $(CH_3)_4N$,Na-V

Plate 3.7.1

The continuous-heating X-ray powder diffraction pattern of species $Na,(CH_3)_4N$-V, heated in air at 0.5 deg./min. from room temperature up to 850°.*

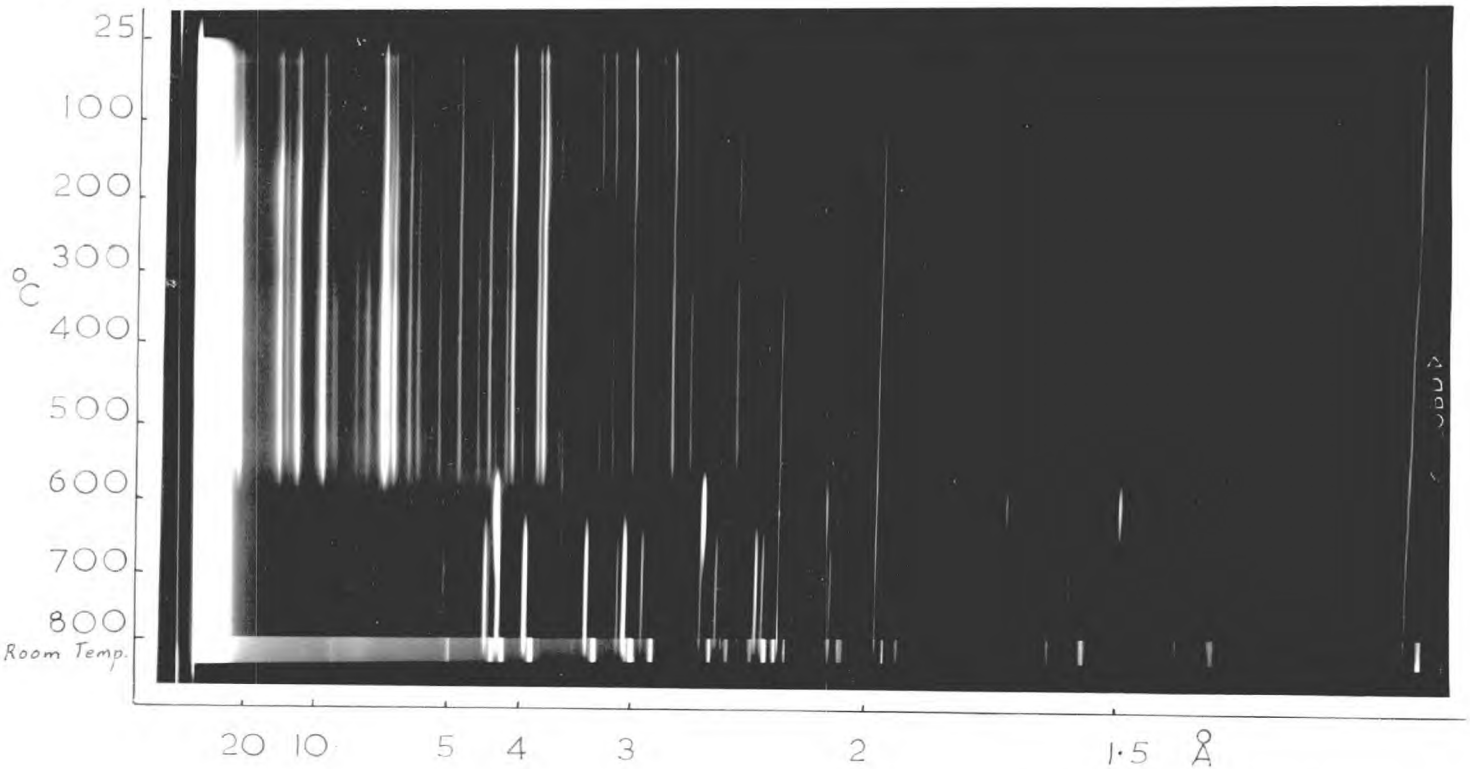

* 1. The superimposed pattern at the end of heating is that of the final product at room temperature.

* 2. The continuous very fine lines are the diffraction lines of the platinum supporting grid. These may be used for calibration.

Table 3.7.5

The d-spacings of the two phases produced by heating species $Na,(CH_3)_4N$-V.

Na - V1		Na - V2	
d_{obs}		d_{obs}	
4.25	s	8.7	mw
3.60	s	5.0	m
2.22	vw	4.35	s
2.13	m	* 4.20	s
1.84	mw	3.85	s
1.69	s	3.35	s
1.50	vs	3.11	ms
1.415	m	3.08	s
1.300	m	2.88	m
1.260	m	2.58	s
1.163	mw	2.50	s
		2.40	m
		2.35	s
		2.31	s
		* 2.17	mw
		2.13	m
		* 2.10	ms
		2.08	ms
		1.99	w
		1.93	m
		1.88	m

* These lines, as shown in Plate 3.7.1 were coincident with and of similar intensity to those of the previous phase.

3.8 The Systems Metakaolinite-Silica-Barium-Potassium Hydroxide-Water

and Metakaolinite-Silica-Barium-Tetramethylammonium Hydroxide-Water

The reactions between metakaolinite + silica and mixed aqueous barium and potassium hydroxides were investigated in an effort to improve the sorbent properties of the previously studied zeolite Ba-G (Section 3.5.2). This zeolite had been found to have the Linde L type framework but did not sorb large molecules, such as cyclohexane. This molecule should have passed readily through the 12-membered ring windows of free diameter 7.5 Å, if these windows were unblocked. Since Linde L had previously been grown from potassium-sodium aluminosilicate gels rich in potassium the barium-potassium system was chosen. The desired product was a zeolite of the L type having the sorption capacities of Linde L yet with a low silica to alumina ratio.

To examine further the influence of the second cation in admixture with barium, this second ion was increased in size by replacing KOH by tetramethylammonium hydroxide. The results are now described and discussed.

The products formed in these two systems have been tabulated and identified below.

Short Reference	Zeolite formula	Description
G1	$(K,Ba)G1_h(210)$ [ch]	members of chabazite like phases K-G(beginning silica alumina ratio 2.10)(Section 3.1.5)
G2	$(Ba,K)G2_H(\ \ )$[L] $((CH_3)_4NBa)G2_h(\ \ )$[L]	members of the L series of zeolites having silica to alumina ratios in the region of 2.1 , Ba-G phase (Section 3.5.4)
L	$(Ba,K)L_H(\ \ )$[L] $((CH_3)_4NBa)L_h(\ \ )$[L]	members of the L series of zeolites having silica to alumina ratios in the region of Linde L (Section 3.1.8)
P	-	hexagonal polymorph of Ba celsian (Section 3.5.7)
T	$\{Ba(OH)_2\}(Ba)$-T(2)[ ]	new barium zeolite (Section 3.5.6)
E	$((CH_3)_4N,Ba)$-$E_h(6)$ [Eri]	erionite type zeolite

3.8.1 Reactions in the System Metakaolinite-BaO-K_2O-SiO_2-H_2O

The reactions of metakaolinite-silica with mixed barium and potassium hydroxides are summarised in Tables 3.8.1 - 3.8.4 The crystallization fields have been plotted in Figures 3.8.1 - 3.8.4.

Table 3.8.1

The general reaction taking place was:

1 metakaolinite + 3.0 - 20.0(m BaO + (1-m)K_2O) + ~275 H_2O

rotated at 85° for 4 days.

Run No.	Concentration of alkali (molality)	Cation fraction $\frac{BaO}{BaO + K_2O}$	Products	Description of products
8-14	0.3	0.05	G1	pr.cr.
8-1	0.3	0.1	G1	pr.cr.
8-2	0.3	0.3	G1 + G2	G1pr.cr.,G2pr.cr.
8-3	0.3	0.5	G2	md.cr.
8-5	0.3	1.0	G2	md.cr.
8-15	0.5	0.05	G1	md.cr.
8-6	0.5	0.1	G2	gd.cr.
8-7	0.5	0.2	G2	gd.cr.
8-8	0.5	0.3	G2 + P	G2gd.cr.,Pmd.cr.
8-9	0.5	0.4	G2 + P	G2gd.cr.,Pmd.cr.
8-10	0.5	0.5	G2	md.cr.
8-13	0.5	1.0	G2	md.cr.
8-17	1.0	0.1	G2	gd.cr.

Table 3.8.1 (continued)

Run No.	Concentration of alkali (molality)	Cation fraction $\frac{BaO}{BaO + K_2O}$	Products	Description of products
8-18	1.0	0.2	G2	md.cr.
8-19	1.0	0.4	P	md.cr.
8-20	1.0	0.6	P	md.cr.
8-21	1.0	0.7	P + G2	Pmd.cr.,G2 tr.
8-22	1.0	0.9	P	gd.cr.
8-25	1.6	0.1	G2 + T	G2pr.cr.,Tmd.cr.
8-26	1.6	0.3	G2 + T	G2pr.cr.,Tmd.cr.
8-27	1.6	0.4	T	gd.cr.
8-28	1.6	0.5	P	md.cr.
8-29	1.6	0.8	P	md.cr.
8-31	2.0	0.1	G2 + T	G2pr.cr.,Tgd.cr.
8-32	2.0	0.3	G2 + T	G2pr.cr.,Tgd.cr.
8-33	2.0	0.5	P + T	Pmd.cr.,Tmd.cr.
8-35	2.0	0.7	P	gd.cr.
8-37	2.0	0.9	P	gd.cr.

Figure 3 8 1 The Crystallization Field Resulting from:

1 Metakaolinite + 3 – 20 (m Ba + (1-m) K_2O) ∓ 275 H_2O

Rotated at 85° for 4 days

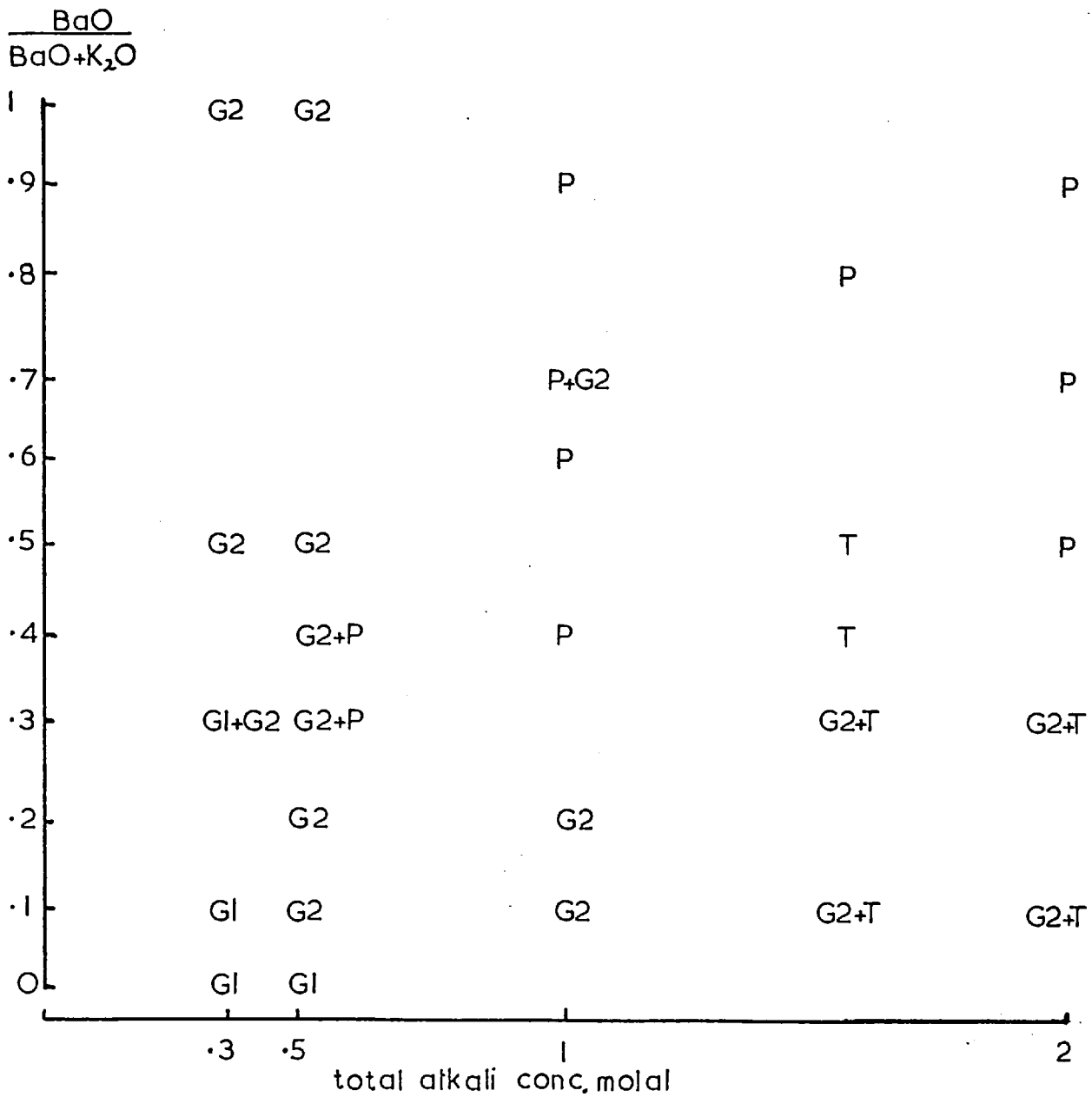

Table 3.8.2

The general reaction composition was

1 metakaolinite + 3.0 - 20.0 ($mBaO+(1-m)K_2O$) + 2 SiO_2 + ~ 275 H_2O

rotated at 85° for 4 days.

Run No.	Concentration of alkali (molality)	Cation fraction $\frac{BaO}{BaO + K_2O}$	Products	Description of products
8-40	0.3	0	G1	pr.cr.
8-41	0.3	0.1	G1 + G2	G1pr.cr.,G2pr.cr.
8-42	0.3	0.2	G1 + G2	G1pr.cr.,G2md.cr.
8-43	0.3	0.3	G2	pr.cr.
8-45	0.3	0.7	P + G2	Pmd.cr.,G2 tr.
8-47	0.5	0.1	G1	md.cr.
8-48	0.5	0.3	G1 + G2	G1md.cr.,G2md.cr.
8-49	0.5	0.5	G1 + G2	G1md.cr.,G2md.cr.
8-50	0.5	0.7	G2 + P	G2md.cr.,Pmd.cr.
8-51	0.5	0.8	P	gd.cr.
8-53	1.0	0.1	G1 + G2	G1gd.cr.,G2md.cr.
8-54	1.0	0.3	G1 + G2	G1md.cr.,G2md.cr.
8-55	1.0	0.5	G1 + G2	G1md.cr.,G2gd.cr.
8-56	1.0	0.6	G2 + P	G2gd.cr.,Pmd.cr.
8-57	1.0	0.8	P	gd.cr.
8-58	1.5	0.1	G2	pr.cr.
8-59	1.5	0.3	T + G2	G2md.cr.,Tmd.cr.
8-60	1.5	0.5	P + G2	G2pr.cr.,Pmd.cr.
8-61	1.5	0.7	P	md.cr.
8-62	2.0	0.1	T + G2	Tgd.cr.,G2md.cr.
8-63	2.0	0.2	T + G2	Tgd.cr.,G2md.cr.
8-64	2.0	0.3	T + G2	Tgd.cr.,G2md.cr.

Figure 3.8.2 The Crystallization Field Resulting from:

1 Metakaolinite +3-20(mBaO+(1-m)K_2O)+2SiO_2 ∓275H_2O

Rotated at 85° for 4days

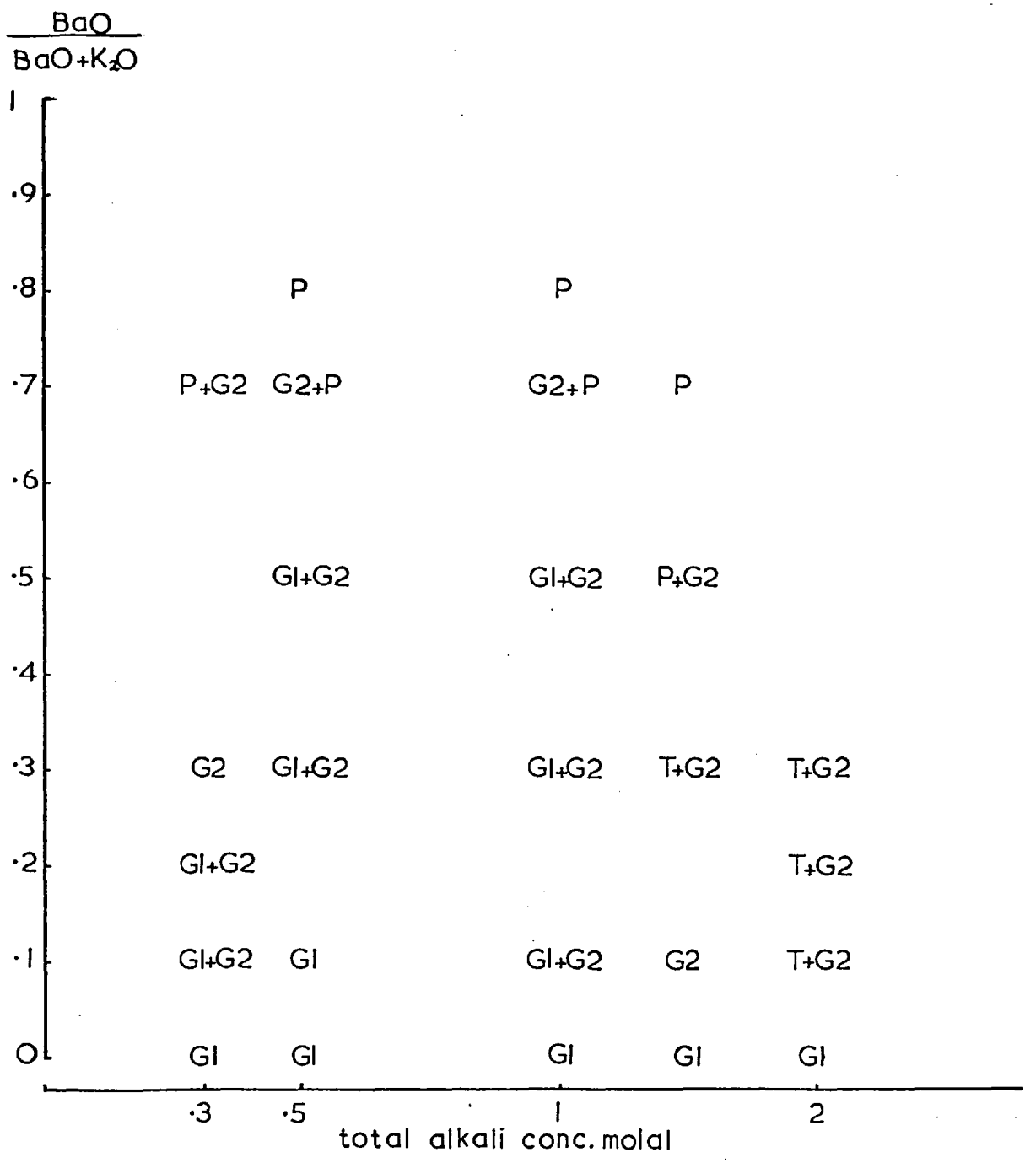

Table 3.8.3

The general reaction composition was

1 metakaolinite + 1.0 - 20.0($mBaO+(1-m)K_2O$) + 4 SiO_2 +~ 275 H_2O

rotated at 85° for 4 days.

Run No.	Concentration of alkali (molality)	Cation fraction $\frac{BaO}{BaO + K_2O}$	Products	Description of products
8-65	0.1	1.0	L	pr.cr.
8-81	0.3	0.05	Gl	pr.cr.
8-66	0.3	0.1	L	md.cr.
8-67	0.3	0.2	L	md.cr.
8-69	0.3	0.5	L	md.cr.
8-70	0.3	0.7	P + L	Ppr.cr.,Lmd.cr.
8-71	0.3	1.0	P + L	Pmd.cr.,Lpr.cr.
8-72	0.5	0.1	Gl + L	Glmd.cr.,Lpr.cr.
8-73	0.5	0.2	Gl + L	Glmd.cr.,Lmd.cr.
8-74	0.5	0.3	L	md.cr.
8-75	0.5	0.6	L	md.cr.
8-76	0.5	0.9	P	md.cr.
8-77	1.0	0.1	Gl + L	Glmd.cr.,Lmd.cr.
8-78	1.0	0.2	L	md.cr.
8-79	1.0	0.4	L + T	Lmd.cr.,Tgd.cr.
8-80	1.0	0.6	L + T	Lmd.cr.,Tgd.cr.
8-82	1.0	0.9	P	gd.cr.
8-83	1.5	0.1	L + T	Lmd.cr.,T tr.
8-84	1.5	0.4	L + T	Lmd.cr.,Tgd.cr.
8-85	1.5	0.6	L + P	Lpr.cr.,Pgd.cr.
8-86	2.0	0.1	L + T	Lpr.cr.,T tr.
8-87	2.0	0.2	L + T	Lpr.cr.,Tgd.cr.
8-88	2.0	0.3	P	md.cr.

Figure 3.8.3 The Crystallization Field Resulting from:

1 Metakaolinite + 1–20 ($mBaO + (1-m)K_2O$) + $4SiO_2$ ∓ $275H_2O$

Rotated at 85° for 4 days

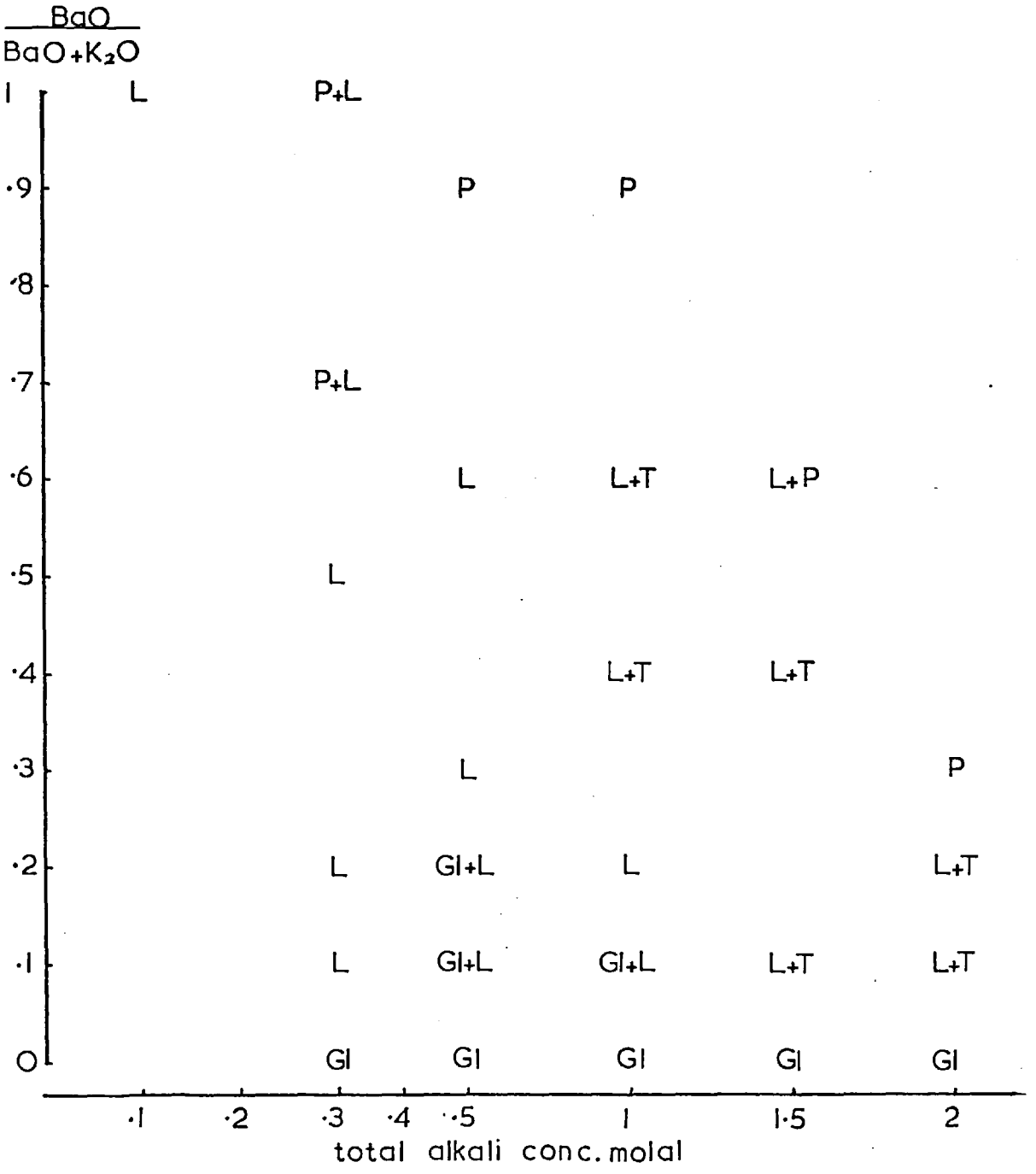

The influence of time of crystallization was examined in the crystallization field of Table 3.8.3 and Figure 3.8.3 by repeating the crystallizations with a duration of eight days in each experiment.

Table 3.8.4

The general reaction composition was:

1 metakaolinite + 1.0 - 20.0($mBaO+(1-m)K_2O$) + 4 SiO_2 + ~ 275 H_2O

rotated at 85° for 8 days.

Run No.	Concentration of alkali (molality)	Cation fraction $\frac{BaO}{BaO + K_2O}$	Products	Description of products
8-90	0.3	0	Gl	pr.cr.
8-91	0.3	0.1	Gl + L	Glmd.cr.,Lmd.cr.
8-92	0.3	0.4	L	md.cr.
8-93	0.3	0.6	P	md.cr.
8-94	0.3	0.8	P	md.cr.
8-95	0.5	0.1	L	md.cr.
8-96	0.5	0.2	L	md.cr.
8-97	0.5	0.3	P + L	Ppr.cr.,Lmd.cr.
8-98	0.5	0.6	P + L	Pmd.cr.,Lmd.cr.
8-99	0.5	0.7	P	md.cr.
8-100	0.5	0.9	P	md.cr.
8-101	1.0	0.1	L	md.cr.
8-102	1.0	0.2	L + T	Lmd.cr.,T tr.
8-103	1.0	0.3	L + T	Lpr.cr.,Tpr.cr.
8-105	1.0	0.5	L+P+T	-
8-106	1.5	0.1	L + T	Lmd.cr.,Tmd.cr.
8-107	1.5	0.3	L + T	Lmd.cr.,Tmd.cr.
8-108	1.5	0.6	T	gd.cr.
8-109	2.0	0.1	L + T	Lmd.cr.,Tmd.cr.
8-110	2.0	0.3	T	gd.cr.

Figure 3.8.4 The Crystallization Field Resulting from:

1 Metakaolinite + 3–20 ($mBaO + (1-m)K_2O$) + $4SiO_2$ ∓ 275 H_2O

Rotated at 85° for 8 days

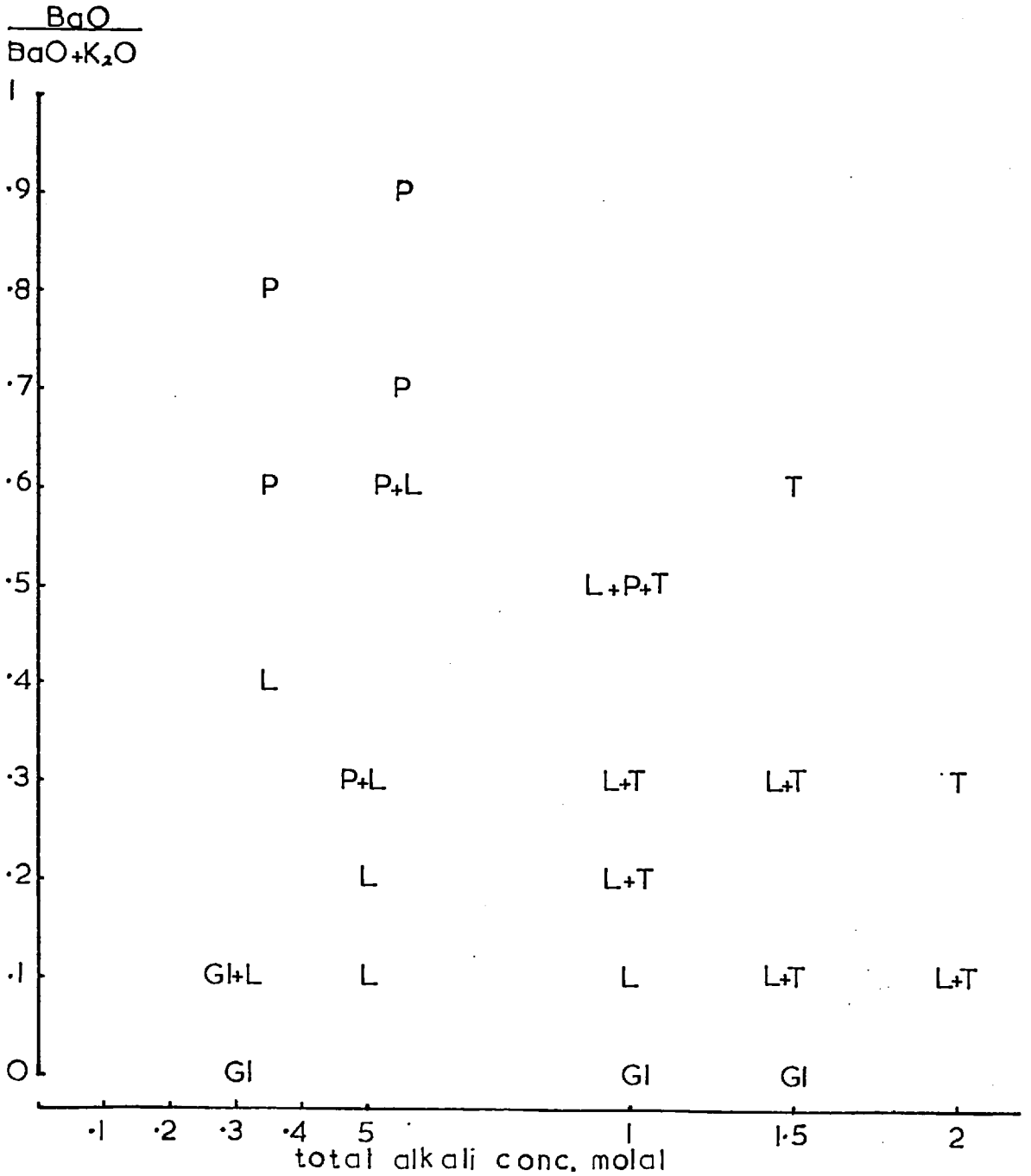

3.8.2 Observations on the System

The crystallization fields plotted in Figures 3.8.1 - 3.8.4 show that a large area is dominated by barium zeolites. These accommodate potassium in the cases of G2 and L. It was found by analysis of P that 90% of the cations present were barium. Probably barium was the only cation present in the hexagonal polymorph of Ba celsian-P, with the potassium in the sample present in uncrystallized gel.

The areas of the crystallization fields where the chabazite-like phase G1 is formed are outlined by dotted lines. As the silica to alumina ratio of the magma is increased from 2 to 4 this area increases and then decreases as the ratio is again increased from 4 to 6. Thus the area of formation of the L-type phases G2 and L is a minimum when the reacting composition has a silica to alumina ratio between those of Ba-G (2.5) (Section 3.5.4) and L (6.05) (Section 3.1.8). The crystallization field resulting from a silica to alumina ratio of 4 shows that species G2 nearly always crystallized together with a second product. In the two preparations (Runs 8-43, 8-58) where G2 was the sole product it was not well crystallized and could not be analysed due to the large amount of gel present. Thus the L type framework preferentially grows from magmas having

either the Ba-G or the L framework composition and also probably crystallizes best with these compositions.

The main effect of increasing the time from four to eight days was to increase the area of formation of non-hydrated products. Thus for reaction periods of four days and concentrations of 0.5 molal, a barium cation fraction of 0.3 yields L but in eight days it yields P + L (Figures 3.8.3, 3.8.4).

3.8.3 The Species Ba, K-G2

This product was identical with Ba-G (Section 3.5.2) which has been shown to have the zeolite L-type framework.

The chemical analysis of a sample is given below in terms of weight per cent and molar proportions respectively:

	% by weight	molar ratio
K_2O	3.3	0.15
BaO	31.0	0.85
Al_2O_3	24.2	1.0
SiO_2	30.4	2.14
H_2O (by difference)	11.1	2.6

Thermogravimetric analysis of the product showed a total water loss of 10.8%, in close agreement with the value found in the chemical analysis. The curve is shown in Figure 3.8.5. The D.T.A. curve of the original Ba/K form of G2 was heated to 600° and then rehydrated without significant change in the resulting D.T.A. and T.G.A. curves. A sample of the original Ba,K-G2 was heated in the Lenné-Guinier camera to 800°. There was no lattice change other than thermal expansion, which was small. The resulting diffraction pattern is shown in Plate 3.8.1

Plate 3.8.1

The continuous-heating X-ray diffraction pattern of species Ba, K-G2 heated in air at 0.5 deg./min. from room temperature up to 800° (Plate 3.7.1*)

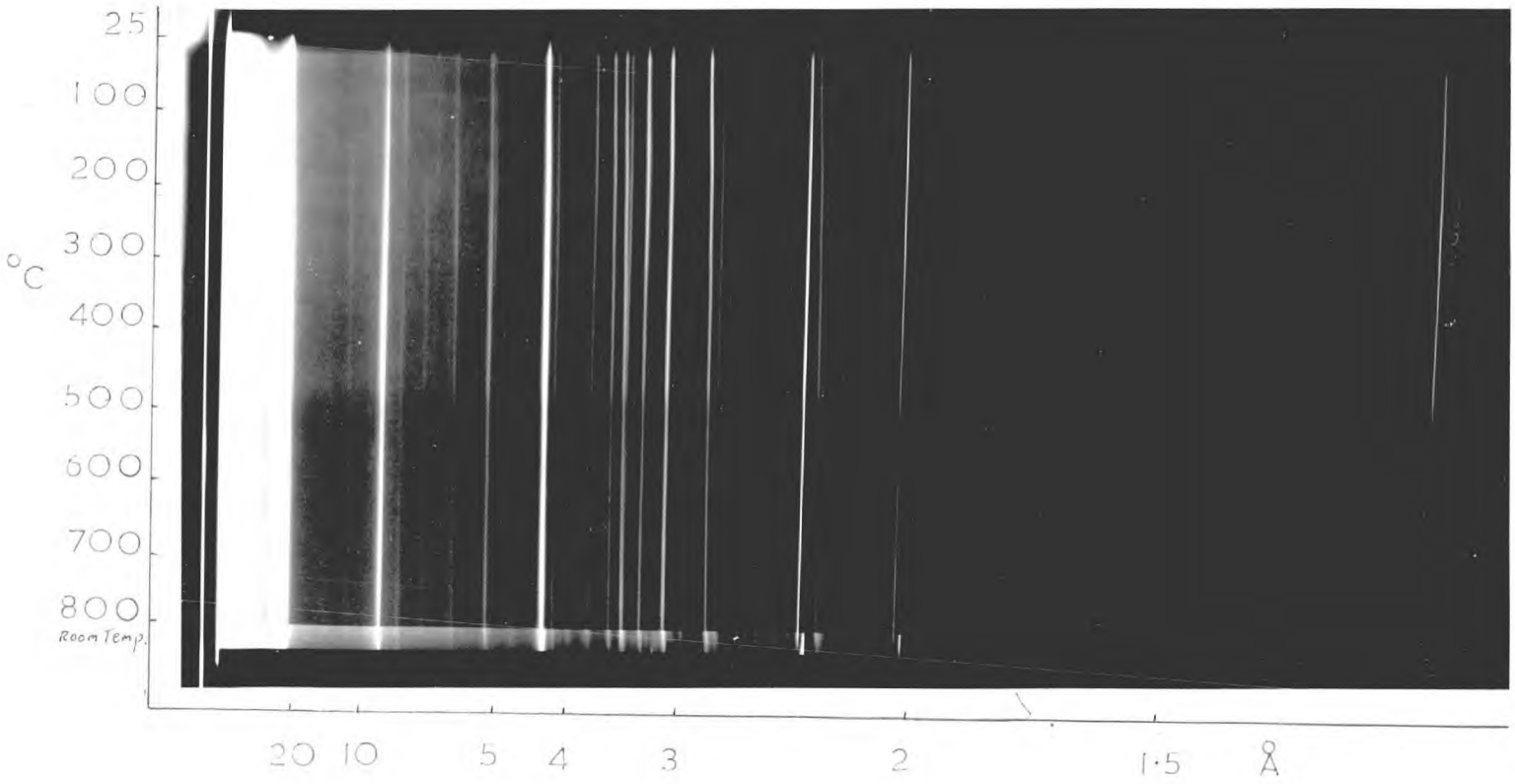

Figure 3.8.5 Dehydration of Various Cationic Forms of K Ba-G2

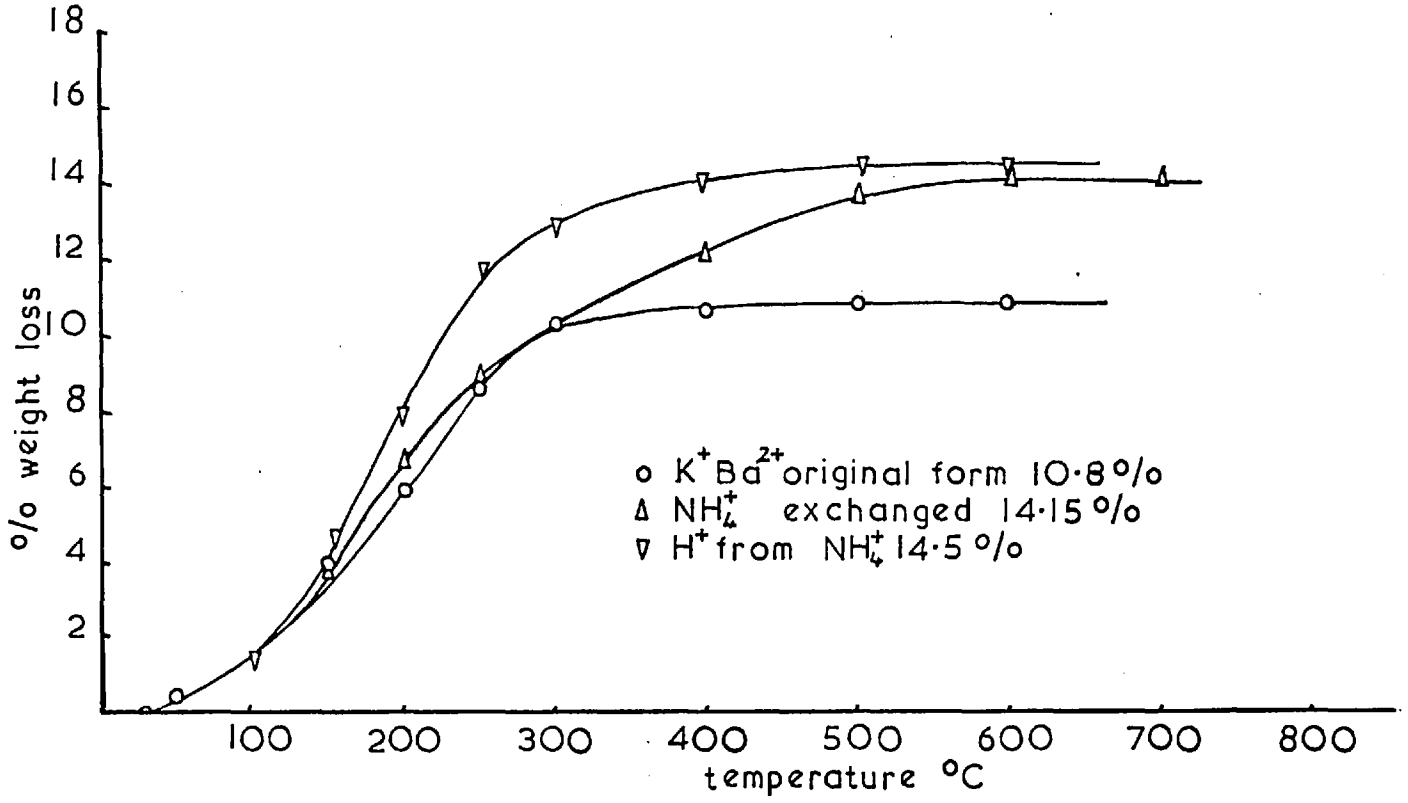

The originally synthesized form of G2 showed remarkable thermal stability for a zeolite having a low silica to alumina ratio (2.14). Due to the high thermal stability the hydrogen form of Ba,K-G2 was investigated with respect to hydration, sorption and stability. The original sample of K,Ba-G2 was exchanged to the ammonium form and then thermally decomposed at 375°. This product was then rehydrated. The T.G.A. and D.T.A. curves of both the ammonium exchanged form and the hydrogen form are given in Figures 3.8.6, 3.8.5. The following results for the extent of hydrogen ion formation were obtained.

Initial composition of Ba,K-G2:

$(0.15\ K_2O,\ 0.85\ BaO)\cdot Al_2O_3,\ 2.14\ SiO_2,\ 2.6\ H_2O$

Sample	% wt.loss	% wt.loss expressed as equivalent % of initial Ba/K form
Initial Ba/K product	10.8	10.8
NH_4^+ exchanged form	14.5	12.6
NH_4^+ decomposition product	14.5	12.7

Composition of NH_4^+ exchanged form

	% by weight	mole ratio
NH_4^+	1.8	0.41
Al_2O_3	25.8	1
SiO_2	31.9	2.16
H_2O	12.3	2.8
$(0.15\ K_2O+0.85\ BaO)$	20.2	0.64 *

Figure 3.8.6 The DTA of Various Forms of Ba,K-G2

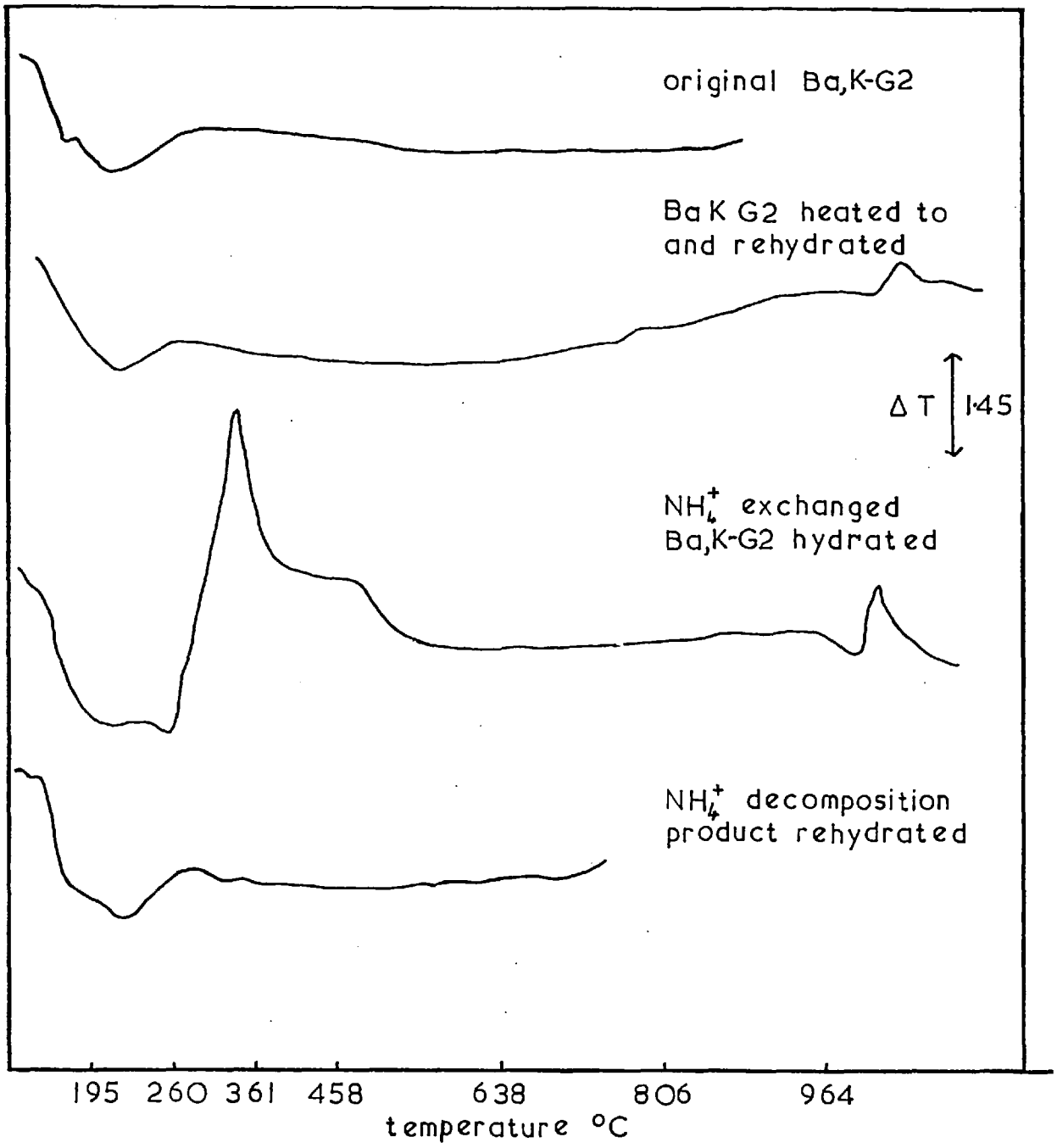

Figure 3.8.6a Zeolite Ba-G of Section 3.5.3

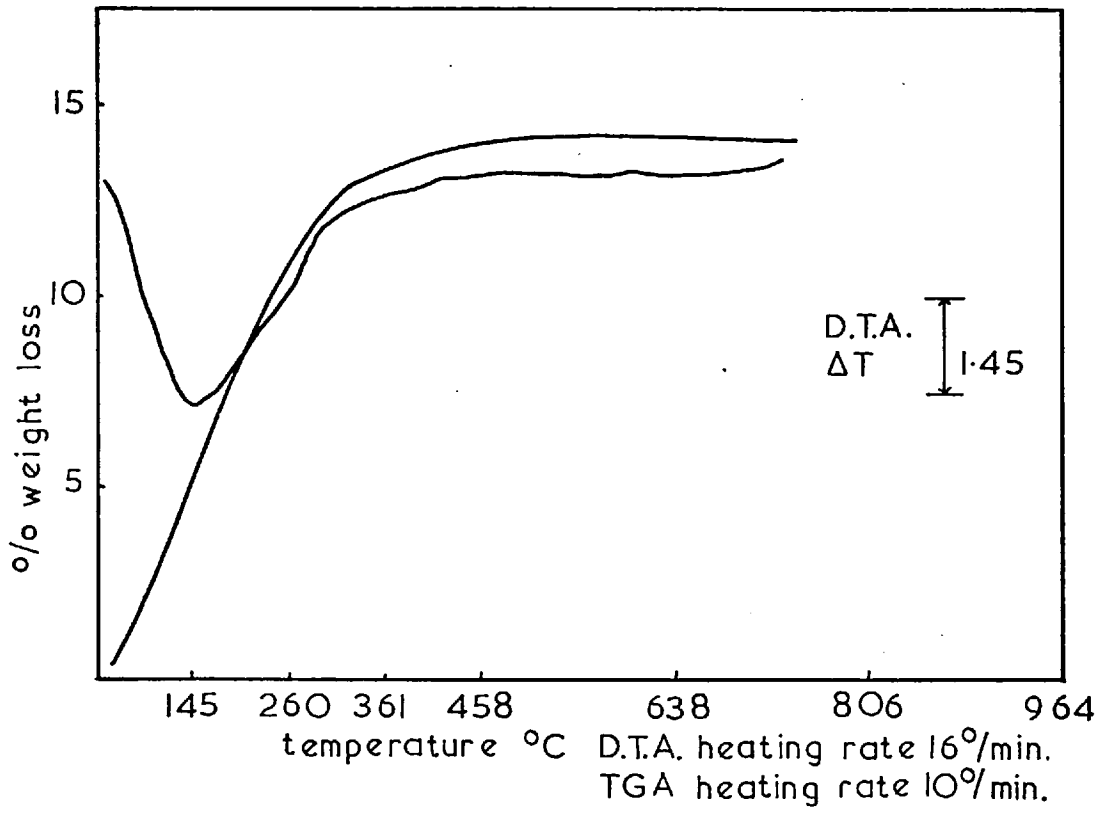

Table 3.8.5

The calculated and observed d-spacings of K,Ba-G2

a = 18.699± 0.001

c = 7.502± 0.001

Indices	d_{obs}	d_{calc}
100		16.194
001	7.474	7.502
101	6.804	6.807
210	6.141	6.121
300	5.399	5.398
211	4.737	4.742
220	4.679	4.675
310	4.484	4.491
301	4.380	4.381
221	3.962	3.967
311	3.853	3.853
002	3.748	3.751
320	3.715	3.715
102	3.659	3.654
410	3.523	3.534
112	3.478	3.481
202	3.396	3.403
321	3.331	3.329
500	3.241	3.239
212	3.199	3.198
302	3.082	3.080
420	3.060	3.060
501	2.975	2.973
222	2.924	2.925
312	2.878	2.879
421	2.834	2.834
402	2.751	2.752
600	2.698	2.699
322	2.638	2.639

Table 3.8.5 (continued)

Indices	d_{obs}	d_{calc}
520	2.593	2.593
412	2.569	2.572
601	2.541	2.540
431	2.509	2.509
103	2.471	2.471
521	2.450	2.451
113	2.415	2.416

The cell dimensions here for the Ba/K form can be compared with those of the Ba form given in Section 3.5.2. The a dimension is identical but c is smaller and approaches that of K-L. The observed and calculated d-spacings are given in Table 3.8.5.

The sorption properties of different preparations of the G2 and L members have been investigated both for oxygen and hydrocarbons. In Table 3.8.6 the sorption capacities of three of these products are compared with those of Ba-G (Section 3.5.2) and Linde L.

A comparison of Ba-G2 with Ba,K-G2 shows that the oxygen capacity is slightly smaller in the product synthesized with potassium. This is probably due to a greater volume occupied by the monovalent potassium cations. Yet the hydrocarbon sorption capacities are greater and Ba,K-G2 sorbed large amounts of neo-pentane. This demonstrates that the 7.5 Å windows along the main channel are unblocked.

Synthesis in the region of the Linde L composition (silica to alumina ratio of 6.05) gave products having silica to alumina ratios comparable to L but lower sorption capacities. This is probably due to poor overall crystallinity and/or the presence of aluminosilicate gel in the cavities.

Table 3.8.6 Comparison of the Approximate Saturation Capacities of Species having the L-type Framework

System Cations Present	SiO_2/Al_2O_3		Saturation Capacities cm^3 at ST P/g.				Thermal Stability
	During Synthesis	In the Product	Oxygen 78°K	n-Butane 273°K	iso-Butane 273°K	neo-pentane 273°K	Lattice Stable at:-
Ba	2	2·50	87	12·2	9·7	nil	—
K Ba	2	2·08	82	23·5	19·4	13·0	800
K Ba	6	5·40	74	11·0	10·9	—	800
Ba	5	4·80	72	9·5	—	—	—
K*	15-28	6·4	—	25	20	10	—

*Linde K-L approximate values taken from isotherms of Lee(1967) and Breck and Acara (1958)

Figure 3.8.7 Sorption of Oxygen at 78°K on K,Ba-G2 (L)

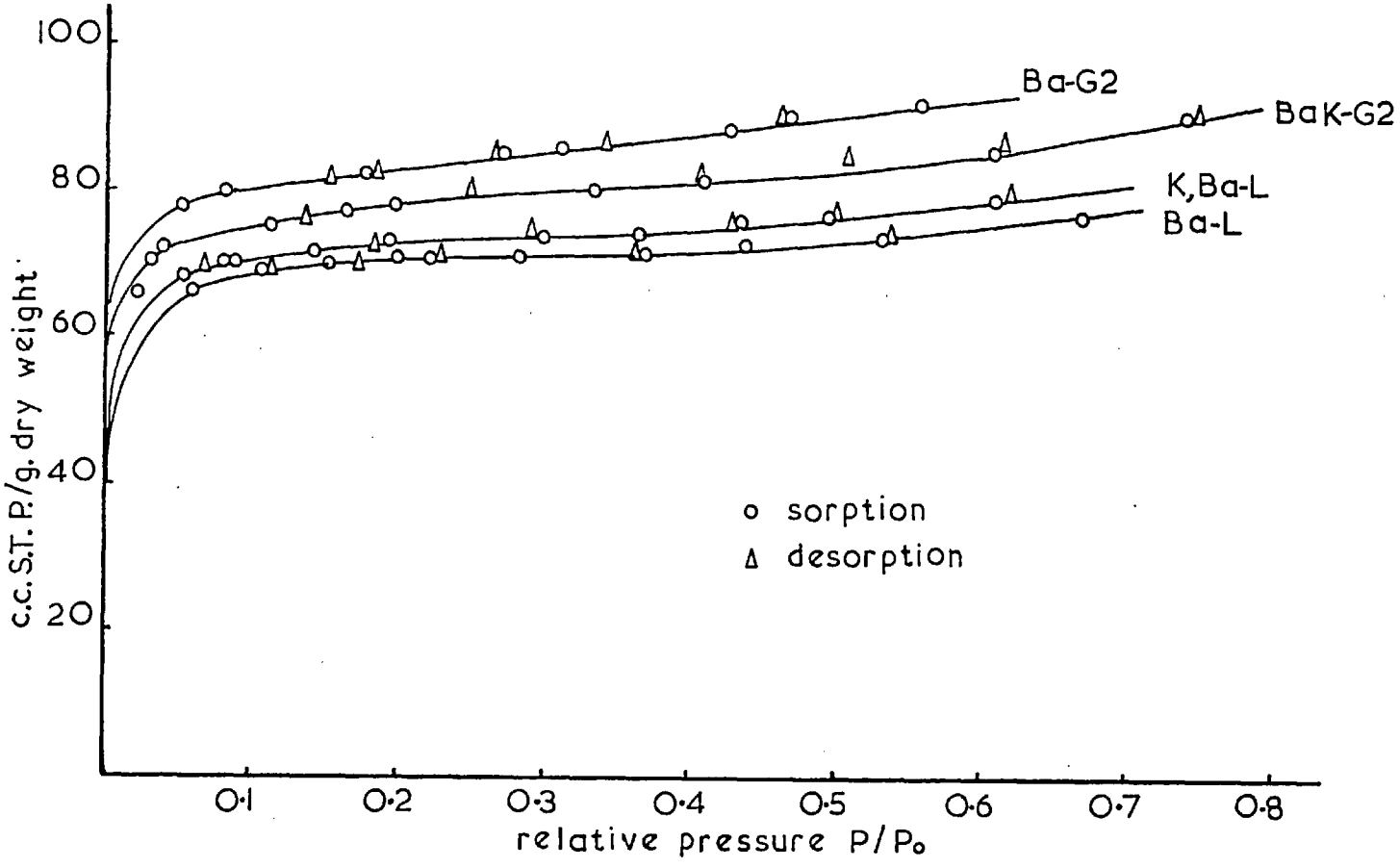

In Figures 3.8.7 - 3.8.9 the isotherms of the better crystallized products are shown. Also included is a kinetic curve showing the rate of uptake of neopentane by Ba,K-G2 at 0° C. This is a rapid process with almost complete sorption after five minutes.

Cyclohexane was sorbed both by the original Ba,K-G2 and by the hydrogen form produced by thermal decomposition of the ammonium cation-exchanged form. The results are given below where they are compared with those obtained using Ba-G2 and Linde L.

Sample	Temp. °C	Pressure mm.Hg	Cyclohexane-wt.%
Ba-G2	20.0	20	0
Ba,K-G2	19.0	21	7.7
H^+,(Ba,K)-G2	18.0	20	7.4
Linde K-L	25.0	10	8.6

The Ba,K-G2 sample had a cyclohexane sorption capacity below that of the Linde K-L. This probably resulted from presence of small amounts of uncrystallized gel. The lower sorption capacity of the hydrogen form was ascribed to a little lattice damage, probably due to local heating during the exothermic decomposition of the ammonium cation in air. This was not detectable in the X-ray diffraction pattern of the product.

Figure 3.8.8 Sorption of Hydrocarbons on K-BaG at O°C

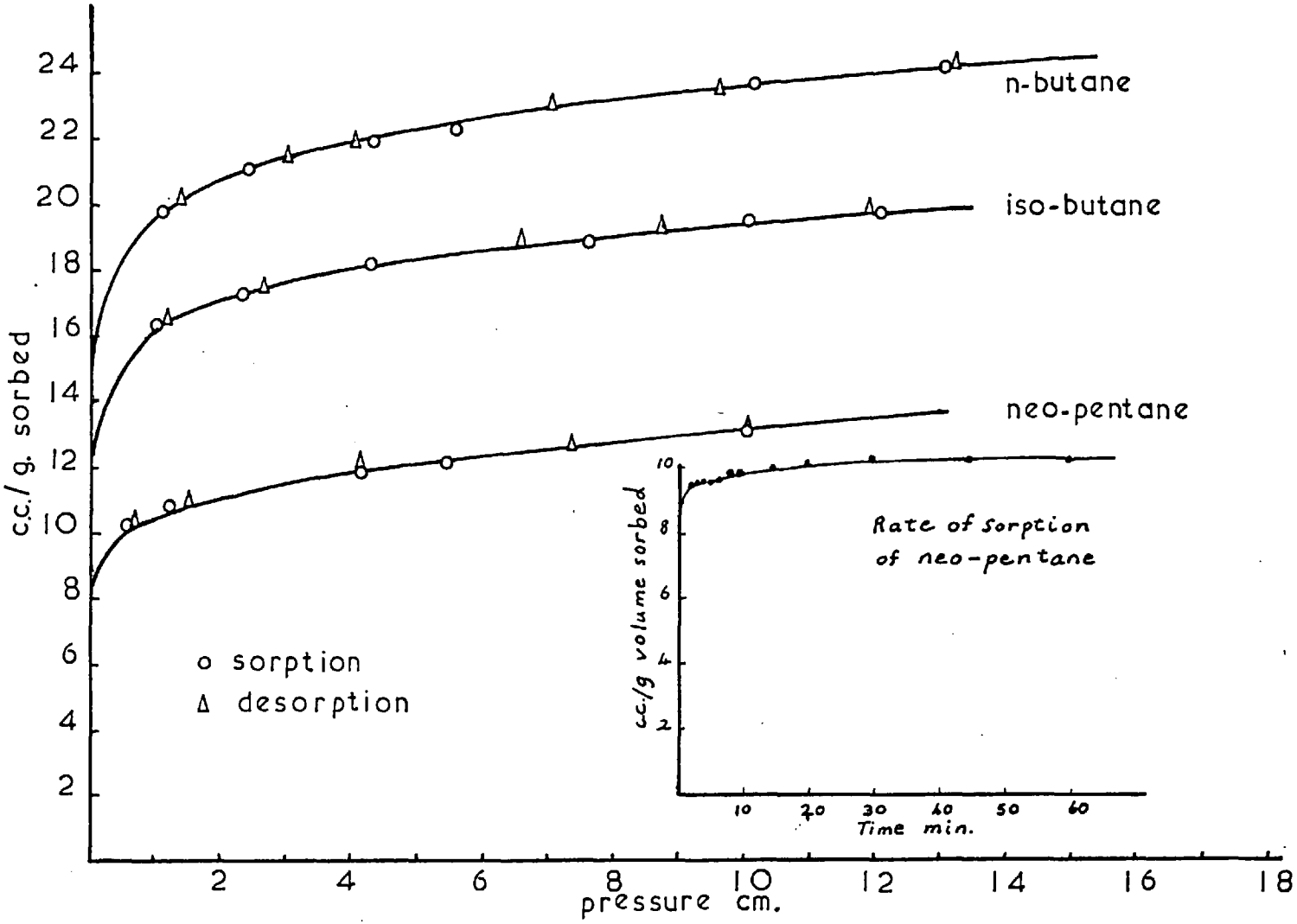

Figure 3.8.9 Sorption of iso-Butane at 273°K

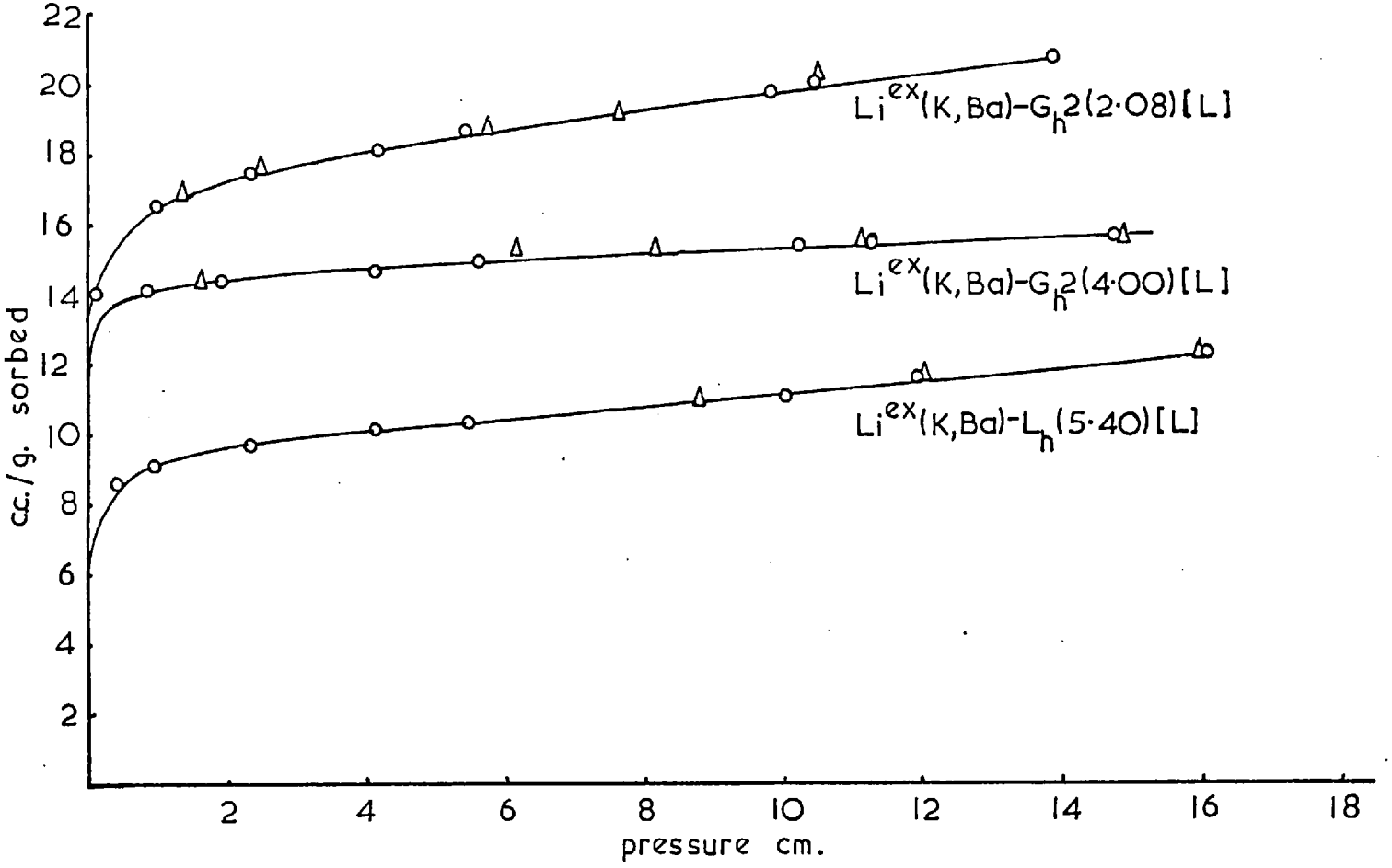

3.8.4 Reactions in the System Metakaolinite - BaO-$[(CH_3)_4N]_2O$-SiO_2-H_2O

The reactions of metakaolinite + silica with mixed aqueous barium and tetramethylammonium hydroxides are summarised in Tables 3.8.7 - 3.8.9. The crystallization fields have been plotted in Figures 3.8.10 - 3.8.12.

Table 3.8.7

The general reaction composition was: 1 metakaolinite + 2.0 - 10.0(mBaO + (1-m)$[(CH_3)_4N]_2O$) + ~ 275 H_2O rotated at 85° for 7 days.

Run No.	Concentration of alkali (molality)	Cation fraction $\frac{BaO}{BaO + [(CH_3)_4N]_2O}$	Products	Description of products
8-120	0.125	0.1	G2	pr.cr.
8-121	0.125	0.3	G2	pr.cr.
8-122	0.125	0.5	G2	pr.cr.
8-123	0.125	0.7	G2 + P	G2md.cr.,Ppr.cr.
8-124	0.2	0.1	G2	pr.cr.
8-125	0.2	0.4	G2	md.cr.
8-126	0.2	0.6	P	md.cr.
8-127	0.25	0.1	G2	md.cr.
8-128	0.25	0.3	G2 + P	G2md.cr.,Ppr.cr.
8-129	0.25	0.5	P	md.cr.
8-130	0.25	0.9	P	gd.cr.
8-135	0.5	0.1	G2 + P	G2md.cr.,Ppr.cr.
8-136	0.5	0.2	P	md.cr.
8-137	0.5	0.5	P	md.cr.
8-138	1.0	0.2	P	md.cr.
8-139	1.0	0.5	P	gd.cr.
8-140	1.0	0.9	P	gd.cr.

Figure 3 8 10 The Crystallization Field Resulting from:

1 Metakaolinite + 2–10 (m BaO + (1-m) $[(CH_3)_4N]_2O$ ∓ 275 H_2O

Rotated at 85° for 7 days

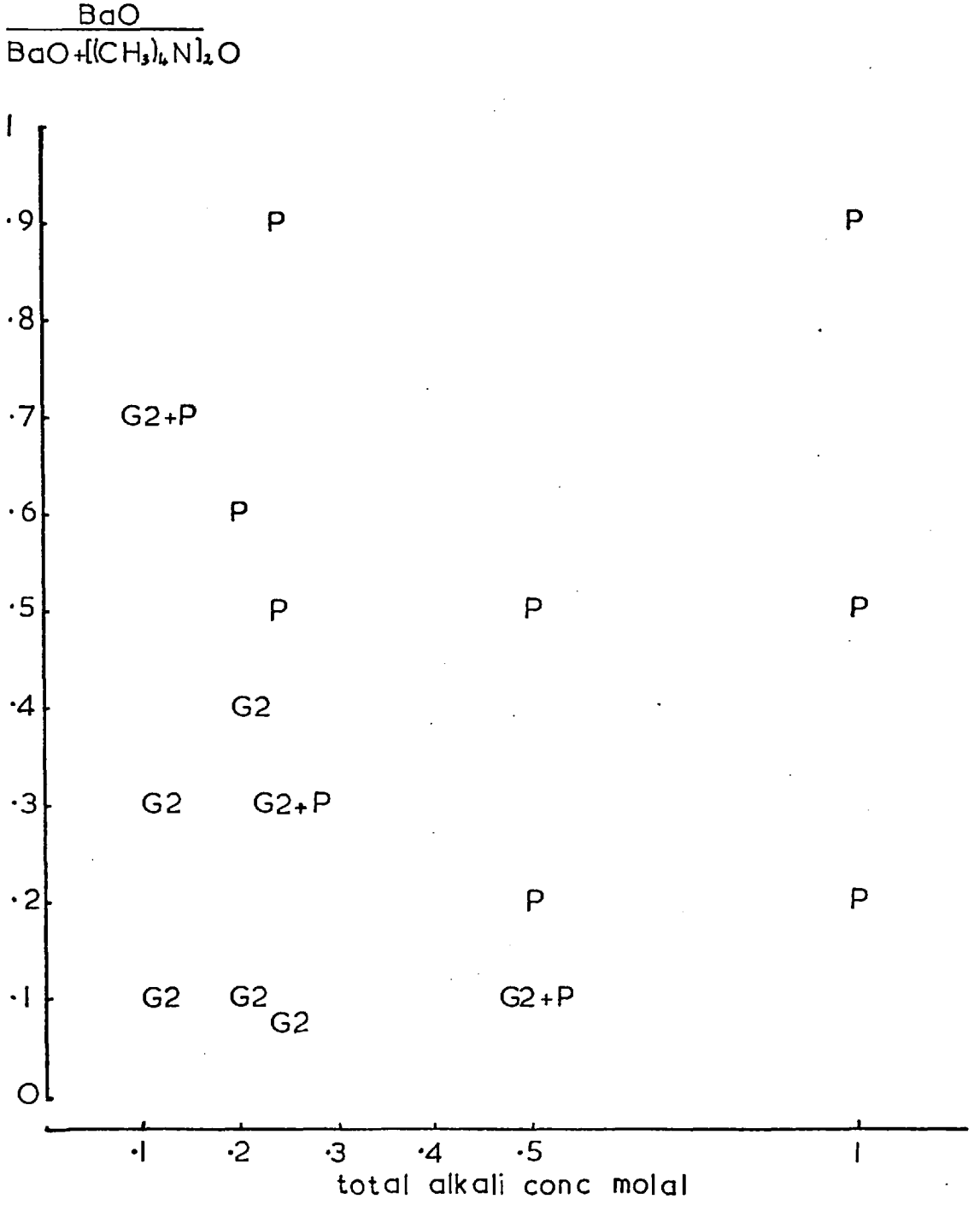

Table 3.8.8

The general reaction composition was:

1 metakaolinite + 2.0 - 10.0($mBaO+(1-m)[(CH_3)_4N]_2O$) + 4 SiO_2 + 275 H_2O rotated at 85° for 7 days.

Run No.	Concentration of alkali (molality)	Cation fraction $\frac{BaO}{BaO+[(CH_3)_4N]_2O}$	Products	Description of products
8-141	0.2	0.1	L	pr.cr.
8-142	0.2	0.2	L	pr.cr.
8-143	0.2	0.5	L + P	G2pr.cr.,Pmd.cr.
8-147	0.2	0.8	T	pr.cr.
8-148	0.25	0.1	L	pr.cr.
8-149	0.25	0.2	L	md.cr.
8-150	0.3	0.1	L	md.cr.
8-151	0.3	0.3	L + T	G2md.cr.,Tmd.cr.
8-153	0.3	0.5	P + T	Pmd.cr.,Tmd.cr.
8-154	0.3	0.7	P + T	Pmd.cr.,Tgd.cr.
8-155	0.3	0.9	P + T	Pmd.cr.,Tgd.cr.
8-156	0.5	0.1	L	md.cr.
8-157	0.5	0.3	P + L	Ppr.cr.,Lmd.cr.
8-158	0.5	0.5	P + L	Pmd.cr.,Lmd.cr.
8-159	0.5	0.7	P + L	Pmd.cr.,Lgd.cr.
8-160	0.5	0.9	P + L	Pmd.cr.,Lgd.cr.
8-161	1.0	0.1	T +L	T gd.cr.,Lmd.cr.
8-162	1.0	0.3	P + L	Pmd.cr.,Lmd.cr.
8-163	1.0	0.7	P + L	Pmd.cr.,Lmd.cr.
8-164	1.0	0.9	P + L	Pgd.cr.,Lgd.cr.

Figure 3.8.11 The Crystallization Field Resulting from:

$1\,Metakaolinite + 2-10(mBaO + (1-m)[(CH_3)_4N]_2O + 4SiO_2 \mp 275H_2O$

Rotated at 85° for 7 days

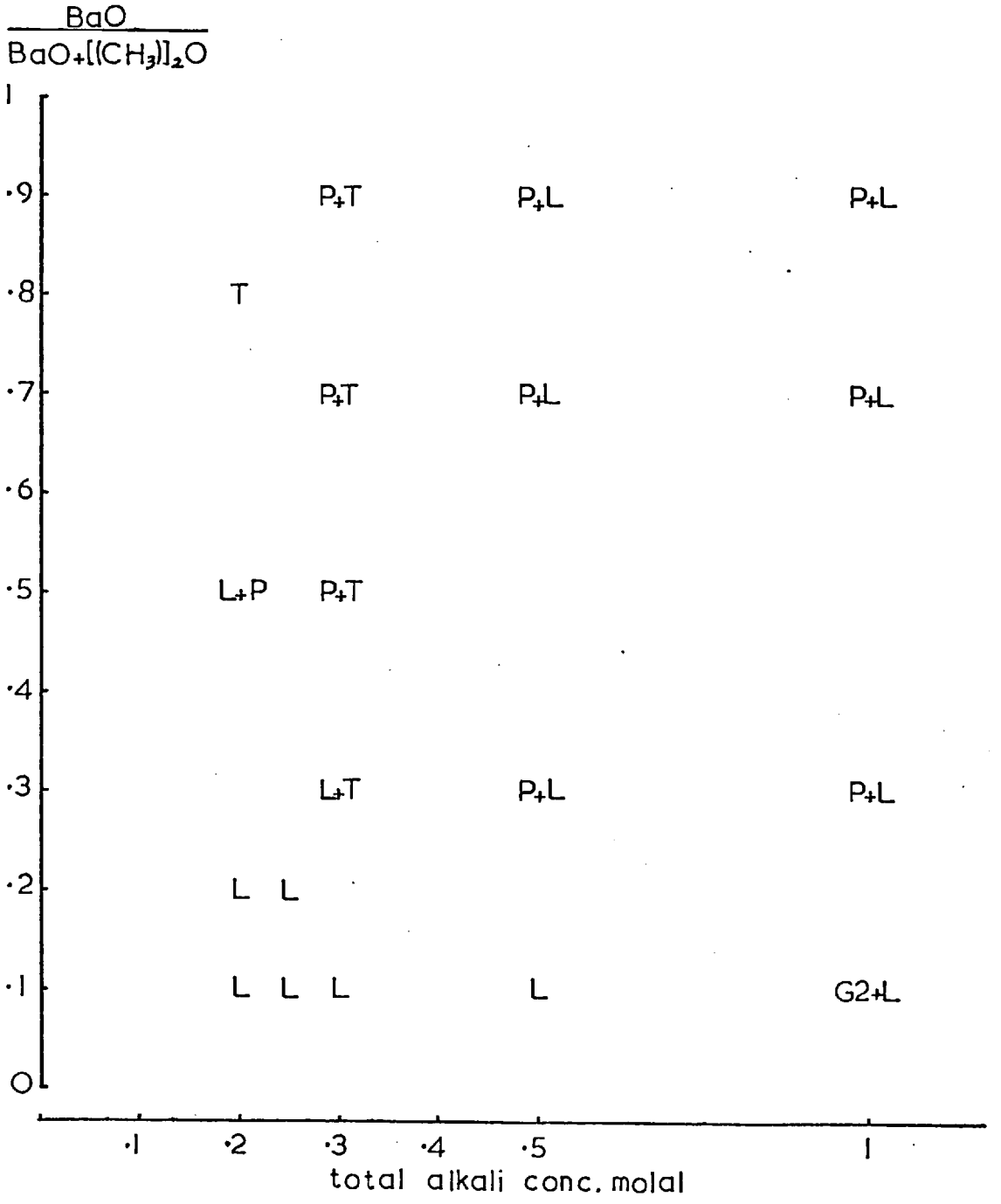

Table 3.8.9

The general composition was:

1 metakaolinite + 2.0 - 10.0($mBaO+(1-m)[(CH_3)_4N]_2O$) + 6 SiO_2 + 275 H_2O rotated at 85° for 7 days.

Run No.	Concentration of alkali (molality)	Cation fraction $\frac{BaO}{BaO+[(CH_3)_4N]_2O}$	Products	Description of products
8-165	0.2	0	Am	-
8-166	0.2	0.1	L + E	L pr.cr., Emd.cr.
8-167	0.2	0.2	L + E	L pr.cr., Epr.cr.
8-168	0.2	0.4	L	pr.cr.
8-170	0.2	0.7	L	pr.cr.
8-171	0.2	0.9	P + T	Ppr.cr., Tmd.cr.
8-177	0.25	0.15	L + E	L pr.cr., Emd.cr.
8-178	0.25	0.25	L + E	L pr.cr., Emd.cr.
8-172	0.3	0.1	L + E	L pr.cr., Emd.cr.
8-173	0.3	0.2	L + E	L pr.cr., Emd.cr.
8-174	0.3	0.4	L	md.cr.
8-176	0.3	0.8	P + T	Ppr.cr., Tmd.cr.
8-181	0.5	0.2	L + E	L md.cr., Emd.cr.
8-182	0.5	0.4	L	md.cr.
8-183	0.5	0.7	L + T	L md.cr., Tmd.cr.
8-184	1.0	0.1	L + T	L md.cr., Tmd.cr.
8-185	1.0	0.2	L + T	L md.cr., Tmd.cr.
8-186	1.0	0.4	L+T+P	L md.cr., Tmd.cr., Ppr.cr.
8-187	1.0	0.7	L+T+P	L md.cr., Tmd.cr., Pgd.cr.
8-188	1.0	0.9	P + T	Pgd.cr., Tgd.cr.

Figure 3.8.12 The Crystallization Field Resulting from : 1 Metakaolinite +2-10 ($mBaO + (1-m)[(CH_3)_4N]_2O$) + $6SiO_2$ + ~275 H_2O Rotated at 85° for 7 Days

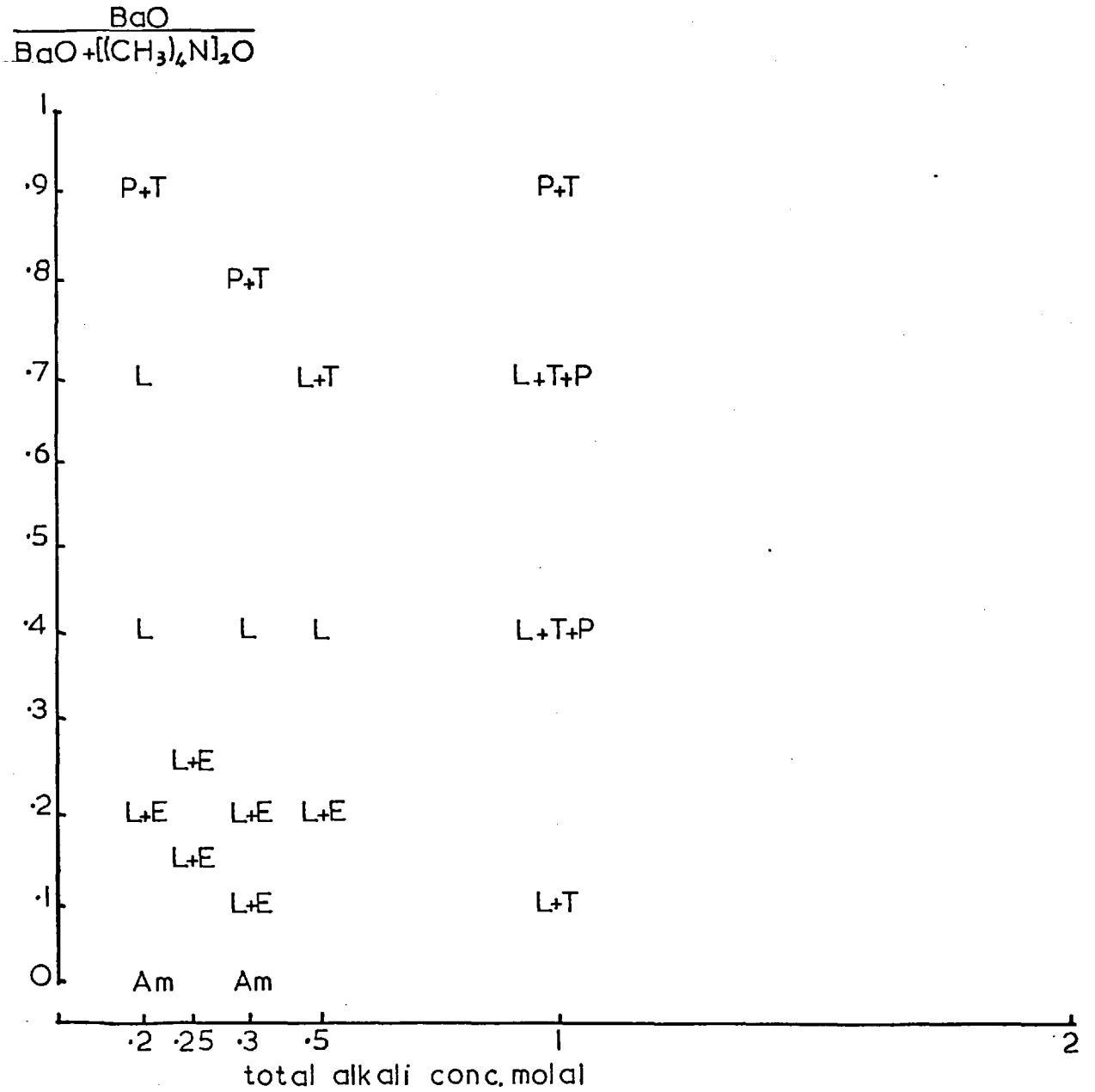

The barium cation in the mixed barium + tetramethylammonium hydroxides has the dominating role in the crystallization. At low silica to alumina ratios (2 and 6 shown in Figures 3.8.10, 3.8.11) the crystallization yielded typical barium species. Tetramethylammonium hydroxide tends to give zeolites rich in silica (Barrer and Denny, 1961; Baerlocher and Meier 1969). Thus the reacting magma may have been too aluminous for such products and yielded the less siliceous barium species Ba-P and Ba-T. However, over a large part of the tetramethylammonium rich area of the crystallization field species G2 formed, which could accommodate the large tetramethylammonium cations in the main channels.

With increased silica content (Figure 3.8.12) synthetic erionite crystallized in the section of the crystallization field which had a high tetramethylammonium fraction and a low total concentration. Thus formation of erionite is probably favoured by a low barium content in the reacting magma.

3.8.5 The Species $(CH_3)N_4Ba$-E

Lately there has been considerable study of the crystallization and properties of the related zeolites erionite, offretite and Linde L (Section 1.1). In this work a new synthesis of erionite from a system containing barium has been found. As previously noted E crystallized from mixtures with a low barium content. In all experiments the erionite, E, co-crystallized with L. This resembles the co-crystallizations of erionite, offretite and L in presence of mixed aqueous NaOH and KOH found by Barrer and Galabova (1970), but contrasts with the crystallizations in presence of mixed sodium, potassium and tetramethylammonium hydroxides reported by Aiello and Barrer (1970). Here no co-crystallizations of erionite and zeolite L were reported.

Due to the presence of the L-type product with erionite, no chemical analysis of the product was possible. The structure of erionite as described by Staples and Gard (1959) contains 23-hedral cages, cancrinite (11-hedral) cages and hexagonal prisms. Due to their size, the tetramethylammonium cations must be in the 23-hedral while barium may be either there or in the cancrinite cages.

The X-ray diffraction pattern was measured and gave the spacings in Table 3.8.10. Here it is compared both with a synthetic erionite having the composition:

$$0.33\,[(CH_3)_4N]_2O,\ 0.73\,Na_2O,\ 5.8\,SiO_2,\ 3.7\,H_2O$$

and with a natural erionite from Tecopa U.S.A. having the approximate composition:

$$0.09\,CaO,\ 0.20\,MgO,\ 0.32\,K_2O,\ 0.51\,Na_2O,\ 8\,SiO_2,\ 6\,H_2O.$$

The line positions are very similar in the diffraction patterns but there is a large variation in relative intensities.

Table 3.8.10

A comparison of the d-spacings of species E synthetic tetramethylammonium offretite and natural offretite

$(CH_3)_4N$,Ba-E		$(CH_3)_4N$,Na-E (Aiello and Barrer 1970)		natural erionite (Sheppard and Gude 1969)	
11.50	ms	11.58	vw	11.41	100
9.20	w	9.21	vs	9.07	11
7.65	w	7.64	w	7.51	7
6.63	m	6.66	vs	6.61	73
6.40	m	6.38	mw	6.28	5
5.80	mw			5.72	16
5.45	mw	5.39	mw	5.34	14
4.60	m	4.60	m	4.595	8
				4.551	12
				4.322	67
		4.19	ms	4.156	24
3.82	ms	3.83	m	3.813	37
3.75	s	3.78	s	3.746	65
3.65 *	m	3.62	ms	3.570	24
				3.402	4
3.35	mw	3.32	mw	3.303	39
				3.276	25
3.24 *	m			3.271	25
		3.182	w		
3.125	w	3.120	vw	3.106	12
				-	5
3.050 *	w	3.042	vw	-	5
2.940	m	2.942	mw	2.923	10
				2.910	10
				2.869	60
2.865	m	2.864	m	2.839	50
2.825	m	2.825	ms	2.812	52

* lines obscured by those of the co-crystallized G2.

Section 4. General Discussion

Many of the reactions of metakaolinite previously described are similar to those using raw kaolinite or aluminosilicate gels. But there exist some distinct differences. The most important of these is the crystallization of zeolite Na-Q (Linde A) from metakaolinite. This industrially important zeolite readily crystallizes from mixtures of metakaolinite and 2 molal sodium hydroxide when maintained at 80° for 24 hours, (Section 3.2.6). This is in contrast with the reaction of kaolinite under these conditions, where the product is basic sodalite (Barrer, Cole and Sticher 1968). As with metakaolinite the product obtained from aqueous alkaline aluminosilicate gels is zeolite Na-Q.

Similarly zeolite Na, $(CH_3)_4N$-V crystallizes rapidly from mixed sodium and tetramethylammonium hydroxide when it reacts with either metakaolinite (Section 3.7.1) or aluminosilicate gel (Acara 1968). No synthesis of this species has yet been reported from kaolinite or other highly crystalline alumina and silica source.

The crystallization field in the system kaolinite-K_2O-H_2O reported by Barrer, Cole and Sticher (1968) is very similar to that of metakaolinite-K_2O/H_2O (Section 3.1) with the

exception of the large area of formation of K-I in the former, which with metakaolinite is replaced by the near-chabazite K-G.

Roy, Roy and Francis (1955) have described metakaolinite as having large pseudo flakes apparently no different from unheated kaolinite, but rehydrated metakaolinite as consisting of much smaller particles. This indicated that the original large particles are broken down in the rehydration process or in the case of synthesis when put in contact with the hydroxide solution. Thus its increased rate of dissolution in alkaline solution above that of crystalline kaolinite as observed by Stricher and Bach (1969) is due to the increased surface area as well as the previously described instability of metakaolinite. The increased rate of dissolution tends to make metakaolinite produce a reacting gel-solution mixture, from which zeolite crystallization occurs, with a greater similarity to aqueous alkaline aluminosilicate gels than kaolinite. This is a more probable explanation for the difference in the reactions of kaolinite and metakaolinite than the assumption that the surface of the feed stock plays an important role in directing the mechanism of the crystallization towards different products, since metakaolinite maintains essentially the original structure in the ab plane (Section 1.4). Also Cole (1970) found that the substitution of metakaolinite for

kaolinite in crystallizations of sodalites and cancrinites in the presence of salts did not usually determine which of these two products was formed. The importance of the rate of attainment of a solution of a specific composition is demonstrated by the similarity of the products obtained from metakaolinite and from aluminosilicate gels. Here different products were found only at low alkalinity and low temperatures.

The close relationship between the formation of natural zeolites and synthetic zeolite preparation is stressed by recent work on sedimentary zeolites. Most early zeolite occurrences were from fracture and vesicle fillings in basic igneous rocks (e.g. Walker 1951, 1959). A review of sedimentary deposits of zeolites by Sheppard (1970) shows only analcime, chabazite, clinoptilolite, erionite, mordenite and phillipsite occurred extensively as sedimentary deposits. Most zeolites in sedimentary rocks formed by the reaction of siliceous vitric material (e.g. tuffs) with interstitial water where there was a relatively high pH and a high alkali ion concentration (Sheppard 1970). In Section 3.1.11 the trend from silica rich species to those low in silica was seen to occur with increasing alkalinity of the magma. Thus siliceous chabazites were obtained from magmas that were not

only silica-rich but low in alkalinity. Gude and Sheppard (1966) have found a very similar occurrence in nature. Silica-rich chabazite and the silica-rich clinoptilolite formed from rhyolitic volcanic glass in a sedimentary environment whereas most chabazite and the aluminous heulandite occurred in more basic igneous rocks. Other examples of zeolites with sedimentary varieties rich in silica are: analcime, phillipsite, and erionite. Sheppard and Gude (1969) have found that erionite, which tended to be more siliceous than offretite, had sedimentary origins while offretite and one aluminous erionite (Harada, Shigeki and Kuniaki 1967) occurred in the more basic igneous rocks.

The low temperature hydrothermal crystallization employed here produced several anhydrous products with typical high temperature origins. These were K-D (kaliophilite) and Ba-P (hexagonal polymorph of barium celsian) at 80°, and K-N (kalsilite) at 170°. Together with the early preparation of potassium felspar by Barrer and Hinds (1950) they represent low temperature laboratory syntheses of possible geological interest. Many of the syntheses of zeolites from metakaolinite were at temperatures below those previously used when synthesis took place from alkaline aluminosilicate gels. Examples are K-F (Section 3.1.7) and Na-B analcime (Section 3.2.9).

References

Acara, N.A. (1968), Union Carbide Corp., U.S.P. 3414602.

Adamson, O.J. (1942), Geol. För. Förh, Stockholm, 64, 19.

Addison, W.E. and Barrer, R.M. (1955), J.chem. Soc., 757.

Aiello, R. and Barrer, R.M. (1970), J. chem. Soc., 1470.

Aiello, R., Barrer, R.M. and Kerr, I.S. (1970), Second Int. Conf. on Molecular Sieve Zeolites, Worcester, Mass.

Ames, L.L. (1961), Amer. Mineral., 46, 1120.

Ames, L.L. (1963), Amer. Mineral., 48, 1374.

Ames, L.L. (1964a), Amer. Mineral., 49, 127.

Ames, L.L. (1964b), Amer. Mineral., 49, 1099.

Amphlett, C.B. (1964), "Inorganic Ion Exchangers", Elsevier.

Appleman, D.E. (1960), Acta Cryst., 13, 1002.

Avery, W.F. and Lee, M.N.Y. (1962), Oil Gas Journ., 60, 121.

Azaroff, L.V. and Buerger M.J. (1958), "The Powder Method", McGraw-Hill Co.

Baerlocher, Ch. and Meier, W.M. (1969), Helv. Chim. Acta, 52, 1853.

Baerlocher,Ch. and Meier, W.M. (1970), in press.

Baerlocher, Ch., Barrer, R.M., Mainwaring, D.E. and Marcilly, Ch.R. (1970) to be published.

Barrer, R.M. (1948a), J. chem. Soc., 127.

Barrer, R.M. (1948b), J. chem. Soc., 2158.

Barrer, R.M. (1949), Discuss. Farad. Soc., 5, 326.

Barrer, R.M. (1949b), Trans. Farad. Soc., 45, 358.

Barrer, R.M. (1959), Brit. Chem. Eng., May Issue 1.

Barrer, R.M. (1960), J. Phys. Chem. Solids, 16, 84.

Barrer, R.M. (1966), J. Colloid and Interface Sci., 21, 415.

Barrer, R.M. (1968), Chemistry and Industry, 1203.

Barrer, R.M. (1968b), "Molecular Sieves", Soc. Chem. Ind., London, p.39.

Barrer, R.M. and Baynham, J.W. (1956a), J. chem. Soc., 757.

Barrer, R.M. and Baynham, J.W. (1956b), J. chem. Soc., 2892.

Barrer, R.M., Baynham, J.W., Bultitude, F.W. and Meier, W.M. (1959), J. chem. Soc., 195.

Barrer, R.M. and Bratt, G.C. (1959), J. Phys. Chem. Solids, 12, 30.

Barrer, R.M. and Brook, D.W. (1953a), Trans. Farad. Soc., 49, 940.

Barrer, R.M. and Brook, D.W. (1953b), Trans. Farad. Soc., 49, 1049.

Barrer, R.M., Bultitude, F.W. and Kerr, I.S. (1959), J. chem. Soc., 1521.

Barrer, R.M., Buser, W. and Grutter, W.F. (1956), Helv. Chim. Acta, 39, 518.

Barrer, R.M. and Cole, J.F. (1970), J. chem. Soc. (A), 2475.

Barrer, R.M., Cole, J.F. and Sticher, H. (1968), J. chem. Soc.(A), 2475.

Barrer, R.M., Davies, J.A. and Rees, L.V.C. (1968), J. inorg. and nucl. chem., 31, 219.

Barrer, R.M. and Davies, J.A. (1970) in press.

Barrer, R.M. and Denny, P.J. (1961), J. chem. Soc., 971.

Barrer, R.M. and Falconer, J.D. (1956), Proc. Roy. Soc. A, 236, 227.

Barrer, R.M. and Hinds, L. (1950), Nature, London, 165, 562.

Barrer, R.M., Hinds, L. and White, E.A. (1956), J. chem. Soc., 1466.

Barrer, R.M. and Ibbitson, D.A. (1944a), Trans. Farad. Soc., 40, 194.

Barrer, R.M. and Kerr, I.S. (1959), Trans. Farad. Soc., 55, 1915.

Barrer, R.M. and Langley, D.A. (1958), J. chem. Soc., Part I 3804, Part II 3811, Part III 3817.

Barrer, R.M. and Lee, J.A. (1968), Surface Sci. 12, 341.

Barrer, R.M. and McCallum, N. (1951), Nature, London, 167, 1071.

Barrer, R.M. and McCallum, N. (1953), J. chem. Soc., 4029.

Barrer, R.M. and McCallum, N. (1953b), J. chem. Soc., 4035.

Barrer, R.M. and Marcilly, Ch. R. (1970), J. chem. Soc., in press.

Barrer, R.M. and Marshall, D.J. (1964), J. chem. Soc., 2296.

Barrer, R.M. and Marshall, D.J. (1965), J. chem. Soc., 6621.

Barrer, R.M. and Marshall, D.J. (1965b), J. chem. Soc., 6616.

Barrer, R.M. and Munday, B.M. (1970), to be published.

Barrer, R.M. and Sammon, D. (1955), J. chem. Soc., 2838.

Barrer, R.M. and Vaughan, D.E.W. (1967), Trans. Farad. Soc., 63, 2275.

Barrer, R.M. and Vaughan, D.E.W. (1967a) unpublished results.

Barrer, R.M. and Villiger, H. (1969a) Zeit. Krist., 128, 352.

Barrer, R.M. and Villiger, H. (1969b), Chem. Comm. No. 468.

Barrer, R.M. and Walker, A.J. (1964), Trans. Farad. Soc., 60, 171.

Barrer, R.M. and White, E.A.D. (1951a) J. chem. Soc., 1561.

Barrer, R.M. and White, E.A.D. (1951b), J. chem. Soc., 1267.

Beattie, J.R. and Dyer, A. (1957), J. chem. Soc., 4387.

Bergerhoff, G.B., Bauer, W.H. and Nowacki, W. (1958), Neues Jahrb. Mineral. Monatash., 193.

Borer, H. (1969), Ph.D. Thesis, E.T.H. Zurich.

Borer, H. and Meier, W. (1970), Second Int. Conf. on Molecular Sieve Zeolites, Worcester, Mass.

Bowen, N.L. (1917), Amer. J. Sci., 4th Series, 43, 115.

Breck, D.W. (1970), Second Int. Conf. on Molecular Sieve Zeolites, Worcester, Mass.

Breck, D.W. and Acara, N.A. (1958), Union Carbide Corp., B.P. Applic. 909, 264.

Breck, D.W. and Acara, N.A. (1965), Union Carbide Corp., U.S.P. 3,216, 789.

Breck, D.W., Eversole, W.G. and Milton, R.M. (1956a), J. Amer. Chem. Soc., 78, 2338.

Breck, D.W., Eversole, W.G., Milton, R.M., Reed, T.B. and Thomas, T.L. (1956b), J. Amer. Chem. Soc., 78, 5963.

Breck, D.W. and Flanigen, E.M. (1968), "Molecular Sieves", Soc. Chem. Ind., London, p. 47.

Brindley, G.W. and Nakahira, M. (1958), Nature, London, 181, 1333.

Brindley, G.W., Sharp, J.H., Patterson, J.H. and Narahari, B.N., (1967), Amer. Mineral., 52, 201.

Brown, G. (1961), "The X-ray Identification and Crystal Structures of Clay Minerals, Mineralogical Soc. London.

Ciric, J. (1968), J. Colloid and Interface Sci., 28, 315.

Ciric, J. (1968b), Mobil Oil Corp., U.S.P. 3411874.

Cole, W.F., Sörum, H. and Taylor, W.H. (1951), Acta, Cryst., 4,20.

Cole, J.F. (1970), Ph.D. Thesis, Univ. of London.

Conviser, S.A. (1968), Oil Gas J., 63, 130.

Coombs, D.S. (1955), Mineral. Mag., 30, 699.

Coombs, D.S., Ellis, A.F., Fyfe, W.S. and Taylor, A.M. (1959), Geochim. Cosmochim. Acta, 17, 53.

Dominé, D. and Quobex, J. (1968), "Molecular Sieves", Soc. Chem. Ind., London, p. 78.

Dent, L. and Smith, J.V. (1958), Nature, London, 181, 179.

Deer, W.A., Howie, R.A. and Zussmann, J. (1963), "Rock Forming Minerals", Vol. 4, J. Wiley and Sons, New York.

DiPiazza, J.J., Regis, A.J. and Sand, L.B. (1959), Bull. Geol. Soc. Amer., 70, 1589.

Dubinin, M.M. and Polstyanov, E.F. (1966), Russ. J. Inorg. Chem., 40, 631.

Dyer, A. and Molyneux, A. (1968), J. inorg. nucl. chem., 30, 2831.

Ebdon, J.F. (1965), Gas, 41, 66.

Edgar, A.D. (1964), Amer. Mineral., 49, 1139.

Eitel, W. (1966), "Silicate Science", Vol. 4, Academic Press, New York.

Eitel, W., Müller, H.O. and Radczewski, O.E. (1939), Ceram. Abstr., 18, 8, 222.

Fahlke, B., Wieker, W. and Thilo, E. (1966), Zeit. Anorg. u. allg. Chemie, 347, 82.

Faust, G.T. (1963), Schweiz mineral. petr. Mitt, 43, 165.

Fischer, K. (1963), Amer. Mineral., 48, 664.

Fischer, K. (1966), Neues Jahrb. Mineral. Mh., 1.

Fischer, K. and Meier, W.M. (1965), Fortschr. Mineral., 42, 50.

Flanigen, E.M. and Breck, D.W. (1960), 137th Meeting of the Amer. Chem. Soc., Cleveland, Ohio.

Flanigen, E.M. and Grose, R.W. (1970), Second Int. Conf. on Molecular Sieve Zeolites, Worcester, Mass.

Foster, M.D. (1965), U.S. Geol. Surv. Prof. Paper 504-E.

Fyfe, W.S. (1960), J. Geol., 68, 553.

Fyfe, W.S. and Verhoogen, J. (1958), Geol. Soc. Amer. Mem. 73.

Garden, L.A., Kington, G.L. and Laing, W.L. (1955), Trans. Farad. Soc., 51, 1558.

Ginsburg, A.S. (1923), Mineral. Abs., 2, 153.

Goldsmith, J.R. (1953), J. Geol., 61, 439.

Goldsmith, J.R. and Laves, F. (1955), Zeit. Krist., 106, 213.

Gottardi, G. and Meier, W.M. (1963), Zeit. Krist., 119, 53.

Gude, A.J. and Sheppard, R.A. (1966), Amer. Mineral. 51, 909.

Gusseva, I.V. and Liliev, I.S. (1965), Zh. Neorg. Khim., 10, 92.

Guth, J.-L. (1965), Rev. de Chemie Minerale, 2, 127.

Guyer, A., Ineichen, M. and Guyer, P. (1957), Helv. Chim. Acta, 40, 1603.

Harada, K., Shigeki, I. and Kuniaki, K., (1967), Amer. Mineral., 52, 1785.

Hay, R.L. (1964), Amer. Mineral., 49, 1366.

Hendricks, S.B. (1929), Zeit. Krist., 71 (3), 269.

Hey, M.H. (1930), Mineral. Mag.,22, Part I 422.

Hey, M.H. (1932), Mineral. Mag., 23, Part II 51; Part III 243.

Hoss, H. and Roy, R. (1959), Bull. Geol. Soc. Amer., 70, 1620.

Hoss, H. and Roy, R. (1960), Beitr. Mineral. u. Petrog. 7, 389.

Hurlbat, C.S. (1957), Amer. Mineral. (a) 792, (b) 768.

Keller, W.D. (1952), J. Sediment. Petrol., 22, 70.

Keller, W.D. (1953), J. Sediment. Petrol., 23, 10.

Kerr, G.T. (1966), J. Phys. Chem., 70, 1947.

Kerr, G.T. (1966b), Inorg. Chem., 5, 1539.

Kerr, G.T. (1968), J. Phys. Chem., 72, 1385.

Kerr, I.S., Gard, J.A., Barrer, R.M. and Galabova, I.M., (1970), Amer. Mineral., 55, 441.

Kerr, I.S. (1970), Private Communication.

Kokotailo, G.T. and Lawton, S.L. (1964), Nature, London, 203, 621.

Kopp, O.C., Harris, L.A., Clark, G.W. and Yakel, H.L. (1963), Amer. Mineral., 48, 100.

Kühl, G.H. (1967), Mobil Oil Corp., U.S.P. 3355246.

Kühl, G.H. (1968), "Molecular Sieves", Soc. Chem. Ind., London, p. 85.

Kühl, G.H. (1969), Amer. Mineral., 54, 1607.

Lam, A.H.T., Univ. of Sheffield, A.S.T.M. index 15-519.

Lee, J.A. (1967), Ph.D. Thesis, Univ. of London.

Loens, J. and Schulz, H. (1967), Acta, Cryst., 23, 434.

Loewenstein, W. (1954), Amer. Mineral., 39, 92.

Lukesh, J.S. and Buerger, M.J. (1942), Amer. Mineral., 27, 226.

Mason, B. (1962), Amer. Mineral., 47, 985.

Mason, B. and Sand, L.B. (1960), Amer. Mineral., 45, 341.

Mays, R.L. and Pickert, P.E. (1968), "Molecular Sieves", Soc. Chem. Ind., London, p. 112.

McConnell, D. (1952), Amer. Mineral., 37, 609.

Meier, W.M. (1957), Ph.D. Thesis, Univ. of London.

Meier, W.M. (1961), Zeit. Krist., 115, 439.

Meier, W.M. (1968), "Molecular Sieves", Soc. Chem. Ind., London, p. 10.

Meier, W.M. and Olsen, D.H. (1970), Second Int. Conf. on Molecular Sieve Zeolites, Worcester, Mass.

Milton, R.M. (1959), Union Carbide Corp., U.S.P. 2882244.

Milton, R.M. (1961), Union Carbide Corp., U.S.P. 3012853.

Mobil Oil Corp. (1968), Dutch Pat. 6805355.

Mumpton, F.A. (1960), Amer. Mineral., 45, 351.

Munday, B.M. (1969), Ph.D. Thesis, Univ. of London.

Newnham, R.E. (1956), See Brown, G. (1961)

Nuffield, E.W. (1966), "X-ray Diffraction Methods", J. Wiley and Sons, Inc., New York.

Ovoepyan, M.E. and Zhdanov, S.P. (1965), Izv. A.N.S.S.S.R. Ser. Khim., 1, 11.

Pauling, L. (1930), Proc. Nat. Acad. Sci., Wash., 16, 578.

Peng, C.J. (1955), Amer. Mineral., 40, 834.

Pierce, J.E. and Stiegham, D.L., Hydrocarbon Process Petrol. Refin., 45, 170.

Plyushchev, V.E. (1959), Zapiski Vsesoyuz. Mineral. Obshchestra, 88, 152.

Reed, T.B. and Breck, D.W. (1956), J. Amer. Chem. Soc., 78, 5972.

Regis, A.J., Sand, L.B., Calmon, C. and Gilwood, M.E. (1960), J. Phys. Chem., 64, 1567.

Roy, R., Roy, D.M. and Francis, E.E. (1955), J. Amer. ceram. Soc., 38, 198.

Ruiz-Menacho, C. and Roy, R. (1959), Bull. Geol. Soc. Amer., 70, 1666.

Saha, P. (1959), Amer. Mineral., 44, 300.

Saha, P. (1961), Amer. Mineral., 46, 859.

Sand, L.B. (1968), "Molecular Sieves", Soc. Chem. Ind., London, p. 71.

Sand, M.L., Coblenz, W.S. and Sand, L.B. (1970), Second Int. Conf. on Molecular Sieve Zeolites, Worcester, Mass.

Saneshima, J.S. and Morita, N. (1935), Bull. Chem. Soc. Japan, 10, 485.

Senderov, E.E. and Khitarov, N.I. (1970), Second Int. Conf. on Molecular Sieve Zeolites, Worcester, Mass.

Sheppard, R.A. (1970), Second Int. Conf. on Molecular Sieve Zeolites, Worcester, Mass.

Sheppard, R.A. and Gude, A.J. (1968), Geol. Surv. Prof. Pap., 597.

Sheppard, R.A. and Gude, A.J. (1969), Amer. Mineral., 54, 875.

Sherry, H.S. (1966), J. Phys. Chem., 70, 1158.

Sherry, H.S. (1968a), J. Phys. Chem., 72, 4086.

Sherry, H.S. (1968b), J. Phys. Chem., 72, 4095.

Smith, J.V. (1958), Nature, London, 181, 1794.

Smith, J.V, (1963), Mineral. Soc. of Amer., Special Paper No. 1.

Smith, J.V. (1964), J. chem. Soc., 3759.

Smith, J.V. and Bailey, S.W. (1963), Acta, Cryst., 16, 801.

Smith, J.V., Rinaldi, F. and Dent-Glasser, L.S. (1963), Acta Cryst., 16, 45.

Smith, J.V. and Tuttle, O.F. (1957), Amer. Journ. Sci., 255, 282.

Sorrel, C.A. (1962), Amer. Mineral., 47, 291.

Staples, L.W. and Gard, J.A. (1959), Mineral. Mag., 32, 261.

Steinfink, H. (1962), Acta Cryst., 15, 644.

Sticher, H. and Bach, R. (1969), Helvetica Chim. Acta, 52, 543.

Stranski, I.N. and Totomanov, D. (1933), Zeit. Phys. Chem., A 163, 399.

Strunz, H. (1936), Zeit. Krist., 95, 1.

Taggart, Le R., Eden, L. and Riband, G.L. (1964), Union Carbide Corp., U.S.P. 3119659.

Takahashi, H. and Nishimura, Y. (1966), Int. Conf. Clays and Clay Minerals, p. 185.

Takeuchi, Y. (1958), Mineral. J. Japan, 2, 311.

Taylor, A.M. and Roy, R. (1964), Amer. Mineral. 49, 656.

Taylor, A.M. and Roy, R. (1965), J. chem. Soc., 4028.

Taylor, H.F.W. (1949), J. chem. Soc., 1253.

Taylor, W.H. (1930), Zeit. Krist., 74, 1.

Taylor, W.H. and Jackson, R. (1933), Zeit. Krist., 86, 53.

Tscheischwili, L., Buessem, W. and Weyl, W. (1939), Ceram. Abstr., 18, 10,279.

Ueda, S. and Koizumi, M. (1970), Second Int. Conf. on Molecular Sieve Zeolites, Worcester, Mass.

Union Carbide Corp. (1967), Dutch Patent 6710729.

Vaughan, D.A. (1966), Acta Cryst., 21, 983.

Venuto, P.B. (1970), Second Int. Conf. on Molecular Sieve Zeolites, Worcester, Mass.

Venuto, P.B. and Landis, P. (1968), Adv. Catalysis, 18, 259.

Villiger, H. (1970), Ph.D. Thesis, Univ. of London.

Walker, G.P.L. (1951), Mineral. Mag., 29, 773.

Walker, G.P.L. (1959), Mineral. Mag., 32, 202.

Walker, G.P.L. (1970), Private Communication.

Wells, A.F. (1950), "Structural Inorganic Chemistry", The Clarendon Press, Oxford.

Wise, W.S., Nokleberg, W.J. and Kokinos, M. (1969), Amer. Mineral., 54, 887.

Young, D.M. and Crowell, A.D. (1962), "Physical Adsorption of Gases", Butterworths Ltd.

Zhdanov, S.P. (1965), Izv. Akad. Nauk. S.S.S.R., Ser. Khim., 6, 950.

Zhdanov, S.P. (1968), "Molecular Sieves", Soc. Chem. Ind., London, p. 62.

Zhdanov, S.P. (1970), Second Int. Conf. on Molecular Sieve Zeolites, Worcester, Mass.

Zhdanov, S.P., Samulevich, N.N. and Egorova, E.N. (1963), Izv. Akad. Nauk. Ser. Khim., 11, 2061.

Appendix 1. Zeolite Nomenclature

The designation of natural zeolites has followed the traditional pattern of mineralogy. The development of molecular sieves in technology and industry has, however, resulted in the synthesis of many varients of naturally occurring species and also in synthesis of a number of structures which have no natural counterparts. Further, a large number of novel zeolitic aluminosilicate frameworks can be constructed, some at least of which will probably be synthesized in the future.

The nomenclature of the synthetic variants and of novel synthetic zeolites has so far been very confused, because listing has been different in each laboratory. To introduce order into this complicated situation various aspects for the systematic description of synthetic zeolites were proposed (Barrer and Mainwaring 1970) which can be used equally well for natural zeolites. Some of the main features have been outlined below with examples to illustrate its usage.

The aims of the formula must be:

(1) to give as full information as possible;

(2) to provide an overall formula which is unique;

(3) not to become cumbersome; and

(4) to maintain the practice of using a short group of characters, e.g. A, L, P, which by themselves could be used in phase diagrams, isotherms, etc.

The chemistry of zeolites includes the following aspects, about which the formula should provide information, at least briefly:

(1) cation exchange;

(2) isomorphous replacement;

(3) crystallography;

(4) lattice defects of chemical types.

1. Ion Exchange

Suppose we have a synthetic zeolite such as Linde Sieve L (U.S.P. 3,216,789), which in this instance has so far no known natural counterpart.

(a) Let L denote one electrochemical equivalent of the anionic framework.

(b) The cations present in this zeolite as originally synthesised were K^+ and Na^+. This is denoted by (K, Na) so that the zeolite is

$$(K,Na)\text{-}L.$$

If the actual K^+ and Na^+ contents are determined by analysis this information is incorporated by writing the zeolite as

$$(K_{1-x}\ Na_x)\text{-}L$$

(c) If the K^+ and Na^+ are wholly or partially exchanged by other ions, say NH_4^+ and Ca^{++}, then the zeolite composition is written as

$$NH_{4(1-u-w-y)}\ Ca_{u/2}\ K_w\ Na_y\ (K_{1-x}Na_x)\text{-}L$$

If the values of u, w, y etc are not known then the formula becomes

$$NH_4,\ Ca,\ K,\ Na\ (K,Na)\text{-}L.$$

(d) This system easily embraces the natural zeolites. Thus for phillipsite in which the ions actually present are say K, Na and Ca the composition is written

$$(K,\ Na,\ Ca)\text{-Phillipsite}$$

or, if the cation composition is known,

$$(K_{(1-x-y)}Na_xCa_{y/2})\text{-Phillipsite.}$$

For brevity it may be desirable to shorten the name "phillipsite" to "phi", and similarly with other zeolites as suggested in the Table 2 at the end of this paper.

(e) In some novel synthetic zeolites, and variants of natural zeolites the cations may include nitrogenous ones, such as the alkylammonium ions. Thus the zeolite designated Ω by the Linde Co., synthesised with Na^+ and tetramethylammonium (N^+Me_4) ions in the framework, becomes according to (b)

$$(Na_{1-x}(NMe_4)_x)\text{-}\Omega$$

or if the cationic composition is not known

$$(Na,NMe_4)\text{-}\Omega$$

It is also known that tetramethylammonium or other alkylammonium ions can hydrolyse under hydrothermal conditions to give for example with NMe_4^+:

$$N^+HMe_3\ ,\ N^+H_2Me_2\ ,\ N^+H_3Me \text{ and } N^+H_4$$

It may therefore often be convenient to represent all nitrogenous ions as "N" and write the formula as

$$(Na_{1-x}N_x)\text{-}\Omega$$

(f) Either in listing the ions originally present, or in giving the composition after subsequent ion exchange, the most abundant cation (as equivalents) should be given first and then the other cations in decreasing order of abundance.

2. Isomorphous Replacement

(a) Such replacements as

$$NaAl \rightleftarrows Si$$

$$Ba2Al \rightleftarrows 2Si$$

are common among both natural and synthetic zeolites. They arise as a result of differing synthesis conditions, but cannot be effected directly, after synthesis. Such replacements are indicated by the silica:alumina ratio of the zeolite, which can conveniently be given after the type letter or designation (L, Phi, Ω in foregoing illustrations). Thus for synthetic zeolite X with $SiO_2:Al_2O_3 = 2.67$

one wr es

$$(Na)\text{-}X\ (2.67).$$

If the silica:alumina ratio is not known the bracket can be left empty or omitted.

(b) One may also have, through synthesis, other isomorphous replacements such as

$$Al \rightleftharpoons Ga$$

$$Si \rightleftharpoons Ge$$

If p is the gram atom fraction of Ge replacing Si and q is this fraction for Ga replacing Al, then full information is conveyed, e.g. in the case of known Ga and Ge bearing variants of zeolite X, by writing the composition as

$$(Na)\text{-}X\ (2.67)\begin{matrix}Ge_p\\Ga_q\end{matrix}$$

If the numerical values of p and q are unknown the composition is written

$$(Na)\text{-}X\ (2.67)\begin{matrix}Ge,Si\\Ga,Al\end{matrix}$$

3. Crystallographic Information

Full details of the unit cell and structure must be given separately from the formula itself. However, useful information, often essential for supplementing such letter designations as X, can very easily be conveyed in the formula. Thus zeolite X is cubic, and is a variant of natural faujasite. Then the formula of 2(b) for example becomes

$$(Na)\text{-}X_c\ (2.67)\begin{matrix}Ge_p\\Ga_q\end{matrix}\ [Fau]$$

where [Fau] denotes "having the faujasite type of structure".

In the case of the hexagonal zeolite L which has no natural counterpart, but for which the structure is known, the formula of 1(c) becomes

$$^{NH_4}{}_{(1-u-w-y)}{}^{Ca}{}_{u/2}{}^{K}{}_{w}{}^{Na}{}_{y}(K_{1-x}Na_x)\text{-}L_h\ (\quad)\ [L]$$

The subscript to the letter designation denotes the crystal symmetry and the symbol in the square brackets shows the type of framework structure. The $SiO_2:Al_2O_3$ ratio is assumed not to be known so that the bracket following L_h is left empty, or can be omitted.

4. Some Lattice Defects of Chemical Type

Lattice defects which may be present in high concentration are associated with:

(i) decationation;

(ii) decationation plus dehydroxylation;

(iii) dealumination;

(iv) dealumination plus dehydroxylation.

These will be briefly considered in turn and a possible nomenclature indicated. The nomenclature can then if desired be incorporated into the compositional formula quite readily.

4.1. Decationation Defects Although not a simple term "decationation" describes a process in which metallic ions are eliminated from a zeolite, usually by forming the ammonium zeolite and then by heating this:

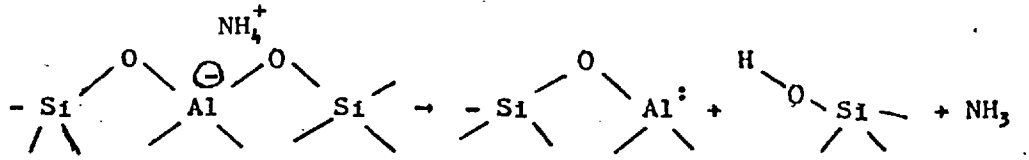

Therefore this process yields a Lewis acid site and a Bronsted acid site. It is proposed that a decationated zeolite be written, for example if derived from natural chabazite initially with Na^+ and Ca^{2+} ions, as

$$\{H\}(Na,Ca)\text{-Chabazite}_h \quad (\quad)$$

It is sometimes possible by appropriate means, for instance by treatment with suitable dilute or weak acid, to form a hydroxium ion exchanged zeolite. By contrast with the decationated zeolite, this normal ion exchanged form is written

$$H_3O\ (Na,Ca)\text{-Chabazite}_h \quad (\quad)$$

The chemical defects are always to be enclosed in braces.

4.2. Decationation-dehydroxylation Defects

If a decationated zeolite is heated to a sufficiently high temperature under appropriate conditions further water is evolved. The process is not fully understood, but one reaction, which involves migration of hydroxyl hydrogen, is believed to be

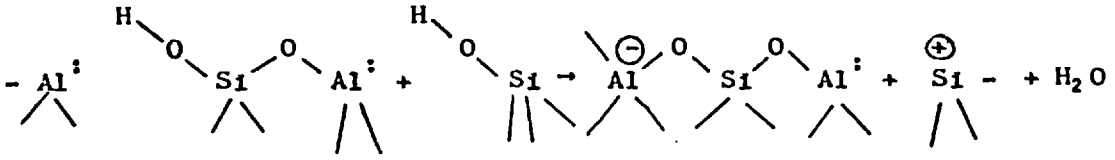

Decationation-dehydroxylation defects of this kind may be incorporated by writing the zeolite as

$$\{H_{(1-x)}(-+)_{x/2}\}\ (Na,Ca)\text{-Chabazite}_h \quad (\quad)$$

If the value of x is not known the formula becomes

$$\{H,\ (-+)\}(Na,Ca)\text{-Chabazite}_h \quad (\quad)$$

4.3. Dealumination Defects

Again under appropriate conditions it is believed that in the presence of small amounts of water Al may be liberated from the framework. If such a reaction goes to completion

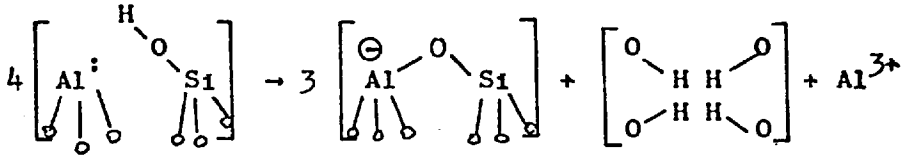

This process can easily be effected in silica-rich zeolites with mineral acids, or for less silica-rich zeolites such as Y with ethylenediaminetetraacetic acid.

Complete dealumination may be possible without significant lattice breakdown as shown by X-ray diffraction (e.g. clinoptilolite). Defects comprising nests of four associated hydroxyls arising from dealumination may be represented as $(-OH)_4$. The fully dealuminated zeolite can be written as

$$\{(-OH)_4\}(Na,Ca)\text{-Clinoptilolite}_m \quad (\quad)$$

A partially decationated partially dealuminated clinoptilolite is written

$$\{H_{1-4x}(-OH)_{4x}\}(Na,Ca)\text{-Clinoptilolite}_m \quad (\quad)$$

4.4. Dealumination - Dehydroxylation Defects

By heating a partially decationated and partially dealuminated zeolite water is evolved. The nests of four hydroxyls are in this reaction able to form two new Si-O-Si bonds with some disordering of the anionic framework, this defect being denoted $\{2(\overset{1}{\underset{1}{O}})\}$. In addition

decationation defects may be converted either to defects $\{-+\}$ or to nests of hydroxyls with further dealumination, which then yields defects $\{2(\phi)\}$. Thus if fully freed of hydroxyl water the product becomes

$$\{-+,\ 2(\phi)\}\ (Na,Ca)\text{-Clinoptilolite}_m\ (\quad)$$

If some decationation defects and hydroxyl nests still remain in unknown amounts the representation would be

$$\{H,(-OH)_4,\ -+,\ 2(\phi)\}\ (Na,Ca)\text{-Clinoptilolite}_m\ (\quad)$$

5. Intercalation Defects

The guest molecules normally present in natural or synthetic zeolites are water molecules, which are driven off during activation of the zeolite. However, it is possible to have non-volatile intercalated guest species which may substantially modify the molecular sieve behaviour, the stability and/or the catalytic properties of the zeolite. It may therefore be important to be able to incorporate these impurities, where they are known, into the formula.

Impurities of this type may be incorporated adventitiously and largely unavoidably during synthesis (silicate or aluminate anions, and additional alkali, for example in cancrinite hydrate); or they may be introduced afterwards by impregnation of the crystals by aqueous or molten salts, e.g. zeolites X, Y or A; or as volatile salts into various zeolites. This impregnation may be followed by chemical breakdown to incorporate metals (e.g. $PtCl_4$ into species X or Y followed by heating or reduction to deposit Pt atoms in the zeolite).

The means of specifying the presence of intercalated material is relatively straightforward: the guest "impurity" can be included with the other defects of §4 within the braces. Thus a

typical decationated zeolite Y carrying Pt atoms and having $SiO_2 : Al_2O_3 = 5.00$ would be

$$\{Pt,H\}(Na)\text{-}Y_c\ (5.00)[Fau]$$

If on the other hand some of the Pt migrates out of the crystal and forms Pt metal externally, the composition is written

$$\{Pt_y,H\}(Na)\text{-}Y_c\ (5.00)\ [Fau] + Pt_{(x-y)}$$

6. Summary and Conclusions

6.1. Not all the elements of nomenclature indicated in this paper may be needed at any one time, so that shortened formulae may be used. However, those elements which are needed should be introduced always in a logical manner according to the sequence of the system.

6.2. In a complete naming of the zeolite the sequence is thus

$$\{\text{Defects}\}\ \text{Cation composition after all treatments}\ \left(\text{Cation composition as synthesised or obtained}\right)\ \text{Naming symbol and crystal symmetry}\ \left(SiO_2 : Al_2O_3 \text{ ratio}\right)\ \left[\text{Symbol for structure type}\right]$$

For a natural zeolite the naming symbol and the structural symbol will be the same. The square bracket and the term in it can in this case be omitted. The naming symbol can if preferred be the full mineralogical name.

6.3. A fuller description exemplified by a decationated platinised zeolite Y would be as in Table 1.

6.4. Further consideration could be given to the question whether synthetic zeolites of novel structure should be allocated names or designated as at present by letters or groups of letters (as in Table 3); and if by letters whether the choice in Table 3 is the most appropriate.

Table 1

$\{Pt_{0.6}H_{0.9}\}$ $(NH_4)_{0.05}$ $Na_{0.05}$ (Na) - Y_c (2.67) $^{Ge_{0.4}}_{Ga_{0.3}}$ [Fau.]

- Framework structure
- Extent of replacement of Si by Ge and Al by Ga
- Ratio $MO_2:M'_2O_3$ where (M=Si, Ge, ... and M'=Al, Ga, ...)
- Designating letter (non-systematic and often varying among authors) and the crystal symmetry where known, as subscript.
- Cation(s) present in crystals as synthesised, or as obtained from natural source.
- Cations remaining after exchange and any other treatments (decationation etc). Subscripts denote g atoms of cations per electrochemical equivalent of original anionic framework.
- Lattice defects present, type and if possible amounts per equivalent of original anionic framework (subscripts).

Table 3

Short designations for some known Zeolite Structures

Zeolite	Suggested Structure Designation	Zeolite	Suggested Structure Designation
Analcime*	Ana	Phillipsite*	Phi
Wairakite*	Wai	Harmotome*	Har
Viscite	Vis	Gismondine	Gis
Kehoite	Keh	Garronite	Gar
Laumontite	Lau	Heulandite*	Heu
Natrolite	Nat	Clinoptilolite*	Cli
Mesolite	Mes	Brewsterite	Bre
Scolecite	Sco	Stilbite	Sti
Thomsonite	Tho	Stellerite	Ste
Gonnardite	Gon	Mordenite	Mor
Edingtonite	Edi	Dachiardite	Dac
Chabazite	Cha	Epistilbite	Epi
Herschelite	Her	Ferrierite	Fer
Gmelinite	Gme	Bikitaite	Bik
Erionite	Eri	Faujasite	Fau
Offretite	Off	Paulingite	Pau
Levyne	Lev	Yugawaralite	Yug
Cancrinite hydrate	Can	Zeolite P	P
		Zeolite A	A
Sodalite hydrate	Sod	Zeolite L	L
		Zeolite Ω	Ω ?
		Zeolite ZK-5	ZK-5 ?

Appendix 2. Sorption Data

Pressure - P cm. Hg

Relative pressure - P/P_o P_o - S.V.P.

Amount - c.c. at S.T.P. per g. dry weight

Sorption of Oxygen at 78°K on:

(a) K-G_h5 (4.51) [Cha]

P/P_o	amount
.07	3
.11	3
.13	3
.16	4
.26	5
.33	5
.41	6
.54	8
.55	8
.41	6
.32	5
.16	4

(b) $Li^{ex}(K)$-G5

P/P_o	amount	P/P_o	amount
.005	156	.81	189
.01	160	.71	185
.06	169	.57	182
.07	170	.51	181
.12	173	.43	180
.16	175	.36	180
.25	177	.29	179
.31	179	.24	177
.46	180	.19	174
.59	182	.11	172
.72	185	.08	171
.82	189	.07	170

(c) $Na^{ex}(K)$-G5

P/P_o	amount	P/P_o	amount
.005	92	.84	116
.03	95	.69	112
.14	103	.54	110
.21	105	.47	110
.34	106	.38	108
.49	109	.26	106
.56	110	.17	104
.61	112	.10	102
.78	115	.08	100
.84	116		

(d) H(K)-G5

P/P_o	amount
.03	94
.12	97
.28	99
.32	99
.43	99
.53	101
.67	100
.77	99
.76	101
.66	99
.51	99
.42	99
.19	97
.09	97

(e) Ca^{ex}(K)-G5

P/P_o	amount	P/P_o	amount
.005	140	.84	182
.01	150	.75	179
.015	151	.64	176
.04	158	.56	174
.07	160	.44	173
.09	162	.42	173
.19	167	.36	172
.26	169	.27	170
.34	171	.23	169
.46	171	.16	167
.55	174	.13	164
.63	177	.08	162
.76	179		
.85	182		

(f) $Ca^{ex}(K)$-Mo(3.3) [Phi]

P/P_o	amount
.06	8
.10	9
.22	11
.36	13
.45	15
.59	17
.72	22
.84	28

(g) $Li^{ex}(K)$-F(3.41) [ ]

P/P_o	amount	P/P_o	amount
.05	20	.61	52
.09	22	.51	48
.28	28	.40	42
.40	30	.28	37
.46	35	.21	28
.56	45	.13	24
.66	47		
.75	56		
.78	66		

(h) $Na\text{-}S_h(4.03)$ [Gme]

P/P_o	amount
.06	96
.07	97
.08	98
.19	101
.30	107
.49	113
.57	117
.73	126
.75	130
.75	130
.64	124
.45	117
.28	114
.24	107
.16	102
.11	100

(i) $Li^{ex}(Na)\text{-}S$

P/P_o	amount
.13	158
.32	164
.56	178
.78	196
.86	206
.87	206
.62	192
.47	182
.29	170
.25	162
.09	157

(j) H(Na)-S

P/P_o	amount
.01	41
.04	47
.06	49
.21	58
.37	64
.54	74
.63	82
.72	91
.82	100
.71	92
.48	83
.41	79
.29	72
.26	68
.23	62
.14	56

(k) NH_4^{ex}(Na)-S

P/P_o	amount
.07	15
.09	16
.13	18
.29	22
.48	26
.69	42
.76	53
.75	53
.55	37
.45	32
.37	30
.26	28
.22	20
.14	18
.07	16

(l) Ba-G_h(2.50)[L]

P/P_o	amount
.05	78
.08	81
.18	83
.27	86
.31	87
.48	89
.52	90
.61	92
.51	90
.34	87
.26	85
.19	83
.15	82

(m) Ca^{ex}(Ba)-G

P/P_o	amount
.01	66
.02	67
.16	76
.23	78
.27	79
.39	84
.47	88
.63	97
.68	101
.47	91
.37	89
.26	83
.23	80
.18	78
.10	74

(n) $Na^{ex}(Ba)$-G

P/P_o	amount
.04	63
.06	65
.14	71
.26	74
.36	77
.54	82
.64	86
.64	86
.43	80
.34	77
.16	71
.09	67

(o) $Ba,K\text{-}G_h2(2.08)[L]$

P/P_o	amount
.03	71
.04	73
.11	75
.17	77
.33	80
.41	81
.61	86
.74	90
.75	90
.62	87
.51	85
.24	80
.13	76

(p) $K,Ba\text{-}L_h(5.40)[L]$

P/P_o	amount
.02	66
.05	68
.08	70
.14	82
.19	83
.30	74
.36	74
.43	76
.49	78
.61	79
.62	80
.50	77
.43	76
.29	75
.07	70

(q) $Ba\text{-}L_h(4.80)[L]$

P/P_o	amount
.06	63
.10	69
.15	71
.20	71
.23	71
.28	70
.37	72
.44	73
.53	74
.67	77
.54	74
.36	72
.23	71
.17	70
.11	69

(r) (at 90.1°K) $Li^{ex}(Na)-S_h(4.03)$ [Gme]

P/P_o	amount
.01	91
.02	95
.03	97
.13	101
.14	105
.17	106
.26	109
.31	111
.31	111
.21	107
.17	109
.14	105
.13	102
.04	98

Sorption of n-butane at 273°K on:

(a) K-G_h5(4.51) [Cha]

P/P_o	amount
.02	1.0
.03	1.5
.07	2.0
.11	2.5
.24	2.5
.34	3.0
.41	3.0
.42	2.8
.36	2.5
.21	2.5

(b) Ca^{ex}(K)-G

P/P_o	amount
.01	43
.02	44
.09	47
.15	49
.23	50
.29	51
.41	52
.48	52
.47	53
.36	52
.27	51
.14	49
.04	45

(c) Li^{ex}(K)-G

P/P_o	amount
.01	35
.02	36
.13	37
.23	39
.29	41
.43	42
.43	42
.29	40
.14	39
.08	36

(d) Li^{ex}(Na)-S_h(4.03) [Gme]

P/P_o	amount	P/P_o	amount
sample 1		sample 2	
.01	35	.01	17
.03	36	.09	19
.08	36	.21	19
.18	36	.32	21
.31	37	.45	22
.44	39	.44	22
.52	40	.26	20
.43	38	.19	19
.23	36		
.14	35		

(e) K,Ba-G_h2(2.08)[L]

P	amount
1.1	19.8
2.4	21.1
4.4	21.9
5.6	22.3
10.2	23.7
13.1	24.2
13.2	24.2
9.6	23.7
7.1	23.0
4.0	22.0
3.1	21.6
1.4	20.1

Sorption of iso-butane at 273°K on:

(a) K,Ba-G_h2(2.08)[L]

P	amount
.1	14
1.1	16.3
2.4	17.3
4.3	18.2
7.6	18.9
10.1	19.5
12.1	19.7
11.9	19.7
8.7	19.3
6.6	17.9
2.7	17.5
1.2	16.5

(b) Li^{ex}(K,Ba)-G_h2(2.08)[L]

P	amount
.2	14.2
1.0	16.7
2.3	17.5
4.1	18.2
5.4	18.7
9.8	19.8
10.4	20.0
13.8	20.8
10.5	20.2
7.6	19.1
5.7	18.8
2.5	17.7
1.4	16.8

(c) $Li^{ex}(K,Ba)-G_h2(4.00)[L]$

P	amount
.8	14.2
1.9	14.4
4.1	14.8
5.6	15.0
10.2	15.5
11.2	15.6
14.7	15.8
14.9	15.7
11.1	15.6
8.1	15.3
6.2	15.3
1.6	14.3

(d) $Li^{ex}(K,Ba)-L_h(5.40)[L]$

P	amount
.4	8.7
.9	9.2
2.3	9.8
4.1	10.2
5.4	10.4
10.0	11.1
11.9	11.7
16.0	12.4
15.9	12.3
12.0	11.8
8.7	10.0

Sorption of neo-pentane at 273°K on:

$K,Ba-G_h2(2.08)[L]$

P	amount
.6	10.3
1.3	10.9
4.2	11.9
5.4	12.1
10.1	13.1
10.1	13.3
7.4	12.7
4.1	12.1
1.5	11.0
0.7	10.4